ADDIS ABABA UNIVERSITY

ADDIS ABABA INSTITUTE OF TECHNOLOGY

SCHOOL OF ELECTRICAL AND COMPUTER ENGINEERING

SCHOOL OF GRADUATE STUDIES

Studies on Ethiopian High Voltage Grid Security Enhancement Using UPFC

A thesis submitted to Addis Ababa University, Addis Ababa Institute of Technology, School of Electrical and Computer Engineering in partial fulfillment of requirements for the Master of Degree in Electrical Power Engineering

Submitted by

Gezahegn Shituneh Alene

(ID No. 6634/09)

Advisor: Dr. Ing. Getachew Biru Worku

July 12, 2021

Addis Ababa, Ethiopia

ADDIS ABABA UNIVERSITY

ADDIS ABABA INSTITUTE OF TECHNOLOGY

SCHOOL OF ELECTRICAL AND COMPUTER ENGINEERING

SCHOOL OF GRADUATE STUDIES

Studies on Ethiopian High Voltage Grid Security Enhancement Using UPFC

APPROVAL BY BOARD OF EXAMINERS

SN.	NAME	SIGNATURE
1.	CHAIRMAN DEPARTMENT OF GRADUATE COMMITTEE	
	Dr. Yalemzewd Negash	_____
2.	ADVISOR	
	Dr.-Ing. Getachew Biru Worku	_____
3.	INTERNAL EXAMINER	
	Mr. Dawit Habtu (PhD Candidate)	_____
4.	EXTERNAL EXAMINER	
	Prof. N.P. Singh	_____

Declaration

I, Gezahegn Shituneh, want to declare that this MSc thesis is my original work, and it has not been submitted in part or in whole at any other university. The sources used are cited and credited properly. All contributions provided from the organizations and individuals during the development of this study are acknowledged as well.

Name of the student	**Signature & Date**
Gezahegn Shituneh	----------

As the student's academic advisor, I certify that the thesis written by the student is his own work under my supervision.

Name of the Advisor	**Signature & Date**
Dr. Ing. Getachew Biru Worku	----------

Acknowledgment

First and foremost, I would like to thank Almighty God for strengthening me to go ahead through difficulty times and giving persistence to complete this study.

Secondly, I would like to forward my deepest gratitude to my advisor Dr. Ing. Getachew Biru Worku for his valuable, timely, motivative and constructive comments, and all about patience and inspirational guidance to complete this fruitful study. Really, what an inspirational guidance you did it. Dr., I have no words to say all about you except saying “THANK YOU IN ADVANCE !”. I wish you a long life !!!

I would also like to express my sincere thanks to Dr. Getachew Bekele for his effort in empowering us to grasp all about research concepts from starting to end of his all classes. Specially, I learnt a lot from “Research Method for Engineering” course so that I am able to be persistent to complete this study with a little bit wider scope.

I greatly thank Moges Alemu Tikuneh for his input and support to develop this study. Thanks again and keep it up being an open-minded !

Thank you my colleagues specially, Erkeselam Luelseged and Aemiro Tiruneh for what you support. Thank you all of my classmates specially, Kibru Zewdie.

I would also like to forward my appreciations and sincere gratitude to staffs of EEP, typically members of NLDC for their support by providing necessary input data for conducting this study.

I would like to say thank you my family for tireless support throughout my life. My lovely wife, this MSc program was started on the behalf of your encouragement & I would like to forward my special thanks for you. Thank you Nahom for your understanding !

At last, but not least, my special gratitude goes to mother “Askale T/Medhin” for all what she did. I cannot list all and I would like to say “THANK YOU ALL” who contribute directly or indirectly for successful completion of this study.

Abstract

Nowadays, more attention is given for electrical energy transportation system security. Securing electrical energy transportation system in such a way that it can deliver the demanded energy both under normal steady state operation (NSSO) and contingency conditions is very important in a power system.

Ethiopian Electric Power (EEP) manages and operates national power system centrally which consists of geographically dispersed generation stations and long-interconnected transportation system. In this study, existing national grid is modeled and the model under study has network elements of 106 buses, 146 transmission or sub-transmission lines, 51 transformers, 17 power plants, 23 lumped shunts and 69 merged loads.

The grid is simulated using Power System Analysis Toolbox (PSAT) in MATLAB so that 30 top ranked MVA line flows of transmission lines (TLs) and 11 top ranked installed capacity of power plants (PPs) are selected for further outage case studies. The criticality of the selected contingent elements are ranked by using Overall Composite Severity Index (OCSI). Moreover, feasible locations for the UPFC deployment are identified using OCSI and Individual Severity Indice (ISI). Then, grid model with unified power flow controller (UPFC) is simulated both under normal steady state operation (NSSO) and contingency conditions. After all, the results obtained without and with UPFC deployment is compared in terms of TL loading and bus voltage of NSSO condition and in terms of Line Stability Index (LSI), Real Power Performance Index (PPI), Individual Composite Severity Index (ICSI) and OCSI for all outage case studies.

At NSSO condition, 37 bus voltage limit violations (far below acceptable minimum voltage) without UPFC but 27 bus voltage limit violations with UPFC deployment yet appreciably improved. In addition, 400 kV TL from Gilgel Gibe II to Wolyta Sodo , 11_GG-II PP to 7_Wolyta, is overloaded without UPFC deployment hence, its line flow determined is 12.217675 pu apparently where its thermal limit is 12.17 pu but solved after UPFC is deployed i.e., the line flow changed from 12.217675 pu to 3.796130 pu. It is investigated from the simulations of the grid before UPFC deployment that 140 statically instable TLs when evaluated in terms of LSI, 5 overloaded TLs when evaluated in terms of PPI and 27 TLs' limit violated when evaluated in terms of ICSI. Following the same procedures but with UPFC devices deployed on the grid: 90 TLs are statically stabilized, 41 TLs improved, and 9 TLs negatively impacted when evaluated in terms of LSI; overloading status of 2 TLs solved, and 3 TLs are a little bit negatively impacted when evaluated in terms of PPI and 17 limit violated TLs solved, 1 TL improved, and 9 TLs are negatively impacted when evaluated in terms of ICSI. Finally, the security of grid with UPFC deployed is enhanced for 38 contingency case simulations whereas for 2 contingency cases, it is negatively impacted as evaluated in terms of OCSI.

As per the grid security enhancement evaluation carried out by using UPFC, the existing grid security is weak, and implementation of this study is highly recommended.

KEY WORDS: Overall Composite Severity Index (OCSI), Individual Composite Severity Index (ICSI), Real Power Performance Index (PPI), Line Stability Index (LSI), Individual Severity Index (ISI), Outage, Contingency, Unified Power Flow Controller (UPFC), Power System Analysis Toolbox (PSAT), Security, Grid Model and Contingency Ranking

Table of Contents

List of Figures

List of Tables

Acronyms

ATC	Available Transfer Capability
CPF	Continuation Power Flow
CSI	Composite Severity Index
EEP	Ethiopian Electric Power
FACTS	Flexible AC Transmission System
GERD	Great Ethiopian Renaissance Dam
GG	Gilgel Gibe
GUI	Graphical User Interface
HV	High Voltage
ICS	Interconnected System
ICSI	Individual Composite Severity Index
ISI	Individual Severity Index
L	Line Stability Index
LSI	Line Stability Index
MVA	Megavolt Ampere
MWM	Megawatt Margin
NGCC	National Grid Control Center
NLDC	National Load Dispatch Center
NSSO	Normal Steady State Operation
OCSI	Overall Composite Severity Index
PI_{lf}	Line Performance Index
PI_{P}	Active Power Performance Index
PI_{rp}	Reactive Power Performance Index

PI_v	Voltage Performance Index
PP	Power Plant
PPI	Real Power Performance Index
PSAT	Power Analysis Toolbox
PSS	Power System Stabilizer
SSSC	Static Synchronous Series Controller
STATCOM	Static Synchronous Compensator
SVC	Shunt Voltage Controller
SVS	Synchronous Voltage Source
TCPAR	Thyristor Controlled Phase Angle Regulator
TCPST	Thyristor Controlled Phase Angle Transformer
TCSC	Thyristor controlled Series Capacitor
TL	Transmission Line
UPFC	Unified Power Flow Controller
VSC	Voltage Source Controller
VSI	Voltage Source Inverter

CHAPTER 1

INTRODUCTION

1.1 Background

Power system operation may be affected more or less by different phenomena: natural and technical problems; from second to a minute, minutes to an hour, an hour to hours etc. In other words, power system network cannot be hundred percent free in every aspects from natural phenomenon and technical problems.

As per past power system records, Ethiopia lacks secured power system network. The country has faced sever power system disturbances at different times that sometimes escalated to major grid disturbances resulting in partial or total blackouts. In past studies [1] [2] [3], it is investigated that minor to major disturbances including partial or total blackouts at their worst cases were caused by the system outages, system overload, short circuits, voltage collapses and slow protective actions to clear faults. A cascade of power system outages is also a frequent problem making the power system unsecure. To combat these incidents, power system security study is the basic task to be performed and ways to enhance a grid security should be investigated.

In Ethiopia, a commonly used sub-or main-transmission line base ratings are 45, 66, 132, 230, and 400 kV whereas for distribution system 33, 15 and 11 kV distribution lines are in use. Transmission lines, 230 and 400 kV, are relatively at highest voltage levels in Ethiopia's grid and the most important lines for power transmission from far and dispersed generation plants to the desired stations [4] [5].

As per the news released at EEP's official website [5], currently, the total stretched high voltage transmission lines has reached more than 17,000 km across the country ranging from 132 kV to 500 kV. This includes [1]500 kV Hidase-Didesa-Holeta, 400 kV Wolayta Soddo II-Addis Ababa,

[1] *It is important to note that the construction of 500 kV transmission line from Hidase (generation station) -Didessa substation-Holeta substation is completed but not energized when seen from the intended plan perspective since GERD is under construction phase. In contrast, 400 kV busbar of Holeta substation is fully deployed within existing network and energized so that currently*

230 kV koka-Hurso-Dire Dawa, 230 kV Alaba-Hosana-Giligel GibeII-Jimma-Agaro-Bedele, and 230 kV Metu- Gambela transmission lines which are under operation. The number of Substations has reached 163 substations ranging from 132 kV to 500 kV. 500 kV Didesa and Holeta substations, 400 kV Gibe III, 230 kV Hurso, Gambela and Mehoni substations are among the 163 substations currently under operation across the country. The circuit diagram of the national transmission network of EEP [4] is attached in Appendix A.

It is obviously known that electrical energy demand is growing sharply in high rates from time to time. Consequently, Ethiopia focuses mostly on constructing new electrical energy generation plants as only option to account for sharply growing demands. Nowadays putting effort on generation side only cannot be a solution to respond for enormously growing demand. Accordingly, it is important to pay more attention and give focus on project works of securing both transmission and distribution lines too in a such a way that it enables to transport and provide the electrical energy securely.

The past decade has witnessed a big growth in Ethiopia's electricity sector [1] [6]. This steep growth in the electricity sector has led to significant constraints on EEP's power grid.

Moreover, while the generation has been at the forefront of energy developments in Ethiopia, the weaknesses in the transmission network are not receiving due attention. These weaknesses affect the customers, the government, the economy and social welfare of the society. Due to these facts, fault(s) in the transmission system are threatening the operation of the power system, and thereby the national grid's vulnerability [1].

giving the service. Even 500 kV Busbar of Holeta substation is energized and usually the 500 kV transmission line from Holeta to Didessa is used for power transmission to Didessa substation when it is needed till the GERD starts operation.

400 kV busbars of the Holeta are included in the system study as the most recent numerical data are provided including 400 kV transmission lines running from Sebeta II 400 kV- Holeta 400 kV, Gelan 400 kV- Holeta 400 kV and Sululta 400 kV- Holeta 400 kV busbar as it is fully deployed within existing grid and under operation though not updated on the EEP's single line diagram (see Appendix-A).

It is important to evaluate the power system network performance for likely contingency threat of power system elements to find ways for security improvement of the system. Any power system element contingency can be categorized under either planned or unplanned outage occurrences [7].

In recent years, many researchers are looking how to control the power flow effectively to alleviate congestion without building new transmission. Accordingly, they have looked for FACTS devices which can provide fast control of Active and Reactive power through power system network.

Ethiopia's electric power transmission network is more challenging due to a centralized grid interconnection system with very wide geographic spread. Therefore, a loss of one transmission line from the network will gradually disturb the rest of the system. The network needs latest autonomous control and protective mechanisms on the selected transmission line to make the system secure [2].

FACTS devices can provide fast control of Active and Reactive power in Power system. Among the converter-based FACTS devices Static Synchronous Compensator (STATCOM) and Unified Power Flow Controller (UPFC) are the popular FACTS devices. Unified Power Flow Controller (UPFC) is a power electronic based device that has capability of controlling the power flow through the line by controlling appropriately its series and shunt parameter. It has been reported that UPFC can improve transient stability of a system [8].

The UPFC is the most versatile FACTS controller developed so far, with all-encompassing capabilities of voltage regulation, series compensation, and phase shifting. It can independently and very rapidly control both real and reactive power flows in a transmission line. It is an electrical device for providing fast-acting Reactive power compensation on high-voltage electricity transmission networks [9].

A ways to enhance a grid security should be investigated. Thus, this study aims at finding the required knowledge and information to alleviate the problem. Finally, grid security evaluation using UPFC, FACTS device family, is going to be performed in terms how much the device is effective to mitigate the most threatening security problems investigated so far.

1.2 Statements of the Problem

It is frequently observed phenomena that Ethiopia is facing sever grid disturbances at different times that sometimes escalated to major grid disturbances resulting in partial or total blackouts. The outage of power system elements can be initiated by system overload, short circuit incidents, bus voltage limit violation and faulty protective device decision. Whatever the causative agent is, the phenomenon affects the grid's performance to operate securely. Consequently, a failure of specific power system element exposes a grid to enter to the different disturbance levels of alert, emergency and restorative states. Unanticipated effect of transmission element or generation plant outage affects individual transmission lines of a grid and cascaded effect might enforce a grid to enter to the major disturbance, and then partial or total blackout incidents at worst case.

The challenges have been become more and more serious as the country tries to manage and operate the national power system centrally in which the generation stations are geographically dispersed nationwide, and very long and interconnected transmission lines. The complexity of the grid leads into difficulties to manage and operate even at little bit disturbance when a single power system component or element is out of the service so that the system fails to serve the customers partly or wholly depending on the criticality of the outage phenomena.

The incapability of the grid to withstand the disturbances and fail to regain its steady state operation further leads to the failure of supplying the required amount of energy partly or wholly to the customers. A secured power system should have to assure that the demand can be satisfied in all circumstances i.e., both under steady state operation and any system failure scenarios.

In this thesis, outage analysis based security study of Ethiopian HV Grid is conducted. The most threatening outage cases with potential impact on the grid are identified and selected. To do so, TLs with relatively highest MVA line flows determined from the grid model simulation and generation power plants (PPs) with highest installed capacity are considered to manage the volume of the study. Accordingly, the selected case studies are: 30 transmission lines (TLs) i.e., eight of 400 kV TLs, nineteen of 230 kV TLs and three of 132 of kV TLs, and eleven power plants (PPs) i.e., GG III PP 2200 MVA, GG II PP 500 MVA, Tekeze PP 344 MVA, GG I PP 219 MVA,

M/Wakena PP 180 MVA, Fincha PP 160 MVA, Amerti Neshi PP 106 MVA, Tis Abay II PP 80 MVA, Koka PP 60 MVA, Awash II PP 40 MVA and Awash III PP 40 MVA.

The ultimate goal of this study is to study security status of the grid under selected contingency cases above and investigate the most security threatening problems of Ethiopian high voltage grid. Finally, to evaluate the security enhancement possibilities by using UPFC and to summarize overall findings of the study.

1.3 Objectives

The general objective of the thesis is to study and evaluate the security enhancement possibilities of Ethiopian high voltage grid by using Unified Power Flow Controller (UPFC).

The specific objectives of the thesis are as follows:

- ✓ To develop mathematical study model of the existing Ethiopian high voltage (HV) grid.
- ✓ To simulate the grid at normal and various contingency conditions.
- ✓ To observe HV grid performance in terms of bus voltage and transmission line loading.
- ✓ To identify the most security threatening outages
- ✓ To evaluate the static security of the grid without UPFC in terms of Real Power Performance Index (PPI), Line Stability Index (LSI)), Individual Composite Severity Index (ICSI) and Overall Composite Severity Index (OCSI)
- ✓ To determine feasible locations for UPFC deployment
- ✓ To size UPFC mathematically, deploy and simulate the high voltage grid with UPFC
- ✓ To study the static security of the grid with UPFC in terms of PPI, LSI, ICSI and OCSI
- ✓ To compare the performance of the high voltage grid before and after UPFC deployment under normal steady state operation (NSSO) and contingency conditions.
- ✓ To summarize the overall findings of the study.
- ✓ To forward recommendations to EEP as per the evaluation results obtained

1.4 Significance of the Study

It is fact that secure power transport and delivery is required to satisfy the customer demand while keeping the system safer from transmission line overloading and bus voltage limit violations. In

other words, these limit violations are known as thermal and voltage limits which are related to the static security issue of the power system. The static security study is chosen to evaluate the bus voltage statuses whereas thermal and static line stability are chosen to evaluate the transmission lines performance.

In this study, cascaded outage case studies are not carried out i.e., only N-1 contingency case simulations are performed for selected contingency conditions of transmission lines (TLs) and power plants (PPs). As far as a grid security is demanded, the worst possible incident should be also taken into consideration as it is usually happening phenomenon. Accordingly, PP outage case studies are included to evaluate HV grid performance at worst cases. In this thesis, static security assessment method is used hence, the variables under study are bus voltage limit, and thermal limit and static stability limit of the transmission lines. This study is intended to evaluate the grid performance with respect to stated limit violations before and after subjected to the contingency condition.

The results investigated in this study may further help both planners and operation personnel of EEP to have awareness about cause and effect of grid element outages which can be either planned or unplanned outage of TLs and PPs when seen from the scope of this study. It may also help to have overlook on security status of the existing national power system. Moreover, the study will open up research interest on this area.

1.5 Scope of the Thesis

The scope of this thesis is conducting static security study of selected transmission line and generation power plant outage conditions of Ethiopian HV grid model using PSAT toolbox in MATLAB. Outage analysis based security study of Ethiopian HV Grid is conducted for most threatening outage cases of high potential impact on the grid. To do so, 30 TLs with relatively highest MVA line flows determined from the grid model simulation and 11 generation power plants (PPs) with highest installed capacity are selected to manage the volume of the study. Accordingly, the selected case studies are: 30 transmission lines (TLs) i.e., eight of 400 kV TLs, nineteen of 230 kV TLs and three of 132 of kV TLs, and 11 power plants (PPs) i.e., GG III PP 2200 MVA, GG II PP 500 MVA, Tekeze PP 344 MVA, GG I PP 219 MVA, M/Wakena PP 180

MVA, Fincha PP 160 MVA, Amerti Neshi PP 106 MVA, Tis Abay II PP 80 MVA, Koka PP 60 MVA, Awash II PP 40 MVA and Awash III PP 40 MVA.

It is important to note that only single contingency case study is considered. Moreover, double or triple circuit transmission lines (TLs) are also treated as a single outage case study. Under this study, only N-1 contingency simulations are performed for selected contingent elements i.e., transmission lines (TLs) and power plants (PPs). This study is intended to evaluate the grid performance in terms of bus voltage and TL thermal limit under NSSO whereas TLs in terms of real power performance index (PPI), static stability index (LSI), individual composite severity index (ICSI) and overall composite severity index (OCSI) under contingency conditions with and without UPFC deployment. Just to note, the cost estimation analysis is not the scope of this study.

1.6 Organization of the Thesis

The thesis includes five chapters organized as follows:

Chapter one gives a background information on the study, including problem formulation, objectives, methodology, and scope of the thesis.

The theoretical background and related literature reviews are explored in chapter two of the study.

Whereas chapter three consists of all about methods of the study including input data collection, compiling and mathematical model development.

In chapter four, security enhancement evaluation of Ethiopian HV grid using UPFC, simulation case studies and analysis of the results are presented.

Conclusions, recommendations and suggestions for future work are presented in chapter five of the thesis.

CHAPTER 2

POWER SYSTEM SECURITY ANALYSIS AND ENHANCEMENT

2.1 Introduction

Power system security refers to the degree of risk in a power system's ability to survive imminent disturbances and, hence, depends on the system operating condition as well as the contingent probability of disturbance. Security assessment is an important study which has to be carried out in an energy management system to determine the security and stability of the system under unfrozen contingencies. Power systems are being operated closer to the stability limit nowadays with several new economic objectives for operation. As power transactions increase, weak connections, unexpected events, and hidden failures in protection systems, human errors and other reasons may cause the system to lose balance and even lead to catastrophic failures [10] [11].

Power system security itself has different assessment categories. Amongst, a static security assessment evaluates a power system in terms of voltage and thermal limits after subjected to contingency condition/s i.e., neglects transient behavior of the system. The second power system security assessment category is dynamic or transient which is intended to evaluate time dependent transition from pre- to post- contingent state and primarily, it deals with stability issues including voltage stability, angular stability and frequency stability. Contingency based analysis technique is widely used to analyze the power system security and jointly, different security indices are used for the prediction of power system performance and operation status as elaborated in sub-section 2.2 of the thesis.

Though power system security enhancement can be achieved by different mechanisms, FACTS technology is looked in this study among which UPFC device is chosen. Accordingly, components of UPFC, its operation and enhancement possibilities of power system security using UPFC devices are going to be presented in most general expression as presented in sub-section 2.3. The most related literatures are reviewed and presented in summarized way at the end of the chapter's sub-section.

2.2 Power System Security Analysis

It is well known that power system is a complex network consisting of numerous equipments like generators, transformers, transmission lines, circuit breakers etc. Failure of any of these equipments during its operation harms the reliability of the system and hence leading to outages. Thus, one of the major agenda of power system planning and its operation is to study the effect of outages in terms of its severity [11] [12].

Generally, a power system assessment categories are as depicted in Figure 2.1.

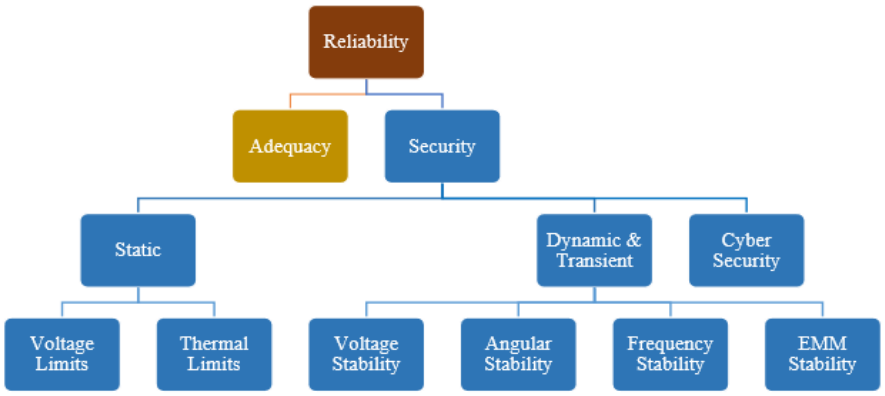

Figure 2.1. Power system security assessment categories, including both static and dynamic analysis [7]

Among security assessment categories, static security assessment evaluates the system voltage and the equipment's thermal limit violations after any contingency to ensure that they remain within acceptable intervals [7].

Power system security (Gupta, 1977) is best thought of as a measure of satisfactory performance of the system following the occurrence of anyone of a pre-specified set of contingencies. A typical contingency set may consist of one or more possible disturbances like: loss of line; loss of a generator; loss of load and sudden change in tie-line flow [13].

Contingency analysis technique is being widely used to predict the effect of outages like failure of power system components such as generator, transformer, transmission line etc., and to take necessary action to keep the power system secure and reliable. Use of offline analysis to predict the effect of individual contingency is a tedious task as a power system contains large number of

components. Practically, only selected contingencies will lead to severe conditions in power system. The process of identifying severe contingencies is referred as contingency selection and this can be done by calculating performance indices for each type of contingency [14].

Contingency analysis avoids system troubles before they occur by studying the outage events and alerting the operators to any potential overloads or serious voltage violations. The major components of contingency analysis are contingency definition, contingency ranking, contingency Selection and contingency evaluation [14].

Contingency Definition: involves preparing a list of probable contingencies.

Contingency Ranking: ranking in descending order according to the obtained value of a scalar index, normally called as severity index.

Contingency Selection: process consists of selecting the set of most probable contingencies; they need to be evaluated in terms of potential risk to the system.

Contingency Evaluation: Finally, the selected contingencies are ranked in order of their severity, till no violation of operating limits is observed.

2.2.1 Static and Dynamic Security

One of the main aspects of power system security is static security. Static security is defined as the ability of the system to reach a state within the specified secure region following a contingency. The standard approach to the security assessment problem is to perform the static security analysis followed by dynamic security analysis. Static security analysis evaluates the post-contingent steady state of the system neglecting the transient behavior and any other time-dependent variations due to changes in load generation conditions. On the other hand, dynamic security analysis evaluates the time-dependent transition from the pre- to the post-contingent state. Most of the energy management systems perform only static security analysis [15].

In the Figure 2.2 [11] [16], arrowed lines represent involuntary transitions between levels 1 to 5 due to contingencies. The removal of violations from level 4 normally requires corrective rescheduling or remedial action bringing the system to level 3, from where it can return to either level 1 or 2 by preventive rescheduling depending upon the desired operational security objectives.

Levels 1 and 2 represent normal power system operation. Level 1 has the ideal security but is too conservative and costly. Level 2 is more economical but depends on post contingency corrective rescheduling to alleviate violations without loss of load, within a specified period of time.

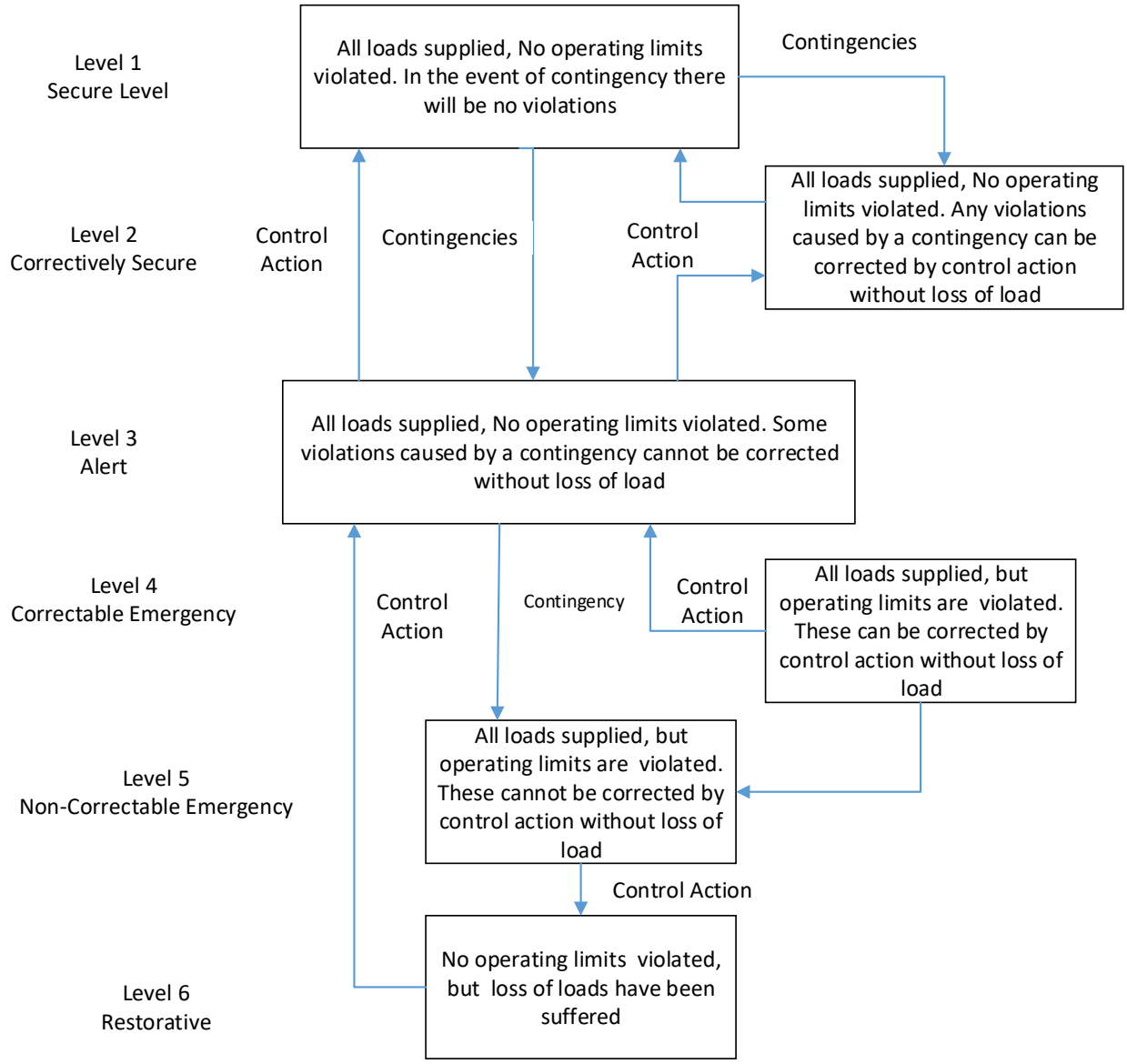

Figure 2.2. Static security levels of power system [11] [16]

2.2.2 Security Indices

There are many indices for the prediction of power system performance and operation status. Among, some indices are listed and explained by different authors as follows.

The indices provide effective information regarding identification of system weaknesses, comparison for alternative system designs, and the justification of new facilities. Performance indices are used to predict proximity to voltage collapse which have been a permanent concern in power system operation and design. These indices are used online or off-line to help operators determine the closeness of the systems from possible collapses. The various performance indices are (1-4) [17]:

1. Loading Margin (λ)
2. Voltage Stability Index (L-index)
3. Real Power flow performance index
4. Reactive power flow performance index
5. Composite Severity Index (CSI) [18]

Continuation Power flow (CPF)

CPF is the method that finds successive load flow solutions according to a load scenario. Method comprises of two steps i.e., prediction and correction step. Predictor step is used to estimate solution for designated pattern of load enlargement with a known base solution. The corrector step determined by the N-R method. After that, a next predictor step based upon the next tangent vector after that the corrector step is applied on load. This process goes till the critical point reached. Once the tangent vector becomes null, then critical point is reached. The curve of predictor-corrector scheme is depicted in Figure 2.3 [19].

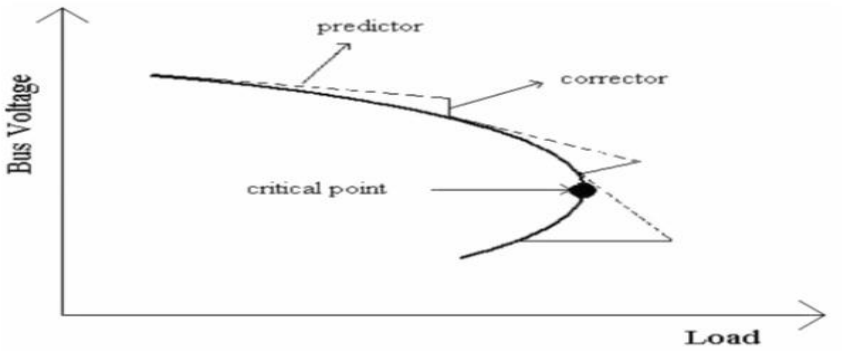

Figure 2.3. Bus Voltage-Load Curve [19]

Loading Margin (λ) [17]: The system loading margin is the amount of additional load increase for a particular-operating point until the voltage collapses. This index is most widely accepted index to measure the voltage collapse. If the system load is chosen to be the variable parameter, then a system P-V curves can be drawn where the loading margin to voltage collapse would be the change in loads between the operating point and the nose of the curve. The changes in loading can be measured by the sum of the absolute changes in load powers. However, for large systems, such approach would be prohibitively time consuming even for a single component contingency.

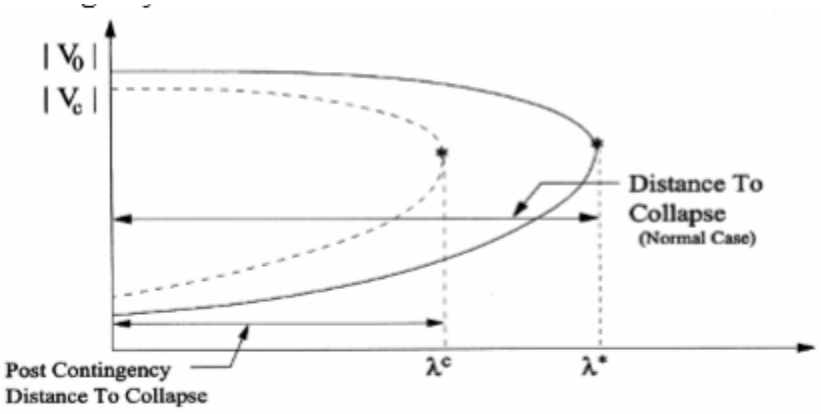

Figure 2.4. Voltage Collapse Point at Pre-Contingency and Post-Contingency [20]

Voltage Stability Index (L-index):

Even though voltage stability is a dynamic problem, static indexes still plays a very important role in voltage stability analysis and helps operators to know how close the current operation point is to static stability limit. The static indexes that are currently used by system planners and operators are four and these indexes are all kept less than the critical value for system stable operation. All the four indexes are based on power flow concept. The four indexes are fast voltage stability index (FVSI), line stability index (L_{mn}), online stability index (LVSI) and line stability factor (LQP). Static voltage stability analysis can be conducted by assuming the system is operating in the steady state and the load is a linear load. The static load models are expressed in terms of active and reactive powers which are functions of the bus voltages [21] et al..

Based on the transmission concept, M. Moghavvemi's [22] derived a line stability index to find the voltage of an interconnected system in a reduced single line network. In this formulation the

discriminator of the voltage quadratic equation is set to be greater or equal than zero to maintain stability. A typical single transmission line where index is derived from is illustrated in Figure 2.5.

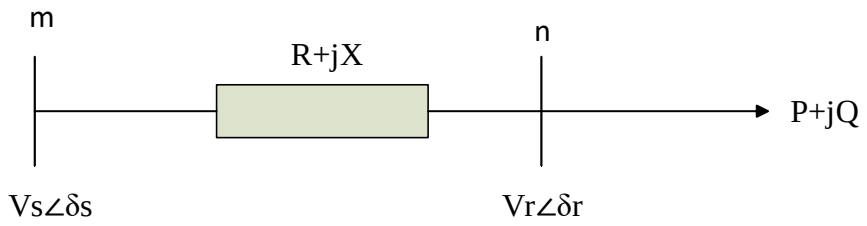

Figure 2.5. Single line diagram of a transmission line in the power system [22]

where,

$V_s\angle\delta_s$, $V_r\angle\delta r$ are the sending end and receiving end voltages

R+jX is the impedance of the transmission line

P+jQ is the receiving end apparent power

θ is the line impedance angle

δ is the angle difference between the supply voltage and the receiving end voltage

The line stability index is expressed by L_{mn}, proposed by Moghavvemi and Omar (1998) is formulated based on a power transmission concept in a single line. The line stability index L_{mn} is given by [18] [22] et al,

$$L_{mn} = {4xQ_r}\Big/{[V_m \sin(\theta - \delta)]^2} \tag{2.1}$$

where,

$$\delta = \delta_m - \delta_n \tag{2.2}$$

$$\theta = \tan^{-1} X/R \tag{2.3}$$

$\boldsymbol{\delta}$- is the angle between voltage and current

X- is the reactance of line between bus m and n

R- is the resistance of line between bus m and n

$\boldsymbol{\delta}_m$- voltage phase angle of bus m

$\boldsymbol{\delta}_n$- voltage phase angle of bus n

Q_n- is the reactive power at bus n

V_m- is the voltage magnitude at bus m

Line flow performance index (PI_{lf}): This is the index which helps in determining the extent of line overloads [11].

$$PI_{lf} = \sum_{l=1}^{nl}(W/2n)(P_l^{new} / P_{llimit})^{2n} \quad (2.4)$$

Where,

P_l^{new}- is the MW power flow of line l

P_{llimit}- is the MW capacity of line l

n_l-is the number of lines of the system

W- is the real non-negative weighting factor, value = 1

n- is exponent of penalty function, value =1

Reactive power performance index (PI_{rp}): This is the index which helps in determining bus Voltage limit violation [11].

$$PI_{rp} = \sum_{l=1}^{nb}\left(\frac{W}{2n}\right)\{(|V_i| - |V_i^{sp}|)/\Delta V_i^{lim}\}^{2n} + \sum_{l=1}^{Ng}(W/2n)(Q_i / Q_i^{limit})^{2n} \quad (2.5)$$

where,

$|V_i|$- is the voltage magnitude at i^{th} bus

$|V_i^{sp}|$- is the specified (rated) voltage magnitude at i^{th} bus

ΔV_i^{lim}- is the derivation limit of the voltage

n- is the exponent of penalty function and value =1

N_b- is the number of buses in the system

Q_i- is the produced reactive power at ith bus

$Q_{ilimit-}$ is the reactive power production limit

N_g - is the number of generating units in the system

Composite Severity Index (CSI) [18]:

Real power performance index (PI) gives an estimate of line overloads in terms of real power. Line stability index (L_{mn}) indicates the voltage stability of the system. Both indices have been combined to form a Composite Severity Index, which is used to get an accurate estimation of overall stress on the line. After obtaining the PI and L_{mn} values of all the lines for a particular line outage, the composite severity index is calculated as [22]:

$$CSI = w_1 * PI + w_2 * L_{mn} \tag{2.6}$$

where,

w_1 and w_2 are the weighting factors of the two indices for each line. The weighting factors may be used to reflect the relative importance of the indices.

The indice PI is given by:

$$PI_{ij} = \sum_{m=1}^{NL} \frac{W_m}{2n} \left(\frac{P_{lm}}{P_{lm}^{max}}\right)^{2n} \tag{2.7}$$

where,

P_{lm} - is the real power flow

P_{lm}^{max} – is max is the rated real power capacity of line m

n - is the exponent

w_m - is a real non-negative weighting factor which may be used to show a relative importance of the lines

N_L is the total number of lines in the network

The indice L_{mn} is given by:

$$L_{mn} = {4xQ_r}\Big/{[V_m \sin(\theta - \delta)]^2} \tag{2.8}$$

where,

$$\delta = \delta_m - \delta_n \tag{2.9}$$

$$\theta = \tan^{-1} X/R \tag{2.10}$$

$\boldsymbol{\delta}$- is the angle between voltage and current

X- is the reactance of line between bus m and n

R- is the resistance of line between bus m and n

$\boldsymbol{\delta}_m$- voltage phase angle of bus m

$\boldsymbol{\delta}_n$- voltage phase angle of bus n

Q_n- is the reactive power at bus n

V_m- is the voltage magnitude at bus m

2.3 Power System Security Enhancement

Since late 1960s, power system industries have undertaken considerable effort to develop and implement preventive and corrective measures to reduce the possibility and extent of system outage. Several techniques had been adopted to plan the power system restoration improvement. But with the advent and usage of the FACTS devices like SVC, UPFC, IPFC have made the system restoration significantly improved along with combined effort of system analysts, operating personal and the concurrent use of on-line and off-line computer facilities at the operating center. Any large disruption in generation and load balance in a massively interconnected system can lead to undesirable variations in power flows and bus voltages. Occasionally, this imbalance can spread uncontrollably over an entire system causing blackout of large parts of the system. As the digital age prevails, more efficient manufacturing processes, based on computers and power electronics, have come to dominate the power industry [10].

[13] The IEEE defines FACTS as "Alternating Current Transmission Systems incorporating power electronics-based and other static controllers to enhance controllability and power transfer

capability." This technology allows for improvement in transmission system operation with minimal infrastructure impact, environment impact and the time frame when compared with the construction of new transmission lines (Paserba, 2005). FACTS technology is a collection of high power controllers which can be applied on individual basis or in coordination with other controllers to control one or more of the interrelated system parameters. The following are the effects of lack of fast reliable controllers:

1. Inability of using transmission line at its thermal limits as a result of transient stability problems.
2. Power flow through unintended lines.
3. Abnormal voltage level and higher losses due to undesirable reactive power flow (Putrus, 2010).

FACTS controllers can be used for various applications to enhance power system performance. One of the greatest advantages of using FACTS controllers is that it can be used in all the three states of the power system, namely:

1. Steady state
2. Transient
3. Post transient steady state

However, the conventional devices find little application during system transient or contingency condition.

Among FACTS devices so far developed, UPFC is advanced and promising device which is one of the FACTS device family with unique capabilities. It comprises all-in-one controlling capabilities by integrating different control actions which was only possible by specific device for which it is purposely intended to do so. Basic concept of this device arises from the combined functions of the independent functions of the shunt and series FACTS devices, STATCOM and SSSC, respectively. These components, STATCOM and SSSC, are voltage source converters (VSC) when combined with coupling capacitor provide the UPFC device with unique characteristic. The detail of the device is to be discussed in upcoming sub-sections.

The operation of the UPFC is explained in different articles, [23] [24] et al., and it is summarized by using single line diagram of the UPFC device as depicted in Figure 2.6.

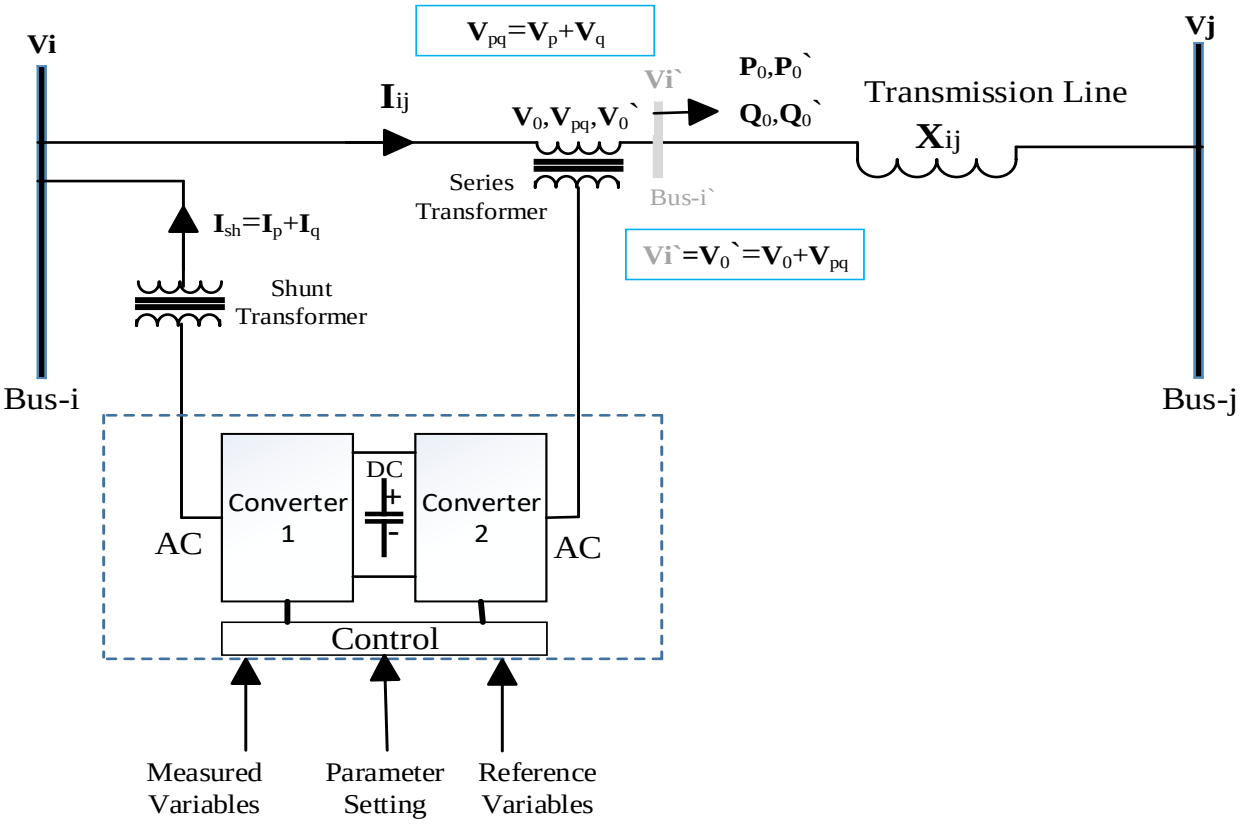

Figure 2.6. Single line diagram of the UPFC

Basically, the UPFC device concept is derived from the integration of the static synchronous compensator (STATCOM) and static synchronous series compensator (SSSC) principle independently and its circuit is constructed by incorporating the circuits of both FACTS devices as its name 'unified' indicates too. UPFC device consists of two voltage source converters, shunt converter denoted as converter 1 and series converter denoted as converter 2, which are coupled to the transmission line via shunt and series transformer respectively and coupled each other with capacitor DC link. Each component of the UPFC functions, series and shunt component, and the capacitor DC link is as explored below.

Series Component of UPFC (converter 2):

This component constitutes the main function of UPFC device with the capability of injecting controllable series voltage ($\mathbf{V}_{pq}$) both in magnitude and phase angle within controllability range of $0 \leq V_{pq} \leq V_{pq,max.}$ and $0^{\circ} \leq \gamma \leq 360^{\circ}$ respectively in accordance with the power frequency of the system via coupled series insertion transformer. The real and reactive power exchange between the series injected voltage ($\mathbf{V}_{pq}$) via insertion series transformer and converter 2 occur while the transmission line current (I_{ij}), from bus i to j, flows through this ac terminal voltage. The exchanged reactive power is either generated or absorbed electronically by converter 2 whereas the AC real power exchanged is converted to DC power by the converter itself and appears at the terminals of the capacitor as negative or positive power demand so as to enable it to communicate with converter 1.

Shunt Component of UPFC (converter 1):

This component is intended to supply or absorb the requested real power demand at the coupling capacitor terminal, then converts back to AC and further exchange this power with transmission line, either draw or inject to the connection point of the TL, via coupling shunt transformer. Moreover, this component is responsible to maintain the DC voltage level of the capacitor. Jointly, it is important to note that there is no reactive power exchange between converters so that the reactive power is only feasible on their side of the connection, shunt or series side, and the components are responsible independently for reactive power exchange as long as they are coupled with capacitor. Accordingly, the shunt component is capable of either absorb or supply reactive power independently to maintain the voltage magnitude at predefined value at the connected bus, bus i, as per the single line diagram depicted in Figure 2.6.

Coupling Capacitor:

The coupling capacitor is the linking element of both components and primarily used for energy storage and as communication medium of the stated components. In addition, it is a great role playing coupling element to inhibit the reactive power exchange between the components so that the reactive power management is to be handled independently at both sides. Contrastingly, the allowable power exchange between the two components via the capacitor link is real power alone.

The various power flow control concepts of the UPFC is described in Figure 2.7 (a)-(e) [24] et al.

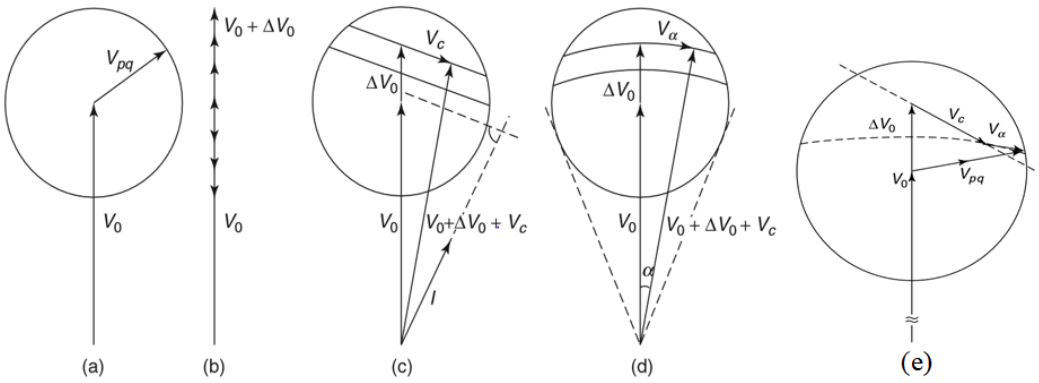

Figure 2.7. A phasor diagram illustrating various (a)-(d) and the general concept (e) of series-voltage injection and attainable power-flow control functions [24] et al.

(a) Series Voltage Injection

This is the concept of series voltage injection, V_{pq}, performed by series component of the UPFC where the voltage is controllable both in terms of magnitude and phase angle. Therefore, the resultant vector voltage, $V_0^{`}$, becomes the sum of the prior voltage, V_0, and injected voltage, V_{pq}, vectorially. Furtherly, V_{pq} is the series injected vector voltage which is the vector sum of the in-phase component, V_p, and quadrature component, V_q, with the line current and to be discussed in coming section in detail. Mathematically,

$$V_0^{`} = V_0 + V_{pq} \tag{2.11}$$

(b) Terminal Voltage Regulation

This is the concept where the terminal voltage can be achieved by in-phase series voltage injection with V_0. In this concept, the series injected voltage (V_{pq}) is equal to the change of voltage injected (ΔV_0), i.e., $V_{pq} = \Delta V_0 = V_0^{`} - V_0$. So,

$$V_0^{`} = V_0 + \Delta V_0 \tag{2.12}$$

(c) Terminal Voltage and Line Impedance Regulation

It is the combined concept of the terminal voltage in (b), and line impedance or series capacitor compensation (V_c) as shown in Figure 2.7 (c). Here, $V_{pq} = \Delta V_0 + V_c$ so,

$$V_0^{`} = V_0 + V_{pq} = V_0 + \Delta V_0 + V_c \quad (2.13)$$

(d) Terminal Voltage and Phase Angle Regulation

It is the combined concept of the terminal voltage regulation component in (b) and phase shifting voltage component (V_α) as shown in Figure 2.7 (d). The function of the V_α is to shift the regulated voltage $V_0 + \Delta V_0$ by an angle α. Here, the series injected voltage is given by $V_{pq} = \Delta V_0 + V_\alpha$ so,

$$V_0^{`} = V_0 + V_{pq} = V_0 + \Delta V_0 + V_\alpha \quad (2.14)$$

(e) Simultaneous Regulation

This is the complete combined concept of the terminal voltage, line impedance, and phase angle to perform appropriate series voltage injection via converter 2 of the UPFC. Here, the series injected voltage is given by $V_{pq} = \Delta V_0 + V_\alpha$. In this case, the function of the V_α is to shift the regulated voltage $V_0 + V_c + \Delta V_0$ by an angle α. Accordingly,

$$V_0^{`} = V_0 + V_{pq} = V_0 + \Delta V_0 + V_c + V_\alpha \quad (2.15)$$

2.4 Literature Review

Moges Alemu Tikuneh and Getachew Biru Worku (PhD) [1] presented a study entitled "Analysis of the Power Blackout in the Ethiopian Electric Power Grid" and assessed, identified and summarized the causes, reasons, mechanisms and extent of the past blackout of the 6th January 2016 blackout, in the EEP grid using DIgSILENT PowerFactory software. It has been investigated that the causes for the blackout incident are power plant generator tripping (outage), line tripping (outage), slow fault clearing time of protection devices. Moreover, it is presented that the sequence of events in the blackout typically, the analysis of the 6th January 2016 blackout, was linked to the slow breaker actions (not clearing the short circuit fault as fast as possible). Slow fault clearing time settings of the protective relays was explored and summarized as root cause for the blackout incident.

Mohammed Ahmed Woday, Gezahegn Shituneh et al [2] conducted the study on "Contingency Analysis of Ethiopia's 230 kV Transmission Network" at very limited scope. The paper's work was observing the effect of the 230 kV TL/s outage, identifying the most critical outage using Line

outage Distribution Factor (LODF), and mitigating the problem investigated using Distributed Flexible AC Transmission System (D-FACTS) devices using Power World Simulator.

Moges Alemu Tikuneh and Getachew Biru Worku (PhD) [3], described a framework for identifying the Ethiopian electric power system vulnerabilities, largely based on performance indices and supported by power flow and line outage analyses using active power performance index (PIp) and voltage performance index (PIv) in DIgSILENT PowerFactory software. This work has identified and ranked the most severe line outages based on performance indices and the network vulnerabilities are evaluated based on: Numbers of outages that lead to voltage limit violation of buses and element overload. Finally, it is summarized that the most network vulnerabilities with respect to bus voltage violations and element overloading are occurred on those buses and elements found at the high load centers.

Sunil Malival [17] studied Power System Security of Indian Utility 62 Bus System using a Maximum Loading Margin for ranking of the contingencies expected to cause steady state bus voltage and power flow violations. The paper demonstrated the effectiveness of the proposed approach on Indian Utility 62 bus power system using PSAT and stated that contingencies related to voltage violations and power line overloading have been responsible for power system collapse. Finally, it is summarized that contingency ranking and analysis is very important from the viewpoint of power system security.

Neelesh Sahu, Dr. K.T. Chaturvedi [11], conducted the study on contingency analysis & security of 6 bus power system network using 'Line flow performance index (PI_{lf})' and 'Reactive power performance index (PIrp)' for single transmission line outage with the help of Newton Raphson load flow analysis. The PI_{lf} and PIrp is calculated in MATLAB environment and contingency ranking is made independently then 'Overall performance index', the summation of two performance index, is determined in which one of the performance index determines line overloading and the other performance index determines bus voltage drop limit violation and named as Line flow performance index (PI_{lf}) and reactive power performance index (PIrp) respectively.

Mostafa Alinezhad and Mehrdad Ahmadi Kamarposhti [20], carried out the study on "Static Voltage Stability Assessment Considering the Power System Contingencies using Continuation Power Flow Method" using IEEE 14-Bus Test System with the help of PSAT toolbox in Matlab environment. The study stated that increasing utilization in power system leads the transmission lines and power plants often operate in stability boundary and system probably lose its stable condition by overloading or occurring disturbance. Moreover, the study explored the importance of prediction and recognition of voltage instability in power to make network security stronger. To generalize, the study focused on Mega Watt Margin (MWM) and maximum loading point indices in order to analyze the static voltage stability using continuation power flow (CPF) method by considering power system contingency based effects and results are presented.

Dr. Shobha Shanka et al [25], conducted the study on "Identification of Unified Power Flow Controller Location under Line Outage Contingencies" and it is presented that an approach for identifying optimal location of Unified Power Flow Controller under line outage contingencies using Fuzzy approach to combine the effect of voltage stability margin indicated by Minimum Singular Value of load flow Jacobian matrix (MSV) and voltage change to identify the optimal location. The study tested the proposed method on 24 bus 400 kV Southern grid of India with simulated condition and concluded that the voltage stability margin of the system is enhanced, and voltage profiles are improved with unified power flow controller deployed at optimal location.

CHAPTER 3

MODELLING AND SECURITY ASSESSMENT OF ETHIOPIAN HIGH VOLTAGE GRID

3.1 Introduction

It is obvious that security study of a grid requires contingency analysis technique. In other words, list of probable contingencies with high potential impact must be prepared at start. Then, the selected contingent elements must be ranked by using severity index and their potential risk must be evaluated as well.

To conduct this study, national grid system data collection is the primary task performed. The system data collected itself requires methods of compiling to prepare it in a such a way that it can be used in accordance with the study's requirement. The gathered data are furtherly used for grid model development, validation and carrying out overall case studies.

Besides numerical input data preparation, mathematical model development of the Ethiopian high voltage grid requires network reduction technique hence, only meshed network is interest of this study. Accordingly, the grid's element (TLs, shunts, loads, etc.,) are modeled mathematically as each of them are building components of a power system. The model under study has network elements of 106 buses, 146 transmission or sub-transmission lines, 51 transformers, 17 power plants, 23 lumped shunts and 69 merged loads.

Power flow studies and grid model validation based on simulation is performed by using Power System Analysis Toolbox (PSAT) in MATLAB. Power flow study is the pre-request to evaluate the grid performance both under NSSO and contingency condition. In other words, the power flow report obtained from the simulation of a grid must be well understood and interpreted as well. The validity of grid model developed is verified in terms of state variables under NSSO i.e., bus bar voltage magnitudes, transmission line thermal flow limits apparently, transformer capacity limits apparently, power generation limits and all loads being served is checked as well.

It is important to set the guideline/s to prioritize a transmission line (TL) or power plant (PP) to conduct outage case study as it is difficult to carry out all contingency studies for the case of large

grid. The grid model is simulated at scaled peak (scale factor=1.33) so that 30 top ranked MVA line flows of transmission lines (TLs) and 11 top ranked installed capacity of power plants (PPs) are selected for further outage case studies. In this study, different contingency ranking indices are used. Those are: Overall Composite Severity Index (OCSI) which is determined from Individual Severity Indices (ISI) i.e., Individual Composite Severity Index (ICSI), Real Power Performance Index (PPI) and Line Stability Index (LSI).

The grid model is simulated under 41 contingent elements and their criticalities are ranked by using OCSI which is determined from ISI i.e., ICSI, PPI and LSI. The contingent element with highest OCSI value is ranked at first implying that its outage impact on the grid is very high.

3.2 Data Collection and Compiling

The data consists of numerical data of transmission lines, bus bars, generators, transformers and shunt elements of the grid and recorded peak load demand collected from EEP's archive.

Data compilation is an important task for this work as it is the basis for the analysis of the system. The data is analyzed quantitatively and used for modeling the grid as well as to carry out further simulation studies.

1. Network Loads

All the radially connected sub-transmission or distribution substations are considered as loads being supplied from its respective buses or nodes of interconnected system (ICS). Series of all transmission or distribution substation loads being cascaded radially are summed up and considered as a single load being supplied from the corresponding nodes of the ICS.

In this thesis, load scale factor (sf) =1.33 is used to scale the peak load recorded and then, overall outage study of this work is conducted at this load as it is also used by the NLDC too, to perform generation dispatch scheduling and daily peak load forecasting. The stated load scale factor is reasonably used in order not to be pivoted at record of specific past load data as energy demand varies from time to time. It is also intended to account for omitted radial transmission or sub-transmission line losses and aimed to conduct the study at widened margin demand.

2. Transmission Lines

In this study, part of transmission or sub-transmission lines of the national grid are considered to come up with interconnected system (ICS). In other words, the radial transmission or sub-transmission lines are omitted, and their loss contribution is considered within network equivalent load.

3. Transformers

Both two- and three-winding transformers exist in the national power system grid. Although most of the transmission substations have two winding and less dominantly three winding transformers but three winding transformers are treated as equivalent two winding transformers in this study. In both cases, the resistance of windings is neglected and obviously the capacitive reactance is negligible in transformer operation as compared to the magnetizing reactance of the machine.

4. Generation Units

The generation units of each plant data are summed up and the plant installed capacity is represented with a single unit hence, analysis tool used requires doing so. In order not to ignore generation from wind farms, maximally 30% of the installed capacity is assumed to be generated and included in the network model.

3.3 Modelling of Ethiopian High Voltage Grid

In order to conduct the study, valid model development is important task. Accordingly, all the methods used for model developing and validating are under discussed. The methods consist of national grid reduction and Ethiopian HV grid model development.

3.3.1 Grid Model Reduction

As it is obviously known, the whole Ethiopia's network is too large (see the single line diagram in Appendix-A). However, most of the network parts are radially connected and substations can be considered as load being supplied from the HV grid and merged with careful calculation and tracing of single line diagrams. Finally, it is possible to arrive at grid with its respective merged loads.

1. Merging Load

All the radially connected sub-transmission or distribution substations are considered as loads being supplied from its respective nodes. The recorded peak load data of radially connected and cascaded distribution substations are summed up in which furtherly considered as a single and network equivalent load being supplied from the respective node of grid.

2. Generation Units

The generation units of each power plant data are summed up and a power plant installed capacity is represented with a single unit hence, analysis tool used requires doing so. Generator connected buses are not taken into part of the network reduction in order to keep network accuracy.

3. Busbars

Importantly, it is necessary to note that single busbar configuration is considered in this study though different bus bar configurations are existing due to the consideration that the action does not affect the study from the stated scope perspective.

4. Shunt Reactors

Shunt reactors of the transmission lines are lumped at their respective buses of reduced grid model. Moreover, both fixed and switched shunts are modeled as constant loads though almost all shunts are fixed type.

By combining all the methods discussed above, the national grid is reduced to interested one as depicted in Figure 3.1.

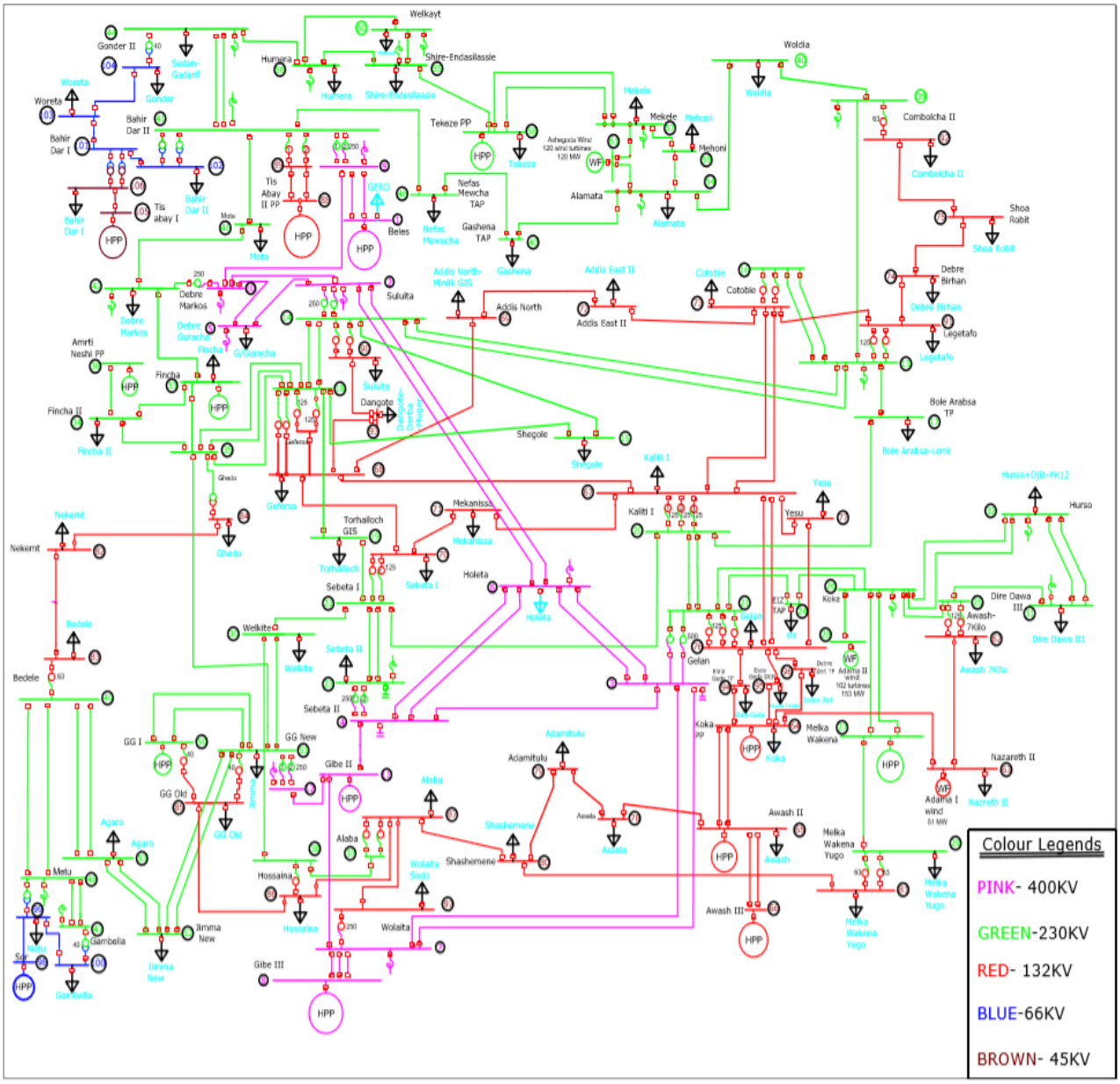

Figure 3.1. Reduced grid model of national grid

3.3.2 Ethiopian High Voltage Grid Modelling

It is obvious that any practical power system consists of generation, transmission, and distribution system when looked from the perspective of operations performed. The elements of a power system are generation units, transformers, transmission lines, shunts and loads.

In this thesis, actual system data collected are used to model, validate and study the system by incorporating the compiled data within the stated analysis software. The basic and foremost task performed is the modeling each power system component before going ahead to the grid modeling as each of the components is the building elements of the grid system.

Load Modeling:

However, there are different types of load modeling methodologies; constant load modeling scheme is followed in this study as specified quantity of real and reactive power at a specific bus. It is necessary to note that constant load is kept constant as long as the voltages at respective load buses are within prescribed limits, otherwise it is converted into constant impedance and given by [26],

$$P_L = {PV^2}\Big/{V_{lim}^2} \tag{3.1}$$

$$Q_L = {QV^2}\Big/{V_{lim}^2} \tag{3.2}$$

where, V_{lim} is $V_{min.}$ or $V_{max.}$ depending on the case.

For the specific bus i, the complex load demand is given by,

$$S_d^i = P_d^i + jQ_d^i \tag{3.3}$$

This complex load demand equation denotes the $n_b \times 1$ vector of complex loads at all buses in MW and MVAr respectively or pu equivalents; where, n_b is the number of the buses in a power system. Here it is important to note that all the pu values are defined with respect to base MVA of each bus at which the load is connected.

Generally, summing and merging the radially connected loads at sub-transmission or distribution substations to the respective interconnected buses can be governed by the equation,

$$Total\ power\ demand\ at\ intersted\ bus = \sum_{i=1}^{n} S_{di} + \sum_{i=1}^{j,\ i\neq j, i\rightarrow j} S\,{}_i^j - line\ loss \tag{3.4}$$

where,

S_{di}– the complex power demand at specific radial bus

$S_i^j - line\ loss$- is the complex power loss over radial line from bus i to j noting i≠j and if i to j, then j to i does not hold true

i – specific radial bus number, i=1,2,3…, n

n – total number of the radial buses at which the power demands is to be summed and merged to its respective interconnected bus

In this study, the loss over radial lines is neglected so that the cumulative load data of all radially connected sub-transmission or distribution substations at each of the respective buses is given by,

$$Total\ power\ demand\ at\ bus\ i = \sum_{i=1}^{n} S_{di} \tag{3.5}$$

Moreover, it is important to note that the apparent power demand at specific bus i is given by,

$$S_{di} = \sqrt{P_{di}^2 + Q_{di}^2} \tag{3.6}$$

Cumulative load data at respective interconnected bus of the grid model is tabulated in Appendix B.

Transmission Line Modeling:

In this study, all transmission lines are modeled using π-transmission line model with series impedance given by $Z_s = R_s + jX_s$ and total lumped charging susceptance b_c which is used for formulating the network admittance matrix, Y. Generally, the complex power flow through the specific transmission line between bus i and j is governed by the equation,

$$S_{i-j}^{fl} = P_{i-j}^{fl} + jQ_{i-j}^{fl} \tag{3.7}$$

For better understanding, let us consider the assumed power flow from bus i (sender end) to Bus j (receiver end) in Figure 3.2.

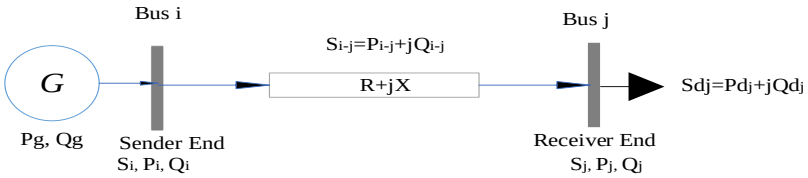

Figure 3.2. Two power flow representation from bus i to j

For this case, the complex power flow equation is given by as equation 3.7,

$$S_{i-j}^{fl} = P_{i-j}^{fl} + jQ_{i-j}^{fl}$$

Thermal limit of the apparent power flow through the specific transmission line between bus i and j depends on permissible thermal current ($I_{thermal}$) and can be calculated using equation,

$$S_{limit} = \sqrt{3} * V_{LL-Nominal} * I_{thermal} \quad (3.8)$$

The per unit expression of overall transmission line input data compiled, prepared and used for this study are defined on the basis of their respective ratings of voltages and MVAs in order to match the input data requirement analysis tool, PSAT software, used. Accordingly, the overall transmission line input data tabulated in Appendix C.

Transformer Modeling:

There are two types of transformers incorporated in the grid. Those are two- and three-winding transformers. It is important to note in this study that all transformers are modeled with resistance neglection, fixed transformer tap ratio and with fixed phase shift. In other words, voltage and phase angle control capability of the transformers is set to be fixed so that automatic controls and regulations cannot be performed with the help of incorporated transformers in the grid.

Two-winding transformers are modeled as series reactance neglecting iron and winding losses. The input data of overall two winding transformers used in this study are as tabulated in Appendix E.

In PSAT [26], three-winding transformers are internally modeled as two two-winding transformers and one transmission line in a Y connection, as depicted in Figure 3.3. PSAT processes three-winding transformer data before running the power flow for the first time and adds one bus in the 'Bus structure' and three new lines in the 'Line structure'.

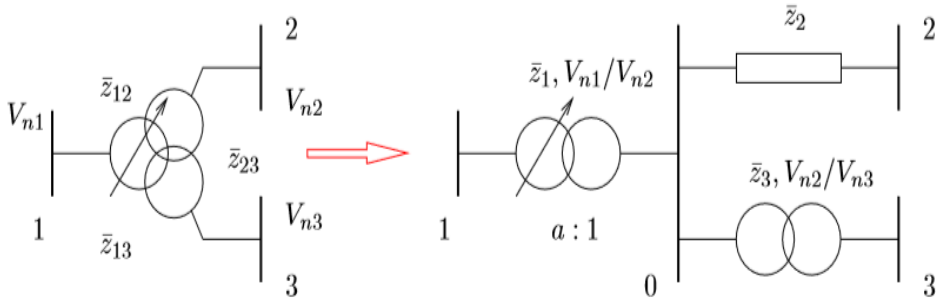

Figure 3.3. Three-winding transformer equivalent circuit [26]

The data format of three-winding transformer allows setting impedances of the triangle branches, whose relationships with the resulting star impedances are as follows.

$$\left.\begin{aligned} \widetilde{z_{12}} &= \widetilde{z_1} + \widetilde{z_2} \\ \widetilde{z_{13}} &= \widetilde{z_1} + \widetilde{z_3} \\ \widetilde{z_{23}} &= \widetilde{z_2} + \widetilde{z_3} \end{aligned}\right\} \tag{3.9}$$

Where,

$$\left.\begin{aligned} \widetilde{z_1} &= (\widetilde{z_{12}} + \widetilde{z_{13}} - \widetilde{z_{23}})/2 \\ \widetilde{z_2} &= (\widetilde{z_{12}} + \widetilde{z_{23}} - \widetilde{z_{13}})/2 \\ \widetilde{z_3} &= (\widetilde{z_{13}} + \widetilde{z_{23}} - \widetilde{z_{12}})/2 \end{aligned}\right\} \tag{3.10}$$

$\widetilde{z_{12}}$- The impedance obtained by shorting winding 2 and supplying winding 1 with voltage till the rated current flows through shorted winding 2 while winding 3 left open. In simple term it is a test data and the same way for $\widetilde{z_{13}}$ and $\widetilde{z_{23}}$.

$\widetilde{z_1}$, $\widetilde{z_2}$ and $\widetilde{z_3}$- Equivalent three winding transformer leakage impedances

In this study, three winding transformers are treated as equivalent two winding transformers as explained above in which the tertiary winding part is omitted. This consideration is due to reason that it is considered as star connected transmission line by PSAT simulation package so that only the impedance from primary to secondary ($X_{1\text{-}2}$) is used and the input data formulation is as tabulated in Appendix G.

Shunt Reactors (Capacitors) Modeling:

A shunt connected capacitor or reactor at bus can be modeled as a fixed or switched impedance to ground. The admittance of shunt element connected at specific bus i can be governed by the equation,

$$y_{sh}^{i} = g_{sh}^{i} + jb_{sh}^{i} \tag{3.11}$$

$Y_{sh} = G_{sh} + jB_{sh}$ denotes the $n_b \times 1$ vector of complex shunts at all buses where, n_b is the number of the buses in a power system.

where,

y^{i}_{sh} - shunt admittance of bus i

g^{i}_{sh} - shunt conductance of bus i

b^{i}_{sh} - shunt susceptance of bus i

n_b - number of the buses in a power system

The power injection at buses due to shunt impedances is given by [26]

$$P = gV^2 \tag{3.12}$$

$$Q = bV^2$$

Where, V is the bus voltage and susceptance b is negative for inductive charges but positive for capacitive ones.

Under this study, fixed or switched shunt reactors and capacitors are modeled as a constant impedance load. Here it is important to note that all the pu values of shunts are defined with respect to base MVA of each shunt element connected. The installed capacity of reactors includes the reactors of the transmission line if any which is merged and lumped to its respective buses. The input data are tabulated in Appendix H.

Bus Modeling:

The network topology is defined by “bus” components, in which the basic input data is defined by bus number and its base voltage. In other words, bus numbers, which can be in any order, and

voltage ratings, V_b, are mandatory. Moreover, the area and region number of the buses can be set but it is optional.

In PSAT, [26] Voltage magnitudes V_0 and phases θ_0 can be optionally set if the power flow solution is known or if a custom initial guess is needed. If voltages are not specified, a flat start is used (V = 1 at all buses except for the PV and slack generator buses, and θ = 0).

In this study, double bus bar configurations are considered as single busbar system and actual data collected from the NLDC is used and set as initial guess data, Voltage (pu) and Angle (rad), for starting power flow solution. In addition, the busbar data includes the permissible limits of voltage (pu) under both normal and emergency operation states as defined by the NLDC though this may not hold true in practical operation of the national grid as it is observed from the data collected from the dispatch center. Overall input data of the buses used throughout this study are tabulated in Appendix D.

Power Generation Modeling:

A generator can be considered as complex power injecting element at a specific bus of power system network. Let us consider the simple radial network given in Figure 3.4.

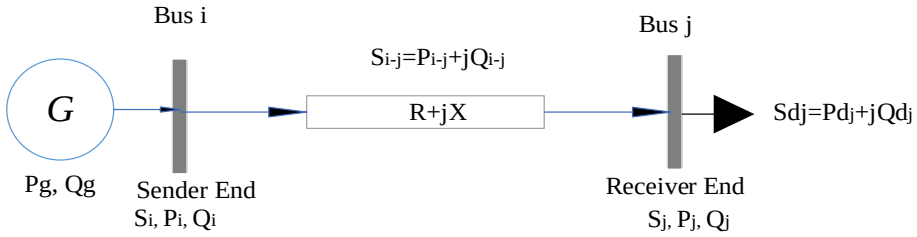

Figure 3.4. Two bus radial power system network

From the simple two bus radial network in Figure 3.9, the complex power injected at bus i by generator 'G' is given by,

$$S_g^i = P_g^i + jQ_g^i \tag{3.13}$$

This complex power injection denotes the $n_b \times 1$ vector of complex power injected at all buses in MW and MVAr respectively or pu equivalents; where, n_b is the number of the buses in a power

system. In this study, the cumulative power injection capacity of each plants is considered as a single generator as tabulated in Appendix E.

$$Total\ Power\ Injection\ at\ bus\ i = \sum_{i=1}^{n} Inj\ U_i \tag{3.14}$$

Where, U is generation unit.

In power system network, under mentioned constraints must be satisfied in normal operating condition.

$$\begin{aligned} P_g^{NS} &= P_d^{NS} + P_{loss}^{NS} \\ P_g^i &= P_{g\_sch}^i + P_{g\_loss}^{i\_LPF} \\ Q_{min}^i &\le Q_g^i \le Q_{max}^i \end{aligned} \tag{3.15}$$

where,

P_g^{NS}- the total real power generation in Network System (NS)

P_d^{NS}- the total real power demand in Network System (NS)

P_{loss}^{NS}- the total real power loss in Network System (NS)

P_g^i- real power generation by unit i

$P_{g\_sch}^i$- the scheduled real power generation by unit i

$P_{g\_loss}^{i\_LPF}$- real power generation by unit i for loss compensation as per the provided loss participation factor (LPF)

$Q_{min}^i\ and\ Q_{max}^i$ – permissible lower and upper generation limits of unit i

3.4 Power Flow Studies and Model Validation

The analysis tools used are Power System Analysis Toolbox (PSAT), Matlab toolbox to design the network as well as to input the data user friendly, and Excel Microsoft office for accessing and handling the power flow report data. PSAT is open source Matlab toolbox for electric power system analysis and control, and it has Simulink based library which provides a user-friendly tool for network design.

The base case network model was developed with the help of Power System Analysis Toolbox (PSAT), Matlab toolbox, using the latest peak load demand data accessed from EEP's record.

3.4.1 Power Flow Studies

Power flow study is the pre-request to evaluate the grid performance both under NSSO and contingency condition. In other words, the power flow report obtained from the simulation of a grid must be well understood and interpreted as well. This in turn requires background knowledge on the concept of power flow. To recap the power flow concepts, power flow and admittance matrix problem formulations are discussed below.

3.4.1.1 Power Flow Problem Formulation

Let us consider a transmission line of two bus system in Figure 3.5 to recapture the power flow problem formulation.

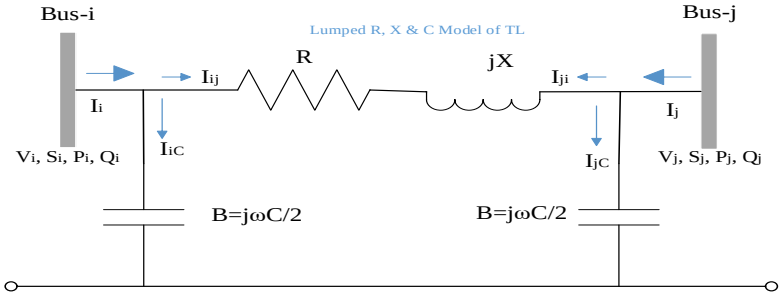

Figure 3.5. Circuit schematic of two bus radial power system network

$$jB_i = {}^{jwc_i}/_{2} \tag{3.16}$$

$$Z = R + jX, \text{ then} \quad Y = {}^{1}/_{Z} = G - jB \tag{3.17}$$

$$Y = \frac{1}{R+jX} = \frac{R-jX}{R^2+X^2} = \frac{R}{R^2+X^2} - j\frac{X}{R^2+X^2}$$

Then by equating equations above,

$$G - jB = \frac{R}{R^2+X^2} - j\frac{X}{R^2+X^2}$$

$$G_{ij} = {}^{R}/_{(R^2+X^2)} \tag{3.18}$$

$$-jB_{ij} = {-jX}\Big/{(R^2 + X^2)}$$

where, R+jX- series impedance, C- capacitance, G- conductance, B-susceptance and Y-admittance of the line running from bus i to j.

In order to formulate the general power flow equation of the given power system, Figure 3.5 is re-used for the simplicity of understanding and the derivation is as follows.

$$S_{ij} = V_i I_i^* = P_{ij} + jQ_{ij} \text{ and } I_i = I_{iC} + I_{ij} = V_i \frac{j\omega C}{2} + \frac{V_i - V_j}{R + jX} \tag{3.19}$$

$$S_{ij} = V_i \, Conj.\left\{V_i \frac{j\omega C}{2} + \frac{V_i - V_j}{R + jX}\right\}$$

$$S_{ij} = V_i \, Conj.\left\{V_i \frac{j\omega C}{2} + \frac{(R - jX)(V_i - V_j)}{R^2 + X^2}\right\}$$

$$S_{ij} = Conj.\left\{V_i^*.V_i \frac{j\omega C}{2} + \frac{(R - jX)(V_i^*.V_j - V_i^*.V_j)}{R^2 + X^2}\right\}$$

$$S_{ij} = V_i.V_i^* \frac{-j\omega C}{2} + \frac{(R + jX)(V_i.V_j^* - V_i.V_j^*)}{R^2 + X^2}$$

Let $V_i = |V_i| < \theta_i$, $V_j = |V_j| < \theta_j$ and $\theta_{ij} = \theta_i - \theta_j$, then

$$S_{ij} = V_i.V_i^* \frac{-j\omega C}{2} + \frac{(R + jX)(|V_i| < \theta_i.|V_j| < -\theta_j \quad - |V_i| < \theta_i.|V_j| < -\theta_j)}{R^2 + X^2}$$

After completing and re-arranging the general complex power flow equation above the result below is obtained.

$$S_{ij} = \{G_{ij}[V_i^2 - V_iV_j \cos\theta_{ij}] + B_{ij}V_iV_j \sin\theta_{ij}\} + j\{-B_iV_i^2 - G_{ij}V_iV_j \sin\theta_{ij} + B_{ij}[V_i^2 - V_iV_j \cos\theta_{ij}]\}$$

By equating the above equation with $S_{ij} = P_{ij} + jQ_{ij}$, then

$$P_{ij} = G_{ij}[V_i^2 - V_iV_j \cos\theta_{ij}] + B_{ij}V_iV_j \sin\theta_{ij} \tag{3.20}$$

$$Q_{ij} = -B_iV_i^2 - G_{ij}V_iV_j \sin\theta_{ij} + B_{ij}[V_i^2 - V_iV_j \cos\theta_{ij}] \tag{3.21}$$

To summarize, the general power flow equations formulated above holds true for the transmission line power flow between two buses of general n-bus power system network noting that i ≠ j.

3.4.1.2 Admittance Matrix Formulation

Admittance matrix problem can be formulated and understood easily by using the simple radial network in Figure 3.6 and the derivation is as under discussed.

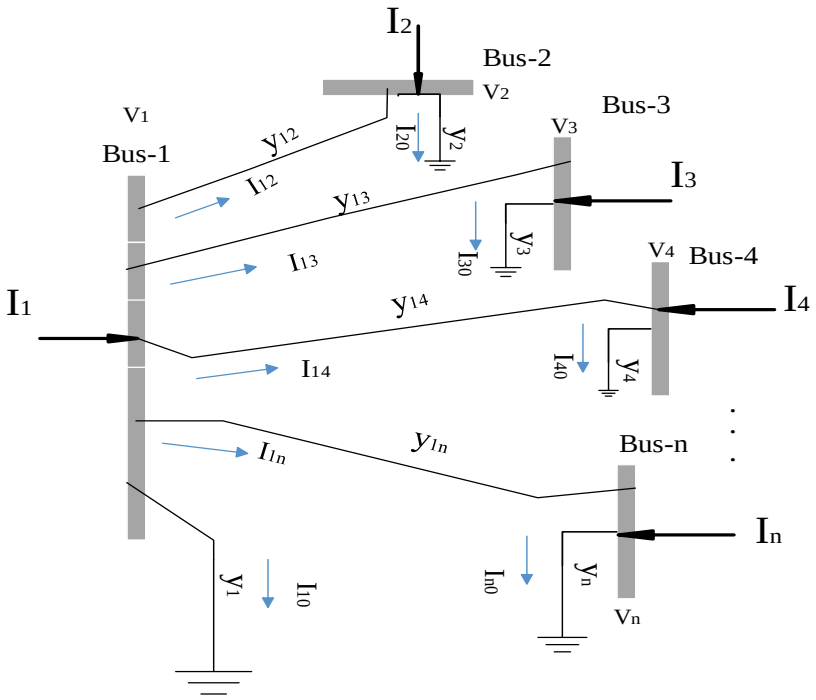

Figure 3.6. Net power injection of n-bus power system

The net injected power of any bus can be evaluated using Kirchhoff's Current Law (KCL), i.e.

$$\mathbf{I_1} = I_{10} + I_{12} + I_{13} + I_{14} + \cdots + I_{1n}$$

Similarly, net power injection at any individual buses can be written using KCL as below.

$$\mathbf{I_2} = I_{20} + I_{21} + I_{23} + I_{24} + \cdots + I_{2n}$$

$$\mathbf{I_3} = I_{30} + I_{31} + I_{32} + I_{34} + \cdots + I_{3n}$$

$$\mathbf{I_4} = I_{40} + I_{41} + I_{42} + I_{43} + \cdots + I_{4n}$$

$$\mathbf{I_n} = I_{n0} + I_{n1} + I_{n2} + I_{n3} + \cdots + I_{2n} \quad (3.22)$$

The net injected power of any bus can be further expanded and evaluated using KCL equations as explained but below, only the net power injected at bus 1 is used for further derivation and intended to observe easily how the arrangements of admittance of power system looks like.

$$\mathbf{I_1} = V_1 y_1 + y_{12}(V_1 - V_2) + y_{13}(V_1 - V_3) + y_{14}(V_1 - V_4) + \cdots + y_{1n}(V_1 - V_n)$$

Rearranging the terms of equation above, we can obtain the net current injected at bus becomes.

$$\mathbf{I_1} = V_1(y_1 + y_{12} + y_{13} + y_{14} + \cdots + y_{1n}) - V_2 y_{12} - V_3 y_{13} - V_4 y_{14} - V_n y_{1n}$$

$$\boldsymbol{I_1 = Y_1 V_1}$$

Where and in this case, it is observed clearly that

$$\boldsymbol{Y_1} = [y_1 + y_{12} + y_{13} + y_{14} \quad -y_{12} \quad -y_{13} \quad -y_{14} \quad . \quad . \quad -y_{1n}]$$

From the above, it can be noticed that the arrangement of the admittance matrix looks like as in equation (3.23) for n-bus system considered.

$$\boldsymbol{Y} = \begin{bmatrix} y_1 + y_{12} + y_{13} + y_{14} & -y_{12} & -y_{13} & -y_{14} & . \; . & -y_{1n} \\ -y_{21} & y_2 + y_{21} + y_{23} + y_{24} & -y_{23} & -y_{24} & . \; . & -y_{2n} \\ -y_{31} & -y_{32} & y_3 + y_{31} + y_{32} + y_{34} & -y_{34} & . \; . & -y_{3n} \\ -y_{41} & -y_{42} & -y_{43} & y_4 + y_{41} + y_{42} + y_{43} & . \; . & -y_{4n} \\ . & . & . & . & . \; . & . \\ . & . & . & . & . \; . & . \\ -y_{n1} & -y_{n2} & -y_{n3} & -y_{n4} & . \; . & y_{nn} \end{bmatrix} \tag{3.23}$$

When further re-defined, the admittance matrix of the n-bus power system network becomes,

$$\boldsymbol{Y} = \begin{bmatrix} Y_{11} & Y_{12} & Y_{13} & Y_{14} & . \; . & Y_{1n} \\ Y_{21} & Y_{22} & Y_{23} & Y_{24} & . \; . & Y_{2n} \\ Y_{31} & Y_{32} & Y_{33} & Y_{34} & . \; . & Y_{3n} \\ Y_{41} & Y_{42} & Y_{43} & Y_{44} & . \; . & Y_{4n} \\ . & . & . & . & . \; . & . \\ . & . & . & . & . \; . & . \\ Y_{n1} & Y_{n2} & Y_{n3} & Y_{n4} & . \; . & Y_{nn} \end{bmatrix} \tag{3.24}$$

To generalize,

$$\boldsymbol{I = YV} \tag{3.25}$$

where, $\mathbf{I} = \begin{bmatrix} I_1 \\ I_2 \\ : \\ I_n \end{bmatrix}$ and , $\mathbf{V} = \begin{bmatrix} V_1 \\ V_2 \\ : \\ V_n \end{bmatrix}$ are vector matrices.

3.4.1.3 Bus Net Power Injected Formulation

Admittance matrix problem formulated earlier is used for derivation of general bus net power injection equations. So, let us consider a radial power system network in Figure 3.7.

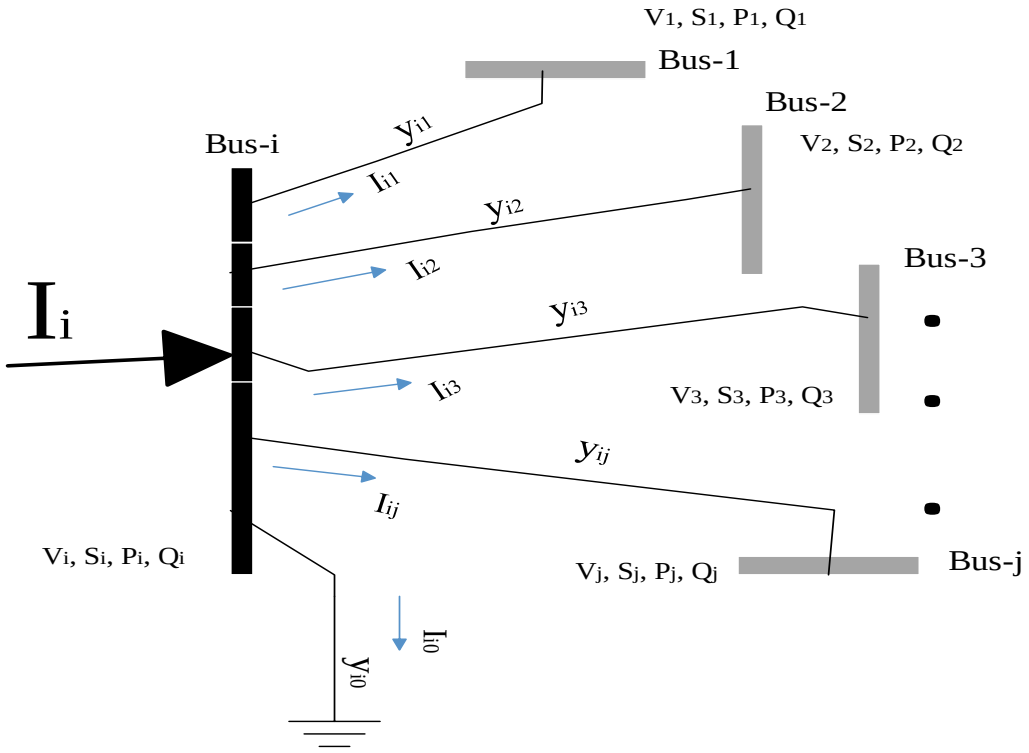

Figure 3.7. Net power injection at Bus-i of radial n-bus power system

It is discussed that the net injected current of any bus, in this case bus i, can be evaluated using Kirchhoff's Current Law (KCL), i.e.

$$I_i = I_{i0} + I_{i1} + I_{i2} + I_{i3} + \cdots + I_{ij}$$

$$I_i = V_i y_{i0} + y_{i1}(V_i - V_1) + y_{i2}(V_i - V_2) + y_{i3}(V_i - V_3) + \cdots + y_{ij}(V_i - V_j)$$

Rearranging the terms of equation above, we can obtain the net current injected at bus i as shown below.

$$I_i = V_i(y_{i0} + y_{i1} + y_{i2} + y_{i3} + \cdots + y_{ij}) - V_1 y_{i1} - V_2 y_{i2} - V_3 y_{i3} - V_j y_{ij}$$

This can be rewritten as,

$$I_i = V_i \sum_{j=0, j\neq i} y_{ij} - \sum_{j=1, j\neq i} y_{ij} V_j = V_i Y_{ii} + \sum_{j=1, j\neq i} Y_{ij} V_j \tag{3.26}$$

The complex Power at any bus i is given by,

$$S_i = V_i I_i^* = P_i + jQ_i \tag{3.27}$$

or by conjugating the above equation both sides,

$$S_i^* = V_i^* I_i = P_i - jQ_i$$

$$S_i^* = V_i^* \left[V_i Y_{ii} + \sum_{j=1, j\neq i} Y_{ij} V_j \right] = P_i - jQ_i$$

Let $V_i = |V_i| < \theta_i$, $V_j = |V_j| < \theta_j$, $Y_{ij} = |Y_{ij}| < \delta_{ij}$,and $Y_{ii} = |Y_{ii}| < \delta_{ii}$, then by equating the part of the equation, which is under summation above, it becomes

$$P_i = \sum_{j=1}^{n} |V_i||V_j||Y_{ij}|\cos(\delta_{ij} - \theta_i + \theta_j) \tag{3.28}$$

$$Q_i = -\sum_{j=1}^{n} |V_i||V_j||Y_{ij}|\sin(\delta_{ij} - \theta_i + \theta_j) \tag{3.29}$$

By solving and completing the equations above, the general equations below can be obtained.

$$P_i = V_i^2 G_{ii} + |V_i| \sum_{j=1, j\neq i}^{n} |V_j| \left[G_{ij} \cos(\theta_i - \theta_j) + B_{ij} \sin(\theta_i - \theta_j) \right] \tag{3.30}$$

$$Q_i = -V_i^2 B_{ii} + |V_i| \sum_{j=1, j\neq i}^{n} |V_j| \left[G_{ij} \sin(\theta_i - \theta_j) - B_{ij} \cos(\theta_i - \theta_j) \right] \tag{3.31}$$

These equations are called general power equations of the power injected at specific bus i of n-bus power system.

3.4.2 Model Validation

In this study, PSAT version 2.1.10 is incorporated with Matlab R2016a to model the grid with the help of PSAT Simulink library, GUI, and execute the overall case simulations as per the requirement.

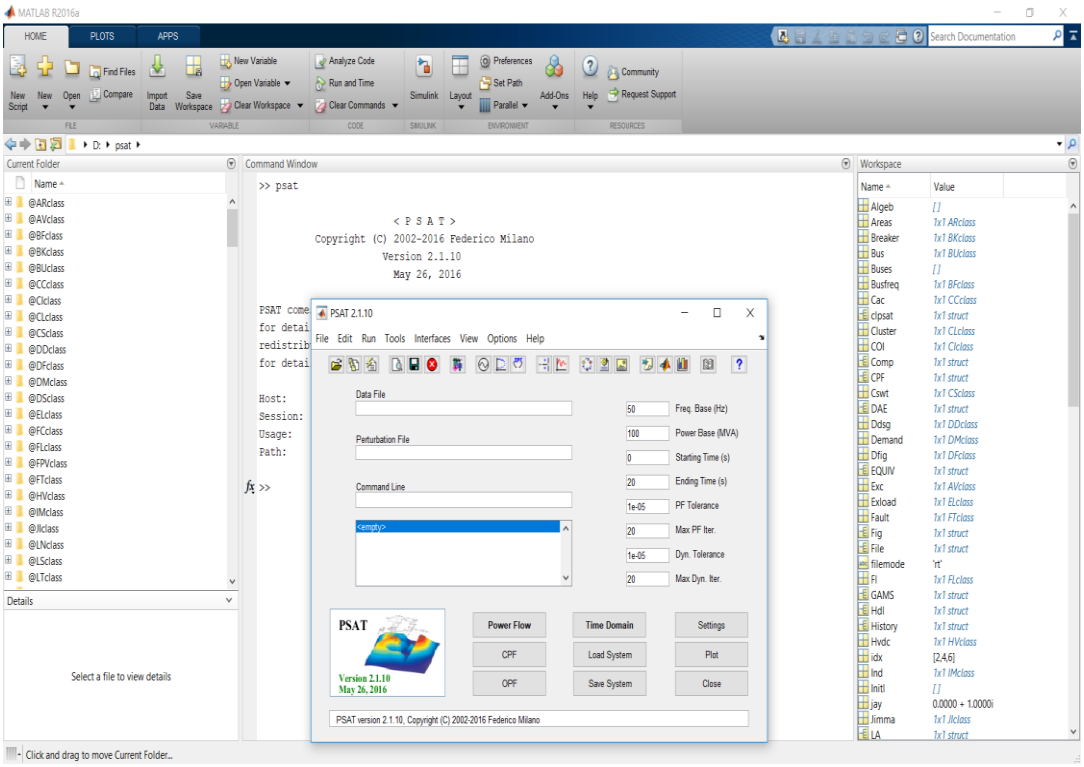

Figure 3.8. Screenshot of launching the PSAT in Graphical User Interface (GUI) mode

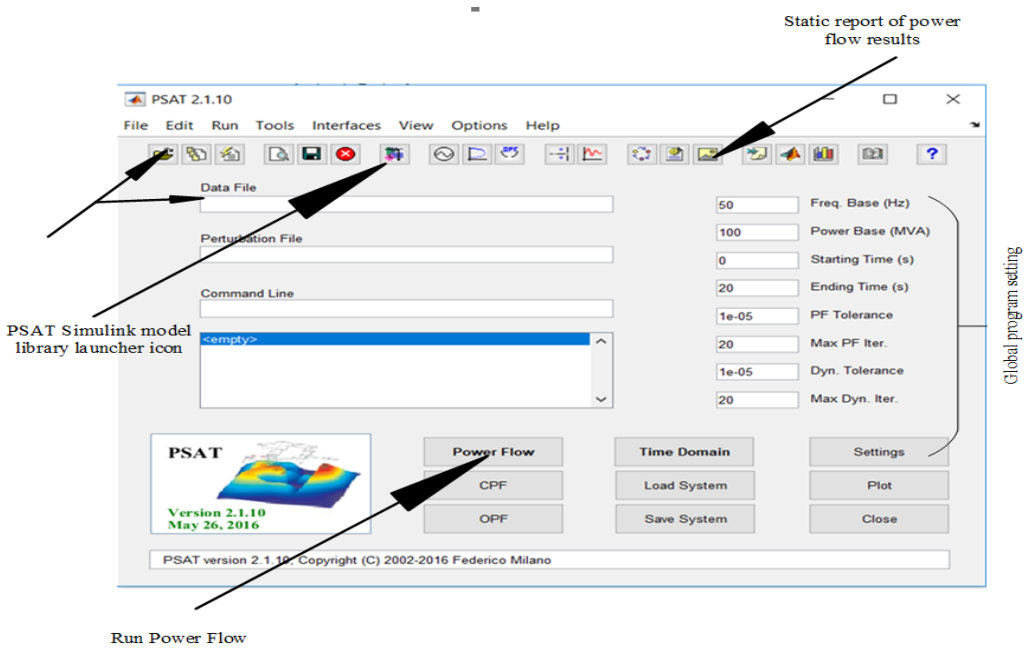

Figure 3.9. Different options and settings of PSAT main page after launched

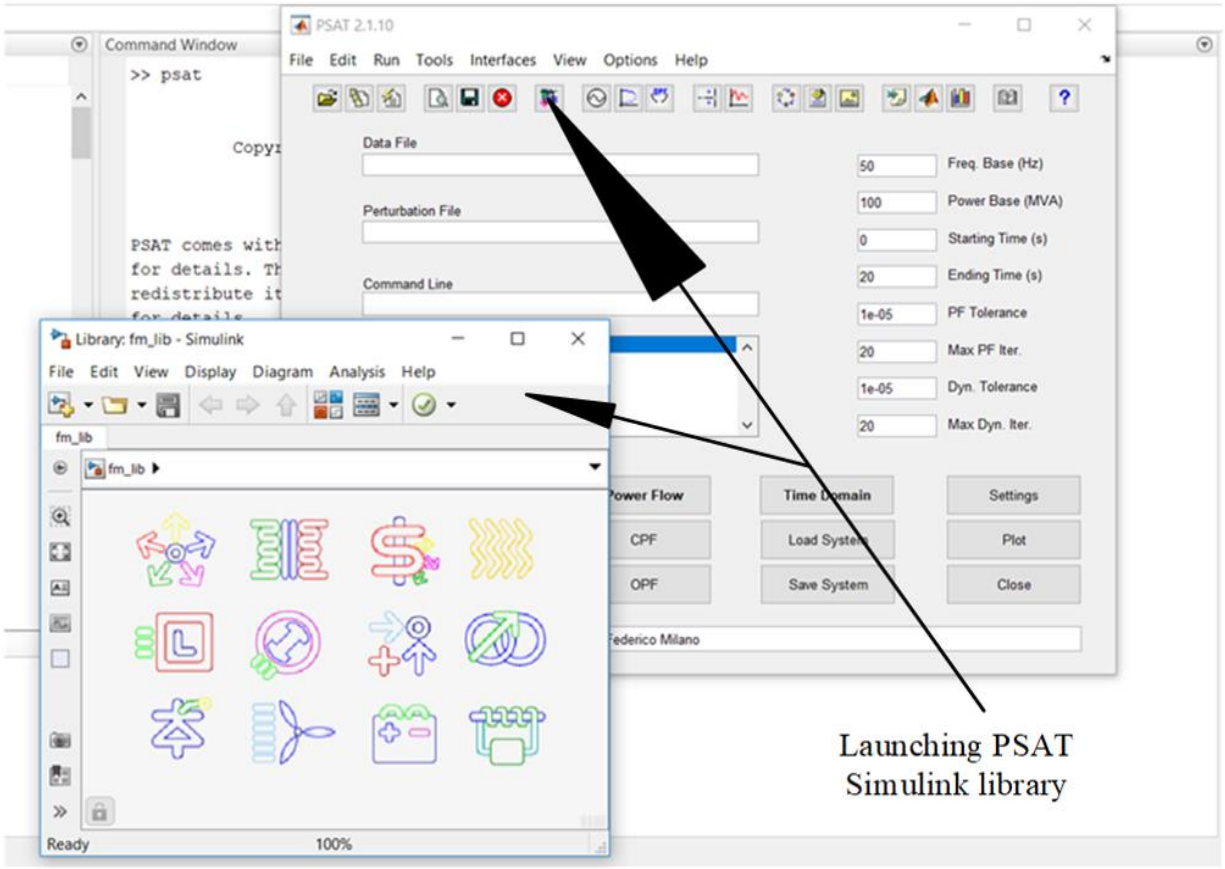

Figure 3.10. Screenshot of launching the PSAT Simulink library

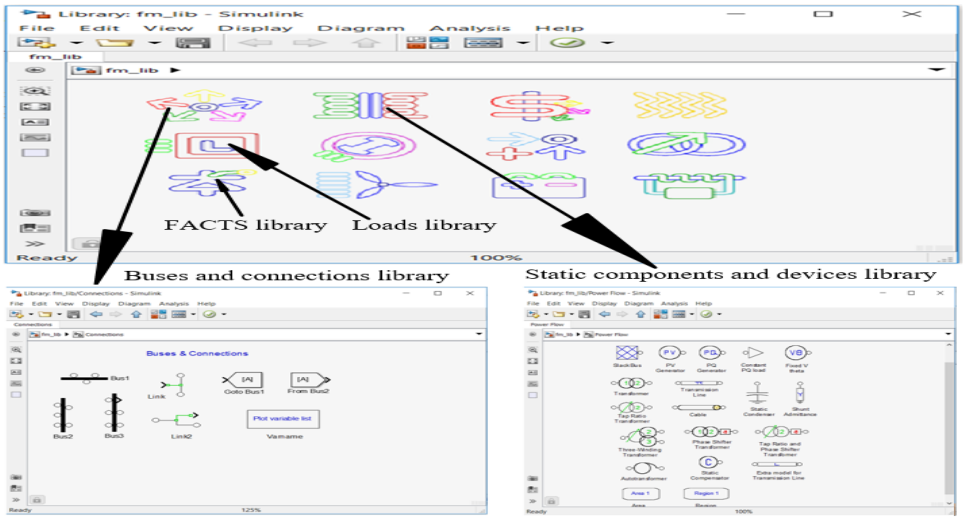

Figure 3.11. Different internal sub-libraries and blocks of Simulink library in PSAT

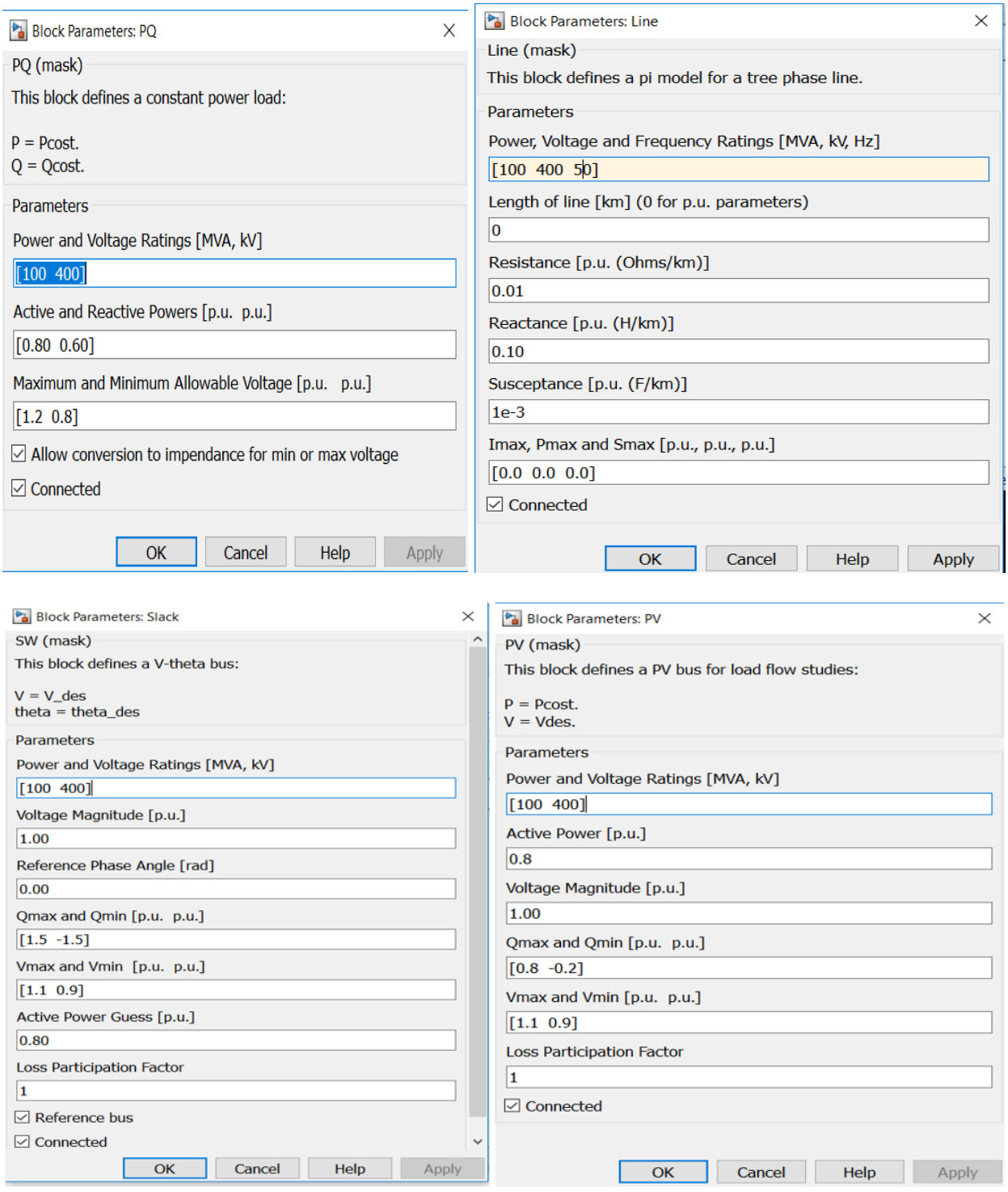

Figure 3.12.Sample of block parameter setting pages

Final reduced grid model has network elements of 106 buses, 146 transmission or sub-transmission lines, 51 transformers, 17 power plants, 23 lumped shunts and 69 loads. This network is modeled in PSAT Simulink library and then the model is tested, validated and pivoted quantitatively using existing system allowable operating limits , bus voltage and MVA loading capacity[2] of transmission lines (TLs), under steady state operation.

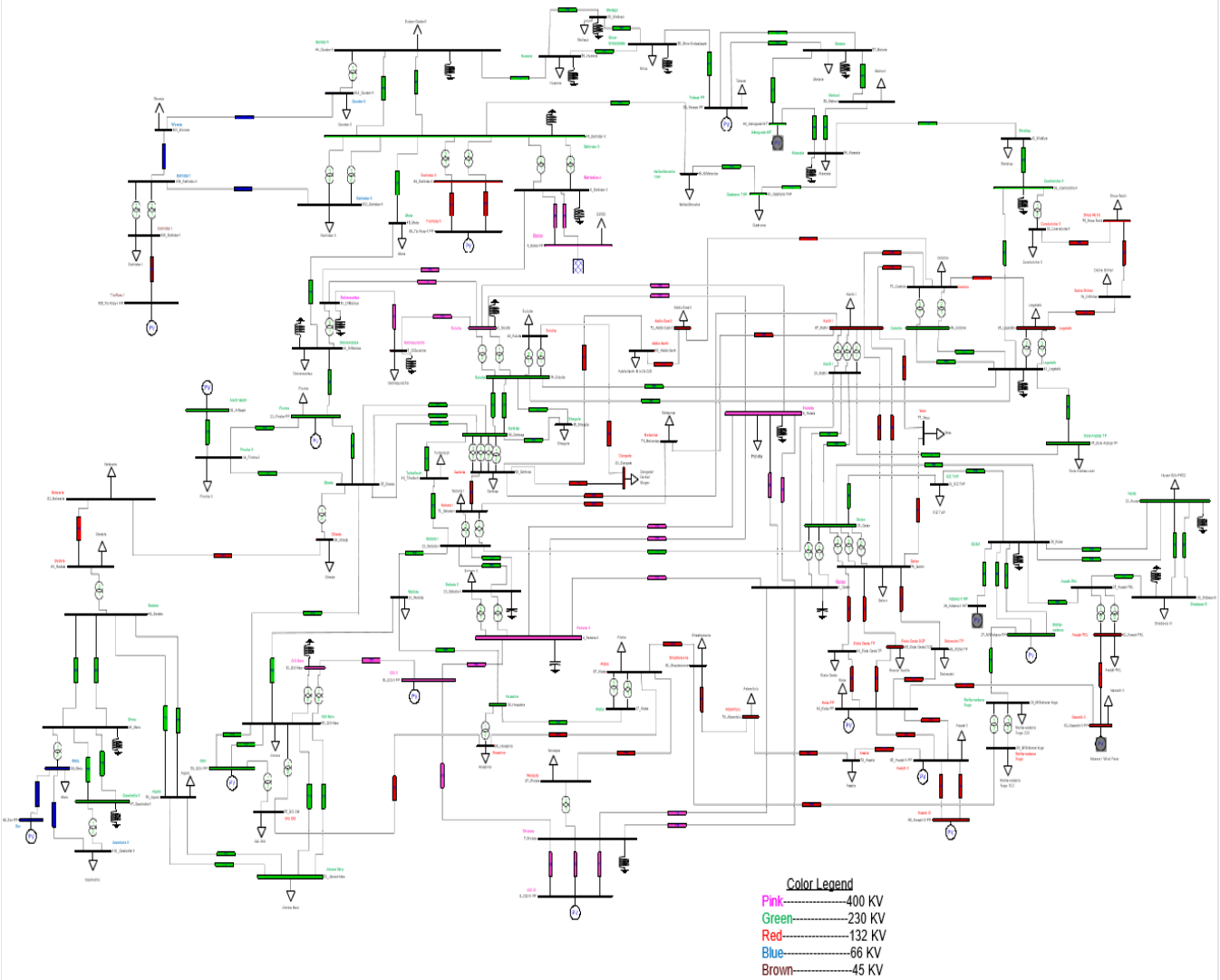

Figure 3.13. Grid model of national power system

[2] *It is important to note that the transmission line (TL) loading capacity, here and in this study, refers to the rated thermal limit of the MVA line flow in pu. Throughout this study, rated thermal MVA limit and calculated MVA line flows in pu are used.*

To assure the grid model validity, it is simulated using Newton Raphson power solver at normal steady state operation so that transmission line MVA flows, bus voltages, power generations and transformer MVA flows are intended to be within the prescribed limits of operation. To do so, the base case simulation is conducted at peak load record of EEP, and the stated constraints are compared quantitatively by using tables in Appendix I and bar graph chart Figures 3.14-3.18.

It is important to note that all the per unit values of the grid model are defined using global apparent power base (S_{base}) of 100 MVA. This value may result in pu values of greater than 1 based on the magnitude of actual value converted.

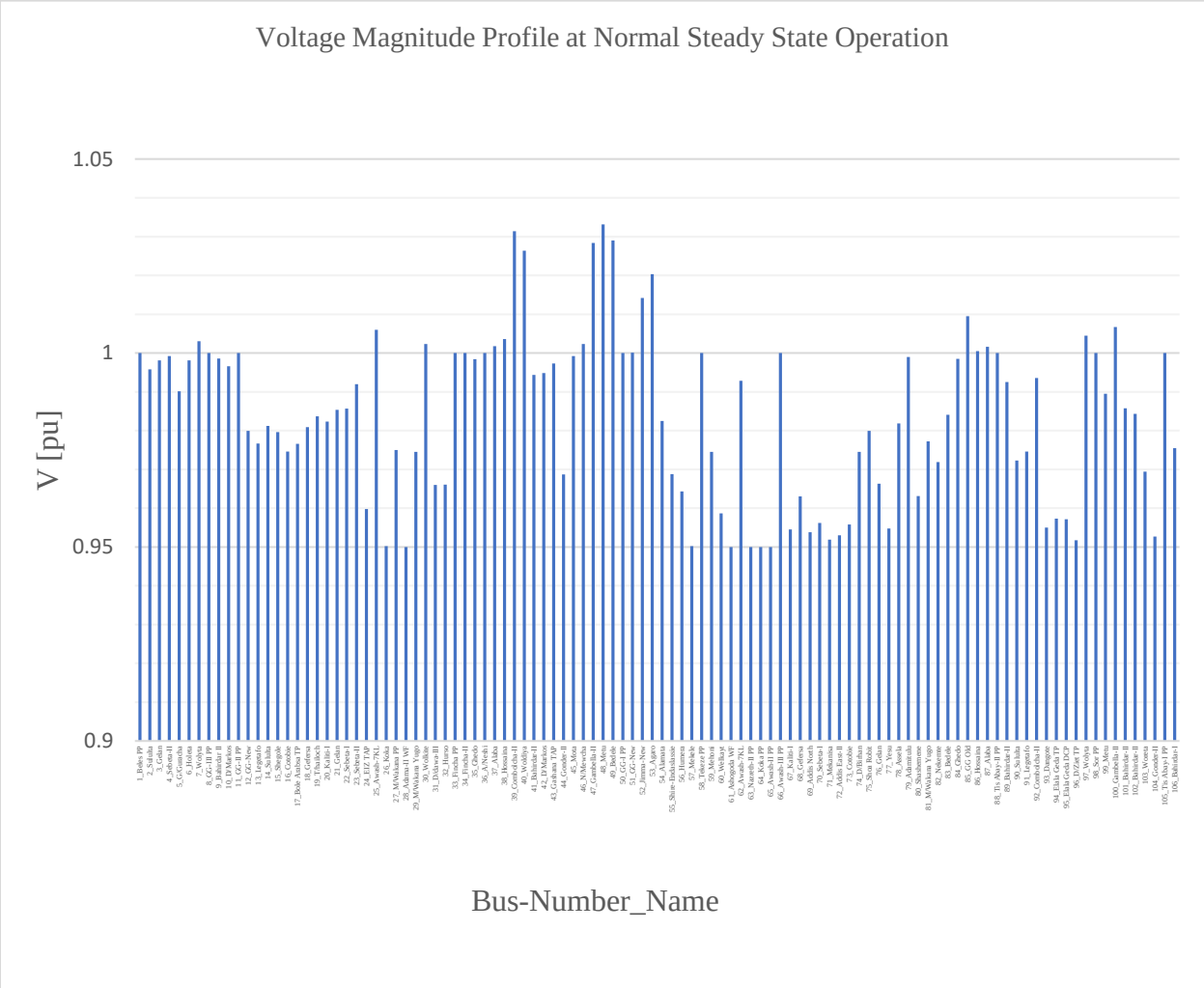

Figure 3.14. Voltage magnitude Profile of the grid model at normal operation condition

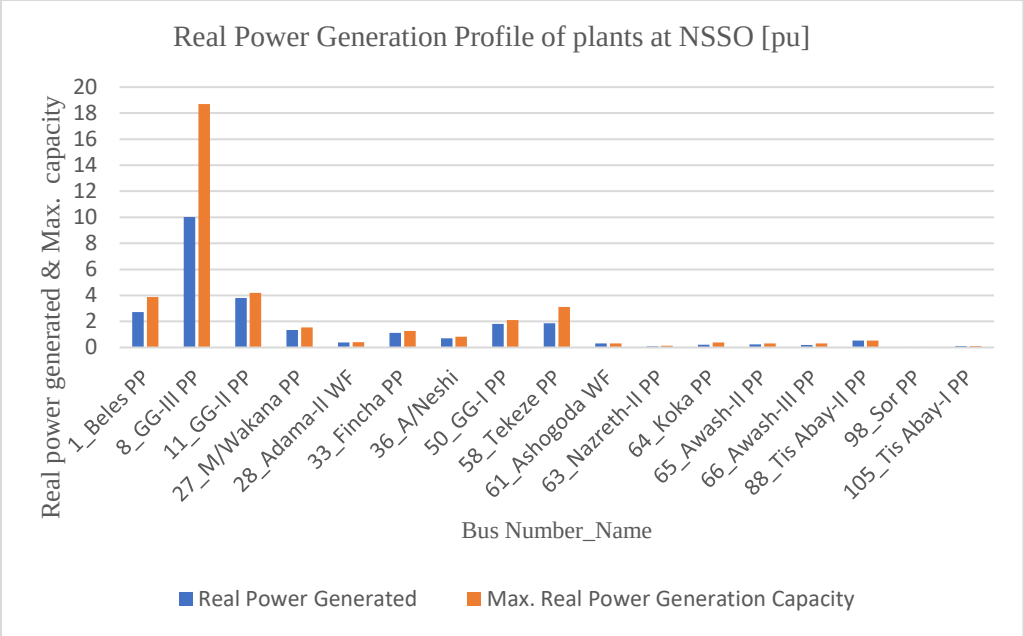

Figure 3.15. Real power generation profile of the grid model at normal operation condition

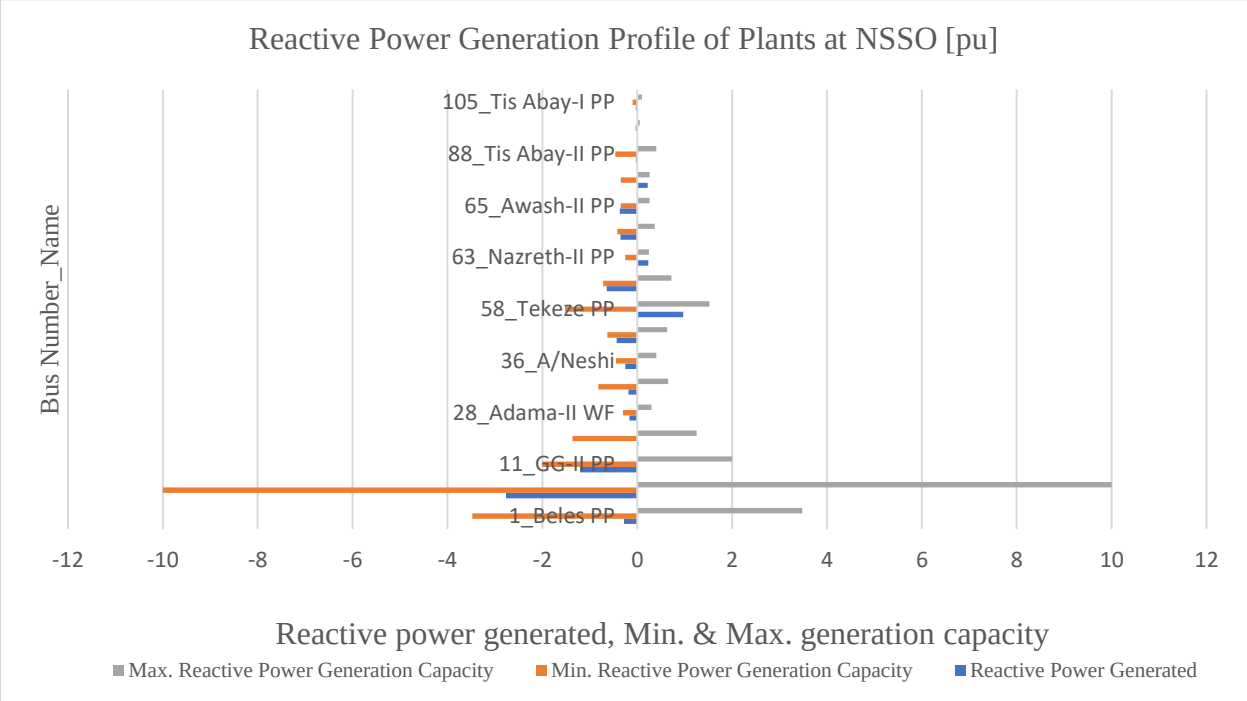

Figure 3.16. Reactive power generation profile of the grid model at normal operation condition

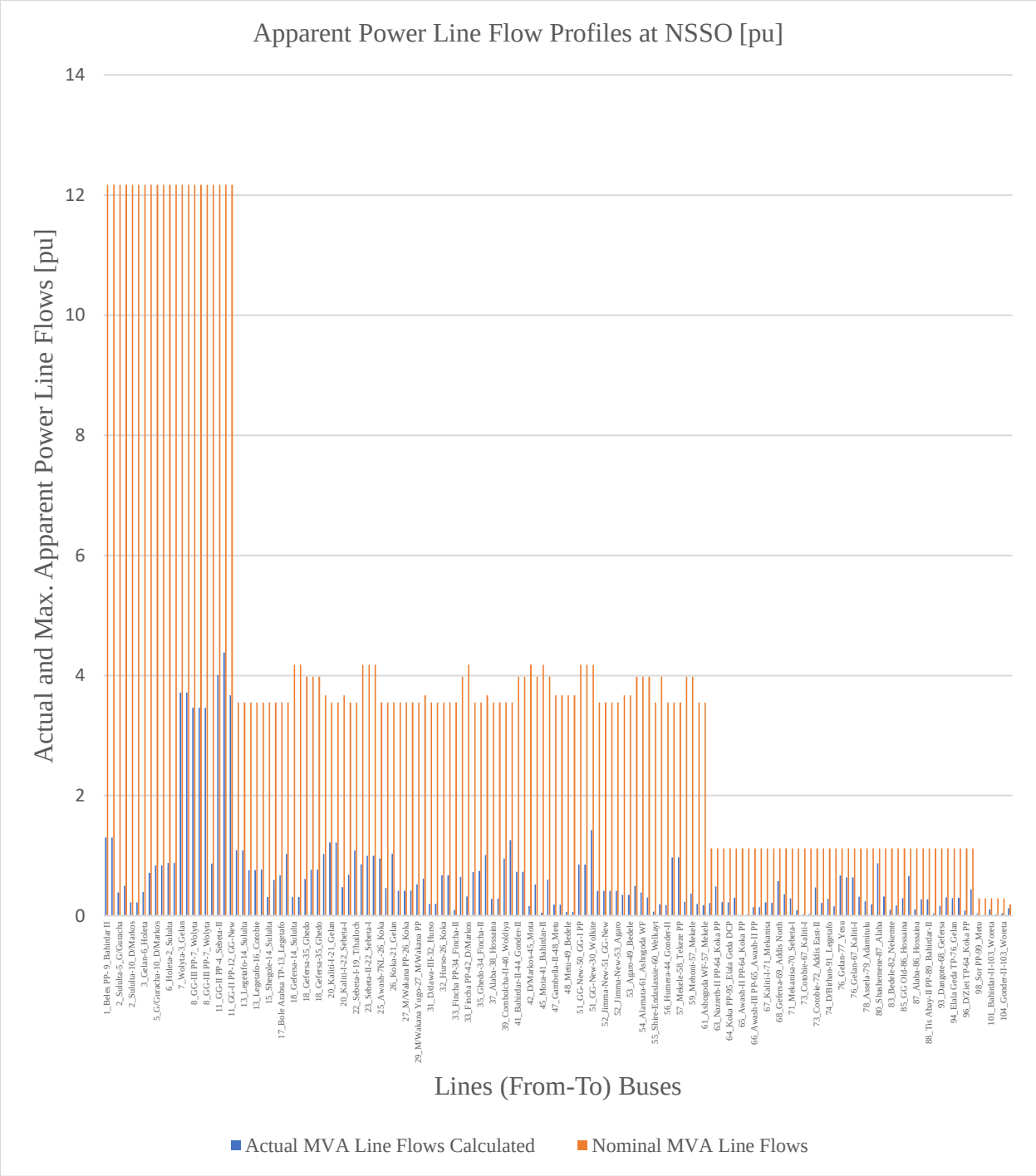

Figure 3.17. Apparent power line flows and respective flow limits

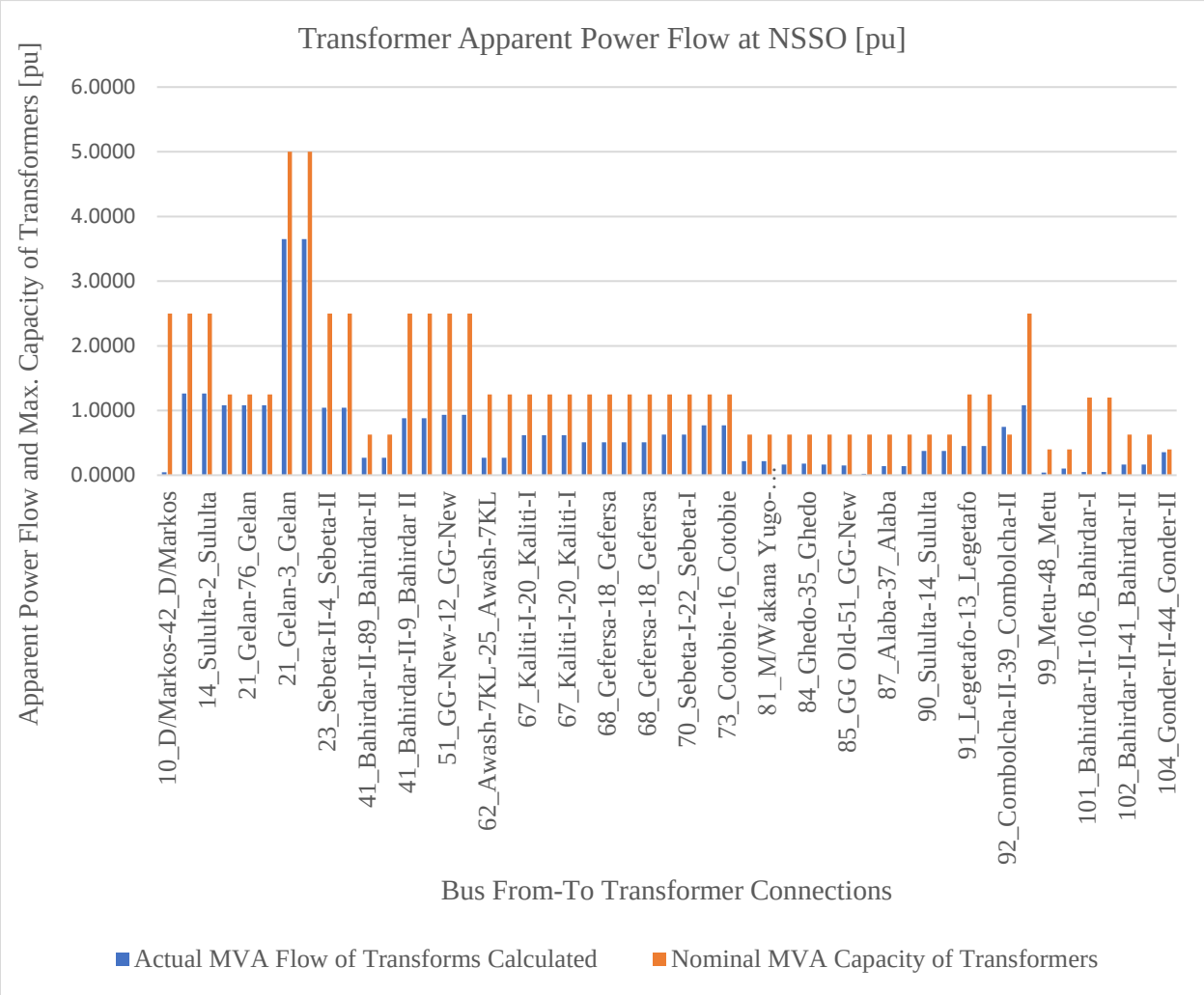

Figure 3.18. Transformer flow reports and comparison with their respective nominal capacities

To conclude, the overall power flow report verify that all the parameters are within permissible and binding limits. All the power flow results being withing binding limits assure that the grid model intended for further study requirement is valid. Hereafter, this grid model is termed as 'Grid Model' and it is the basis for further intended case studies to be carried out.

Let us see the study flow chart shown in Figure 3.19. It is intended to show how overall study is conducted.

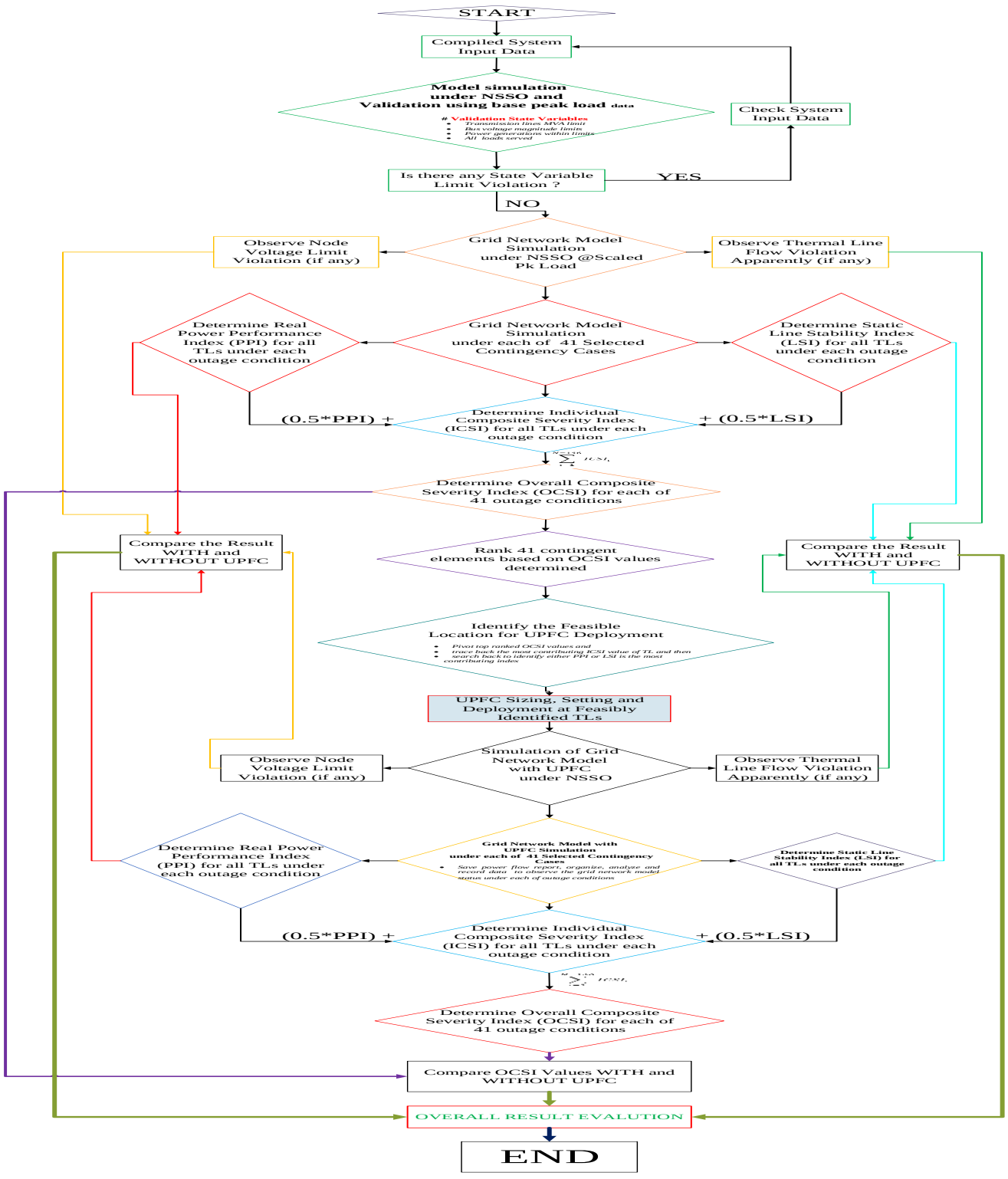

Figure 3.19. Flows of overall study.

3.5 Contingency Analysis of High Voltage Grid

It is important to set the guideline/s to prioritize a transmission line or power plant to conduct outage study as it is difficult to perform all contingency studies for the case of large grid. To conduct this study, different guidelines, techniques and methods are clearly defined and stated for the prioritizing, sorting, ranking and managing overall data as discussed below.

3.5.1 Prioritizing the Transmission Lines for Contingency Analysis

Here, the methodology followed is that the lines with the highest power flow are prioritized and sorted from largest to the smallest and chosen accordingly to perform the study. The prioritizing based on the MVA flow is looked due to the intention that the outage of TLs with highest MVA flow will contribute the highest MVA flow to the rest of network so that it will be critical line to be selected and studied.

Generally, the guiding rules for this methodology are as under listed:

1. Scaling up the each of the peak load recorded at normal steady state operation by the factor of 1.33 as the NLDC does too, for forecasting daily peak load and generation dispatch scheduling.
2. For prioritizing and sorting, the line Flow MVAs of double and more circuits are summed up
3. The single line outage with highest to smallest (up to interested) is looked
4. Double and more circuits are considered as single circuit outage
5. The TLs that will possibly isolate the power plant completely from the grid, equivalently power plant outage, are not part of the outages to be looked
6. Transformer branches are not considered for the outage case studies

As per the defined guidelines above, eight 400 kV (all), nineteen 230 kV and three 132 kV TLs in which a total of 30 feasible TLs (either single or parallel TLs) are screened out and feasibly selected to conduct the intended study as tabulated in Table 3.1.

Table 3.1. Overall TLs sorted and ranked based on MVA line flows

MVA Line Flow Ranking									
From Bus	To Bus	Line No.	P Flow [pu]	Q Flow [pu]	Calculated S(pu) Flow	TL Thermal Limit S(pu)	Network Voltage Level (kV)	Overall MVA flows for sorting	MVA Flow Rank
11_GG-II PP	7_Wolyta	53	-2.91974	-11.86367	12.21768	12.17	400	12.21768	1
7_Wolyta	3_Gelan	25	4.32933	-0.20782	4.33432	12.17	400	8.66864	2
7_Wolyta	3_Gelan	36	4.32933	-0.20782	4.33432	12.17	400		
11_GG-II PP	4_Sebeta-II	47	4.77953	0.43561	4.79934	12.17	400	4.79934	3
20_Kaliti-I	21_Gelan	77	-1.46268	-0.68173	1.61375	3.55	230	3.22750	4
20_Kaliti-I	21_Gelan	78	-1.46268	-0.68173	1.61375	3.55	230		
18_Gefersa	35_Ghedo	73	-0.66721	-0.32983	0.74429	3.98	230	2.62113	5
18_Gefersa	35_Ghedo	74	-0.89178	-0.29215	0.93842	3.98	230		
18_Gefersa	35_Ghedo	75	-0.89178	-0.29215	0.93842	3.98	230		
13_Legetafo	14_Sululta	61	-1.23181	-0.34856	1.28018	3.55	230	2.56035	6
13_Legetafo	14_Sululta	62	-1.23181	-0.34856	1.28018	3.55	230		
23_Sebeta-II	22_Sebeta-I	83	1.10591	0.50540	1.21592	4.18	230	2.43184	7
23_Sebeta-II	22_Sebeta-I	84	1.10591	0.50540	1.21592	4.18	230		
57_Mekele	58_Tekeze PP	138	-1.10469	-0.46861	1.19997	3.55	230	2.39995	8
57_Mekele	58_Tekeze PP	139	-1.10469	-0.46861	1.19997	3.55	230		
11_GG-II PP	12_GG-New	92	2.32021	0.59964	2.39645	12.17	400	2.39645	9
6_Holeta	2_Sululta	114	1.00213	0.33004	1.05508	12.17	400	2.11017	10
6_Holeta	2_Sululta	125	1.00213	0.33004	1.05508	12.17	400		
6_Holeta	4_Sebeta-II	2	-0.94296	-0.35114	1.00622	12.17	400	2.01244	11
6_Holeta	4_Sebeta-II	59	-0.94296	-0.35114	1.00622	12.17	400		
13_Legetafo	16_Cotobie	63	0.88807	0.33173	0.94801	3.55	230	1.89602	12
13_Legetafo	16_Cotobie	64	0.88807	0.33173	0.94801	3.55	230		
76_Gelan	67_Kaliti-I	37	0.69783	0.54096	0.88295	1.12	132	1.76590	13
76_Gelan	67_Kaliti-I	38	0.69783	0.54096	0.88295	1.12	132		
51_GG-New	30_Wolkite	97	1.63040	0.20960	1.64381	4.18	230	1.64381	14
51_GG-New	50_GG-I PP	52	-0.80905	0.11768	0.81756	4.18	230	1.638965	15
51_GG-New	50_GG-I PP	146	-0.80905	0.11768	0.81756	4.18	230		
32_Hurso	26_Koka	93	-0.75359	-0.28512	0.80573	3.55	230	1.61146	16
32_Hurso	26_Koka	94	-0.75359	-0.28512	0.80573	3.55	230		
41_Bahirdar-II	44_Gonder-II	111	0.78838	-0.11937	0.79737	3.98	230	1.59474	17
41_Bahirdar-II	44_Gonder-II	112	0.78838	-0.11937	0.79737	3.98	230		
22_Sebeta-I	19_T/hailoch	76	1.31351	0.33487	1.35552	3.55	230	1.35552	18
17_B/Arabsa TP	20_Kaliti-I	109	-1.22257	-0.40248	1.28712	3.55	230	1.28712	19
19_T/hailoch	18_Gefersa	72	1.23750	0.30797	1.27524	3.67	230	1.27524	20

35_Ghedo	51_GG-New	106	-1.22378	0.03339	1.22423	3.67	230	1.22423	21
25_Awash-7KL	26_Koka	87	-1.03104	-0.17493	1.04577	3.55	230	1.04577	22
26_Koka	21_Gelan	82	-1.01405	0.21036	1.03564	3.55	230	1.03564	23
9_Bahirdar II	10_D/Markos	103	1.00460	0.14001	1.01431	12.17	400	1.01431	24
22_Sebeta-I	30_Wolkite	85	-1.00000	-0.04436	1.00099	4.18	230	1.00099	25
5_G/Guracha	10_D/Markos	136	-0.49029	-0.80839	0.94545	12.17	400	0.94545	26
80_Shashemene	87_Alaba	39	-0.93084	-0.02628	0.93121	1.12	132	0.93121	27
76_Gelan	77_Yesu	26	0.72560	0.56572	0.92007	1.12	132	0.92007	28
27_M/Wakana PP	26_Koka	89	0.44905	0.00759	0.44911	3.55	230	0.89823	29
27_M/Wakana PP	26_Koka	90	0.44905	0.00759	0.44911	3.55	230		
35_Ghedo	34_Fincha-II	104	-0.84683	-0.23727	0.87944	3.55	230	0.87944	30

These are 30 TLs ranked based on the magnitude of the line flows in pu apparently. The TL with the highest line flow is given highest severity weight due to intension that the outage of relatively loaded TL will expose the grid to worse disturbance.

3.5.2 Prioritizing Power Plants for Contingency Analysis

Case studies of power plants with highest installed capacity (MVA) are prioritized. The selection criteria is due to the fact that the outage of power plants with relatively higher capacities and duties will affect the grid more severely. Here, it is important to note that Wind Farms (WF) and small or medium scale hydro-plants are not part of the case studies.

The guidelines for prioritizing the outage of power plants for this methodology are:

1. The highest MVA installed capacity is prioritized at first as expected as their potential impact on the grid is higher
2. The slack generation plant, Beles PP, is not included as part of the outage study (even if it is selected the analysis tool does not allow to do so)
3. Wind Farms (WF) are not considered hence, they are not included in the scope of this study
4. Power plants with small installed capacities are ignored for the outage study

Table 3.2. Power Plants selected for the outage study

Power Plant Name	No. of units	Generator Bus Number	Generator Bus Name	Bus Type	Sn [MVA]	Rank of Sn [MVA]
GG III Plant	10	8	Gilgel Gibe III	PV	2200	1
GG II Plant	4	11	Gilgel Gibe II	PV	500	2

Tekeze Plant	4	58	Tekeze	PV	344	3
GG I Plant	3	50	Gilgel Gibe I	PV	219	4
M/Wakena Plant	4	27	Melka Wakena	PV	180	5
Fincha Plant	4	33	Fincha	PV	160	6
Amerti Neshi Plant	2	36	Amerti Neshi	PV	106	7
Tis Abay II Plant	2	88	Tis Abay II	PV	80	8
Koka Hydro Plant	3	64	Koka	PV	60	9
Awash II Plant	2	65	Awash II	PV	40	10
Awash III Plant	2	66	Awash III	PV	40	11

Power flow simulations are made for all, 30 Transmission Lines and 11 Power Plants, under every outage condition of the contingent component screened above based on the stated guidelines. Then, simulated power flow report of each and every outage conditions are read, observed, the effect of each contingent on the grid is evaluated and finally the effects are to be recorded for further works.

3.5.3 Contingency Ranking Index

In this study, overall composite severity index (OCSI) is used for ranking the criticality of both contingent transmission line and power plant of the grid model under study. Here, overall composite severity index (OCSI) stands two incorporated severity indices, Real Power Performance Index (PPI) and Line Stability Index (LSI), which are selected to perform the intended study. Each of the severity indices are separately described below.

3.5.3.1 Real Power Performance Index (PPI)

Real power performance index (PPI) is the measure of the grid performance in terms of line loading whenever contingency occurs. Let us consider the single line diagram of the radial power system in Figure 3.20.

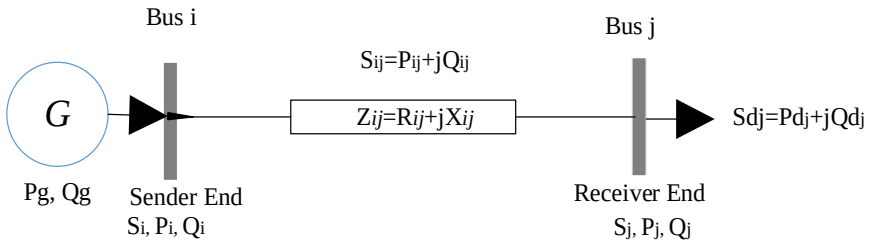

Figure 3.20. Single line diagram of radial power system

Radial power system in Figure 3.20 is intended to observe and understand the parameters of severity indices to be used and it can be observed that the individual real power performance index of a transmission line from bus i to j, $l_{ij,}$ for each of the contingent transmission lines (TLs) or generation plants (PPs) can be evaluated using equation 3.40.

$$PPI_{ij} = \left(\frac{W_{ij}}{2n}\right)\left[\frac{P_{ij}}{P_{ij}^{limit}}\right]^{2n} \tag{3.32}$$

Where,

PPI_{ij}- Real power performance index of the line from bus i to j

W_{ij}- Weighting factor of the line from bus i to j indicating the importance of that line

n- Penalty factor

P_{ij}- Actual real power flow from bus i to j

P_{ij}^{limit}- Permissible limit of power flow allowed from bus i to j and given by

$$P_{ij}^{limit} = {(V_i^{max} * V_j^{max})}\Big/{X_{ij}} \tag{3.33}$$

The case where, $\delta_{ij} = \delta_i - \delta_j = 90°$

V_i^{max}- Max. bus i voltage allowed

V_j^{max}- Max. bus j voltage allowed

X_{ij}- Line reactance from bus i to j (constant impedance from this study perspective)

Moreover, overall real power performance index (PPI) of the power system network for the outage of a transmission line or plant can be given by

$$PPI = \sum_{i\to j, i\neq j}^{N_l}\left(\frac{W_{ij}}{2n}\right)\left[\frac{P_{ij}}{P_{ij}^{limit}}\right]^{2n} \tag{3.34}$$

The implication of the real power performance index is that very small value stands for the line being underloaded condition, high value stands for the line being overloaded condition and its value between these bounds indicates that it is within limits. It is important to note that the

weighting and penalty factors are set to be 1 throughout this study so that the real power performance index formula becomes,

$$PPI = \sum_{i\to j, i\neq j}^{N_l} \left(\frac{1}{2}\right)\left[\frac{P_{ij}}{P_{ij}^{limit}}\right]^2 \tag{3.35}$$

From the eventual simplified formula, it is clearly observed that the critical point of the transmission loading is 0.5 if and only if the real power flow alone is considered.

3.5.3.2 Line Stability Index (LSI)

Even though voltage stability is a dynamic problem, static indexes still plays a very important role in voltage stability analysis and helps operators to know how close the current operation point is to static stability limit [38]. Line Stability index (LSI) is one the voltage indices which is sometimes known as voltage stability index and used in this study as static index to determine the static stability limit of the transmission lines (TLs).

From the context of this study, it is a measure of static line stability in terms of the voltage proximity indicator after the grid is subjected to contingency condition. Again, let us recall Figure 3.20, to have an idea about the stated index, which is given by,

$$L_{ij} = {}^{4X_{ij}Q_j}\Big/_{[V_i \sin(\theta - \delta_{ij})]^2} \tag{3.36}$$

where,

L_{ij}- line stability index of the line from bus i to j

Q_j- reactive power at the receiving end bus j

θ- the impedance angle and given by $\theta = \tan^{-1}\left(\frac{X_{ij}}{R_{ij}}\right)$

δ_{ij}- the voltage angle differences of bus i and j, and given by $\delta_{ij} = \delta_i - \delta_j$

V_i- Actual voltage reading of bus i

The implication of the Line Stability Index (LSI) is that its value less than 1 stands for a transmission line (TL) being in stable condition while the value beyond stands for a transmission line (TL) being in unstable condition.

3.5.3.3 Overall Composite Severity Index (OCSI)

Overall Composite Severity Index (OCSI) combines the characteristics of both indices discussed above and it helps to estimate the whole network stress more accurately under contingency condition, a transmission line or power plant contingency, from the scope of this study.

Composite severity index of the individual line from bus i to j ($ICSI_{ij}$) can be given by

$$ICSI_{ij} = w_{ij-PPI} * PPI_{ij} + w_{ij-L} * L_{ij} \tag{3.37}$$

Where, $w_{ij\text{-}PPI}$ and $w_{ij\text{-}L}$ are weighting factors of real power performance and line stability indices respectively, intended to weigh the importance of the indices. In this study, equal importance is given for both indices i.e., 50 % for each. Accordingly, equation 3.45 can be rewritten as,

$$ICSI_{ij} = 0.5 * PPI_{ij} + 0.5 * L_{ij} \tag{3.38}$$

To generalize, the overall composite severity index (OCSI) of the grid for each of the contingent elements, a transmission line or power plant from the context of this study, is given by

$$OCSI = \sum_{i\to j, i\neq j}^{N_L} ICSI_{ij} = \sum_{i\to j, i\neq j}^{N_L} 0.5 * \left[PPI_{ij} + L_{ij}\right] \tag{3.39}$$

3.6 Simulation Studies and Analysis of Results

As already mentioned in different sections of this work, the case studies are conducted using the verified and validated grid model but at scaled peak load record of EEP with the load scale factor of the 1.33. This factor is chosen with the reason that the planning department of the NLDC uses it for forecasting daily peak load and generation dispatch scheduling. The simulation result of grid model at scaled peak load is tabulated in Appendix J but bar graph charts of voltage magnitude profiles (pu) and line flows apparently (pu) are as shown in Figure 3.21 and 3.22, respectively.

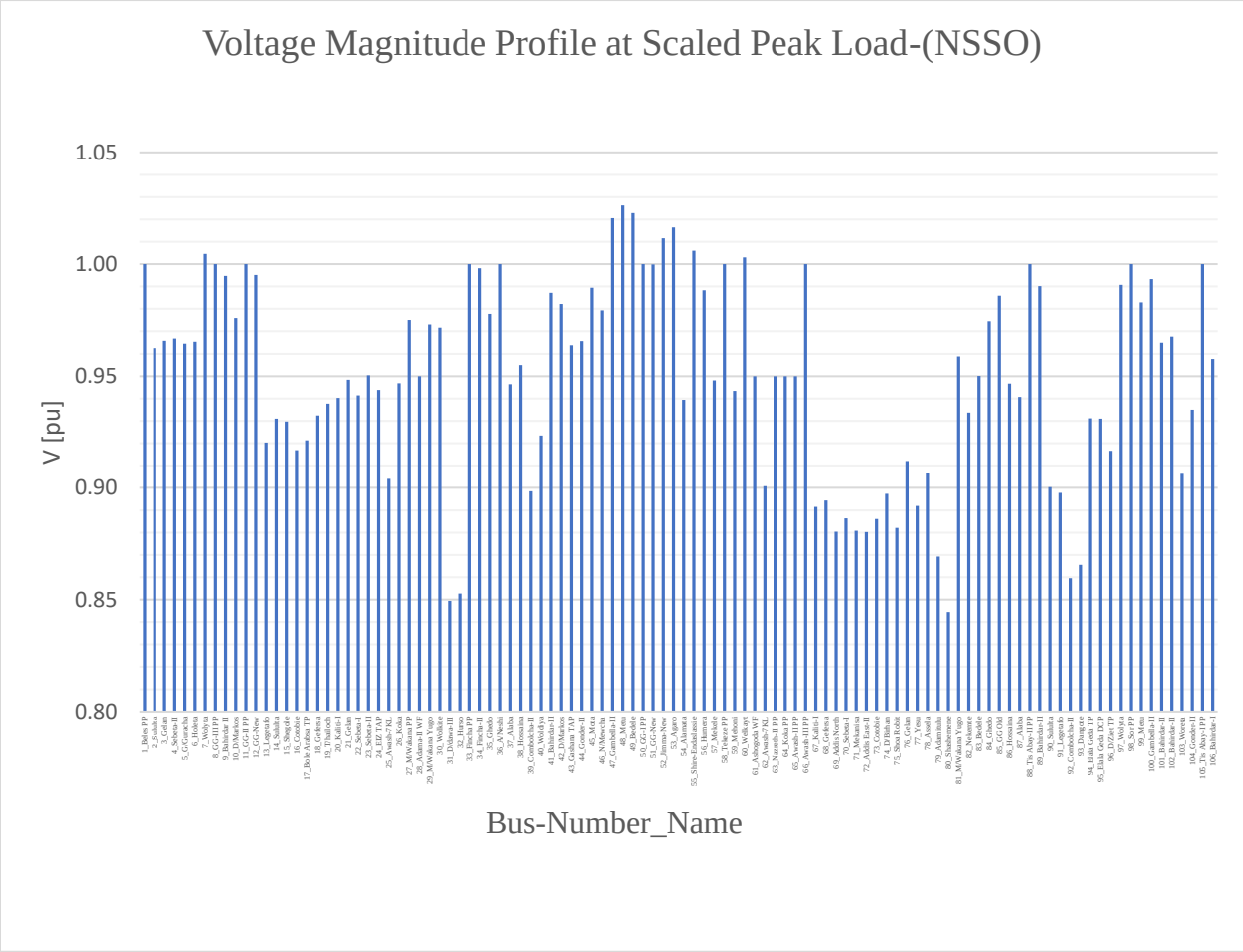

Figure 3.21. Voltage magnitude Profile of the grid model at normal operating condition of scaled peak load

It is clearly observable from voltage magnitude profiles of the grid model which is simulated at scaled peak load that the voltage magnitude of some buses is slashed below the minimally prescribed value of 0.95 pu. It is necessary to bear in mind that this result is obtained from simulation of the grid model under normal steady state operating condition but at scaled peak load yet with the scaling factor of 1.33. This assures that how much the network voltage profile is sensitive with respect to load changes.

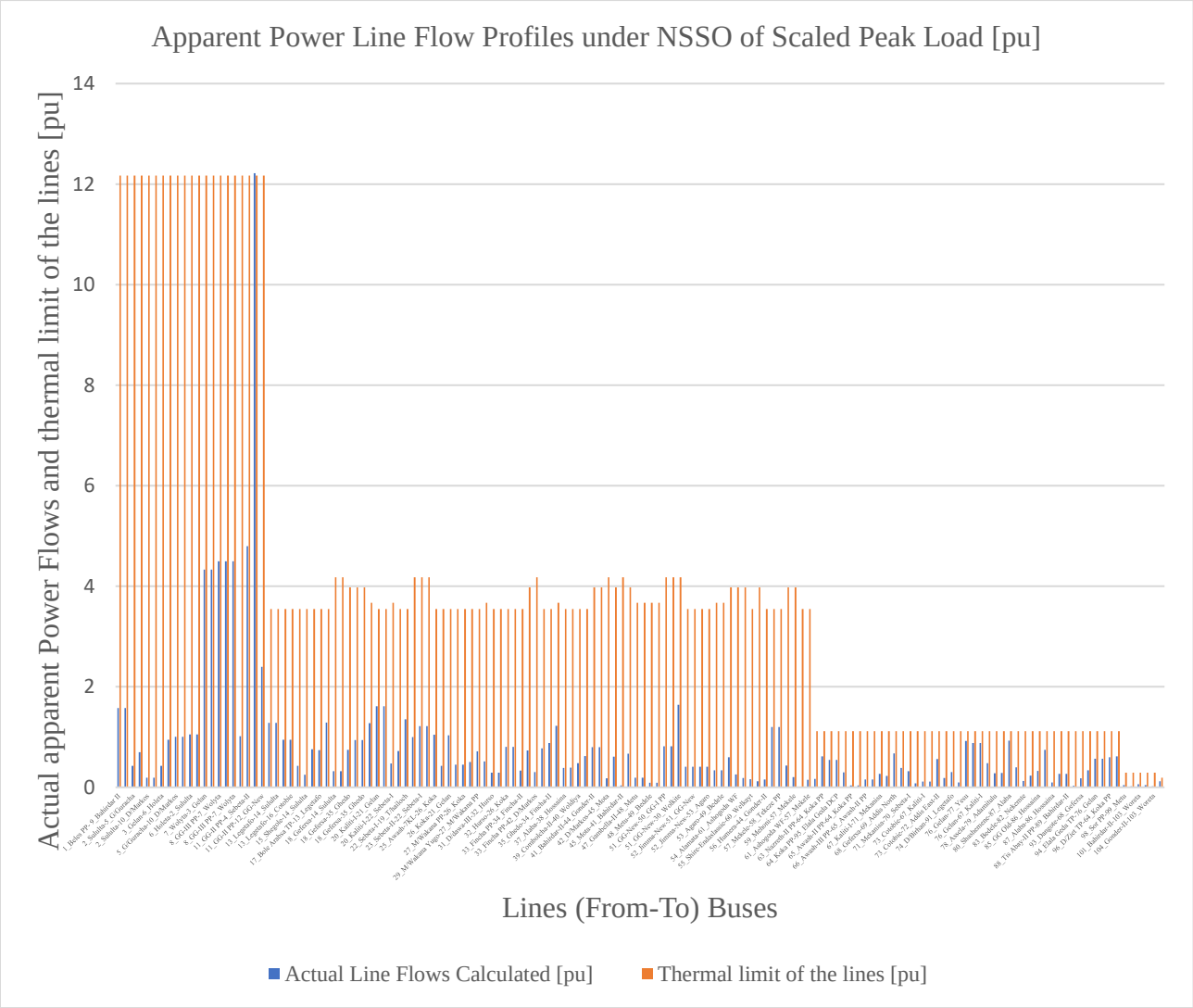

Figure 3.22. Apparent power line flows and respective thermal limits

It is observed from the simulation that all the line MVA flows are within prescribed thermal limits except 11_GG-II PP to 7_Wolyta 400 kV TL which is likely to violate the stated transmission line constraint.

3.6.1.1 Ranking Transmission Line Outages

Under this subsection, power flow report for each of the feasible contingent transmission lines is ranked and sorted from the most sever to the least one on the basis of overall composite severity index (OCSI) value obtained.

In this study, transmission line (TL) loading apparently is the core parameter for sorting and ranking the severity. All the TLs selected for outage case studies are simulated and their effects on the overall grid is calculated and then overall effect of the outage line/s on the grid is ranked based on the overall composite severity index (OCSI) value obtained.

Table 3.3. Ranking of the grid vulnerability level for respective Transmission line (TL) outage load based on Overall Composite Severity Index (OCSI)

Ranking of the grid vulnerability level for respective outage of TL based on OCSI					
Outage TL	Line No.	Thermal S(pu)	TL Voltage Level (kV)	OCSI of the Grid	OCSI Rank
7_Wolyta-3_Gelan	25	12.17	400	19.734291	1
7_Wolyta-3_Gelan	36	12.17	400		
57_Mekele-58_Tekeze PP	138	3.55	230	19.529040	2
57_Mekele-58_Tekeze PP	139	3.55	230		
11_GG-II PP-4_Sebeta-II	47	12.17	400	17.394284	3
6_Holeta-2_Sululta	114	12.17	400	16.973824	4
6_Holeta-2_Sululta	125	12.17	400		
41_Bahirdar-II-44_Gonder-II	111	3.98	230	16.758072	5
41_Bahirdar-II-44_Gonder-II	112	3.98	230		
20_Kaliti-I-21_Gelan	77	3.55	230	16.152047	6
20_Kaliti-I-21_Gelan	78	3.55	230		
27_M/Wakana PP-26_Koka	89	3.55	230	16.094193	7
27_M/Wakana PP-26_Koka	90	3.55	230		
51_GG-New-50_GG-I PP	52	4.18	230	16.089706	8
51_GG-New-50_GG-I PP	146	4.18	230		
23_Sebeta-II-22_Sebeta-I	83	4.18	230	16.005241	9
23_Sebeta-II-22_Sebeta-I	84	4.18	230		
76_Gelan-67_Kaliti-I	37	1.12	132	15.993119	10
76_Gelan-67_Kaliti-I	38	1.12	132		
11_GG-II PP-12_GG-New	92	12.17	400	15.927937	11
32_Hurso-26_Koka	93	3.55	230	15.838092	12

32_Hurso-26_Koka	94	3.55	230		
13_Legetafo-14_Sululta	61	3.55	230	15.721317	13
13_Legetafo-14_Sululta	62	3.55	230		
13_Legetafo-16_Cotobie	63	3.55	230	15.597021	14
13_Legetafo-16_Cotobie	64	3.55	230		
25_Awash-7KL-26_Koka	87	3.55	230	15.578001	15
80_Shashemene-87_Alaba	39	1.12	132	15.538855	16
17_B/Arabsa TP-20_Kaliti-I	109	3.55	230	15.516683	17
26_Koka-21_Gelan	82	3.55	230	15.450951	18
35_Ghedo-51_GG-New	106	3.67	230	15.427357	19
76_Gelan-77_Yesu	26	1.12	132	15.402822	20
22_Sebeta-I-19_T/hailoch	76	3.55	230	15.384544	21
19_T/hailoch-18_Gefersa	72	3.67	230	15.372170	22
6_Holeta-4_Sebeta-II	2	12.17	400	15.366177	23
6_Holeta-4_Sebeta-II	59	12.17	400		
5_G/Guracha-10_D/Markos	136	12.17	400	15.236055	24
18_Gefersa-35_Ghedo	74	3.98	230	15.178510	25
18_Gefersa-35_Ghedo	75	3.98	230		
18_Gefersa-35_Ghedo	73	3.98	230		
51_GG-New-30_Wolkite	97	4.18	230	15.170635	26
35_Ghedo-34_Fincha-II	104	3.55	230	15.143248	27
22_Sebeta-I-30_Wolkite	85	4.18	230	15.039452	28
11_GG-II PP-7_Wolyta	53	12.17	400	14.641239	29
9_Bahirdar II-10_D/Markos	103	12.17	400	14.397400	30

Simulation for all of the selected 30 transmission lines (TL) is carried out under each of the contingency conditions and their criticality is ranked based on the corresponding OCSI value calculated as shown in Table 3.3. Amongst, double circuit transmission line (TL) from Wolyta 400 kV substation to Gelan 400 kV substation, 7_Wolyta-3_Gelan, takes top rank. It is to mean that it is very critical transmission line (TL), and its outage incidence will lead to the worst grid disturbance. The transmission lines (TLs) and their rank based on OCSI defines the criticality level for the grid security.

3.6.1.2 Ranking Power Plant Outages

Under this case study, the real power generation profile setting of each PP is updated to account for the coverage of outage PP plant proportionally. The real power generation setting of each PP

is updated proportionally in a such a way that the actively working PPs are able to share the power generation duty of the contingent plant providing that maximum allowable real power generation capacity is not violated. The breakdown of the setting for each of the PPs with respect to capacity of outage PP being under study at a time is tabulated in Appendix K.

For this case study, power flow report of all selected contingent power plants (PPs) are ranked from the most sever to the least one using overall composite severity index (OCSI).

Table 3.4. Ranking of the grid vulnerability level for respective outage of power plant (PP) based on Overall Composite Severity Index (OCSI)

Ranking of the grid vulnerability level for respective outage of PP based on OCSI					
Outage PP	Bus No.	PP Nominal S(pu)	Bus Voltage Level (kV)	OCSI of the Grid	OCSI Rank
GG III Plant	8	22	400	23.091850	1
M/Wakena Plant	27	1.8	230	19.293922	2
Tekeze Plant	58	3.44	230	16.720615	3
GG II Plant	11	5	400	16.153597	4
Fincha Plant	33	0.16	230	15.633733	5
Awash II Plant	65	0.4	132	15.472644	6
GG I Plant	50	2.19	230	15.456055	7
Koka Hydro Plant	64	0.6	132	15.392289	8
Awash III Plant	66	0.4	132	15.319376	9
Amerti Neshi Plant	36	1.06	230	15.288097	10
Tis Abay II Plant	88	0.8	132	15.272171	11

Contingency simulations for selected 11 power plants (PPs) are conducted and their severity is ranked based on the corresponding OCSI values determined as shown in Table 3.4. As per the simulation result, GG III power plant outage is serious incident that results Beles power plant to receive extreme over loading beyond its capacity . The real phenomenon for this plant outage is the grid blackout incidence hence, no sufficient power generation. This is the expected case due

to reason that the plant is with largest installed capacity among actively working PPs in Ethiopia's grid.

3.6.1.3 Ranking Overall Outages

This is the final stage to sort and re-rank the severities determined using OCSI values under both case studies, a TL or power plant outage, in order to identify the grid vulnerability level for 41 selected contingency case studies.

Table 3.5. Re-ranking of the grid vulnerability level for 41 selected contingency case studies based on Overall Composite Severity Index (OCSI)

Re-ranking of the grid vulnerability level for respective outage of TL/PP based on OCSI						
Outage Element	TL/PP	Line/Bus No.	Nominal PP/ Thermal TL S(pu)	TL/Bus Voltage Level (kV)	OCSI of the Grid	OCSI Rank
GG III Plant	PP	8	22	400	23.091850	1
7_Wolyta-3_Gelan	TL	25	12.17	400	19.734291	2
7_Wolyta-3_Gelan	TL	36	12.17	400		
57_Mekele-58_Tekeze PP	TL	138	3.55	230	19.529040	3
57_Mekele-58_Tekeze PP	TL	139	3.55	230		
M/Wakena Plant	PP	27	1.8	230	19.293922	4
11_GG-II PP-4_Sebeta-II	TL	47	12.17	400	17.394284	5
6_Holeta-2_Sululta	TL	114	12.17	400	16.973824	6
6_Holeta-2_Sululta	TL	125	12.17	400		
41_Bahirdar-II-44_Gonder-II	TL	111	3.98	230	16.758072	7
41_Bahirdar-II-44_Gonder-II	TL	112	3.98	230		
Tekeze Plant	PP	58	3.44	230	16.720615	8
GG II Plant	PP	11	5	400	16.153597	9
20_Kaliti-I-21_Gelan	TL	77	3.55	230	16.152047	10
20_Kaliti-I-21_Gelan	TL	78	3.55	230		
27_M/Wakana PP-26_Koka	TL	89	3.55	230	16.094193	11
27_M/Wakana PP-26_Koka	TL	90	3.55	230		
51_GG-New-50_GG-I PP	TL	52	4.18	230	16.089706	12

51_GG-New-50_GG-I PP	TL	146	4.18	230		
23_Sebeta-II-22_Sebeta-I	TL	83	4.18	230	16.005241	13
23_Sebeta-II-22_Sebeta-I	TL	84	4.18	230		
76_Gelan-67_Kaliti-I	TL	37	1.12	132	15.993119	14
76_Gelan-67_Kaliti-I	TL	38	1.12	132		
11_GG-II PP-12_GG-New	TL	92	12.17	400	15.927937	15
32_Hurso-26_Koka	TL	93	3.55	230	15.838092	16
32_Hurso-26_Koka	TL	94	3.55	230		
13_Legetafo-14_Sululta	TL	61	3.55	230	15.721317	17
13_Legetafo-14_Sululta	TL	62	3.55	230		
Fincha Plant	PP	33	0.16	230	15.633733	18
13_Legetafo-16_Cotobie	TL	63	3.55	230	15.597021	19
13_Legetafo-16_Cotobie	TL	64	3.55	230		
25_Awash-7KL-26_Koka	TL	87	3.55	230	15.578001	20
80_Shashemene-87_Alaba	TL	39	1.12	132	15.538855	21
17_B/Arabsa TP-20_Kaliti-I	TL	109	3.55	230	15.516683	22
Awash II Plant	PP	65	0.4	132	15.472644	23
GG I Plant	PP	50	2.19	230	15.456055	24
26_Koka-21_Gelan	TL	82	3.55	230	15.450951	25
35_Ghedo-51_GG-New	TL	106	3.67	230	15.427357	26
76_Gelan-77_Yesu	TL	26	1.12	132	15.402822	27
Koka Hydro Plant	PP	64	0.6	132	15.392289	28
22_Sebeta-I-19_T/hailoch	TL	76	3.55	230	15.384544	29
19_T/hailoch-18_Gefersa	TL	72	3.67	230	15.372170	30
6_Holeta-4_Sebeta-II	TL	2	12.17	400	15.366177	31
6_Holeta-4_Sebeta-II	TL	59	12.17	400		
Awash III Plant	PP	66	0.4	132	15.319376	32
Amerti Neshi Plant	PP	36	1.06	230	15.288097	33
Tis Abay II Plant	PP	88	0.8	132	15.272171	34
5_G/Guracha-10_D/Markos	TL	136	12.17	400	15.236055	35
18_Gefersa-35_Ghedo	TL	74	3.98	230	15.178510	36
18_Gefersa-35_Ghedo	TL	75	3.98	230		
18_Gefersa-35_Ghedo	TL	73	3.98	230		
51_GG-New-30_Wolkite	TL	97	4.18	230	15.170635	37
35_Ghedo-34_Fincha-II	TL	104	3.55	230	15.143248	38
22_Sebeta-I-30_Wolkite	TL	85	4.18	230	15.039452	39
11_GG-II PP-7_Wolyta	TL	53	12.17	400	14.641239	40
9_Bahirdar II-10_D/Markos	TL	103	12.17	400	14.397400	41

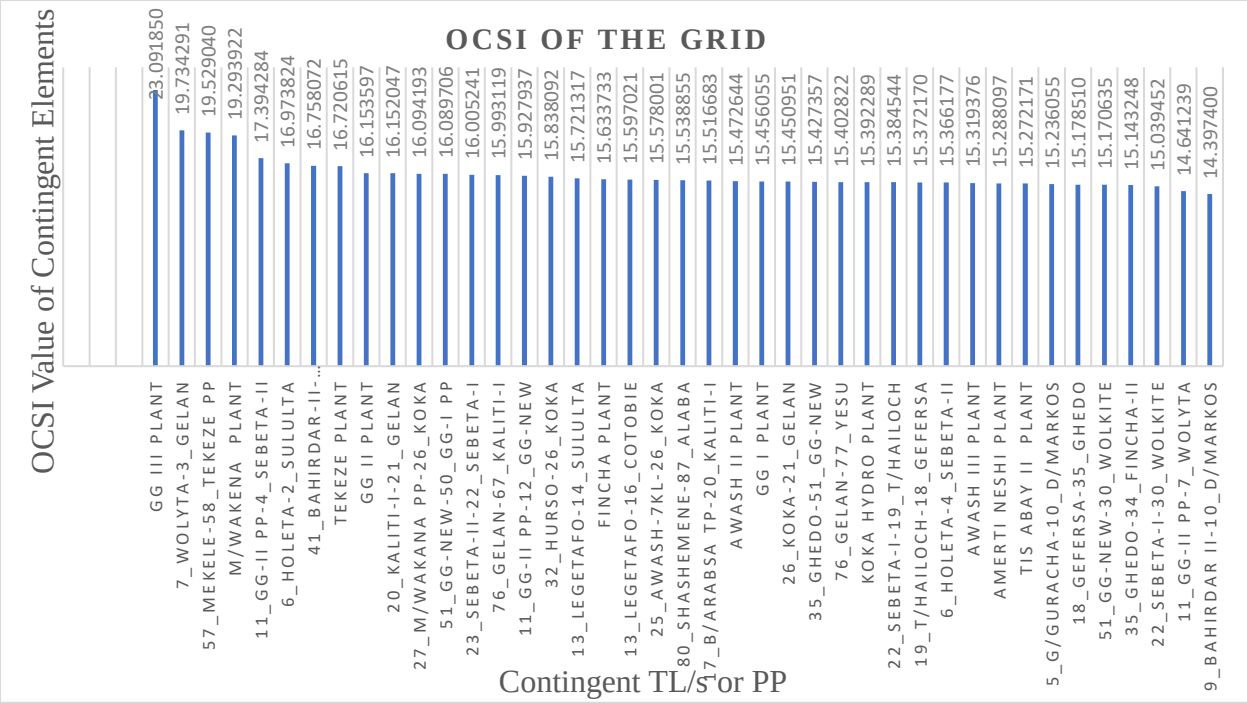

Figure 3.23. Overall ranking of grid vulnerability level based on the overall Composite Severity Index (OCSI) for 41 contingent elements selected

As per the context of this study, the maximum allowable overall network composite severity index range can be defined ideally as 0<OCSI<109.5 provided that each values of individual composite severity index (ICSI)) of 146 transmission line branches are less than 0.75 while holding true for both Real Power Performance Index (PPI_{ij}) and Line Stability Index (L_{ij}) of respective line with PPI_{ij} <0.5 and L_{ij} <1, respectively. As it can be observed from both Table 3.5 and Figure 3.23, double circuit transmission line (TL) from Wolyta 400 kV substation to Gelan 400 kV substation, 7_Wolyta-3_Gelan, and Gilgel Gibe III ([3]GG III) PP are the most top ranked and critical contingent power system components of the national grid.

[3] *In fact, it is observed that the outage of GG-III PP leads to insufficiency of the generation power from over all network power plants (PP) and serious blackout though the remaining power plants are assumed as if they are scheduled to run at maximum power generation capacity. Consequently, the Beles PP receives full duty to respond for the overall demand gap as it is openly and freely acting for any changes yet there is provided limits to do so, and which holds practically true.*

CHAPTER 4

SECURITY ENHANCEMENT OF HIGH VOLTAGE GRID USING UNIFIED POWER FLOW CONTROLLER

4.1 Introduction

The UPFC came into operation at the end of year 2004 in Keepco power system in Korea. It was the largest single procurement order ever placed by Keepco. UPFC devices can save the system from potential threat of system collapse, which can have very serious consequences on other economic sector as well. It can help to avoid the widespread blackout [27]. Amongst these controllers, UPFC is the recently advanced and matured FACTS device family so far developed with controlling capability of all in one.

Transmission line loading management and bus voltage improvements are amongst grid security enhancement possibilities using UPFC. As repeatedly explored, UPFC is the advanced and promising device among the FACTS device which has the unique performance of the integrating various control actions. Power System Analysis Toolbox (PSAT) which is Matlab toolbox provides FACTS device group in SIMULINK library and lets user friendly input parameter setting via dialog box. Mathematical formulation based UPFC parameter setting gives overall clues which is calculated based on the control objective to be achieved hence, appropriate UPFC parameter setting is required. At the first step, the grid model is simulated under the specified values of the state variables, calculated magnitude of series voltage injection and 0^0 flat start of the UPFC reference angle (γ), so that the power flow report is observed. Furtherly, the effect of the output with UPFC is compared with respect to the desired output. The magnitude of the series voltage to be injected is pivoted and the UPFC reference angle (γ) is varied with the step of 10^0 till the desired result is obtained. In addition to mathematical sizing of UPFC, feasible locations for the UPFC devices is identified using OCSI with ISIs. and deployed accordingly to enhance the grid security.

Finally, simulation studies of Ethiopian high voltage grid with UPFC is carried out. After all, simulation results of affected TLs and busbars in terms of TL thermal limit and bus voltage limit under NSSO respectively, and in terms of LSI, PPI, ICSI and OCSI under contingency conditions

without and with UPFC deployment is compared accordingly in order to evaluate how much the grid's security is enhanced.

4.2 Security Enhancement Using UPFC

As long as the power system is under control, it is possible to attain the improved power system emanated from the capability of controlling its different controllable variables namely, voltage, impedance, and phase angle both under steady state operation and disturbance (e.g., contingency) conditions. Power system security enhancement under different operating states is the one of the benefits obtained from the controlled power system using either conventional controllers or advanced controllers though the level of benefits is different depending on the controller looked.

As stated well in [27], the FACTS devices can be used for various applications to boost the power system performance as they have a capability to operate in various states: steady state, transient and post transient steady state conditions. However, the conventional devices find little application during system transient or contingency condition.

As already and repeatedly explored, UPFC is the advanced and promising device among the FACTS device which has the unique performance of the integrating various control actions in one as its name indicates too. To generalize, UPFC has a capability to manage congestion, balance and control power flow, reduce impact of contingency, reduce primary disturbance, perform dynamic voltage control during the contingency to prevent voltage collapse and blackout incident at its worst case.

Power System Analysis Toolbox (PSAT) which is Matlab toolbox provides FACTS device group in SIMULINK library and lets user friendly input parameter setting via dialog box for every and each of the looked devices. Accordingly, the required input parameter setting, and sizing is done in this manner in a such a way that the interested output is to be obtained.

In this study, UPFC devices are sized in such a way that they can maximally inject 30 percent of the MVA thermal capacity of the transmission line (TL) on which it is going to be deployed. In addition, it is important to note as limitation that the shunt component of UPFC devices is not working actively to control the voltage of buses at which they are installed. The purpose of the component is to supply the power demanded by series component and to compensate the

converters loss as long as the converter loss is interested to be included but not yet in this study. Instead, series line compensation of UPFC is used jointly with primarily stated function to compensate the line reactance and to improve the bus voltages as it is provided user friendly in PSAT Simulink library option. According to the stated method, the UPFC MVA sizing can be expressed mathematically as,

$$MVA_{UPFC} = 0.3 * Thermal\ MVA_{limit}\ of\ the\ TL\ being\ looked\ to\ install\ the\ device$$

Table 4.1. Selected nominal capacity of the UPFC devices with respect to the TL thermal limit

SN	Affected TL				Proposed UPFC				
	TL From-To Bus	No. of ckts.	Voltage level (kV)	Thermal MVA limit	Voltage (kV)	Frequency (Hz)	Qty. (No.)	Calculated MVA	Chosen Nominal MVA per ckt.
1	32_Hurso-26_Koka	2	230	355	230	50	2	106.5	100
2	2_Sululta-10_D/Markos	1	400	1217	400	50	1	365.1	400
3	7_Wolyta-3_Gelan	2	400	1217	400	50	2	365.1	400
4	5_G/Guracha-10_D/Markos	1	400	1217	400	50	1	365.1	400
5	11_GG-II PP-7_Wolyta	1	400	1217	400	50	1	365.1	400
6	54_Alamata-61_Ashogoda WF	1	230	398	230	50	1	119.4	100
7	13_Legetafo-39_Combolcha-II	1	230	355	230	50	1	106.5	100
8	87_Alaba-97_Wolyta	1	132	112	132	50	1	33.6	50
9	80_Shashemene-87_Alaba	1	132	112	132	50	1	33.6	50
10	56_Humera-44_Gonder-II	1	230	355	230	50	1	106.5	100
11	81_M/Wakana Yugo-80_Shashemene	1	132	112	132	50	1	33.6	50
12	76_Gelan-77_Yesu	1	132	112	132	50	1	33.6	50
13	77_Yesu-67_Kaliti-I	1	132	112	132	50	1	33.6	50
14	31_D/dawa-III-25_Awash-7KL	1	230	367	230	50	1	110.1	100
15	25_Awash-7KL-26_Koka	1	230	355	230	50	1	106.5	100

In this study, UPFC parameter setting is primarily dependent on the specific objectives to be met with the UPFC deployment as per the weakest TLs identified in terms of the indices used. Those are overloaded and the underloaded TLs. Jointly, it is important to note that voltage magnitudes at all buses may or may not be within prescribed limits though there is improvement after the UPFC devices deployment. In fact, voltage magnitude at some buses was deviated to much due to the

reason that load is scaled up with the defined scaling factor of 1.33. It is the direct that the bus voltage magnitude deviation can be solved by installing shunt voltage controllers (SVC) independently .

In general, underloaded TLs are to be enhanced and contrastingly, overloaded lines with high real power performance index (PPI) are to be managed, and weak busses in terms voltage can be also improved with line impedance compensation capability of UPFC being deployed. As it is already explained, the shunt component of the UPFC is not going to be operated actively to exchange the reactive power so as to maintain the pre-set value of the bus voltage at which it is connected so that its application in this study is to exchange real power with series component of the UPFC. However, all the objectives to be achieved with UPFC deployment are greatly dependent on the UPFC parameter setting and the methods to perform the stated task is based on the under mentioned set of equation described previously.

Assuming the lossless converters and neglecting the shunt reactive power compensation, the overall power injections at buses via UPFC are defined with the set of equations as already derived earlier.

Let us recall that

$$|\bar{V}se| = r|\bar{V}i| = \sqrt{(|Vp|^2 + |Vq|^2)}$$

So,

$$rV_i = \sqrt{(|Vp|^2 + |Vq|^2)}$$

where,

$\sqrt{(|\mathrm{Vp}|^2 + |\mathrm{Vq}|^2)}_{\min} \leq \sqrt{(|\mathrm{Vp}|^2 + |\mathrm{Vq}|^2)} \leq \sqrt{(|\mathrm{Vp}|^2 + |\mathrm{Vq}|^2)}_{\max}$ and $0^\circ \leq \gamma \leq 360^\circ$

$|\bar{V}se|_{min} = \sqrt{(|\mathrm{Vp}|^2 + |\mathrm{Vq}|^2)}_{\min}$ determines the initial operating state of the UPFC under normal steady state operation (NSSO) condition whereas $|\bar{V}se|_{max} = \sqrt{(|\mathrm{Vp}|^2 + |\mathrm{Vq}|^2)}_{\max}$ determines the maximum operating capability of the UPFC device under different conditions.

In this study, methods of determining the minimum and maximum values of the series voltage injection are from corresponding grid simulations under normal steady state operation and contingency condition, respectively. Accordingly, the minimum value of series voltage injection at which UPFC is looked to be deployed is determined from the power flow result report of the grid under normal steady state operation without UPFC deployment. Contrastingly, the maximum value of series voltage injection is determined from the same transmission line but to be searched at which contingent element does the maximum limit violation occurs among selected contingency studies.

4.2.1 Line Loading Management

The identified weakest TLs in terms of the line loading, either overload or underload case, as of measured with the joint indices are managed differently when seen from the control parameter setting perspective of the series component of the UPFC. More specifically, the control mode of the quadrature component of the series injected voltage is constant reactance in which the component voltage is varying with respect to the line current so as to keep the line impedance constant. Importantly, the line resistance is neglected under this control mode. The options UPFC operation modes, constant voltage and constant reactance, are shown in depicted Figure 4.1.

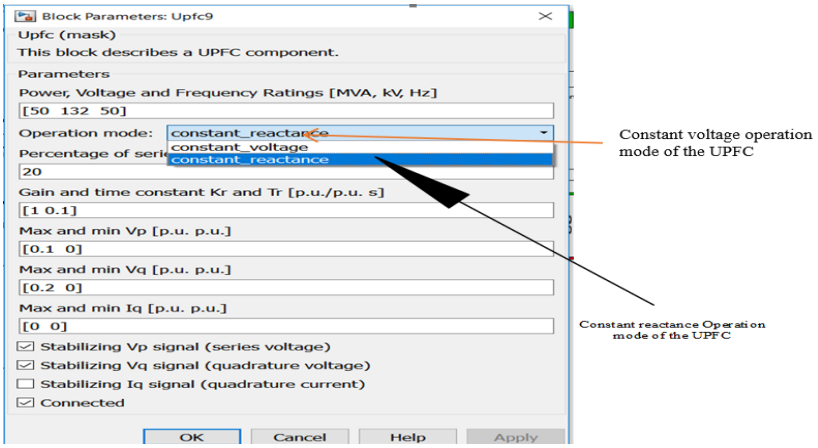

Figure 4.1. Operation modes of the UPFC device

Here, both TL loading (overload and underload) cases are considered, and the cases are independently described as below.

Case 1: Overloaded TL Management

It is investigated that the overloaded transmission lines (TLs) are 132 kV TLs alone as it has been observed throughout the case simulations conducted under selected contingencies. The solution phase of this case study is intended to reduce over duty of those TLs loading as of the results obtained from the simulations under different outage conditions. Under this case, the series injected voltage via series component of the UPFC is to be done in a such a way that the TL loading is to be reduced until the specific objective is achieved.

This role is played with the series voltage injection which greatly depends on the careful parameter setting either to manage the line loading, reduce or advance the magnitude of the power flow, or even change the direction of the power flow as per the interest to do. The minimum series voltage injection is decided based on the interest to keep the value of line flows and the maximum series voltage injection is determined from the stated guideline i.e., maximally, the ceiling of the series voltage injection by UPFC is not greater than 30 percent of the line thermal MVA. In other words, the nominal rating of the UPFC (MVA) is chosen to be 30 percent of the line thermal MVA at which it going to be installed.

Mathematical formulation based UPFC parameter setting gives overall clues which is calculated based on the control objective to be achieved. At the first step, the grid model is simulated under the specified values of the state variables, calculated magnitude of series voltage injection and 0^0 flat start of the UPFC reference angle (γ), so that the power flow report is observed and furtherly, the effect of the output with UPFC is compared with respect to the desired output. The magnitude of the series voltage to be injected is pivoted and the UPFC reference angle (γ) is varied with the step of 10^0 till the desired result is obtained.

For the case study of the overloaded TLs, the focus is mainly on the real power flow through the affected lines as per the calculated indice value from the simulation results obtained. Accordingly, the real power flow equation between buses i and j, by considering bus i as sending end, is given by

$$P_{ij} = b_{ij}V_iV_j\,sin(\delta i - \delta j) + rb_{ij}V_iV_j\,sin(\delta i - \delta j + \gamma) \quad (4.1)$$

It is important to note here that the TL resistance is neglected from the equation for the sake of simplicity to perform the analysis and as it is not also considered by UPFC too. As it is observed from the real power flow equation above, the intended value of the second term which is provided by the UPFC being installed must be negative with respect to first term in order to keep the overloaded TL safer.

Among the set of the UPFC power injection, let us consider the UPFC real power injection at bus i, considered as sending end and shunt side of the UPFC, to determine corresponding minimum and maximum values of series voltage injection.

$$P_{i-UPFC} = -P_{se} + P_i = -rb_{ij}V_iV_j \sin(\delta i - \delta j + \gamma) \tag{4.2}$$

where,

$$rV_i = \sqrt{(|Vp|^2 + |Vq|^2)}$$

Therefore,

$$P_{i-UPFC\_min} = -b_{ij}V_j\sqrt{(|Vp|^2 + |Vq|^2)}_{min} \sin(\delta i - \delta j + \gamma) \tag{4.3}$$

$$P_{i-UPFC\_max} = -b_{ij}V_j\sqrt{(|Vp|^2 + |Vq|^2)}_{max} \sin(\delta i - \delta j + \gamma) \tag{4.4}$$

The interest on the magnitude of the power flow on selected TL at NSSO is the determinant factor to select the minimum real power injection by UPFC in which it is furtherly used to decide the minimum series voltage injection. In contrast, the possibly maximum real power injection capability of the UPFC depends on the maximum line loading resulted from the corresponding contingent among simulated contingencies, then used to determine the maximum series voltage injection. If needed, corresponding reactive power injection due to the series voltage injection by UPFC can be calculated.

Case 2: Underloaded TL Management

It has been observed from the power flow simulation result that most of the TLs are almost underloaded except 132 kV TLs as stated in case 1. In this case, the solution phase is aimed to advance the magnitude of the real power flow for feasibly selected TL at which UPFC device is going to be installed.

However, UPFC parameter setting is in a such a way that the desired objective is met which is contrasting task with case 2. The way and method for both UPFC parameter setting and selection is similar as case 2 as already stated but with different desired specific objective.

4.2.2 Bus Voltage improvement

For transmission line (TL) weakness as evaluated in terms of line voltage stability and line power flow performance, the magnitude of the bus voltage is one of the determinant factor for the used index values. It has been observed that the most overloaded lines are extremely exposed to the voltage slashing from the minimum predefined values. For this, 132 kV system voltages are good examples and the weakest buses which strongly needs independent bus voltage compensation methods.

Under this study, the voltage gets improved with the series line compensation setting of the deployed UPFC in combination with the series voltage injection capability though shunt component of the UPFC is not configured actively yet intended to maintain the desired bus voltage at which it is connected. In other words, keeping the desired series voltage injection to be performed by the UPFC, the bus voltage improvements can be obtained parallelly with the series line compensation setting of the UPFC.

Table 4.2. UPFC selection and parameter settings

Affected Transmission Line (From_To)	No. of TL ckt	UPFC Selection and setting				
		Voltage (kV)	Frequency (Hz)	γ values of UPFC setting (deg)	% Series Compensation (% Cp)	Quadrature Voltage Control Mode
32_Hurso-26_Koka	2	230	50	60	70	Constant Voltage
2_Sululta-10_D/Markos	1	400	50	0	70	Constant Voltage
7_Wolyta-3_Gelan	2	400	50	10	60	Constant Voltage
5_G/Guracha-10_D/Markos	1	400	50	5	70	Constant Voltage
11_GG-II PP-7_Wolyta	1	400	50	120	30	Constant Voltage
54_Alamata-61_Ashogoda WF	1	230	50	5	70	Constant Voltage
13_Legetafo-39_Combolcha-II	1	230	50	170	70	Constant Voltage
87_Alaba-97_Wolyta	1	132	50	90	10	Constant Reactance
80_Shashemene-87_Alaba	1	132	50	90	10	Constant Reactance
56_Humera-44_Gonder-II	1	230	50	5	70	Constant Voltage

81_M/Waka.Yugo-80_Shashemen	1	132	50	90	70	Constant Reactance
76_Gelan-77_Yesu	1	132	50	90	50	Constant Reactance
77_Yesu-67_Kaliti-I	1	132	50	90	-10	Constant Reactance
31_D/dawa-III-25_Awash-7KL	1	230	50	20	70	Constant Voltage
25_Awash-7KL-26_Koka	1	230	50	20	70	Constant Voltage

From Table 4.2, γ values of UPFC are found by searching with increment of 10^0 until satisfactory result is obtained. As already stated, quadrature voltage control mode is constant voltage for statically instable TLs whereas constant reactance for overloaded TLs. Percentage (%) series compensation (% Cp) of TL is chosen based on necessity of TL to be compensated in a such a way to obtain better result.

4.3 Mathematical Modelling of High Voltage Grid with UPFC

The series converter (converter 2) constitutes the main function of the UPFC device whereas the shunt converter (converter 1) is the direct forward function as other controlled shunt voltage compensating devices to maintain the voltage magnitude of that bus at specified value. From the perspective of this study, the shunt converter is maintained at inactive mode so that it is unable to inject the reactive power demanded at the connected bus due to reason that it needs PV (generator connected) bus at its defined sending end bus. Generally, the series converter plays a great role in controlling the power flow through intended transmission line and the mathematical model of the power injection mechanism is going to be dealt here.

Basically, the UPFC concept is derived from the integration of the STATCOM and SSSC device's function and its circuit is constructed by incorporating the circuits of both FACTS devices. It is represented by one series voltage source $\overline{v}s$ and by one shunt current source $\overline{i}sh$, as depicted in Figure 4.2.

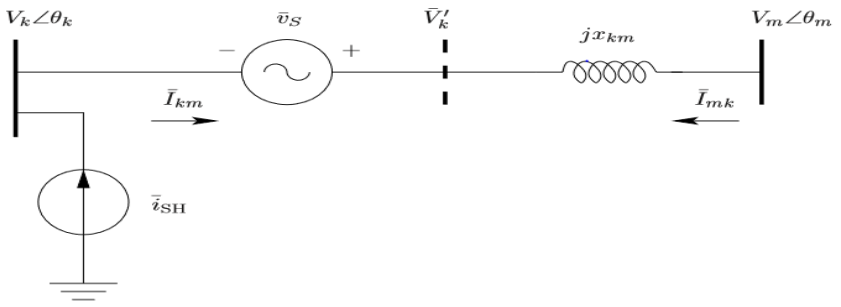

Figure 4.2. Circuit of the UPFC [28]

The series voltage source and the shunt current source are defined as follows [34]:

$$\bar{v}_s = (v_p + v_q)e^{j\varphi} = r\bar{V}ke^{j\gamma} \tag{4.5}$$

$$\bar{\imath}_{SH} = (i_p + i_q)e^{j\theta_k} \tag{4.6}$$

UPFC State Variables [28]:

v_p: This variable represents the component of the series voltage $\bar{v}_s$ that is in phase with the line current.

v_q: This variable represents the component of series voltage $\bar{v}_s$ that is in quadrature with line current. Two control modes are implemented for this variable:

1. Constant voltage: the magnitude of voltage v_q is constant independently of the line current.
2. Constant reactance: the magnitude of the voltage v_q varies proportionally to the line current keeping constant the total impedance (the resistance is actually neglected) of the transmission line.

i_q: This variable represents the component of shunt current $\bar{\imath}_{SH}$which is in quadrature with the bus voltage $\bar{V}_k$.

4.3.1 Mathematical Model of UPFC Series Component

As already explored, the series component of the UPFC stands for converter 2 which is derived from the concept of SSSC basics and represented by series voltage source. According to the definitions provided, let us consider the phasor diagram of the UPFC series voltage source depicted in Figure 4.3.

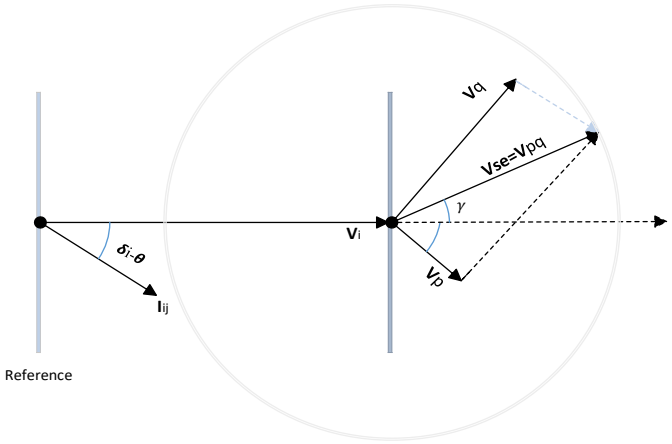

Figure 4.3. Phasor diagram of the UPFC

where,

$\bar{V}_{se}$ - series injected vector voltage $\bar{V}_{pq}$ by converter 2

$\bar{V}_p$ -the component of the series injected voltage in phase with the line current $\bar{I}_{ij}$

$\bar{V}_q$ -the component of the series injected voltage in quadrature with the line current $\bar{I}_{ij}$ so with $\bar{V}_p$

$\bar{I}_{ij}$ -the line current from bus i to j at angle of $(\delta_i - \theta)$ with respect to bus i voltage, V_i

γ- the relative angle of the $\bar{V}_{se}$

From the phasor diagram of the UPFC above, it is observable that the series injected vector voltage , ***V***se or ***V***pq, by series converter is the sum of two vectors ***V***p and ***V***q. Accordingly, it can be expressed as:

$$\bar{V}se = \bar{V}pq = \bar{V}p + \bar{V}q \tag{4.7}$$

According to the definitions,

$$\bar{V}p = |Vp|\angle(\delta i - \theta) = |Vp|e^{j(\delta i-\theta)} \tag{4.8}$$

$$\bar{V}q = |Vq|\angle(\delta i - \theta + 90°) = |Vq|e^{j(\delta i-\theta+90°)} \tag{4.9}$$

$$\bar{V}se = |Vp|e^{j(\delta i-\theta)} + |Vq|e^{j(\delta i-\theta+90°)}$$

$$= e^{j(\delta i-\theta)}\left[|Vp| + |Vq|e^{j90}\right]$$

$$= e^{j(\delta i-\theta)}[|Vp| + j|Vq|]$$

$$= e^{j(\delta i-\theta)}\left[\sqrt{(|Vp|^2 + |Vq|^2)}\angle\left(\tan^{-1}\left(\frac{|Vq|}{|Vp|}\right)\right)\right]$$

$$= e^{j(\delta i-\theta)}\left[\sqrt{(|Vp|^2 + |Vq|^2)}\angle(\delta i - \theta + \gamma)\right]$$

$$= \left[\sqrt{(|Vp|^2 + |Vq|^2)}\right] e^{j(2\delta i-2\theta+\gamma)}$$

$$\bar{V}se = \left[\sqrt{(|Vp|^2 + |Vq|^2)}\right]e^{j2(\delta i-\theta)}.e^{j\gamma} \quad (4.10)$$

It can be expressed as that $\bar{V}$se with magnitude of $\sqrt{(|\mathrm{Vp}|^2 + |\mathrm{Vq}|^2)}$ and lying at initial angle of $2(\delta \mathrm{i} - \theta)$ with respect to the line current $\bar{I}$ij is the rotating vector voltage about a circle of radius $\sqrt{(|\mathrm{Vp}|^2 + |\mathrm{Vq}|^2)}$ with variable rotational angle of γ with respect to voltage Vi of bus i axis as a reference. It is possible to deduce the ranges of controlled variables of UPFC series converter component within provided control region as it is shown with circle basics in phasor diagram. The magnitude of controllable series injected voltage by converter 2 can be varied $\left[\sqrt{(|\mathrm{Vp}|^2 + |\mathrm{Vq}|^2)}\right]\mathrm{min.} \leq \sqrt{(|Vp|^2 + |Vq|^2)} \leq \left[\sqrt{(|\mathrm{Vp}|^2 + |\mathrm{Vq}|^2)}\right]\mathrm{max.}$ and γ can be varied throughout the interested control region of the circle with chosen radius $\left[\sqrt{(|\mathrm{Vp}|^2 + |\mathrm{Vq}|^2)}\right]$ i.e., $0^\circ \leq \gamma \leq 360^\circ$.

There are two modes of control for quadrature component of the series injection voltage. Those are: constant voltage mode in which the magnitude of the Vq is kept constant independent of the line current and constant reactance mode where the magnitude of the Vq varies proportionally with line current in order to maintain the reactance constant noting that the line resistance is neglected.

In general, the series voltage injection representation has been expressed in terms of phasor voltage $\bar{V}i$ with multiplying factor r where $r_{min} \leq r \leq r_{max}$.

$$\bar{V}se = r\bar{V}ie^{j\gamma} \quad (4.11)$$

So,

$$\bar{V}se = r\bar{V}ie^{j\gamma} = \left[\sqrt{(|Vp|^2 + |Vq|^2)}\right]e^{j2(\delta i-\theta)}.e^{j\gamma} \quad (4.12)$$

Equating both sides,

$$r\bar{V}i = \left[\sqrt{(|Vp|^2 + |Vq|^2)}\right]e^{j2(\delta i-\theta)} \quad (4.13)$$

$$|\bar{V}se| = r|\bar{V}i| = \sqrt{(|Vp|^2 + |Vq|^2)} \quad (4.14)$$

Let us consider the UPFC circuit deployed between two buses i and j as depicted in Figure 4.4. It can be represented by one series voltage source and one shunt current source between bus i and an imaginary bus i`.

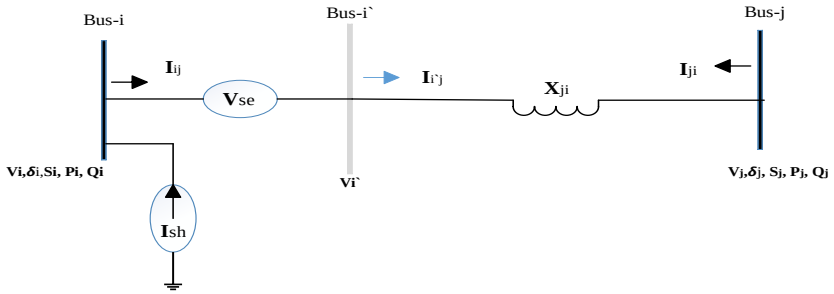

Figure 4.4. The circuit model of the UPFC

To go through the derivations of the power injections by the series component of the UPFC (converter 2), series voltage source can be represented equivalently by shunt current source as depicted in Figure 4.5.

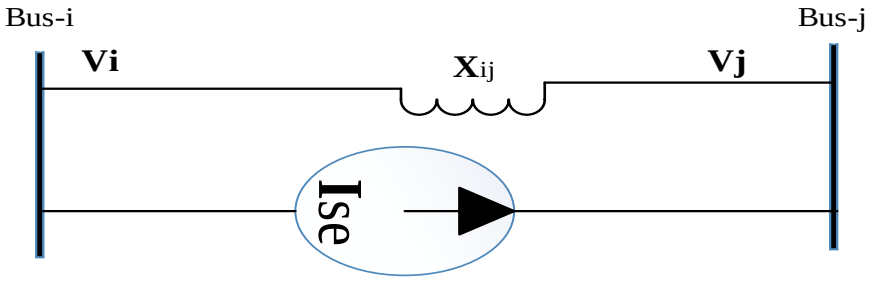

Figure 4.5. Current source representation of series voltage source

From the Figure 4.5,

$$\bar{I}se = -jb_{ij}\bar{V}se \quad (4.15)$$

Where, $b_{ij} = \frac{1}{X_{ij}}$

The corresponding complex power injection at both buses by series component of the UPFC, converter 2, can be obtained as follows. Let us consider Figure 4.6 to perform the derivations with respect to the shunt current source representation of the series voltage source. It is important to note that throughout manipulations, the transmission line resistance is neglected, and lossless converters are considered.

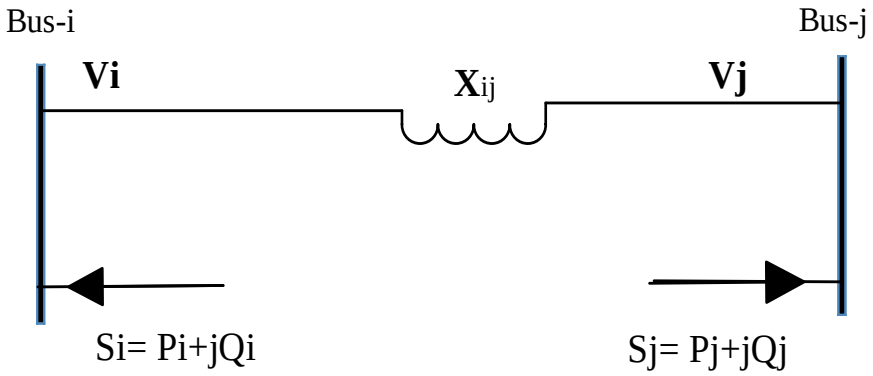

Figure 4.6. Injection model of the series component of the UPFC

Complex power injection at bus i:

$$S_i = \bar{V}i(-\bar{I}se)^* = -\bar{V}i\left(-jb_{ij}\bar{V}se\right)^* = -\bar{V}i\left(-jb_{ij}r\bar{V}ie^{j\gamma}\right)^* \tag{4.16}$$

$$= -rb_{ij}V_i^2 e^{j\delta i}\left(e^{j(\delta i+\gamma-90°)}\right)^*$$

$$= -rb_{ij}V_i^2 e^{j\delta i}e^{-j(\delta i+\gamma-90°)}$$

$$= -rb_{ij}V_i^2 e^{-j(\gamma-90°)}$$

$$= -rb_{ij}V_i^2[\cos(\gamma-90°) - \mathrm{j}\sin(\gamma-90°)]$$

$$S_i = -rb_{ij}V_i^2[\sin\gamma + \mathrm{j}\cos\gamma] = P_i + jQ_i \tag{4.17}$$

$$P_i = -rb_{ij}V_i^2 \sin\gamma \tag{4.18}$$

$$Q_i = -rb_{ij}V_i^2 \cos\gamma \tag{4.19}$$

Complex power injection at bus j:

$$S_j = \bar{V}j(\bar{I}se)^* = \bar{V}j\left(-jb_{ij}\bar{V}se\right)^* = \bar{V}j\left(-jb_{ij}r\bar{V}ie^{j\gamma}\right)^* \tag{4.20}$$

$$= rb_{ij}V_j e^{j\delta j}\left(e^{j(\delta i+\gamma-90°)}\right)^*$$

$$= rb_{ij}V_i V_j e^{j\delta j} e^{-j(\delta i+\gamma-90°)}$$

$$= rb_{ij}V_i V_j e^{-j(\delta i-\delta j+\gamma-90°)}$$

$$= rb_{ij}V_i V_j[\cos(\delta i-\delta j+\gamma-90°)-\mathrm{j}\sin(\delta i-\delta j+\gamma-90°)]$$

$$= rb_{ij}V_i V_j[\sin(\delta i-\delta j+\gamma)+\mathrm{j}\cos(\delta i-\delta j+\gamma)]$$

$$= rb_{ij}V_i V_j[\sin(\delta ij+\gamma)+\mathrm{j}\cos(\delta ij+\gamma)]$$

Where, $\delta_{ij}=\delta_i-\delta_j$

$$S_j = rb_{ij}V_i V_j[\sin(\delta ij+\gamma)+\mathrm{j}\cos(\delta ij+\gamma)] = P_j + jQ_j \quad (4.21)$$

$$P_j = rb_{ij}V_i V_j \sin(\delta ij+\gamma) \quad (4.22)$$

$$Q_j = rb_{ij}V_i V_j \cos(\delta ij+\gamma) \quad (4.23)$$

Furthermore, the power injection due to the series voltage injected via converter 2 can be manipulated using the series component injection model of the UPFC.

$$S_{se} = \bar{V}se(\bar{I}ij)^* = r\bar{V}ie^{j\gamma}\left(\frac{\bar{V}i\grave{}-\bar{V}j}{jX_{ij}}\right)^* = r\bar{V}ie^{j\gamma}\left(\frac{\bar{V}i+\bar{V}se-\bar{V}j}{jX_{ij}}\right)^* \quad (4.24)$$

$$= r\bar{V}ie^{j\gamma}\left(\frac{\bar{V}i+r\bar{V}ie^{j\gamma}-\bar{V}j}{jX_{ij}}\right)^* = rb_{ij}V_i e^{j\delta i}e^{j\gamma}e^{j90°}\left(V_i e^{j\delta i}+rV_i e^{j\delta i}e^{j\gamma}-V_j e^{j\delta j}\right)^*$$

$$= rb_{ij}{V_i}^2 e^{j(\gamma+90°)}+r^2 b_{ij}{V_i}^2 e^{j90°}-rb_{ij}V_i V_j e^{j(\delta i-\delta j+\gamma+90°)}$$

$$= \left\{\left[rb_{ij}{V_i}^2\cos(\gamma+90°)-rb_{ij}V_i V_j\cos(\delta i-\delta j+\gamma+90°)\right]\right.$$
$$\left.+\,j\left[rb_{ij}{V_i}^2\sin(\gamma+90°)+r^2 b_{ij}{V_i}^2-rb_{ij}V_i V_j\sin(\delta i-\delta j+\gamma+90°)\right]\right\}$$

$$S_{se} = \left\{\left[-rb_{ij}{V_i}^2\sin\gamma+rb_{ij}V_i V_j\sin(\delta i-\delta j+\gamma)\right]+j\left[rb_{ij}{V_i}^2\cos\gamma+r^2 b_{ij}{V_i}^2-\right.\right.$$
$$\left.\left.rb_{ij}V_i V_j\cos(\delta i-\delta j+\gamma)\right]\right\} = P_{se}+jQ_{se} \quad (4.25)$$

By equating both sides,

$$P_{se} = -rb_{ij}V_i{}^2 \sin\gamma + rb_{ij}V_iV_j \sin(\delta i - \delta j + \gamma) \quad (4.26)$$

$$Q_{se} = rb_{ij}V_i{}^2 \cos\gamma + r^2 b_{ij}V_i{}^2 - rb_{ij}V_iV_j \cos(\delta i - \delta j + \gamma) \quad (4.27)$$

Power flow through the line from either of the buses including power injected by series converter can be obtained from the manipulations of the equations as under below.

From bus i (shunt) side:

$$S_{ij} = \bar{V}i`(\bar{I}ij)^* = \bar{V}i` \left(\frac{\bar{V}i` - \bar{V}j}{jX_{ij}}\right)^* \quad (4.28)$$

$$S_{ij} = \bar{V}i`(\bar{I}ij)^* = (\bar{V}i + \bar{V}se)\left(\frac{\bar{V}i + \bar{V}se - \bar{V}j}{jX_{ij}}\right)^*$$

$$S_{ij} = jb_{ij}\{\bar{V}i\bar{V}i^* + \bar{V}i\bar{V}se^* - \bar{V}i\bar{V}j^* + \bar{V}se\bar{V}i^* + \bar{V}se\bar{V}se^* - \bar{V}se\bar{V}j^*\}$$

$$S_{ij} = jb_{ij}\{\bar{V}i\bar{V}i^* + \bar{V}i(r\bar{V}ie^{j\gamma})^* - \bar{V}i\bar{V}j^* + (r\bar{V}ie^{j\gamma})\bar{V}i^* + (r\bar{V}ie^{j\gamma})(r\bar{V}ie^{j\gamma})^* - (r\bar{V}ie^{j\gamma})\bar{V}j^*\}$$

$$S_{ij} = b_{ij}e^{j90^\circ}\{V_i^2 + rV_i^2e^{-j\gamma} - V_iV_je^{j(\delta i - \delta j)} + rV_i^2e^{j\gamma} + r^2V_i{}^2 - rV_iV_je^{j(\delta i - \delta j + \gamma)}\}$$

$$S_{ij} = b_{ij}V_i^2e^{j90^\circ} + rb_{ij}V_i^2e^{-j(\gamma - 90^\circ)} - b_{ij}V_iV_je^{j(\delta i - \delta j + 90^\circ)} + rb_{ij}V_i^2e^{j(\gamma + 90^\circ)} + r^2b_{ij}V_i{}^2e^{j90^\circ} - rb_{ij}V_iV_je^{j(\delta i - \delta j + \gamma + 90^\circ)}$$

$$\begin{aligned} S_{ij} = \{&[rb_{ij}V_i^2\, cos(\gamma - 90^\circ) - b_{ij}V_iV_j\, cos(\delta i - \delta j + 90^\circ) \\ &+ rb_{ij}V_i^2\, cos(\gamma + 90^\circ) - rb_{ij}V_iV_j\, cos(\delta i - \delta j + \gamma + 90^\circ)] \\ &+ j[b_{ij}V_i^2 \\ &- rb_{ij}V_i^2\, sin(\gamma - 90^\circ) - b_{ij}V_iV_j sin(\delta i - \delta j + 90^\circ) + rb_{ij}V_i^2 sin(\gamma + 90^\circ) \\ &+ r^2b_{ij}V_i{}^2 - rb_{ij}V_iV_j\, sin(\delta i - \delta j + \gamma + 90^\circ)]\} \end{aligned}$$

$$\begin{aligned} S_{ij} = \{&[rb_{ij}V_i^2\, sin\gamma + b_{ij}V_iV_j\, sin(\delta i - \delta j) - rb_{ij}V_i^2\, sin\gamma + rb_{ij}V_iV_j\, sin(\delta i - \delta j + \gamma)] + \\ &j[b_{ij}V_i^2 + rb_{ij}V_i^2\, cos\gamma - b_{ij}V_iV_j cos(\delta i - \delta j) + rb_{ij}V_i^2 cos\gamma + r^2b_{ij}V_i{}^2 - rb_{ij}V_iV_j\, cos(\delta i - \\ &\delta j + \gamma)]\} = P_{ij} + jQ_{ij} \end{aligned} \quad (4.29)$$

By equating both sides,

$$P_{ij} = b_{ij}V_iV_j\, sin(\delta i - \delta j) + rb_{ij}V_iV_j\, sin(\delta i - \delta j + \gamma) \quad (4.30)$$

$$Q_{ij} = b_{ij}V_i^2 + 2rb_{ij}V_i^2\,cos\gamma - b_{ij}V_iV_jcos(\delta i - \delta j) + r^2b_{ij}V_i^{\,2} - rb_{ij}V_iV_j\,cos(\delta i - \delta j + \gamma) + Q_{conv-1} \quad (4.31)$$

Where, $Q_{conv\text{-}1}$ is the reactive power delivered or absorbed to or from bus i respectively by converter 1, shunt component of the UPFC, to achieve the controlled voltage at bus i if the converter is in active mode state. $P_{ij} = b_{ij}V_iV_j\,sin(\delta i - \delta j)$ and $Q_{ij} = b_{ij}V_i^2 - b_{ij}V_iV_jcos(\delta i - \delta j)$- are the real and reactive power flows respectively at the sending end (bus i) without UPFC deployment on the transmission line whereas the remaining components of both line flow equations are provided by the UPFC device. Moreover, it is important to note that real power flows both at the sending and receiving ends are the same hence, the line resistance is neglected in conducting the analysis though it does not hold true in practical.

From bus j side:

In the same manner, the line power flow can be derived from the receiving end (bus j) side in order to have well understanding about power flows with respect to the either sending or receiving end side.

$$S_{ji} = \bar{V}j(-\bar{I}ij)^* = -\bar{V}j\left(\frac{\bar{V}i` - \bar{V}j}{jX_{ij}}\right)^* \quad (4.32)$$

$$S_{ji} = -\bar{V}j\left(\frac{\bar{V}i + \bar{V}se - \bar{V}j}{jX_{ij}}\right)^*$$

$$S_{ji} = -jb_{ij}\{\bar{V}j\bar{V}i^* + \bar{V}j\bar{V}se^* - \bar{V}j\bar{V}j^*\}$$

$$S_{ji} = -jb_{ij}\{\bar{V}j\bar{V}i^* + \bar{V}j(r\bar{V}ie^{j\gamma})^* - \bar{V}j\bar{V}j^*\}$$

$$S_{ji} = b_{ij}e^{-j90^\circ}\{V_iV_je^{-j(\delta i-\delta j)} + rV_iV_je^{-j(\delta i-\delta j+\gamma)} - V_j^2\}$$

$$S_{ji} = b_{ij}V_iV_je^{-j(\delta i-\delta j+90^\circ)} + rb_{ij}V_iV_je^{-j(\delta i-\delta j+\gamma+90^\circ)} - b_{ij}V_j^2e^{-j90^\circ}$$

$$S_{ji} = \{[b_{ij}V_iV_j\,cos(\delta i - \delta j + 90^\circ) + rb_{ij}V_iV_j\,cos(\delta i - \delta j + \gamma + 90^\circ)] + j[-b_{ij}V_iV_j\,sin(\delta i - \delta j + 90^\circ) - rb_{ij}V_iV_j\,sin(\delta i - \delta j + \gamma + 90^\circ) + b_{ij}V_j^2]\}$$

$$S_{ji} = \{[-b_{ij}V_iV_j \sin(\delta i - \delta j) - rb_{ij}V_iV_j\, sin(\delta i - \delta j + \gamma)] + j[-b_{ij}V_iV_j\, cos(\delta i - \delta j) - rb_{ij}V_iV_j\, cos(\delta i - \delta j + \gamma) + b_{ij}V_j^2] = P_{ji} + jQ_{ji}\} \quad (4.33)$$

Equating both sides,

$$P_{ji} = -b_{ij}V_iV_j \sin(\delta i - \delta j) - rb_{ij}V_iV_j\, sin(\delta i - \delta j + \gamma) = -P_{ij} \quad (4.34)$$

$$Q_{ji} = -b_{ij}V_iV_j\, cos(\delta i - \delta j) - rb_{ij}V_iV_j\, cos(\delta i - \delta j + \gamma) + b_{ij}V_j^2 \quad (4.35)$$

The difference is clearly observable that the reactive power flow components contributed by UPFC are quite different at both ends i.e., at receiving end the losses and reactive power of converter 1, to or from, are not included and vice versa is true for sending end (shunt side of the UPFC).

Generally, the conclusions deduced from the power injection models of series component of the UPFC are summarized as follows. Independently, the vector components of the series voltage source injected have either impacts or no impacts as summarized below.

1. In-phase component ($\mathbf{V}_p$) of the series voltage source ($\mathbf{V}_{se}$)
   - ✓ Case where $\mathbf{V}_q$=0
   - ✓ Component of the series voltage source injected in-phase with the line current
   - ✓ Can control the magnitude of the real power flow prior to the injection but cannot change flow direction
   - ✓ Have no impacts on both magnitude and direction of the reactive power flow prior to the injection
2. Quadrature component ($\mathbf{V}_q$) of the series voltage source ($\mathbf{V}_{se}$)
   - ✓ Case where $\mathbf{V}_p$=0
   - ✓ Component of the series voltage source injected in quadrature with the line current
   - ✓ Cannot control and change both magnitude and direction of the real power flow prior to the injection respectively
   - ✓ Can control magnitude and change direction of the reactive power flow prior to the injection
3. Combined effect of both components ($\mathbf{V}_{se}$)

This is the case where both injected series voltage components are non-zero values. The combination of both vector components of the series voltage source injected constitutes the overall function of the series component (converter 1) of the UPFC device. The series component of the UPFC is an intended component for the power flow control objectives but cannot control bus voltage yet, unless series line compensation is jointly allowed. This characterizes the full function of the series component of the device as under listed.

- ✓ Can control the magnitude of the power flow prior to the injection
- ✓ Can change the direction of the power flow prior to the injection

4.3.2 Mathematical Model of UPFC Shunt Component

As already explored, the shunt component of the UPFC stands for converter 1 which is derived from the concept of STATCOM basics and represented by shunt current source. The main function of this component is to control and maintain the preset value of the voltage at bus i either by supplying or absorbing the reactive power independently and supply the real power demand (P_{se}) by converter 2 plus power losses encountered by converters if the loss of converters is interested to be included. In fact, this component constitutes less important part of the UPFC device in comparison with the series component; the model of reactive power injection at bus i by shunt current source and the real power exchange with series converter (converter 2) are dealt under this sub-section.

The shunt current source injection model can be converted to a voltage source with equivalent series reactance noting that the resistance is neglected, and it can be modelled independently as circuit represented in Figure 4.7.

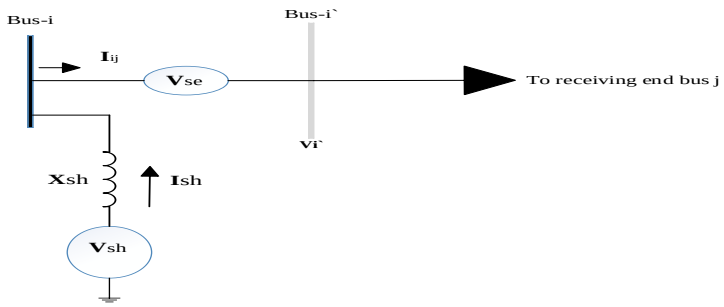

Figure 4.7. The injection model of the shunt component of the UPFC

Moreover, shunt current source can be also decomposed in to in-phase and quadrature component with respect to the voltage Vi at bus i; the concept is derived from the [23] and stated formula in [28]. Of course, in-phase component is not important part of the shunt current source from the bus voltage control perspective so that only quadrature component can be used to meet the stated purpose.

Ip and Iq are respectively the real and imaginary controllable components of ideal shunt current source. Ip, in-phase components with respect to Vi, is determined by active power of shunt converter exchanging with the system and the loss of UPFC. However, Iq is in quadrature components with respect to Vi, which provides independent shunt reactive compensation to maintain bus voltage level where the UPFC is installed [23].

According to the definitions provided, let us consider the phasor diagram of the UPFC shunt current source depicted in Figure 4.8.

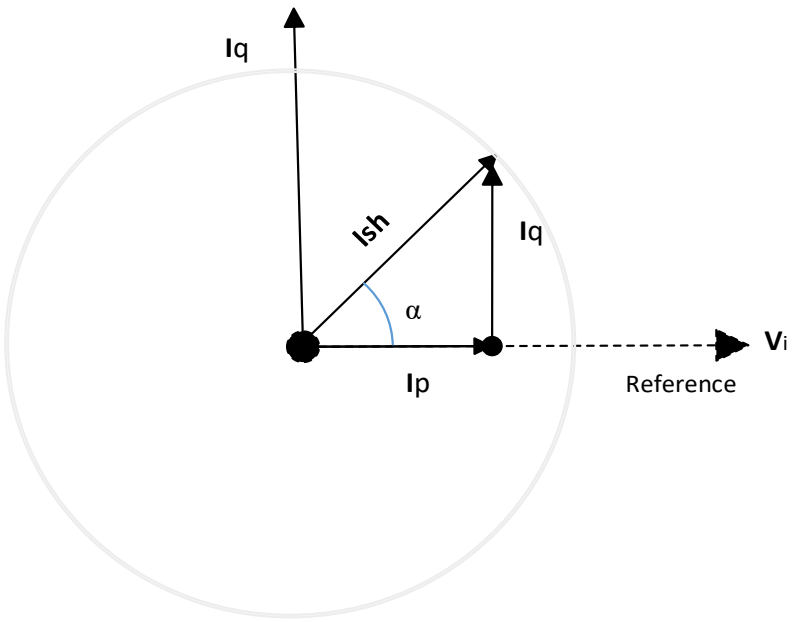

Figure 4.8. The phasor diagram of the shunt component of the UPFC

From the phasor diagram of the shunt component of the UPFC device depicted in Figure 4.8, it is observable that the shunt current source (***I***sh) of shunt converter is the sum of two vector components ***I***p and ***I***q. Accordingly, it can be expressed as:

$$\bar{I}sh = \bar{I}p + \bar{I}q \tag{4.36}$$

$\bar{I}sh$- shunt current source of converter 1

$\bar{I}p$-the component of the shunt current source in-phase with the voltage $\bar{V}i$

$\bar{I}q$-the component of the shunt current source in quadrature with the with the voltage $\bar{V}i$

α- the relative angle of the $\bar{I}sh$ with respect to $\bar{V}i$ as reference

Accordingly, the vectors can be defined as below.

$$\bar{I}p = |Ip|\angle(\delta i) = |Ip|e^{j\delta i} \tag{4.37}$$

$$\bar{I}q = |Iq|\angle(\delta i + 90°) = |Iq|e^{j(\delta i + 90°)} \tag{4.38}$$

$$\bar{I}sh = |Ip|e^{j\delta i} + |Iq|e^{j(\delta i + 90°)}$$

$$= e^{j\delta i}\left[|Ip| + |Iq|e^{j90}\right]$$

$$= e^{j\delta i}[|Ip| + j|Iq|]$$

$$= e^{j\delta i}\left[\sqrt{(|Ip|^2 + |Iq|^2)}\angle\left(\tan^{-1}\left(\frac{|Iq|}{|Ip|}\right)\right)\right]$$

$$= e^{j\delta i}\left[\sqrt{(|Ip|^2 + |Iq|^2)}\angle(\alpha)\right]$$

$$= \left[\sqrt{(|Ip|^2 + |Iq|^2)}\right]e^{j(\delta i + \alpha)}$$

$$\bar{I}sh = \left[\sqrt{(|Ip|^2 + |Iq|^2)}\right]e^{j\delta i}.e^{j\alpha} \tag{4.39}$$

It can be expressed as that $\bar{I}$sh with magnitude of $\sqrt{(|Ip|^2 + |Iq|^2)}$ and lying at initial angle of δi , in-phase, with respect to the voltage $\bar{V}$i is the rotating vector current about a circle of radius $\sqrt{(|Ip|^2 + |Iq|^2)}$ with variable rotational angle of α with respect to voltage Vi of bus i as a reference. It is possible to deduce the ranges of controlled variables of UPFC shunt converter

component within provided control region as it is shown with circle basics in phasor diagram. For lossless converters, the magnitude of controllable reactive power compensation of the bus i, and delivery of real power demand by converter 2 can be varied $\left[\sqrt{(|\mathrm{Ip}|^2+|\mathrm{Iq}|^2)}\right]\min. \leq \sqrt{(|Ip|^2+|Iq|^2)} \leq \left[\sqrt{(|\mathrm{Ip}|^2+|\mathrm{Iq}|^2)}\right]\max.$. Moreover, the variable angle α variation can be achieved with variation of corresponding shunt current components so that the interested control region of the circle with chosen radius $\left[\sqrt{(|\mathrm{Ip}|^2+|\mathrm{Iq}|^2)}\right]$ can be varied through $0^\circ \leq \alpha \leq 360^\circ$. Jointly, it is important to note that the nominal shunt current (Ish-nominal) of the converter 1 must be specified to meet the objective control of the interested parameter.

Furthermore, the complex power of shunt component of UPFC can be obtained by manipulating equations below.

$$Ssh = \bar{V}sh(\bar{I}sh)^* \tag{4.40}$$

Where, $\bar{V}sh$ is obtained from shunt current source conversion and given by,

$$\bar{V}sh = \bar{I}sh(jx_{sh}) = x_{sh}\sqrt{(|Ip|^2+|Iq|^2)}e^{j(\delta i+\alpha+90^\circ)} \tag{4.41}$$

Then,

$$Ssh = \bar{V}sh\left(\frac{\bar{V}sh-\bar{V}i}{jx_{sh}}\right)^* \tag{4.42}$$

$$Ssh = x_{sh}b_{sh}\sqrt{(|Ip|^2+|Iq|^2)}e^{j(\delta i+\alpha+90^\circ+90^\circ)}\left(x_{sh}\sqrt{(|Ip|^2+|Iq|^2)}e^{j(\delta i+\alpha+90^\circ)}-V_ie^{j\delta i}\right)^*$$

$$Ssh = \sqrt{(|Ip|^2+|Iq|^2)}e^{j(\delta i+\alpha+90^\circ+90^\circ)}\left(x_{sh}\sqrt{(|Ip|^2+|Iq|^2)}e^{-j(\delta i+\alpha+90^\circ)}-V_ie^{-j\delta i}\right)$$

$$Ssh = x_{sh}(|Ip|^2+|Iq|^2)e^{j90^\circ}-V_i\sqrt{(|Ip|^2+|Iq|^2)}\ \ e^{j(\alpha+180^\circ)}$$

$$Ssh = \left\{\left[\left(-V_i\sqrt{(|Ip|^2+|Iq|^2)}\right)\cos(\alpha+180^\circ)\right] + j\left[x_{sh}(|Ip|^2+|Iq|^2)-\left(V_i\sqrt{(|Ip|^2+|Iq|^2)}\right)\sin(\alpha+180^\circ)\right]\right\}$$

$$Ssh = \left\{\left[\left(V_i\sqrt{(|Ip|^2+|Iq|^2)}\right)\cos\alpha\right]+j\left[x_{sh}(|Ip|^2+|Iq|^2)+\left(V_i\sqrt{(|Ip|^2+|Iq|^2)}\right)\sin\alpha\right]\right\} = P_{sh}+jQ_{sh} \tag{4.43}$$

Equating both sides,

$$P_{sh} = \left(V_i\sqrt{(|Ip|^2 + |Iq|^2)}\right)\cos\alpha \quad (4.44)$$

$$Q_{sh} = x_{sh}(|Ip|^2 + |Iq|^2) + \left(V_i\sqrt{(|Ip|^2 + |Iq|^2)}\right)\sin\alpha \quad (4.45)$$

Let us denote $|I_{sh}| = I_{sh} = \sqrt{(|Ip|^2 + |Iq|^2)}$, then

$$P_{sh} = V_i I_{sh}\cos\alpha \quad (4.46)$$

$$Q_{sh} = x_{sh}I_{sh}^2 + V_i I_{sh}\sin\alpha \quad (4.47)$$

Where, $x_{sh}(|Ip|^2 + |Iq|^2)$ is the reactive power loss due to shunt converter reactance whereas $\left(V_i\sqrt{(|Ip|^2 + |Iq|^2)}\right)\sin\alpha$ is the reactive power compensation of bus i. In addition, real power of shunt converter, $\left(V_i\sqrt{(|Ip|^2 + |Iq|^2)}\right)\cos\alpha$, is the real power exchange of shunt converter with the transmission line so as to supply the demanded power of series component.

It is important to note here that the real power loss to be encountered by the converters is zero as the resistance is neglected throughout the analysis. Therefore, for the lossless converters assumed, the following constraint equation holds true for the real power exchange between two components of UPFC device.

$$P_{sh} + P_{se} = 0 \quad (4.48)$$

4.3.3 Feasible Location of UPFC Deployment

Nor Rul Hasma Abdullah et al, [29], worked on the placement of the UPFCs in the network using Static Voltage Stability Index (SVSI) technique as tool to determine the location, and then installed in the weakest buses and heavily loaded areas to reduce stressed condition in the system by optimizing the settings the UPFC parameters.

In this study, a feasible location of the UPFC is to be determined and the deployment is based on severity index value obtained i.e., top ranked and critical contingent power system components are considered at first except GG III power plant (PP). To do so, the overall composite severity index (OCSI) value is pivoted at first step, then the most individual composite severity index (ICSI) value which is out of from predefined value is referred and taken as the prior location to implement the UPFC deployment. This procedure continues till the intended output is obtained.

The following UPFC deployment locations are ignored and not taken as feasible ones.

1. Transformer connected branches
2. Generator connected buses with radial branches

From the context of this study, the maximum allowable overall network composite severity index range can be defined ideally as 0<OCSI<109.5 provided that each values of individual composite severity index (ICSI)) of 146 transmission line branches are less than 0.75 while holding true for both Real Power Performance Index (PPI_{ij}) and Line Stability Index (L_{ij}) of respective line that PPI_{ij} <0.5 and L_{ij} <1, respectively. OSCI with relatively highest values are traced and looked back for the most contributing values of ICSI, and if not either Real Power Performance Index of respective line (PPI_{ij}), $PPI_{ij} \geq 0.5$, or Line Stability Index (L_{ij}), $L_{ij} \geq 1$, is to be checked furtherly for each of the contingent elements selected and simulated. Further, this helps as the basic guidelines for identifying the most feasible location of the line/s according to the magnitude of the severity index result obtained and, then deploying UPFC devices to evaluate their performances for improving grid security.

Table 4.3. Screened out of the most contributing severity indices for grid vulnerability

Outage Element/s	Line/ Bus No.	Affected Transmission Lines "From-To"		PPI_{ij}	L_{ij}	$ICSI_{ij}$	OCSI	OCSI Rank
		Bus i_Name	Bus j_Name					
GG III Plant	8	2_Sululta	10_D/Markos	0.075378	4.292656	2.184017	23.091850	1
		2_Sululta	5_G/Guracha	0.070953	3.078783	1.574868		
		1_Beles PP	9_Bahirdar II	0.194493	1.631627	0.913060		
		1_Beles PP	9_Bahirdar II	0.194493	1.631627	0.913060		
		32_Hurso	26_Koka	0.022113	1.364967	0.693540		
		32_Hurso	26_Koka	0.022113	1.364967	0.693540		
		11_GG-II PP	7_Wolyta	0.032856	1.257186	0.645021		
		33_Fincha PP	42_D/Markos	0.073122	1.189387	0.631254		
7_Wolyta-3_Gelan	25	2_Sululta	10_D/Markos	0.000443	2.555346	1.277894	19.734291	2
		32_Hurso	26_Koka	0.021881	1.352247	0.687064		
		32_Hurso	26_Koka	0.021881	1.352247	0.687064		
		5_G/Guracha	10_D/Markos	0.000566	1.298880	0.649723		
	36	13_Legetafo	39_Combolcha-II	0.005300	1.028390	0.516845		
		87_Alaba	97_Wolyta	0.537638	0.172326	0.354982		

		80_Shashemene	87_Alaba	0.532694	0.182779	0.357736		
57_Mekele-58_Tekeze PP	138	56_Humera	44_Gonder-II	0.134740	1.782511	0.958625	19.529040	3
		54_Alamata	61_Ashogoda WF	0.025977	1.629641	0.827809		
		32_Hurso	26_Koka	0.022511	1.360101	0.691306		
	139	32_Hurso	26_Koka	0.022511	1.360101	0.691306		
		2_Sululta	10_D/Markos	0.002269	1.177378	0.589823		
M/Wakana Plant	27	2_Sululta	10_D/Markos	0.001144	1.795850	0.898497	19.293922	4
		28_Adama-II WF	26_Koka	0.006278	1.563302	0.784790		
		7_Wolyta	3_Gelan	0.086014	1.431451	0.758732		
		7_Wolyta	3_Gelan	0.086014	1.431451	0.758732		
		32_Hurso	26_Koka	0.015081	1.113531	0.564306		
		32_Hurso	26_Koka	0.015081	1.113531	0.564306		
		5_G/Guracha	10_D/Markos	0.001324	1.005631	0.503477		
11_GG-II PP-4_Sebeta-II	47	2_Sululta	10_D/Markos	0.000684	1.830921	0.915802	17.394284	5
		7_Wolyta	3_Gelan	0.128914	1.641329	0.885121		
		7_Wolyta	3_Gelan	0.128914	1.641329	0.885121		
		32_Hurso	26_Koka	0.022308	1.357586	0.689947		
		32_Hurso	26_Koka	0.022308	1.357586	0.689947		
		5_G/Guracha	10_D/Markos	0.000834	1.018896	0.509865		
6_Holeta-2_Sululta	114	2_Sululta	10_D/Markos	0.001087	1.954391	0.977739	16.973824	6
		32_Hurso	26_Koka	0.022599	1.359457	0.691028		
	125	32_Hurso	26_Koka	0.022599	1.359457	0.691028		
		5_G/Guracha	10_D/Markos	0.001263	1.070967	0.536115		
		11_GG-II PP	7_Wolyta	0.030973	1.001411	0.516192		
41_Bahirdar-II-44_Gonder-II	111	32_Hurso	26_Koka	0.022531	1.361297	0.691914	16.758072	7
	112	32_Hurso	26_Koka	0.022531	1.361297	0.691914		
		2_Sululta	10_D/Markos	0.001220	1.341630	0.671425		
Tekeze Plant	58	2_Sululta	10_D/Markos	0.000489	1.649087	0.824788	16.720615	8
		32_Hurso	26_Koka	0.022313	1.365400	0.693857		
		32_Hurso	26_Koka	0.022313	1.365400	0.693857		
		54_Alamata	61_Ashogoda WF	0.012267	1.078739	0.545503		
GG II Plant	11	8_GG-III PP	7_Wolyta	0.088959	2.801192	1.445075	16.153597	9
		8_GG-III PP	7_Wolyta	0.088959	2.801192	1.445075		
		8_GG-III PP	7_Wolyta	0.088959	2.801192	1.445075		
		32_Hurso	26_Koka	0.022526	1.371826	0.697176		
		32_Hurso	26_Koka	0.022526	1.371826	0.697176		
20_Kaliti-I-21_Gelan	77	2_Sululta	10_D/Markos	0.000270	1.471601	0.735935	16.152047	10
		32_Hurso	26_Koka	0.022944	1.353982	0.688463		
		32_Hurso	26_Koka	0.022944	1.353982	0.688463		

	78	7_Wolyta	3_Gelan	0.060142	1.011840	0.535991		
		7_Wolyta	3_Gelan	0.060142	1.011840	0.535991		
		11_GG-II PP	7_Wolyta	0.032658	1.002453	0.517556		
27_M/Wakana PP-26_Koka	89	2_Sululta	10_D/Markos	0.000753	1.416840	0.708796	16.094193	11
		32_Hurso	26_Koka	0.021721	1.372879	0.697300		
	90	32_Hurso	26_Koka	0.021721	1.372879	0.697300		
		81_M/Wak. Yugo	80_Shashemene	0.613399	0.495147	0.554273		
51_GG-New-50_GG-I PP	52	2_Sululta	10_D/Markos	0.000644	1.404483	0.702564	16.089706	12
	146	32_Hurso	26_Koka	0.022518	1.361662	0.692090		
		32_Hurso	26_Koka	0.022518	1.361662	0.692090		
23_Sebeta-II-22_Sebeta-I	83	32_Hurso	26_Koka	0.022547	1.359557	0.691052	16.005241	13
		32_Hurso	26_Koka	0.022547	1.359557	0.691052		
	84	2_Sululta	10_D/Markos	0.000384	1.373701	0.687042		
		11_GG-II PP	7_Wolyta	0.029529	1.000097	0.514813		
76_Gelan-67_Kaliti-I	37	2_Sululta	10_D/Markos	0.000417	1.439035	0.719726	15.993119	14
		76_Gelan	77_Yesu	1.224804	0.168176	0.696490		
	38	32_Hurso	26_Koka	0.022350	1.367800	0.695075		
		32_Hurso	26_Koka	0.022350	1.367800	0.695075		
		77_Yesu	67_Kaliti-I	0.698481	0.005292	0.351886		
11_GG-II PP-12_GG-New	92	2_Sululta	10_D/Markos	0.000350	1.485710	0.743030	15.927937	15
		32_Hurso	26_Koka	0.022554	1.360023	0.691289		
		32_Hurso	26_Koka	0.022554	1.360023	0.691289		
32_Hurso-26_Koka	93	31_D/dawa-III	25_Awash-7KL	0.037930	2.703368	1.370649	15.838092	16
	94	2_Sululta	10_D/Markos	0.000017	1.507835	0.753926		
		25_Awash-7KL	26_Koka	0.092102	1.389686	0.740894		
13_Legetafo-14_Sululta	61	32_Hurso	26_Koka	0.022530	1.359325	0.690927	15.721317	17
	62	32_Hurso	26_Koka	0.022530	1.359325	0.690927		
		2_Sululta	10_D/Markos	0.000455	1.380006	0.690230		
Fincha Plant	33	2_Sululta	10_D/Markos	0.000348	1.609197	0.804772	15.633733	18
		32_Hurso	26_Koka	0.022407	1.363017	0.692712		
		32_Hurso	26_Koka	0.022407	1.363017	0.692712		
13_Legetafo-16_Cotobie	63	2_Sululta	10_D/Markos	0.000452	1.408620	0.704536	15.597021	19
	64	32_Hurso	26_Koka	0.022700	1.354827	0.688763		
		32_Hurso	26_Koka	0.022700	1.354827	0.688763		
25_Awash-7KL-26_Koka	87	32_Hurso	26_Koka	0.036408	1.458906	0.747657	15.578001	20
		32_Hurso	26_Koka	0.036408	1.458906	0.747657		
		2_Sululta	10_D/Markos	0.000483	1.417908	0.709196		
80_Shashemene-87_Alaba	39	2_Sululta	10_D/Markos	0.000498	1.439237	0.719868	15.538855	21
		32_Hurso	26_Koka	0.022658	1.356281	0.689470		

		32_Hurso	26_Koka	0.022658	1.356281	0.689470		
17_B/Arabsa TP-20_Kaliti-I	109	2_Sululta	10_D/Markos	0.000504	1.427368	0.713936	15.516683	22
		32_Hurso	26_Koka	0.022592	1.360606	0.691599		
		32_Hurso	26_Koka	0.022592	1.360606	0.691599		
Awash II Plant	65	2_Sululta	10_D/Markos	0.000926	1.380891	0.690908	15.472644	23
		32_Hurso	26_Koka	0.022674	1.327685	0.675179		
		32_Hurso	26_Koka	0.022674	1.327685	0.675179		
		11_GG-II PP	7_Wolyta	0.028691	1.072507	0.550599		
GG I Plant	50	2_Sululta	10_D/Markos	0.000001	1.525828	0.762914	15.456055	24
		32_Hurso	26_Koka	0.022360	1.367398	0.694879		
		32_Hurso	26_Koka	0.022360	1.367398	0.694879		
26_Koka-21_Gelan	82	32_Hurso	26_Koka	0.021746	1.387453	0.704599	15.450951	25
		32_Hurso	26_Koka	0.021746	1.387453	0.704599		
		2_Sululta	10_D/Markos	0.000672	1.401502	0.701087		
35_Ghedo-51_GG-New	106	2_Sululta	10_D/Markos	0.000336	1.476509	0.738422	15.427357	26
		32_Hurso	26_Koka	0.022524	1.360876	0.691700		
		32_Hurso	26_Koka	0.022524	1.360876	0.691700		
76_Gelan-77_Yesu	26	2_Sululta	10_D/Markos	0.000577	1.404660	0.702618	15.402822	27
		32_Hurso	26_Koka	0.022475	1.363706	0.693090		
		32_Hurso	26_Koka	0.022475	1.363706	0.693090		
Koka Hydro Plant	64	2_Sululta	10_D/Markos	0.000914	1.401009	0.700962	15.392289	28
		32_Hurso	26_Koka	0.022764	1.352169	0.687466		
		32_Hurso	26_Koka	0.022764	1.352169	0.687466		
22_Sebeta-I-19_T/hailoch	76	2_Sululta	10_D/Markos	0.000518	1.413217	0.706868	15.384544	29
		32_Hurso	26_Koka	0.022570	1.361024	0.691797		
		32_Hurso	26_Koka	0.022570	1.361024	0.691797		
19_T/hailoch-18_Gefersa	72	2_Sululta	10_D/Markos	0.000526	1.412313	0.706420	15.372170	30
		32_Hurso	26_Koka	0.022567	1.361056	0.691812		
		32_Hurso	26_Koka	0.022567	1.361056	0.691812		
6_Holeta-4_Sebeta-II	2	2_Sululta	10_D/Markos	0.000689	1.489374	0.745031	15.366177	31
	59	32_Hurso	26_Koka	0.022512	1.361316	0.691914		
		32_Hurso	26_Koka	0.022512	1.361316	0.691914		
Awash III Plant	66	32_Hurso	26_Koka	0.022683	1.356354	0.689518	15.319376	32
		32_Hurso	26_Koka	0.022683	1.356354	0.689518		
		2_Sululta	10_D/Markos	0.000959	1.362694	0.681826		
Amerti Neshi Plant	36	32_Hurso	26_Koka	0.022540	1.361708	0.692124	15.288097	33
		32_Hurso	26_Koka	0.022540	1.361708	0.692124		
		2_Sululta	10_D/Markos	0.001352	1.305083	0.653218		
Tis Abay II Plant	88	32_Hurso	26_Koka	0.022531	1.361719	0.692125	15.272171	34
		32_Hurso	26_Koka	0.022531	1.361719	0.692125		

		2_Sululta	10_D/Markos	0.000701	1.372474	0.686587		
5_G/Guracha-10_D/Markos	136	2_Sululta	10_D/Markos	0.001858	1.946772	0.974315	15.236055	35
		32_Hurso	26_Koka	0.022479	1.360682	0.691581		
		32_Hurso	26_Koka	0.022479	1.360682	0.691581		
18_Gefersa-35_Ghedo	74	2_Sululta	10_D/Markos	0.001908	1.556331	0.779119	15.178510	36
	75	32_Hurso	26_Koka	0.022411	1.356264	0.689338		
	73	32_Hurso	26_Koka	0.022411	1.356264	0.689338		
51_GG-New-30_Wolkite	97	2_Sululta	10_D/Markos	0.000587	1.474098	0.737342	15.170635	37
		32_Hurso	26_Koka	0.022516	1.360002	0.691259		
		32_Hurso	26_Koka	0.022516	1.360002	0.691259		
35_Ghedo-34_Fincha-II	104	2_Sululta	10_D/Markos	0.000910	1.389284	0.695097	15.143248	38
		32_Hurso	26_Koka	0.022520	1.361262	0.691891		
		32_Hurso	26_Koka	0.022520	1.361262	0.691891		
22_Sebeta-I-30_Wolkite	85	2_Sululta	10_D/Markos	0.000588	1.468244	0.734416	15.039452	39
		32_Hurso	26_Koka	0.022493	1.360990	0.691741		
		32_Hurso	26_Koka	0.022493	1.360990	0.691741		
11_GG-II PP-7_Wolyta	53	2_Sululta	10_D/Markos	0.000508	1.539834	0.770171	14.641239	40
		32_Hurso	26_Koka	0.022481	1.400602	0.711541		
		32_Hurso	26_Koka	0.022481	1.400602	0.711541		
9_Bahirdar II-10_D/Markos	103	32_Hurso	26_Koka	0.022477	1.360922	0.691699	14.397400	41
		32_Hurso	26_Koka	0.022477	1.360922	0.691699		

From the result of the indices, it can be concluded that static stability limit issue of the transmission lines (TLs) is mostly encountered due to static voltage stability limit problem. This issue is identified by determining line stability index (LSI) for each of the transmission lines (TLs) independently. It is investigated that static voltage stability limit problem is dominant one as it has been observed from the simulation results.

As per the guidelines priorly stated for the feasibility of UPFC device allocation, four transmission lines (TLs) are not feasible for the UPFC deployment. Those are: 400 kV double circuit TLs from Beles to Bahirdar-II (1_Beles PP-9_Bahirdar II), 400 kV triple circuit TLs from GG-III to Wolayta (8_GG-III PP-7_Wolyta), and from Adama-II WF to Koka (28_Adama-II WF-26_Koka). In addition, the two transmission lines, 2_Sululta-5_G/Guracha and 33_Fincha PP-42_D/Markos, are not going to be considered for the deployment of the UPFC device due to the fact that their static stability limit violation occurrence is only under outage condition of GG-III PP which is already omitted from the solution phase.

A 400 kV TL, 11_GG-II PP-7_Wolyta, is the most affected transmission line with the static stability limit violation hence, 5 violations are recorded for corresponding 5 outage cases among which 41 contingency case simulations conducted. The maximum LSI of this line is incurred under outage condition of GG-III PP. Generally, the screened out of affected transmission lines (TLs) for UPFC deployment are presented in Table 4.4.

Table 4.4. Feasible and weakest TLs identified for UPFC deployment with corresponding power flow parameters at NSSO

Affected Transmission Line (From_To)	No. of TL ckt	TL MVA limit (pu)	Simulation results at NSSO						Affected Index (PPI_{ij}/L_{ij})
			V_i (pu)	δ_i (deg)	V_j (pu)	δ_j (deg)	P_{ij} (pu)	Q_{ij} (pu)	
32_Hurso-26_Koka	2	3.55	0.853	-21.714	0.947	-10.556	-0.754	-0.285	L_{ij}
2_Sululta-10_D/Markos	1	12.17	0.962	-4.520	0.976	-3.372	-0.443	-0.539	L_{ij}
7_Wolyta-3_Gelan	2	12.17	1.005	6.703	0.966	-4.162	4.329	-0.208	L_{ij}
5_G/Guracha-10_D/Markos	1	12.17	0.964	-3.860	0.976	-3.372	-0.490	-0.808	L_{ij}
11_GG-II PP-7_Wolyta	1	12.17	1.000	6.557	1.005	6.703	-2.920	-11.864	L_{ij}
54_Alamata-61_Ashogoda WF	1	3.98	0.939	-11.763	0.950	-10.873	-0.202	-0.161	L_{ij}
13_Legetafo-39_Combolcha-II	1	3.55	0.920	-9.779	0.898	-14.288	0.370	-0.219	L_{ij}
87_Alaba-97_Wolyta	1	1.12	0.941	-3.546	0.991	3.619	-0.742	0.058	PPI_{ij}
80_Shashemene-87_Alaba	1	1.12	0.845	-14.018	0.941	-3.546	-0.931	-0.026	PPI_{ij}
56_Humera-44_Gonder-II	1	3.55	0.988	-9.154	0.966	-8.025	-0.099	0.120	L_{ij}
81_M/Wakana Yugo-80_Shashemene	1	1.12	0.959	-8.968	0.845	-14.018	0.344	0.202	PPI_{ij}
76_Gelan-77_Yesu	1	1.12	0.912	-15.615	0.892	-16.311	0.726	0.566	PPI_{ij}
77_Yesu-67_Kaliti-I	1	1.12	0.892	-16.311	0.892	-16.322	0.324	0.358	PPI_{ij}
31_D/dawa-III-25_Awash-7KL	1	3.67	0.849	-21.839	0.904	-17.330	-0.422	-0.293	L_{ij}
25_Awash-7KL-26_Koka	1	3.55	0.904	-17.330	0.947	-10.556	-1.031	-0.175	L_{ij}

The transmission lines (TLs) presented in Table 4.4 are most affected transmission lines screened out for 41 selected contingency case studies conducted which are feasibly selected TLs for the deployment of UPFC devices. The simulation results of voltage, voltage angles and power flows under normal steady state operation (NSSO) are intended to be used for estimating the initial settings of the UPFC devices on the corresponding TLs.

Table 4.5. Causative outages at which maximum index value of the affected TL is obtained and corresponding power flow parameters

Affected TL		Causative outage at which maximum index value of affected TL is obtained	Power flow parameters of affected TLs obtained under simulation of the simulations under corresponding contingency conditions						Max. Index Value (PPI_{ij}/L_{ij})
From bus No.	To bus No.		Vi (pu)	δi (deg)	Vj (pu)	δj (deg)	Pij (pu)	Qij (pu)	
32	26	25_Awash-7KL-26_Koka	0.81	-23.876	0.947	-8.9253	-0.958	-0.280	1.459
2	10	7_Wolyta-3_Gelan	0.916	-3.127	0.949	-2.2091	-0.362	-0.899	2.555
7	3	11_GG-II PP-4_Sebeta-II	1.003	12.368	0.947	-3.4866	6.18	0.410	1.641
5	10	7_Wolyta-3_Gelan	0.93	-2.602	0.949	-2.2091	-0.41	-1.158	1.299
11	7	Awash II Plant	1	-8.1863	1.005	-18.264	-2.915	-11.850	1.073
54	61	57_Mekele-58_Tekeze PP	0.904	-33.813	0.95	-39.842	0.907	-0.890	1.630
13	39	7_Wolyta-3_Gelan	0.882	-7.9462	0.88	-13.116	0.366	-0.300	1.028
87	97	7_Wolyta-3_Gelan	0.918	7.012	0.99	19.037	-1.161	0.206	0.538
80	87	7_Wolyta-3_Gelan	0.823	-7.8392	0.918	7.012	-1.156	0.172	0.533
56	44	57_Mekele-58_Tekeze PP	0.903	11.694	0.916	-1.9495	1.843	-0.658	1.783
81	80	27_M/Wakana PP-26_Koka	0.959	22.607	0.818	-3.3678	1.241	0.141	0.613
76	77	76_Gelan-67_Kaliti-I	0.923	-13.168	0.879	-14.961	1.753	1.201	1.225
77	67	76_Gelan-67_Kaliti-I	0.879	-14.961	0.877	-15.019	1.324	0.910	0.698
31	25	32_Hurso-26_Koka	0.617	-32.401	0.813	-15.49	-1.011	-0.458	2.703
25	26	32_Hurso-26_Koka	0.813	-15.49	0.943	-5.0332	-1.524	-0.650	1.390

In Table 4.5, the highlighted numbers are the determined values of real power performance index (PPI_{ij}) of affected TLs for corresponding contingency case studies carried out. As it can be observed, all the affected lines in terms of this index are 132 kV transmission lines (TLs). Although 132 kV transmission lines (TLs), listed here, are as screened based on the predefined guidelines, it has been observed from the overall results that almost most of the 132 kV TLs are nearly over loaded resulting in bus voltage slashing from their minimum limit defined. In contrast, all of the screened out 230 kV and 400 kV TLs are the weakest TLs as measured in terms of Line Stability Index (LSI); but most of these are under loaded as evaluated in terms of real performance index (PPI).

Among 41 contingency case simulations conducted, outage of double circuit 400 kV TLs from Wolyta to Gelan, 7_Wolyta-3_Gelan, are the critical lines that result overloading of single circuit 132 kV TLs from Alaba to Wolyta, 87_Alaba-97_Wolyta, and Shashemene to Wolyta,

80_Shashemene-87_Alaba, as evaluated using PPI. Outage of the double circuit 230 kV TL from Melka Wakana PP to Koka, 27_M/Wakana PP-26_Koka, are another critical lines that result overloading of single circuit 132 kV TL from Melka Wakana Yugo to Shashemene, 81_M/Wakana Yugo-80_Shashemene, whereas outage of the double circuit 132 kV TL from Gelan to Kaliti, 76_Gelan-67_Kaliti-I, result for the overloading of single circuit 132 kV TLs from Gelan to Yesu, 76_Gelan-77_Yesu, and Yesu to Kaliti, 77_Yesu-67_Kaliti-I, as per the results obtained from simulations. All overloaded TLs as determined using real power performance indice (PPI) are loaded beyond 100 percent of their thermal limit. Specially, it is important to note that the single circuit 132 kV TL from Gelan to Yesu, 76_Gelan-77_Yesu, is overloaded doubly beyond its thermal limit allowed which is caused due to the outage of the double circuit 132 kV TL from Gelan to Kaliti, 76_Gelan-67_Kaliti-I, as it can be observed from Table 4.5.

Similarly, the rest of the outage conditions among 41 contingency case simulations are the causative agents for static stability limit violation of the corresponding TLs as evaluated using line stability index (LSI) which is denoted by L_{ij} as it can be observed from Table 4.5.

4.4 Simulation Studies of High Voltage Grid With UPFC

In this sub-section, simulation studies of Ethiopian high voltage grid with UPFC is carried out. After all, grid performance with UPFC is evaluated using simulation results of affected TLs and busbars in terms of TL thermal limit and bus voltage limit under NSSO respectively, and in terms of LSI, PPI, ICSI and OCSI under contingency conditions.

The grid model with the UPFC devices deployed is as shown in Figure 4.9.

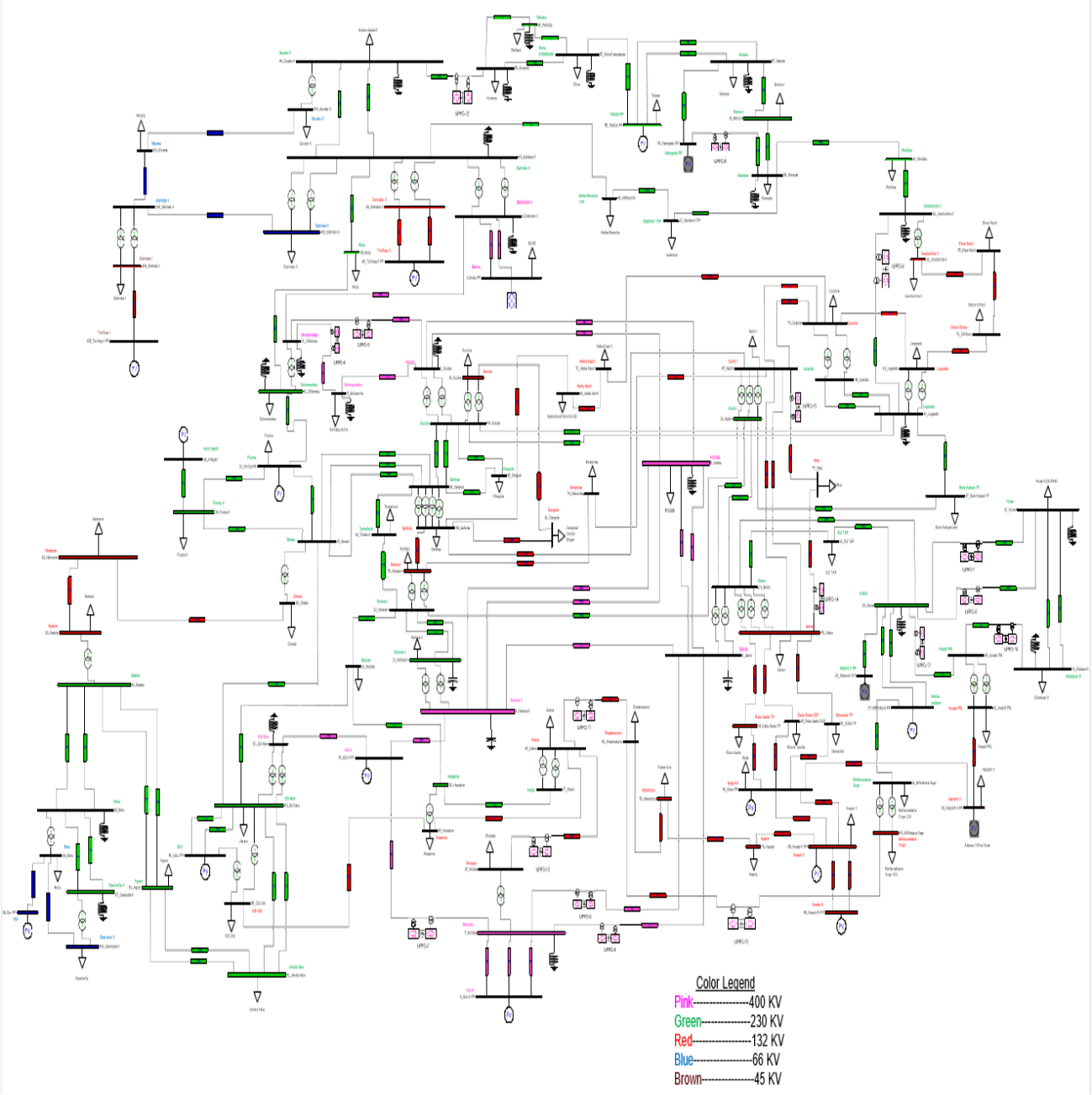

Figure 4.9. Grid model with UPFC deployed

Under this section, the grid model with UPFC devices deployed is simulated and the full simulation result is tabulated in Appendices L. Under this sub-section, only selected bar graphs are included and to be dealt as per the study's interest.

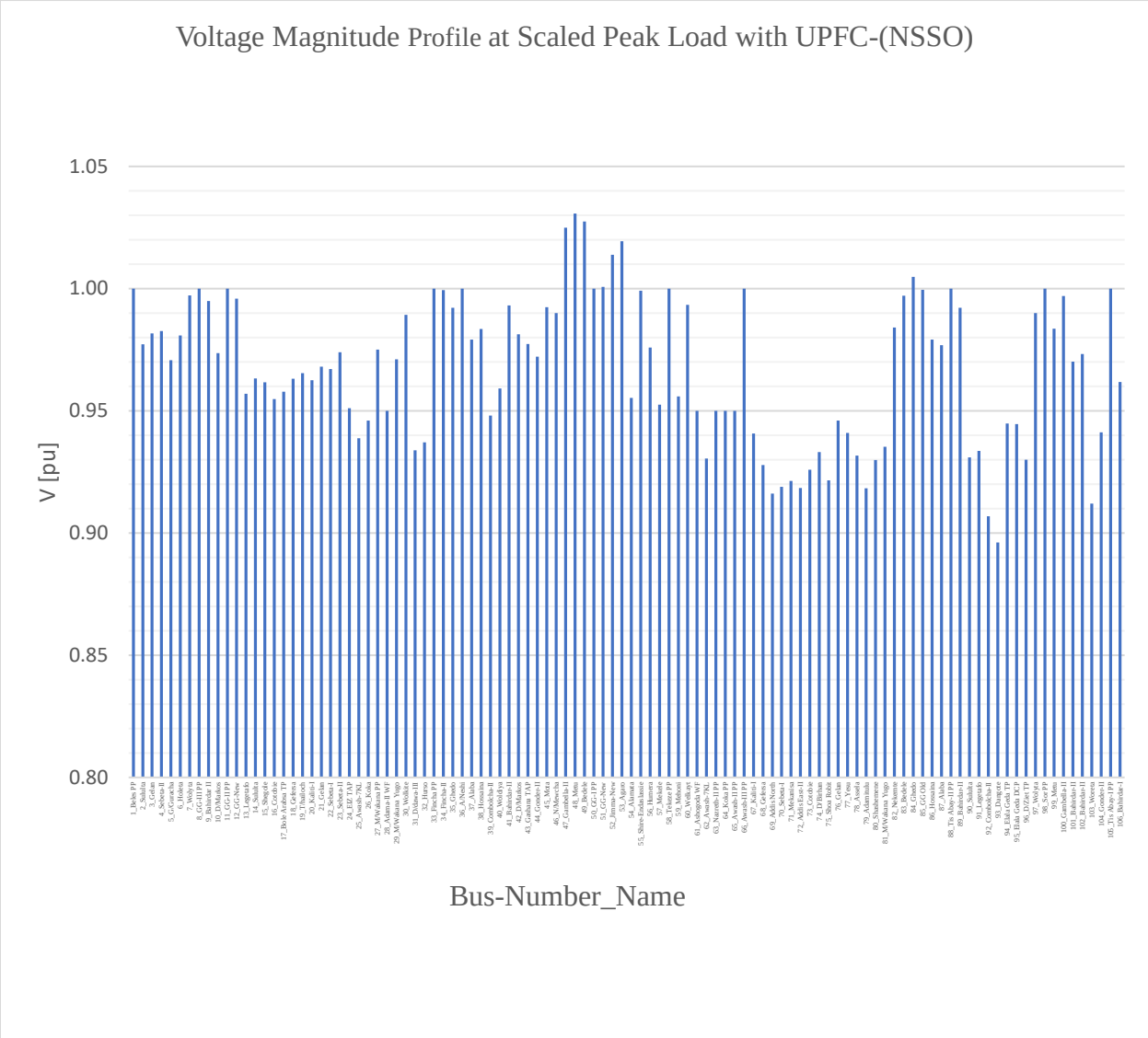

Figure 4.10. Voltage magnitude Profile of the grid model with UPFC at normal operating condition of scaled peak load

It can be visualized from bar graph of Figure 4.10, most of the voltage magnitudes are greater than minimum standard value i.e., 0.95 pu. Though there is appreciable improvement by deploying UPFC, some voltage magnitudes are under predefined value, especially, Dangote busbar is even below 0.9 pu.

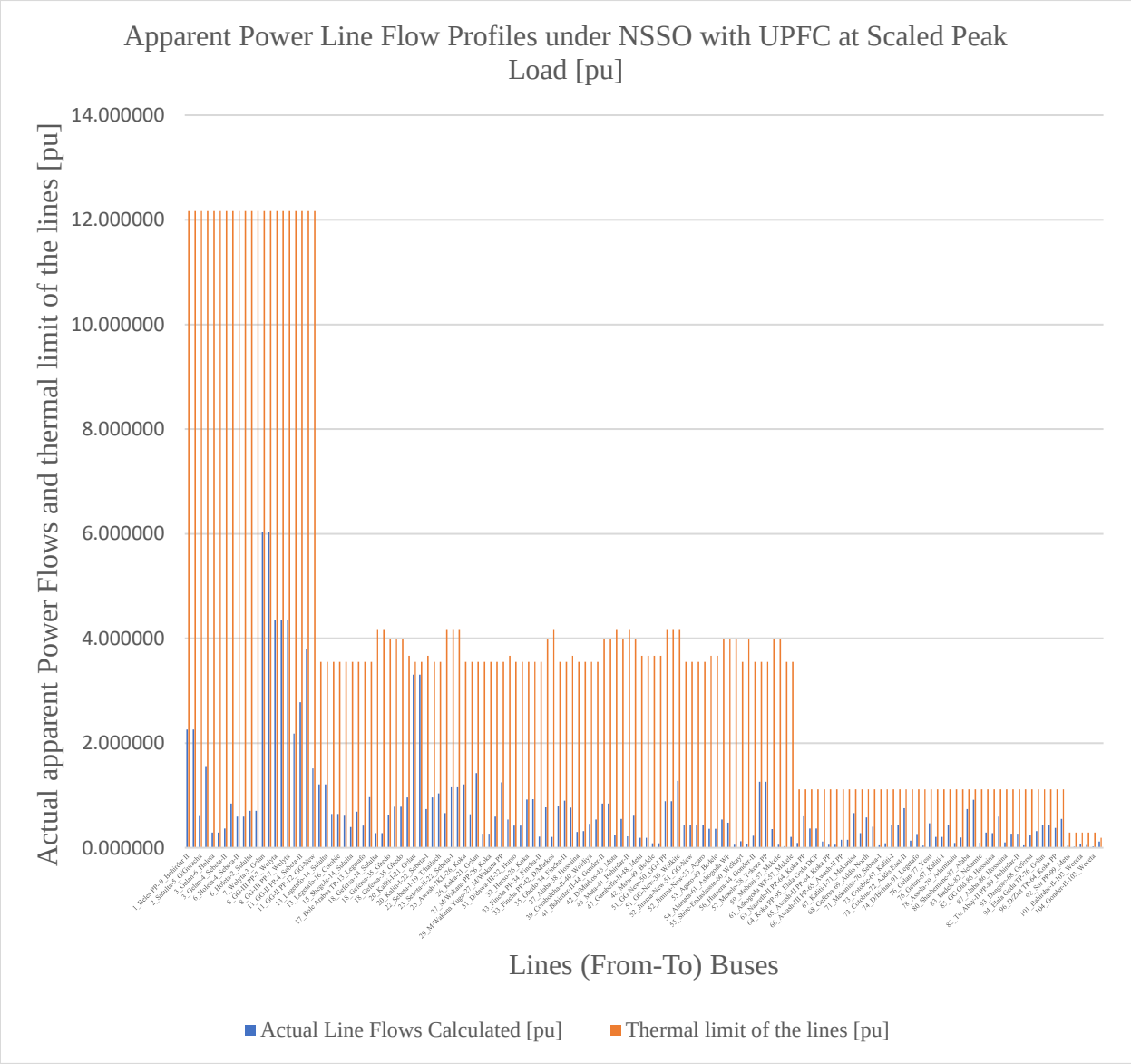

Figure 4.11. Apparent power line flows with UPFC and respective thermal limits

The bar graph chart in Figure 4.11 shows the apparent power flow in pu for each of the transmission lines in which the result is obtained from grid model with UPFC simulation under NSSO. As it can be visualized, all flows are below the maximally allowed thermal limit values.

4.5 Analysis of Results

4.5.1 Simulation Results of Grid Model at NSSO Condition

Here, the simulation result of the grid model at NSSO of scaled peak load with and without UPFC deployment are going to be compared and dealt. The comparison parameters are voltage magnitudes, line power flows and power losses.

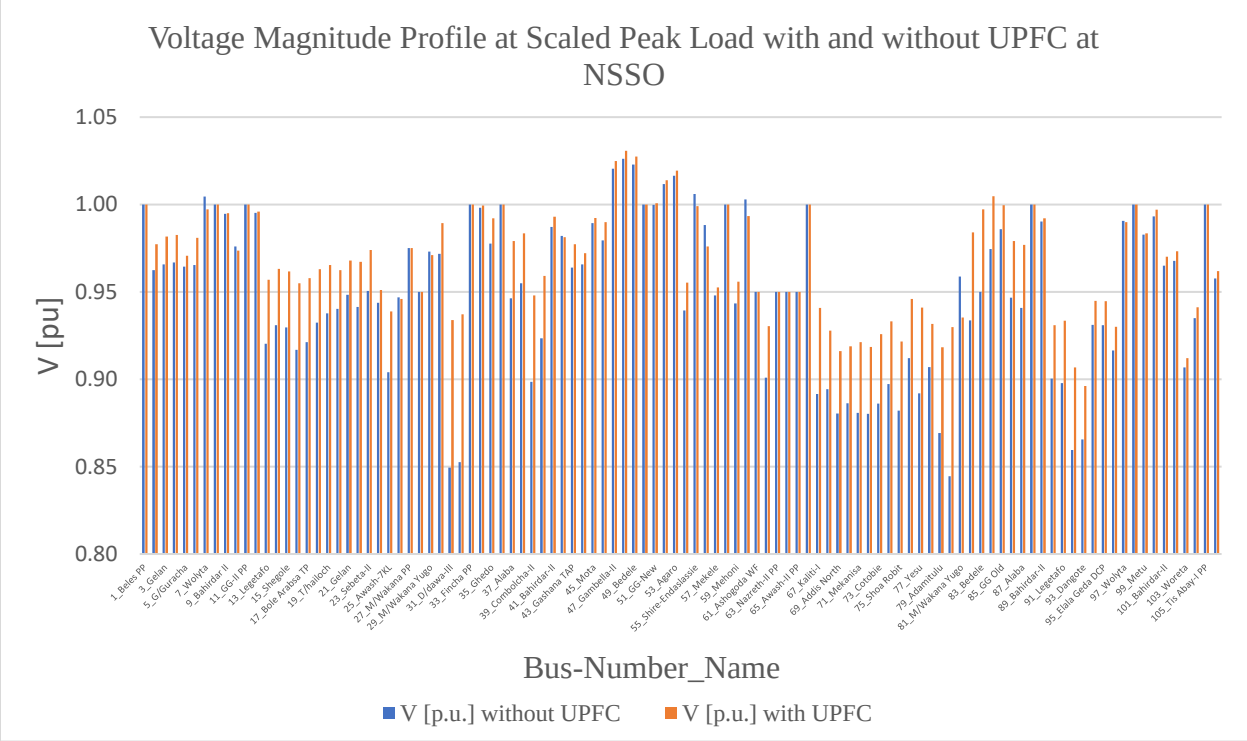

Figure 4.12. Voltage magnitude profile with and without UPFC at NSSO

Figure 4.14 is intended to compare the voltage magnitudes of the grid model without and with deployment of the UPFC devices. As it can be observed, the voltage magnitude improvement with UPFC is appreciable and the difference is visible. Though there are some voltage magnitudes which are still below predefined value (0.95 pu), UPFC devices can be concluded as promising devices to maintain voltage limit. It is important to bear in mind that the results are obtained by operating series component of the UPFC i.e., no reactive power compensation by the shunt component as already stated earlier.

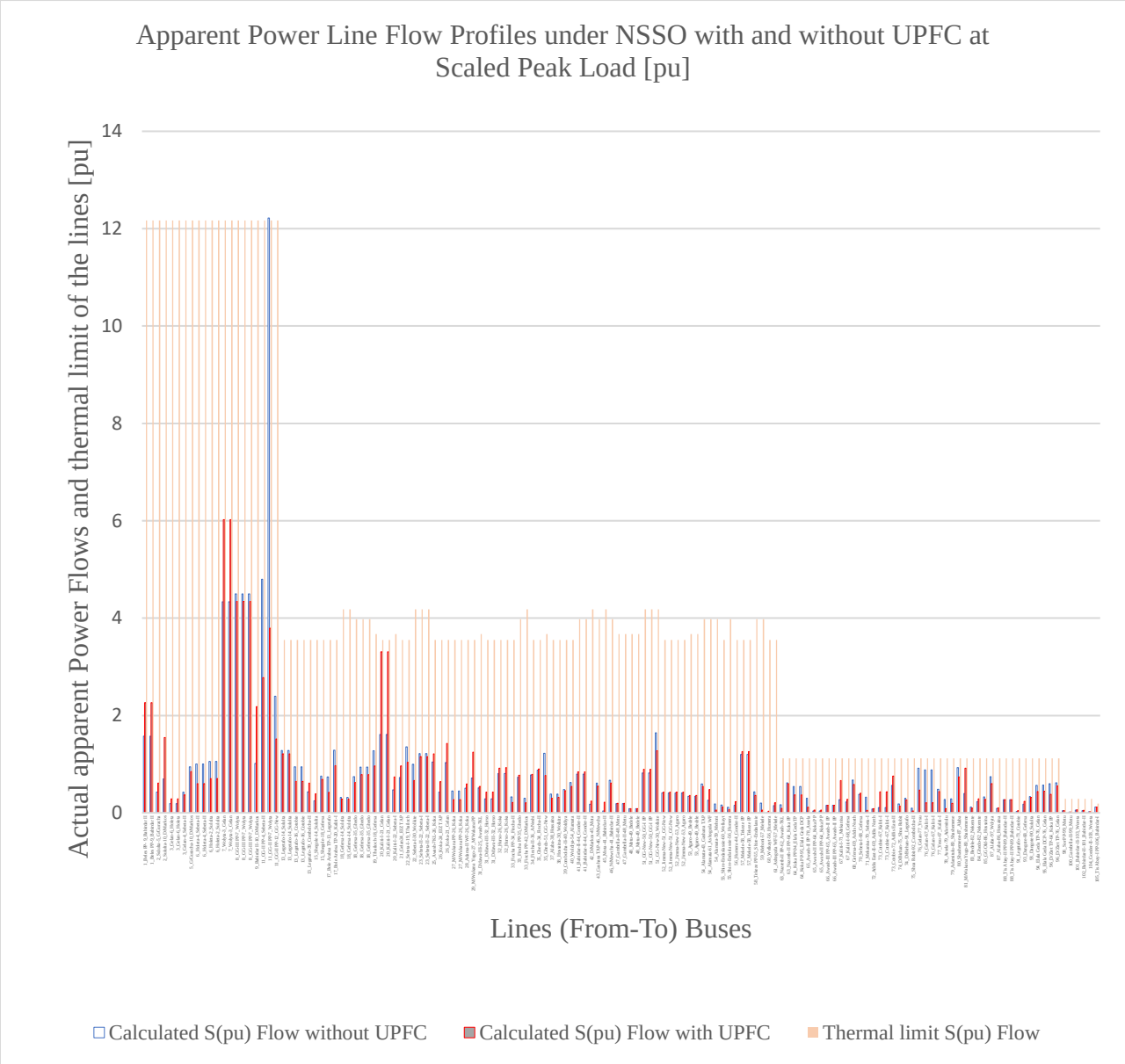

Figure 4.13. Apparent power line flow profile with and without UPFC at NSSO

For the convenience of comparing the results of line flows apparently with and without UPFC, the simulation result is shown in bar graph chart of Figure 4.13. As it can be observed, all line flows are below the maximally defined limits in both cases except 11_GG-II PP to 7_Wolyta 400 kV TL which is likely to violate the stated transmission line limit before UPFC deployment. This case is fully solved after deploying UPFC devices as it can be clearly observed.

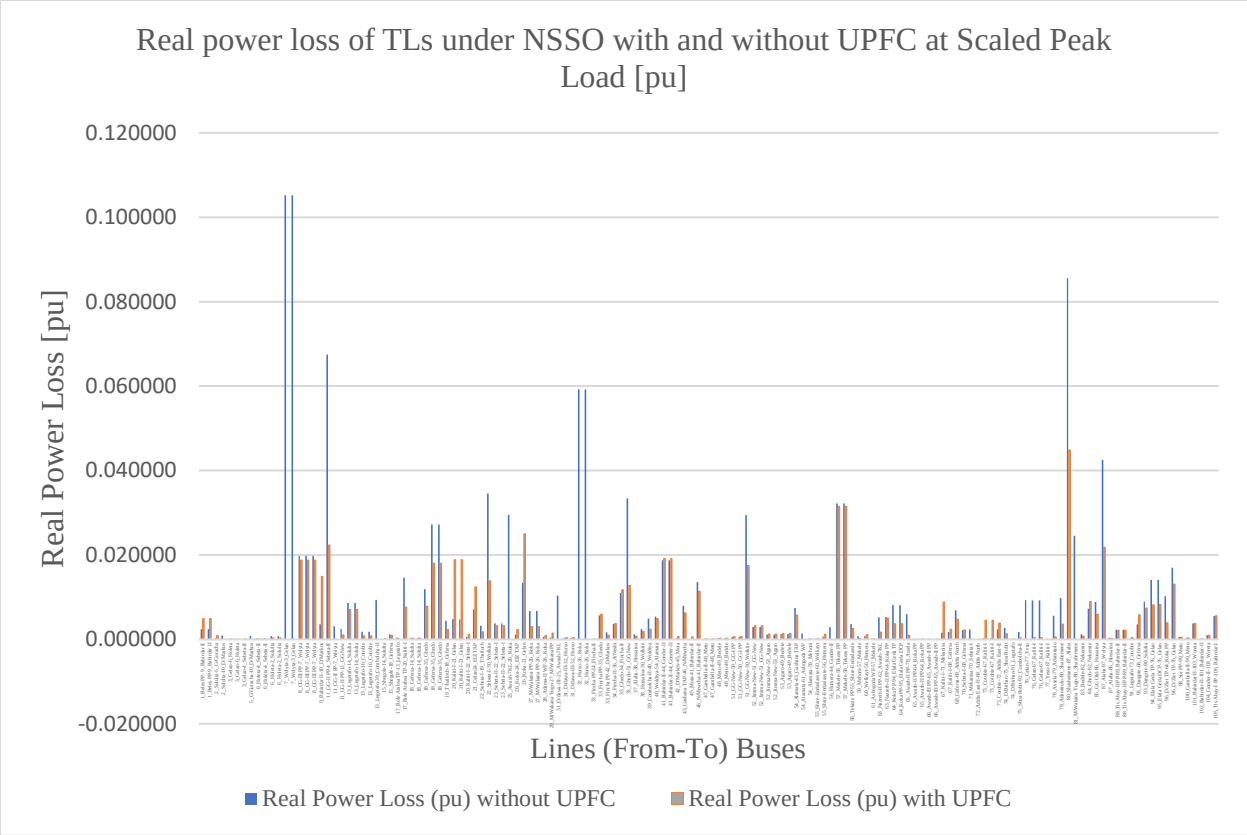

Figure 4.14. Transmission lines (TLs) real power loss with and without UPFC at NSSO

The real power loss representing bar graph chart in Figure 4.14 is just intended to appreciate the performance of the UPFC devices to minimize real power loss. It can be clearly visualized figuratively that how much reduction of real power loss is on each of the transmission lines (TLs) after the simulation of grid with UPFC. The total real power loss is changed from 1.333 pu without UPFC to 0.698 pu with UPFC deployment resulting in net real power saving of the 0.635 pu.

4.5.2 Simulation Results of Grid Model at Contingency Condition

Under this subsection, line power flow of the transmission and evaluation of the identified weak transmission lines based on the indices used for corresponding contingent elements is going to be included and dealt. Accordingly, the simulation is to be conducted for 41 contingent element that are resulting in index violations with respect to the predefined values and the result comparison is conducted with and without UPFC deployment.

4.5.2.1 Power flow results with and without UPFC

Here, the simulation result of the grid model under selected contingency condition of scaled peak load with and without UPFC deployment is going to be compared and dealt. Typically, the parameter to conduct the comparison within this subsection is calculated line power flow apparently (pu) for affected TLs of the grid model.

As is it is observed from transmission line (TL) loading apparently, the simulation result of the grid model which is performed for 41 selected contingency cases with and without UPFC deployment can be easily compared and the difference is clearly visible with both cases. The overall line loading status is appreciably improved with UPFC devices deployment and in contrast, lines which are negatively affected, either thermal loading limit violated or likely to be violated, following the UPFC deployment are to be stated independently.

Accordingly, the most lines which are positively or negatively impacted in terms of line loading apparently either without or with UPFC deployment are summarized in Table 4.6.

Table 4.6. Affected TLs in terms of the apparent power flow either without or with UPFC deployment for corresponding outage condition among 41 contingency case studies performed

Line/PP Outage	Affected TL/s (With or Without UPFC)	Power Flow with and without UPFC Deployment						Thermal loading limit S(pu)
		Power Flow without UPFC			Power Flow with UPFC			
		P(pu)	Q(pu)	S(pu)	P(pu)	Q(pu)	S(pu)	
7_Wolyta-3_Gelan	11_GG-II PP-7_Wolyta	-11.075501	-11.142386	15.710489	-11.088795	2.014647	11.270323	12.17
	80_Shashemene-87_Alaba	-1.156037	0.171918	1.168751	-1.210764	0.482516	1.303369	1.12
	87_Alaba-97_Wolyta	-1.161390	0.206005	1.179518	-1.215970	0.403004	1.281013	1.12
6_Holeta-2_Sululta	11_GG-II PP-7_Wolyta	-3.028993	-11.928007	12.306590	-0.062380	3.539678	3.540228	12.17
	20_Kaliti-I-21_Gelan	-1.933324	-0.747218	2.072698	-3.504856	-0.841582	3.60448	3.55
	20_Kaliti-I-21_Gelan	-1.933324	-0.747218	2.072698	-3.504856	-0.841582	3.60448	3.55
20_Kaliti-I-21_Gelan	11_GG-II PP-7_Wolyta	-3.110309	-11.940649	12.339089	-0.538772	3.880868	3.918088	12.17
	76_Gelan-77_Yesu	0.989074	0.654495	1.186015	1.219166	0.931052	1.534022	1.12
	76_Gelan-67_Kaliti-I	0.956233	0.626064	1.142951	0.681481	0.162497	0.700587	1.12
	76_Gelan-67_Kaliti-I	0.956233	0.626064	1.142951	0.681481	0.162497	0.700587	1.12
	77_Yesu-67_Kaliti-I	0.588288	0.435975	0.732228	0.881425	0.769324	1.169944	1.12
18_Gefersa-35_Ghedo	20_Kaliti-I-21_Gelan	-1.752034	-0.814902	1.932276	-3.589062	-0.769536	3.670634	3.55
	20_Kaliti-I-21_Gelan	-1.752034	-0.814902	1.932276	-3.589062	-0.769536	3.670634	3.55
13_Legetafo-14_Sululta	20_Kaliti-I-21_Gelan	-1.801471	-0.829055	1.983086	-3.642539	-0.829878	3.735878	3.55
	20_Kaliti-I-21_Gelan	-1.801471	-0.829055	1.983086	-3.642539	-0.829878	3.735878	3.55

23_Sebeta-II-22_Sebeta-I	11_GG-II PP-7_Wolyta	-2.957512	-11.912153	12.273804	-0.049574	3.767573	3.767899	12.17
	20_Kaliti-I-21_Gelan	-2.027211	-0.924226	2.227953	-3.900144	-0.842091	3.990018	3.55
	20_Kaliti-I-21_Gelan	-2.027211	-0.924226	2.227953	-3.900144	-0.842091	3.990018	3.55
13_Legetafo-16_Cotobie	11_GG-II PP-7_Wolyta	-2.906078	-11.843100	12.194438	-0.007615	3.932205	3.932212	12.17
	68_Gefersa-69_Addis North	1.108674	0.317261	1.153175	0.858721	0.281978	0.903833	1.12
32_Hurso-26_Koka	11_GG-II PP-7_Wolyta	-2.953916	-11.844995	12.207764	-0.020078	3.795139	3.795192	12.17
41_Bahirdar-II-44_Gonder-II	11_GG-II PP-7_Wolyta	-2.916112	-11.840908	12.194704	-0.015769	3.856939	3.856972	12.17
22_Sebeta-I-19_T/hailoch	11_GG-II PP-7_Wolyta	-2.941463	-11.882748	12.241402	-0.038328	3.792596	3.792790	12.17
17_B/Arabsa TP-20_Kaliti-I	11_GG-II PP-7_Wolyta	-2.955368	-11.872968	12.235259	-0.068134	3.975594	3.976178	12.17
19_T/hailoch-18_Gefersa	11_GG-II PP-7_Wolyta	-2.940264	-11.881051	12.239466	-0.036910	3.795254	3.795434	12.17
25_Awash-7KL-26_Koka	11_GG-II PP-7_Wolyta	-2.930626	-11.851831	12.208787	-0.017901	3.792799	3.792841	12.17
26_Koka-21_Gelan	11_GG-II PP-7_Wolyta	-2.924905	-11.841912	12.197784	-0.042642	3.686736	3.686983	12.17
27_M/Waka. PP-26_Koka	81_M/Waka Yugo-80_S/shemene	1.240522	0.141018	1.248512	1.242762	0.402754	1.306396	1.12
35_Ghedo-34_Fincha-II	11_GG-II PP-7_Wolyta	-2.937678	-11.827389	12.186758	-0.050714	3.812857	3.813194	12.17
76_Gelan-67_Kaliti-I	11_GG-II PP-7_Wolyta	-2.929811	-11.849767	12.206587	-0.017799	3.807221	3.807262	12.17
	76_Gelan-77_Yesu	1.752937	1.201024	2.124911	0.290597	0.700812	0.758673	1.12
	77_Yesu-67_Kaliti-I	1.323763	0.909936	1.606341	-0.159631	0.531309	0.554772	1.12
76_Gelan-77_Yesu	11_GG-II PP-7_Wolyta	-2.922750	-11.859168	12.214022	-0.017530	3.809880	3.809920	12.17
	76_Gelan-67_Kaliti-I	1.006012	0.749882	1.254744	0.175104	0.324272	0.368529	1.12
	76_Gelan-67_Kaliti-I	1.006012	0.749882	1.254744	0.175104	0.324272	0.368529	1.12
8_GG-III PP	11_GG-II PP-7_Wolyta	3.119705	-14.949897	15.271934	3.719850	4.079501	5.520834	12.17
58-Tekeze PP	20_Kaliti-I-21_Gelan	-1.646044	-0.666963	1.776035	-3.554432	-0.631425	3.610081	3.55
	20_Kaliti-I-21_Gelan	-1.646044	-0.666963	1.776035	-3.554432	-0.631425	3.610081	3.55
50-GG-I PP	11_GG-II PP-7_Wolyta	-4.618257	-11.468041	12.363020	-1.556300	4.076519	4.363494	12.17
27-M.Wakena PP	28_Adama-II WF-26_Koka	0.397800	12.107349	12.113882	0.397800	0.420265	0.578677	3.55
Tis Abay-II PP	11_GG-II PP-7_Wolyta	-2.920935	-11.860970	12.215338	-0.018583	3.800312	3.800358	12.17
65-Awash-II PP	11_GG-II PP-7_Wolyta	-2.915269	-11.850219	12.203544	-0.014023	3.810408	3.810434	12.17
66-Awash-III PP	11_GG-II PP-7_Wolyta	-2.915013	-11.852098	12.205308	-0.014030	3.810184	3.810209	12.17

Although 400 kV double transmission lines running from Gilgel Gibe II to Wolyta substation (11_GG-II PP-7_Wolyta) are the most exposed lines for overloading or likely overloaded for most of the contingency cases simulated without UPFC deployment, they are extremely overloaded under contingency case simulation of the 400 kV double transmission lines running from Wolyta to Gelan substation (7_Wolyta-3_Gelan). Quantitatively, the line apparent power flow is changed from 15.710489 pu to 11.270323 pu without and with UPFC deployment respectively in which the line loading is maintained within the prescribed thermal loading limit after UPFC devices deployed. Moreover, the apparent power flow of this line is changed from 12.306590 pu to 3.540228 pu for 6_Holeta-2_Sululta double circuit TL outages , 12.339089 pu to 3.918088 pu for

20_Kaliti-I-21_Gelan double circuit TL outages, 12.273804 pu to 3.767899 pu for 23_Sebeta-II-22_Sebeta-I double circuit TL outages, 12.194438 pu to 3.932212 pu for 13_Legetafo-16_Cotobie double circuit TL outages, 12.207764 pu to 3.795192 pu for 32_Hurso-26_Koka outage, 12.194704 pu to 3.856972 pu for 41_Bahirdar-II-44_Gonder-II outage, 12.241402 pu to 3.792790 pu for 22_Sebeta-I-19_T/hailoch outage, 12.235259 pu to 3.976178 pu for 17_Bole Arabsa TP-20_Kaliti-I outage, 12.239466 pu to 3.795434 pu for 19_T/hailoch-18_Gefersa outage, 12.208787 pu to 3.792841 pu for 25_Awash-7KL-26_Koka outage, 12.197784 pu to 3.686983 pu for 26_Koka-21_Gelan outage, 1.248512 pu to 1.306396 pu for 27_M/Wakana PP-26_Koka double circuit TL outages, 12.186758 pu to 3.813194 pu for 35_Ghedo-34_Fincha-II outage, 12.206587 pu to 3.807262 pu for 76_Gelan-67_Kaliti-I double circuit TL outages, 12.214022 pu to 3.809920 pu for 76_Gelan-77_Yesu outage, 12.363020 pu to 4.363494 pu for 50-GG-I PP, 12.215338 pu to 3.800358 pu for Tis Abay-II PP outage, 12.203544 pu to 3.810434 pu for 65-Awash-II PP Outage and 12.205308 pu to 3.810209 pu for 66-Awash-III PP outage without and with UPFC devices deployment respectively. Appreciably, the loading status of this line in which the loading is beyond its thermal loading limit (12.17 pu) for all outage cases without UPFC device deployment is solved all in all with UPFC deployment.

Furthermore, apparent power flow of the TLs which are effectively managed for corresponding outage/s are: double circuit 132 kV TLs 76_Gelan-67_Kaliti-I for 20_Kaliti-I-21_Gelan double circuit 230 kV TL outages is changed from 1.142951 pu to 0.700587 pu, 76_Gelan-77_Yesu and 77_Yesu-67_Kaliti-I for 76_Gelan-67_Kaliti-I double circuit 132 kV TLs outage is changed from 2.124911 pu to 0.758673 pu and 1.606341 pu to 0.554772 pu respectively, and double circuit 132 kV TLs 76_Gelan-67_Kaliti-I for 76_Gelan-77_Yesu TL outage is changed from 1.254744 pu to 0.368529 pu without and with UPFC devices deployment respectively.

However, the double circuit 230 kV TL from Gelan to Kaliti substation is more or less newly affected TL for some of the outage cases following the UPFC deployment in the grid model as tabulated in Table 4.6. In addition, the 132 kV TLs, 80_Shashemene-87_Alaba and 87_Alaba-97_Wolyta for double circuit TL outages of 7_Wolyta-3_Gelan, 76_Gelan-77_Yesu and 77_Yesu-67_Kaliti-I for double circuit TL outages of 20_Kaliti-I-21_Gelan and 81_M/Wakana Yugo-80_Shashemene for double circuit TL outages of 27_M/Wakana PP-26_Koka are the TLs which

are thermal loading limit violated 132 kV TLs under both without and with UPFC devices deployment. Reasonably, the objective is not able to be achieved due to the fact that the buses, connection points for the loaded or likely loaded TLs, need independent bus voltage compensation besides, inactive mode operations of the shunt component of the UPFC devices deployed due to the previously stated reasons. More overly, the lesson taken is the way of the meshed matters the intended control action effectiveness to assure the security of the grid for which the affected 132 kV TLs are good examples.

4.5.2.2 Individual Severity Indice (ISI) with and without UPFC

In this sub of sub-section, all transmission lines (TLs) affected and selected as per the simulation results obtained without UPFC devices deployment based on individual severity indices (ISI) used, Real Power Performance Index (PPI), Line Stability Index (LSI) and Individual Composite Severity Index (ICSI), are to be discussed. On the basis of the stated ISIs, the security of the affected TLs for the corresponding outage case simulation performed can be compared without and with UPFC devices deployment as tabulated in Table 4.7-4.9.

Line stability index (LSI) is one of the individual severity indices (ISI) used to evaluate the static stability limit of the transmission lines. For the convenience of comparing the transmission lines' static stability limit with and without UPFC deployed, the determined values of LSI from both case simulations are tabulated in Table 4.7. To recap, the critical point of this index is 1.

Table 4.7. Simulation result comparison of TLs affected in terms of the LSI before and after UPFC deployment

Outage Element/s	Line From-To	LSI Without UPFC Deployment	LSI With UPFC Deployment	Result Observation
		L_{ij}	L_{ij}	
7_Wolyta-3_Gelan	2_Sululta-10_D/Markos	2.555346	1.291126	Positive Output
	32_Hurso-26_Koka	1.352247	0.911527	Solved
	32_Hurso-26_Koka	1.352247	1.085112	Positive Output
	5_G/Guracha-10_D/Markos	1.298880	1.291126	Positive Output
	13_Legetafo-39_Combol.-II	1.028390	0.005809	Solved
	56_Humera-44_Gonder-II	1.782511	1.779020	Positive Output

57_Mekele-58_Tekeze PP	54_Alamata-61_Ashogo.WF	1.629641	0.905254	Solved
	32_Hurso-26_Koka	1.360101	0.923330	Solved
	32_Hurso-26_Koka	1.360101	1.096262	Positive Output
	2_Sululta-10_D/Markos	1.177378	0.918680	Solved
M/Wakena Plant	2_Sululta-10_D/Markos	1.795850	0.488537	Solved
	28_Adama-II WF-26_Koka	1.563302	0.056269	Solved
	7_Wolyta-3_Gelan	1.431451	1.796104	Negative Output
	7_Wolyta-3_Gelan	1.431451	1.796104	Negative Output
	32_Hurso-26_Koka	1.113531	0.927520	Solved
	32_Hurso-26_Koka	1.113531	1.099226	Positive Output
	5_G/Guracha-10_D/Markos	1.005631	0.565569	Solved
11_GG-II PP-4_Sebeta-II	2_Sululta-10_D/Markos	1.830921	0.568765	Solved
	7_Wolyta-3_Gelan	1.641329	2.507638	Negative Output
	7_Wolyta-3_Gelan	1.641329	2.507638	Negative Output
	32_Hurso-26_Koka	1.357586	0.922762	Solved
	32_Hurso-26_Koka	1.357586	1.095685	Positive Output
	5_G/Guracha-10_D/Markos	1.018896	0.568765	Solved
6_Holeta-2_Sululta	2_Sululta-10_D/Markos	1.954391	0.617651	Solved
	32_Hurso-26_Koka	1.359457	0.923869	Solved
	32_Hurso-26_Koka	1.359457	1.096794	Positive Output
	5_G/Guracha-10_D/Markos	1.070967	0.732133	Solved
	11_GG-II PP-7_Wolyta	1.001411	0.296584	Solved
41_Bahirdar-II-44_Gonder-II	32_Hurso-26_Koka	1.361297	0.923802	Solved
	32_Hurso-26_Koka	1.361297	1.096679	Positive Output
	2_Sululta-10_D/Markos	1.341630	0.743490	Solved
Tekeze Plant	2_Sululta-10_D/Markos	1.649087	0.373972	Solved
	32_Hurso-26_Koka	1.365400	0.926490	Solved
	32_Hurso-26_Koka	1.365400	1.098367	Positive Output
	54_Alamata-61_Ashog. WF	1.078739	0.242756	Solved
GG II Plant	8_GG-III PP-7_Wolyta	2.801192	0.626289	Solved
	8_GG-III PP-7_Wolyta	2.801192	0.626289	Solved
	8_GG-III PP-7_Wolyta	2.801192	0.626289	Solved
	32_Hurso-26_Koka	1.371826	0.925912	Solved
	32_Hurso-26_Koka	1.371826	1.097622	Positive Output
20_Kaliti-I-21_Gelan	2_Sululta-10_D/Markos	1.471601	0.279845	Solved
	32_Hurso-26_Koka	1.353982	0.910949	Solved
	32_Hurso-26_Koka	1.353982	1.089370	Positive Output
	7_Wolyta-3_Gelan	1.011840	2.467487	Negative Output
	7_Wolyta-3_Gelan	1.011840	2.467487	Negative Output

	11_GG-II PP-7_Wolyta	1.002453	0.325045	Solved
27_M/Wakana PP-26_Koka	2_Sululta-10_D/Markos	1.416840	0.592917	Solved
	32_Hurso-26_Koka	1.372879	0.924639	Solved
	32_Hurso-26_Koka	1.372879	1.095290	Positive Output
51_GG-New-50_GG-I PP	2_Sululta-10_D/Markos	1.404483	0.629412	Solved
	32_Hurso-26_Koka	1.361662	0.923684	Solved
	32_Hurso-26_Koka	1.361662	1.096642	Positive Output
23_Sebeta-II-22_Sebeta-I	32_Hurso-26_Koka	1.359557	0.923153	Solved
	32_Hurso-26_Koka	1.359557	1.096101	Positive Output
	2_Sululta-10_D/Markos	1.373701	0.586952	Solved
	11_GG-II PP-7_Wolyta	1.000097	0.315627	Solved
76_Gelan-67_Kaliti-I	2_Sululta-10_D/Markos	1.439035	0.625993	Solved
	32_Hurso-26_Koka	1.367800	0.910279	Solved
	32_Hurso-26_Koka	1.367800	1.080249	Positive Output
11_GG-II PP-12_GG-New	2_Sululta-10_D/Markos	1.485710	0.599778	Solved
	32_Hurso-26_Koka	1.360023	0.924310	Solved
	32_Hurso-26_Koka	1.360023	1.097105	Positive Output
32_Hurso-26_Koka	31_D/dawa-III-25_Awash-7KL	2.703368	1.277317	Positive Output
	2_Sululta-10_D/Markos	1.507835	0.599417	Solved
	25_Awash-7KL-26_Koka	1.389686	1.704256	Negative Output
13_Legetafo-14_Sululta	32_Hurso-26_Koka	1.359325	0.922503	Solved
	32_Hurso-26_Koka	1.359325	1.095516	Positive Output
	2_Sululta-10_D/Markos	1.380006	0.535746	Solved
Fincha Plant	2_Sululta-10_D/Markos	1.609197	0.599305	Solved
	32_Hurso-26_Koka	1.363017	0.925060	Solved
	32_Hurso-26_Koka	1.363017	1.097533	Positive Output
13_Legetafo-16_Cotobie	2_Sululta-10_D/Markos	1.408620	0.550180	Solved
	32_Hurso-26_Koka	1.354827	0.921828	Solved
	32_Hurso-26_Koka	1.354827	1.095186	Positive Output
25_Awash-7KL-26_Koka	32_Hurso-26_Koka	1.458906	1.657462	Negative Output
	32_Hurso-26_Koka	1.458906	2.046434	Negative Output
	2_Sululta-10_D/Markos	1.417908	0.617234	Solved
80_Shashemene-87_Alaba	2_Sululta-10_D/Markos	1.439237	0.606373	Solved
	32_Hurso-26_Koka	1.356281	0.925525	Solved
	32_Hurso-26_Koka	1.356281	1.097688	Positive Output
17_B/Arabsa TP-20_Kaliti-I	2_Sululta-10_D/Markos	1.427368	0.491623	Solved
	32_Hurso-26_Koka	1.360606	0.922771	Solved
	32_Hurso-26_Koka	1.360606	1.095739	Positive Output
Awash II Plant	2_Sululta-10_D/Markos	1.380891	0.655657	Solved

	32_Hurso-26_Koka	1.327685	0.921371	Solved
	32_Hurso-26_Koka	1.327685	1.095185	Positive Output
	11_GG-II PP-7_Wolyta	1.072507	0.319207	Solved
GG I Plant	2_Sululta-10_D/Markos	1.525828	0.530454	Solved
	32_Hurso-26_Koka	1.367398	0.927520	Solved
	32_Hurso-26_Koka	1.367398	1.099226	Positive Output
26_Koka-21_Gelan	32_Hurso-26_Koka	1.387453	0.941296	Solved
	32_Hurso-26_Koka	1.387453	1.107520	Positive Output
	2_Sululta-10_D/Markos	1.401502	0.685642	Solved
35_Ghedo-51_GG-New	2_Sululta-10_D/Markos	1.476509	0.589973	Solved
	32_Hurso-26_Koka	1.360876	0.923864	Solved
	32_Hurso-26_Koka	1.360876	1.096766	Positive Output
76_Gelan-77_Yesu	2_Sululta-10_D/Markos	1.404660	0.614227	Solved
	32_Hurso-26_Koka	1.363706	0.924282	Solved
	32_Hurso-26_Koka	1.363706	1.097012	Positive Output
Koka Hydro Plant	2_Sululta-10_D/Markos	1.401009	0.640832	Solved
	32_Hurso-26_Koka	1.352169	0.919260	Solved
	32_Hurso-26_Koka	1.352169	1.093787	Positive Output
22_Sebeta-I-19_T/hailoch	2_Sululta-10_D/Markos	1.413217	0.599704	Solved
	32_Hurso-26_Koka	1.361024	0.923838	Solved
	32_Hurso-26_Koka	1.361024	1.096756	Positive Output
19_T/hailoch-18_Gefersa	2_Sululta-10_D/Markos	1.412313	0.600755	Solved
	32_Hurso-26_Koka	1.361056	0.923843	Solved
	32_Hurso-26_Koka	1.361056	1.096754	Positive Output
6_Holeta-4_Sebeta-II	2_Sululta-10_D/Markos	1.489374	0.447826	Solved
	32_Hurso-26_Koka	1.361316	0.923847	Solved
	32_Hurso-26_Koka	1.361316	1.096693	Positive Output
Awash III Plant	32_Hurso-26_Koka	1.356354	0.921281	Solved
	32_Hurso-26_Koka	1.356354	1.095128	Positive Output
	2_Sululta-10_D/Markos	1.362694	0.657538	Solved
Amerti Neshi Plant	32_Hurso-26_Koka	1.361708	0.924075	Solved
	32_Hurso-26_Koka	1.361708	1.096919	Positive Output
	2_Sululta-10_D/Markos	1.305083	0.732021	Solved
Tis Abay II Plant	32_Hurso-26_Koka	1.361719	0.924041	Solved
	32_Hurso-26_Koka	1.361719	1.096879	Positive Output
	2_Sululta-10_D/Markos	1.372474	0.644096	Solved
5_G/Guracha-10_D/Markos	2_Sululta-10_D/Markos	1.946772	0.367418	Solved
	32_Hurso-26_Koka	1.360682	0.923902	Solved
	32_Hurso-26_Koka	1.360682	1.096740	Positive Output
	2_Sululta-10_D/Markos	1.556331	0.625736	Solved

18_Gefersa-35_Ghedo	32_Hurso-26_Koka	1.356264	0.748851	Solved
	32_Hurso-26_Koka	1.356264	0.921925	Solved
51_GG-New-30_Wolkite	2_Sululta-10_D/Markos	1.474098	0.608059	Solved
	32_Hurso-26_Koka	1.360002	1.117101	Positive Output
	32_Hurso-26_Koka	1.360002	1.325959	Solved
35_Ghedo-34_Fincha-II	2_Sululta-10_D/Markos	1.389284	0.641395	Solved
	32_Hurso-26_Koka	1.361262	0.923973	Solved
	32_Hurso-26_Koka	1.361262	1.096818	Positive Output
22_Sebeta-I-30_Wolkite	2_Sululta-10_D/Markos	1.468244	0.563870	Solved
	32_Hurso-26_Koka	1.360990	0.923459	Solved
	32_Hurso-26_Koka	1.360990	1.096395	Positive Output
11_GG-II PP-7_Wolyta	2_Sululta-10_D/Markos	1.539834	0.443169	Solved
	32_Hurso-26_Koka	1.400602	0.923028	Solved
	32_Hurso-26_Koka	1.400602	1.095897	Positive Output
9_Bahirdar II-10_D/Markos	32_Hurso-26_Koka	1.360922	0.923176	Solved
	32_Hurso-26_Koka	1.360922	1.095985	Positive Output

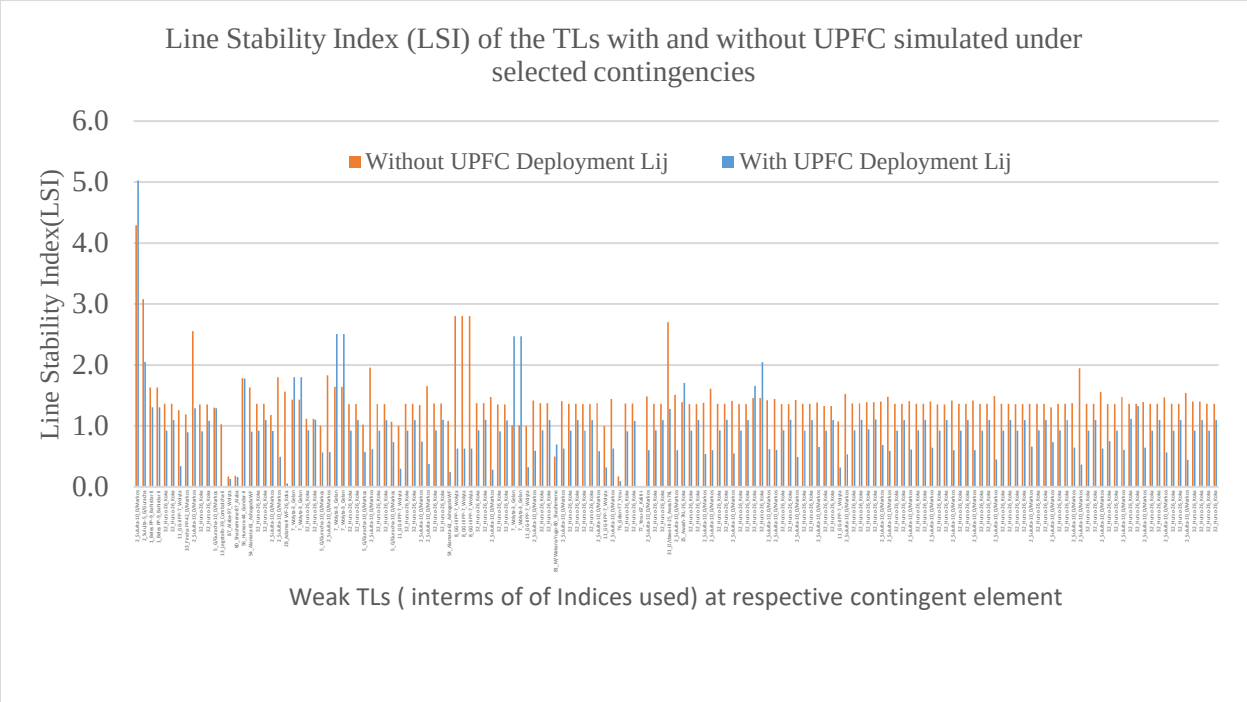

Figure 4.15. Line Stability Index (LSI) of the problematic TLs with and without UPFC simulated under selected contingencies

As it can be observed jointly from Table 4.7 and Figure 4.15, most of the affected TLs in terms of the line stability index (LSI) before the deployment of the UPFC devices are solved by deploying UPFC devices at selected lines. To recap, the critical point for this index, line stability index (LSI), is 1 in which value less than 1 indicating that the lines are [4]statically stable and on the other hand, values beyond 1 indicate statically unstable lines when evaluated in terms of this index alone.

In this study, the result observed using LSI has been classified in to three based on the impact of the UPFC deployment on each of the lines. These are: solved, positive output and negative output. The result observation marked with 'Solved' stands for fully secured TLs in terms of the LSI whereas 'Positive Output' stands for security improved TLs but not fully solved and 'Negative Output' stands for negatively impacted TLs in terms of the LSI following UPFC devices deployment.

Most of the static stability limit problem is solved as it can be observed in Table 4.7. Relatively, some transmission lines (TLs), [5]32_Hurso-26_Koka, 2_Sululta-10_D/Markos, 5_G/Guracha-10_D/Markos, 31_D/dawa-III-25_Awash-7KL and 25_Awash-7KL-26_Koka are statically improved TLs in terms of LSI for corresponding contingency cases as tabulated in Table 4.8. Contrastingly, double circuit 230 kV TLs from Hurso to Koka, 32_Hurso-26_Koka, under 25_Awash-7KL-26_Koka outage condition, 25_Awash-7KL-26_Koka; 25_Awash-7KL-26_Koka TL under 32_Hurso-26_Koka double circuit 230 kV TLs outage and 7_Wolyta-3_Gelan for corresponding contingencies are negatively impacted TLs in terms of LSI following the UPFC deployment.

As it can be observed from the Figure 4.15, the static stability limit violation of the 400 kV TL from Sululta to D/Markos, 2_Sululta-10_D/Markos, goes extremely beyond the critical point even

[4] *Though Voltage Stability is dynamic problem, static indices are playing a great role in determining how close is the current operating point to the static stability limit [38] et al,. Among static indices currently in use, Line Stability Index (LSI) is one which is used by system planners and operators [38] et al,. Here it has been used to determine the static stability limit of the transmission lines.*

[5] *For double circuit 230 kV transmission line (TL) from Hurso to Koka, 32_Hurso-26_Koka, different LSI values have been obtained from the simulation of the grid with UPFC devices deployed. The one with LSI value less than 1 is fully solved and its flow direction has been remaining the same after UPFC deployed. On the other hand, transmission line (TL) with LSI value of a little bit greater than 1 but positive output is measured in opposite direction due to the change of the flow direction following the UPFC deployment.*

worser after UPFC deployed under outage of the GG III PP. This is just to observe though GG III PP is out of this study as per the reason stated in earlier discussion.

Generally, simulation result obtained with UPFC deployed is appreciable which indicates that the UPFC devices are the promising FACTS to assure the grid security as evaluated in terms of the static LSI. If shunt component of the UPFC has been able to put into the active mode operation, the grid security can be assured very well. Furthermore, the UPFC parameter setting is the main determinant factor for better improvement in addition to the interfacing the UPFC components deployed within the grid for improved and optimized utilization but here, it is going to be passed as recommendation and to be a part of future work.

The second jointly used individual severity index (ISI) is real power performance index (PPI) and its determined values of affected transmission lines in terms of real power loading is as tabulated in Table 4.8.

To recap, the critical point for this index, real power performance index (PPI), is 0.5 in which values less than 0.5 indicating that the TL real power loading is within prescribed limit and on the other hand, values beyond 0.5 indicates the TL being overloaded when evaluated in terms of this index alone.

Table 4.8. Simulation result comparison of TLs affected in terms of the PPI before and after UPFC deployment

Outage Element/s	Line From-To	PPI Without UPFC Deployment	PPI With UPFC Deployment	Result Observation
		PPI_{ij}	PPI_{ij}	
7_Wolyta-3_Gelan	87_Alaba-97_Wolyta	0.537638	0.589359	Negative Output
	80_Shashemene-87_Alaba	0.532694	0.584323	Negative Output
27_M/Wakana PP-26_Koka	81_M/Wak. Yugo-80_Shash.	0.613399	0.615616	Negative Output
76_Gelan-67_Kaliti-I	76_Gelan-77_Yesu	1.224804	0.033660	Solved
	77_Yesu-67_Kaliti-I	0.698481	0.010157	Solved

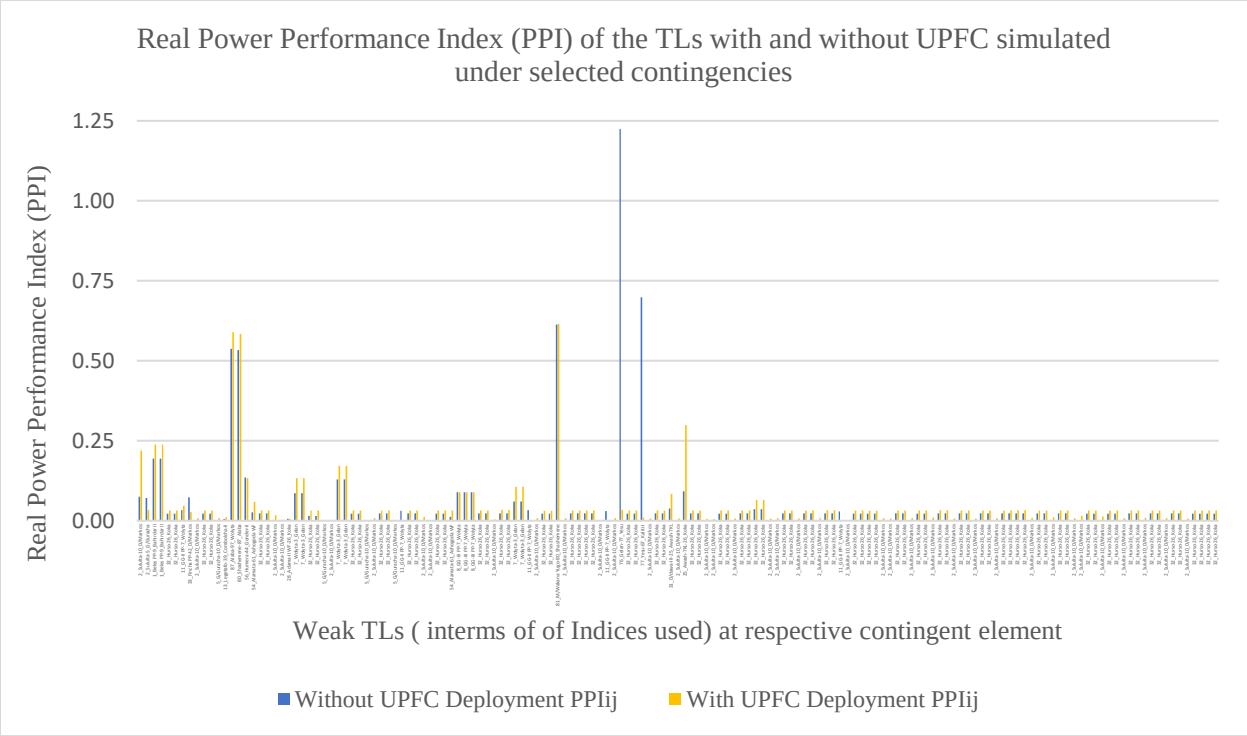

Figure 4.16. Real Power Performance Index (PPI) of the problematic TLs with and without UPFC simulated under selected contingencies

As it can be observed from both Table 4.8 and corresponding bar graph chart in Figure 4.16, extremely affected 76_Gelan-77_Yesu 132 kV TL for 76_Gelan-67_Kaliti-I double circuit 132 kV TL outage in terms of the real power performance index (PPI) before the deployment of the UPFC devices is solved by deploying UPFC devices at selected lines. In addition, 77_Yesu-67_Kaliti-I for 76_Gelan-67_Kaliti-I double circuit 132 kV TL outage is another affected TL prior to the UPFC deployment but latter solved.

In contrast, the real power performance index of the affected TLs before UPFC deployment: 87_Alaba-97_Wolyta and 80_Shashemene-87_Alaba 132 kV TLs for 7_Wolyta-3_Gelan double circuit 400 kV TLs outage, and 81_M/Wakana Yugo-80_Shashemene 132 kV TL for 27_M/Wakana PP-26_Koka double circuit 400 kV TL outage are the negatively impacted TLs following the UPFC deployment. This is due to the fact that the way of the meshed matters the intended control action effectiveness to assure the security of the grid for which the affected 132 kV TLs are good examples as already stated earlier.

The third individual severity index (ISI) is individual composite severity index (ICSI) which is the combination of previously discussed two indices i.e., LSI and PPI. It is intended to evaluate each of the transmission lines (TLs) using combined effect of both indices. To recap, the critical point for this index, Individual Composite Severity Index (ICSI), is 0.75, in which values less than 0.75 indicates that the TL is safe and not weak providing that both Real Power Performance Index (PPI) and Line Stability Index (LSI) are within defined limit and on the other hand, values beyond 0.75 indicates that TL is not safe and weak when evaluated in terms of combined indices (ICSI). But here, only the affected transmission lines are compared in terms of ICSI value by pivoting the stated critical value hence, all transmission lines are evaluated earlier in terms of both individual severity indices separately i.e., PPI and LSI. The determined ICSI values of affected TLs from both case simulation results are as shown in Table 4.9 and ICSI of all affected TLs in terms one of the ISI is shown in Figure 4.17.

Table 4.9. Simulation result comparison of TLs affected in terms of the ICSI before and after UPFC deployment

Outage Element/s	Line From-To	ICSI Without UPFC Deployment	ICSI With UPFC Deployment	Result Observation
		$ICSI_{ij}$	$ICSI_{ij}$	
7_Wolyta-3_Gelan	2_Sululta-10_D/Markos	1.277894	0.649753	Solved
57_Mekele-58_Tekeze PP	56_Humera-44_Gonder-II	0.958625	0.956221	Positive Output
	54_Alamata-61_Ashogo.WF	0.827809	0.482276	Solved
M/Wakena Plant	2_Sululta-10_D/Markos	0.898497	0.245525	Solved
	28_Adama-II WF-26_Koka	0.784790	0.031274	Solved
	7_Wolyta-3_Gelan	0.758732	0.964759	Negative Output
	7_Wolyta-3_Gelan	0.758732	0.964759	Negative Output
11_GG-II PP-4_Sebeta-II	2_Sululta-10_D/Markos	0.915802	0.285136	Solved
	7_Wolyta-3_Gelan	0.885121	1.339537	Negative Output
	7_Wolyta-3_Gelan	0.885121	1.339537	Negative Output
6_Holeta-2_Sululta	2_Sululta-10_D/Markos	0.977739	0.313017	Solved
Tekeze Plant	2_Sululta-10_D/Markos	0.824788	0.187332	Solved
GG II Plant	8_GG-III PP-7_Wolyta	1.445075	0.357624	Solved
	8_GG-III PP-7_Wolyta	1.445075	0.357624	Solved
	8_GG-III PP-7_Wolyta	1.445075	0.357624	Solved

20_Kaliti-I-21_Gelan	7_Wolyta-3_Gelan	0.535991	1.286997	Negative Output
	7_Wolyta-3_Gelan	0.535991	1.286997	Negative Output
32_Hurso-26_Koka	31_D/dawa-III-25_Awash-7KL	1.370649	0.680741	Solved
	2_Sululta-10_D/Markos	0.753926	0.303142	Solved
	25_Awash-7KL-26_Koka	0.740894	1.001801	Negative Output
Fincha Plant	2_Sululta-10_D/Markos	0.804772	0.301987	Solved
25_Awash-7KL-26_Koka	32_Hurso-26_Koka	0.747657	0.861002	Negative Output
	32_Hurso-26_Koka	0.747657	1.055488	Negative Output
GG I Plant	2_Sululta-10_D/Markos	0.762914	0.265402	Solved
5_G/Guracha-10_D/Markos	2_Sululta-10_D/Markos	0.974315	0.191301	Solved
18_Gefersa-35_Ghedo	2_Sululta-10_D/Markos	0.779119	0.319492	Solved
11_GG-II PP-7_Wolyta	2_Sululta-10_D/Markos	0.770171	0.225192	Solved

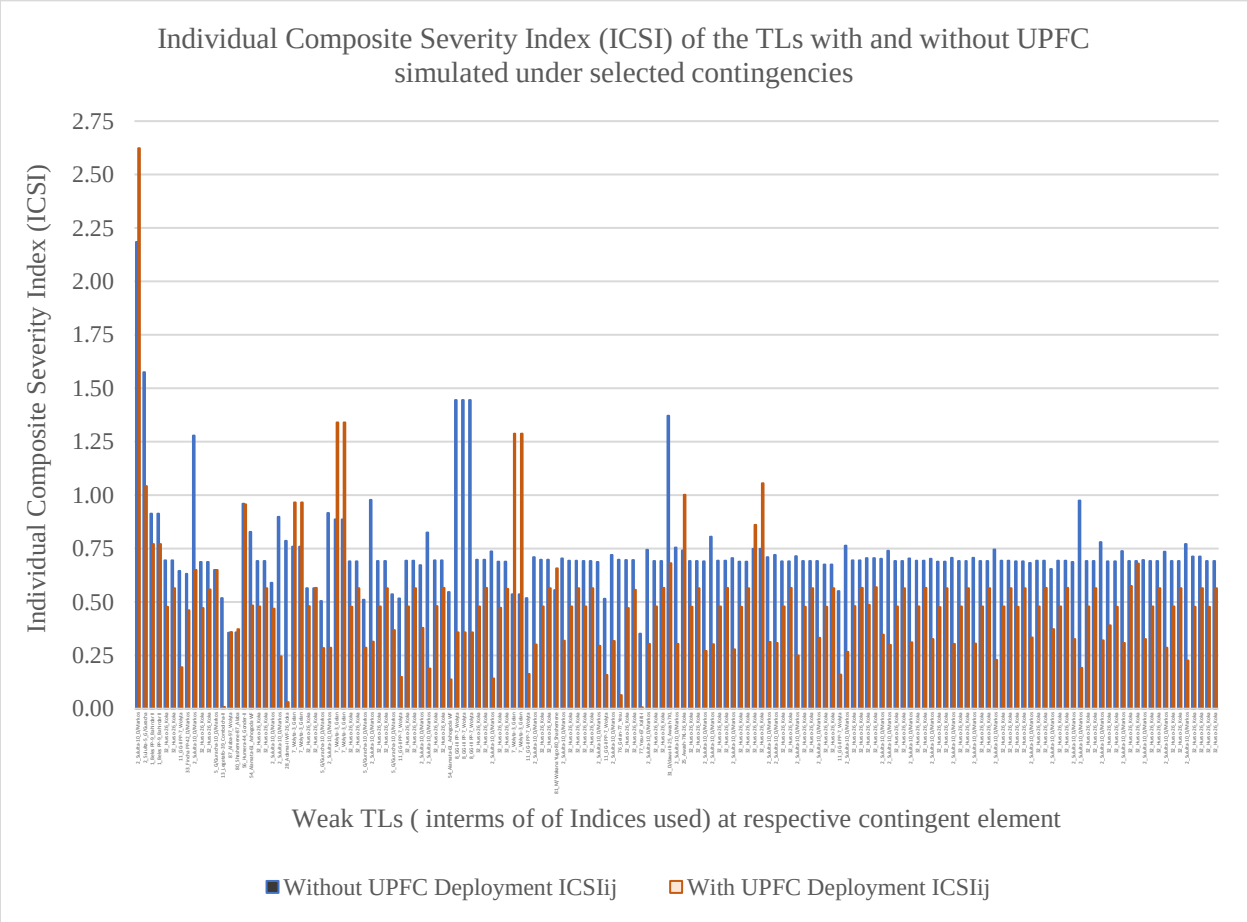

Figure 4.17. Individual Composite Severity Index (ICSI) of all problematic TLs with and without UPFC simulated under selected contingencies

As already stated, here also the impact of the UPFC deployment on each of the lines result is identified as solved, positive output and negative output. The result observation marked with 'Solved' stands for fully secured TLs in terms of the ICSI whereas 'Positive Output' stands for security improved TLs but not fully solved and 'Negative Output' stands for negatively impacted TLs in terms of the ICSI following UPFC devices deployment.

It can be observed jointly from Table 4.9 and bar graph chart of Figure 4.17, almost all affected TLs in terms of the Individual Composite Severity Index (ICSI) are solved by deploying UPFC devices at selected lines. The result is the combined effect of both LSI and PPI of that transmission line (TL) by giving equal weight for both of the indices i.e., 50% weight is considered for each index.

On the other hand, 230 kV TL from Humera to Gonder, 56_Humera-44_Gonder-II, is a little bit improved in terms of ICSI under outage of double circuit 230 kV TL Mekelle to Tekeze PP, 57_Mekele-58_Tekeze PP, whereas double circuit 400 kV TL from Wolyta to Gelan, 7_Wolyta-3_Gelan, 230 kV TL from Awash to Koka, 25_Awash-7KL-26_Koka and one of 230 kV TLs from Hurso to Koka, 32_Hurso-26_Koka, are the negatively impacted TLs under corresponding contingency conditions following UPFC devices deployment. It is to be noted that the outage case study of GG III PP has been included in each of the bar graph figures for visualization of its result.

It can be concluded from the explorations made throughout this study that the line stability issue is the most important index to secure overall grid under selected contingency case. The result shows that further work on the line stability of the Ethiopia's grid is very important. In fact, this limitation is incurred due to the inactive mode operation of the UPFC devices deployed in the model under study.

4.5.2.3 Overall Composite Severity Indices (OCSI) with and without UPFC

The overall composite severity index (OCSI) is intended to measure the overall effect of the selected transmission line (TL) or power plant (PP) outage on grid model. As its name indicates, it is overall sum of individual composite severity index (ICSI) determined for each of the transmission lines (TLs). The determined OCSI values for respective outage of selected

transmission lines (TLs) and power plants (PPs) before and after deployment of UPFC devices are as shown in Table 4.10 and corresponding Figure 4.18.

Table 4.10. OSCI of the grid for respective outage of TL/PP

OSCI of the grid for respective outage of TL/PP					
Outage TL/PP	Nominal PP/ Thermal TL S(pu)	TL/Bus Voltage Level (kV)	OCSI of the Grid Model Simulation without UPFC	OCSI of the Grid Model Simulation with UPFC	Result Observation
GG III Plant	22	400	23.091850	31.671190	Negative Output
7_Wolyta-3_Gelan	12.17	400	19.734291	13.194244	Improved
57_Mekele-58_Tekeze PP	3.55	230	19.529040	17.582851	Improved
M/Wakena Plant	1.8	230	19.293922	13.781072	Improved
11_GG-II PP-4_Sebeta-II	12.17	400	17.394284	14.630370	Improved
6_Holeta-2_Sululta	12.17	400	16.973824	13.720821	Improved
41_Bahirdar-II-44_Gonder-II	3.98	230	16.758072	16.083706	Improved
Tekeze Plant	3.44	230	16.720615	14.363204	Improved
GG II Plant	5	400	16.153597	14.493103	Improved
20_Kaliti-I-21_Gelan	3.55	230	16.152047	15.247087	Improved
27_M/Wakana PP-26_Koka	3.55	230	16.094193	14.088134	Improved
51_GG-New-50_GG-I PP	4.18	230	16.089706	15.243446	Improved
23_Sebeta-II-22_Sebeta-I	4.18	230	16.005241	14.502846	Improved
76_Gelan-67_Kaliti-I	1.12	132	15.993119	15.172807	Improved
11_GG-II PP-12_GG-New	12.17	400	15.927937	14.185750	Improved
32_Hurso-26_Koka	3.55	230	15.838092	14.566636	Improved
13_Legetafo-14_Sululta	3.55	230	15.721317	14.619841	Improved
Fincha Plant	0.16	230	15.633733	14.290149	Improved
13_Legetafo-16_Cotobie	3.55	230	15.597021	14.816201	Improved
25_Awash-7KL-26_Koka	3.55	230	15.578001	15.079702	Improved

80_Shashemene-87_Alaba	1.12	132	15.538855	14.589988	Improved
17_B/Arabsa TP-20_Kaliti-I	3.55	230	15.516683	14.557094	Improved
Awash II Plant	0.4	132	15.472644	14.582781	Improved
GG I Plant	2.19	230	15.456055	13.781072	Improved
26_Koka-21_Gelan	3.55	230	15.450951	14.614845	Improved
35_Ghedo-51_GG-New	3.67	230	15.427357	14.335378	Improved
76_Gelan-77_Yesu	1.12	132	15.402822	14.383320	Improved
Koka Hydro Plant	0.6	132	15.392289	14.734472	Improved
22_Sebeta-I-19_T/hailoch	3.55	230	15.384544	14.335608	Improved
19_T/hailoch-18_Gefersa	3.67	230	15.372170	14.338670	Improved
6_Holeta-4_Sebeta-II	12.17	400	15.366177	14.828129	Improved
Awash III Plant	0.4	132	15.319376	14.607653	Improved
Amerti Neshi Plant	1.06	230	15.288097	14.582393	Improved
Tis Abay II Plant	0.8	132	15.272171	14.373305	Improved
5_G/Guracha-10_D/Markos	12.17	400	15.236055	14.465779	Improved
18_Gefersa-35_Ghedo	3.98	230	15.178510	17.207830	Negative Output
51_GG-New-30_Wolkite	4.18	230	15.170635	14.988342	Improved
35_Ghedo-34_Fincha-II	3.55	230	15.143248	14.450245	Improved
22_Sebeta-I-30_Wolkite	4.18	230	15.039452	14.429302	Improved
11_GG-II PP-7_Wolyta	12.17	400	14.641239	14.093116	Improved
9_Bahirdar II-10_D/Markos	12.17	400	14.397400	16.665166	Negative Output

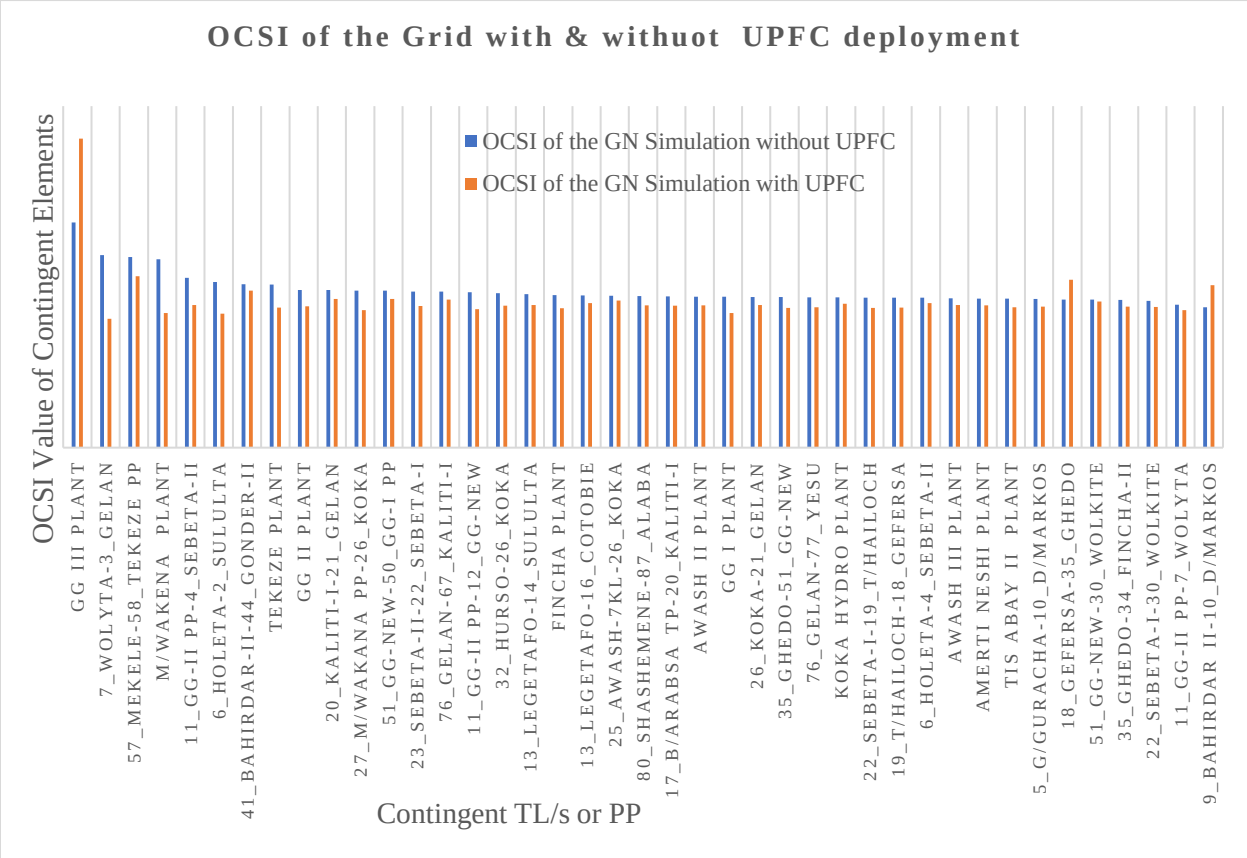

Figure 4.18. OSCI of the grid with and without UPFC for respective outage of TL/PP

It can be observed from Table 4.10 and corresponding bar graph chart of Figure 4.18, OSCI simulation result of the grid model that almost overall security of the TLs are improved by deploying UPFC devices except three contingent elements. The contingent elements for which OCSI is negatively impacted following UPFC deployment are GG III PP (of course it is omitted from the solution phase), triple circuit 230 kV TL from Gefersa to Ghedo, 18_Gefersa-35_Ghedo, and 400 kV TL from Bahirdar to D/Markos, 9_Bahirdar II-10_D/Markos,.

To conclude, the security of the grid model has improved as evaluated in terms of both individual and composite indices. This in turn assures that UPFC devices have performance to secure the grid.

CHAPTER 5

CONCLUSIONS, RECOMMENDATION AND FUTURE WORK

5.1 Conclusions

This thesis presents security enhancement of Ethiopia high voltage grid using UPFC. Accordingly, the existing national grid is modeled and validated using collected data from EEP and then, the whole study is carried out by scaling the load at each of the nodes by 1.33 as it is also used by NLDC planners for generation scheduling and daily peak load forecasting. The grid is simulated so that 30 transmission lines (TLs) are selected based on the magnitude of MVA flow ranks and also 11 power plants (PPs) are selected based on the installed capacity ranks for further outage case studies. These 41 contingent elements are simulated under corresponding outage condition using PSAT in MATLAB and their criticalities are ranked by using OCSI. Moreover, feasible locations for the UPFC deployment are identified using OCSI and individual severity indices (ISI) jointly. Then, grid model with UPFC deployed is simulated under both NSSO and each of the contingency conditions. After all, simulation results of affected elements in terms of TL thermal limit and bus voltage limit under NSSO, and in terms of LSI, PPI, ICSI and OCSI under contingency conditions are identified and screened out. The simulation results obtained without and with UPFC deployment is compared accordingly in order to evaluate how much the grid's security is enhanced.

The results obtained from grid model simulation without UPFC deployed at NSSO are 37 bus voltage limit violations (far below acceptable minimum voltage) and all MVA flows are within prescribed thermal limits except 11_GG-II PP to 7_Wolyta 400 kV TL hence, its loading is 12.217675 pu apparently where its thermal limit is 12.17 pu. The results obtained at NSSO when UPFC devices are deployed are 27 bus voltage limit violations but appreciably improved and all MVA flows are within prescribed thermal limits including 11_GG-II PP to 7_Wolyta 400 kV TL hence, the line overload problem apparently is solved i.e., changed from 12.217675 pu without UPFC to 3.796130 pu with UPFC.

The results obtained from grid model simulation in terms of ISI without UPFC deployment under selected 40 contingency conditions (GG III PP outage case omitted) are 140 statically instable TLs

when evaluated in terms of LSI, 5 overloaded TLs when evaluated in terms of PPI and 27 TLs' limit violated when evaluated in terms of ICSI. But the results obtained after UPFC deployment are 90 TLs are statically stabilized, 41 TLs improved, and 9 TLs negatively impacted when evaluated in terms of LSI; 2 TLs overloading status solved, and 3 TLs are a little bit negatively impacted when evaluated in terms of PPI; and 17 limit violated TLs solved, 1 TL improved, and 9 TLs are negatively impacted when evaluated in terms of ICSI.

The security of grid model with UPFC deployed is enhanced for 38 contingency case simulations whereas for 2 contingency cases, it is negatively impacted i.e., for outage condition of triple circuit 230 kV TLs from Gefersa to Ghedo, 18_Gefersa-35_Ghedo, and 400 kV TL from Bahirdar to D/Markos, 9_Bahirdar II-10_D/Markos, as evaluated in terms of OCSI.

5.2 Recommendations

As per the study results obtained, we would like to forward our recommendations to EEP as follows.

It is observed from the case studies carried out that GG III PP outage has high impact on the grid i.e., more care should be taken on its operation as it will expose the grid for total blackout incident. Existing national grid security is weak as it has been evaluated in this study and more attention ought to be paid to secure it. Overall simulation results of case studies carried out with UPFC deployment is appreciable which indicates that FACTS devices are good choice to enhance the grid security as it has been evaluated throughout this study using UPFC.

It has been observed from the overall results that relatively, some of the 132 kV TLs are nearly overloaded even under NSSO resulting in bus voltage slashing from their minimum limit defined. At minimum level, permanently switched fixed reactors and capacitors shall be changed by autonomous reactive power compensation FACTS devices to enhance the grid security. In other words, weak buses ought to be supported by autonomous reactive power compensator to improve bus voltage and static stability of transmission lines (TLs).

As per the grid security enhancement evaluation carried out by using UPFC, implementation of this study is highly recommended.

5.3 Suggestions for Future Work

For the continuation of this study, future work directions are suggested as under below.

Inclusion of 500 kV system in future study upon the completion of the GERD and when actively deployed into grid is one the suggestions for future works. Moreover, identifying the optimal placement of UPFC using different and the latest techniques such as Artificial Intelligence (AI) is suggested. At advanced level, interfacing the UPFC devices deployed so as to enable them to communicate each other for improved and optimized utilization can be looked.

REFERENCES

[1] Moges Alemu Tikuneh, Getachew Biru Worku (PhD), "Analysis of the Power Blackout in the Ethiopian Electric Power Grid", Science Journal of Circuits, Systems and Signal Processing. Vol. 8, No. 2, 2019, pp. 53-65, accessed on October 13, 2019.

[2] Mohammed Ahmed Woday, Gezahegn Shituneh et al.," Contingency Analysis of Ethiopia's 230 kV Transmission Network", International Journal of Engineering Technologies, Vol. 1, No. 4, 2015.

[3] Moges Alemu Tikuneh and Getachew Biru Worku (PhD), "Identification of system vulnerabilities in the Ethiopian electric power system", Global Energy Interconnection Development and Corporation Organizations, Vol. 1 No. 3 Aug. 2018, accessed on April 10, 2019.

[4] Existing General Transmission Network of EEP "LDC Operational Planning and System Study Department" Version-24 drawn in February 2018 accessed on June 23, 2019.

[5]. https://www.eep.com.et/en/power-transmission/ , "EEP's Official website"-2019

[6] World Bank Group - International Development Association, "International Development Association Project Paper on a Proposed Additional Credit to the Federal Democratic Republic of Ethiopia for the Electricity Network Reinforcement and Expansion Project", World bank, Ethiopia, May 6, 2016

[7]. Bahram Shakerighadi et al., "A New Guideline for Security Assessment of Power Systems with a High Penetration of Wind Turbines", Applied Sciences, published: 3 May 2020, accessed on November 30, 2020.

[8]. Rajesh Kr Ahuja and Mukul Chankaya, "Transient Stability Analysis of Power System with UPFC Using PSAT", International Journal of Emerging Technology and Advanced Engineering, Volume 2, Issue 12, December 2012, accessed on May 12, 2019.

[9]. Dr. P.R. Sharma, Dr. Rajesh Kr. Ahuja, Shakti Vashisth, "Performance Analysis of Multi-Machine System Using UPFC", Vol. 3, Issue 6, June 2014, accessed on May 21, 2019

[10]. T.A. Ramesh Kumaar et al, "Power System Security Enhancement using FACTS devices in a Power System Network with Voltage Dependent Loads and ZIP Loads", International Journal of Computer Applications (0975 – 8887), Volume 45– No.4, May 2012, accessed on March 02, 2019.

[11]. NEELESH SAHU, Dr. K.T. CHATURVEDI, "CONTINGENCY ANALYSIS & SECURITY OF 6 BUS POWER SYSTEM NETWORK", International Research Journal of Engineering and Technology (IRJET), Volume: 05 Issue: 05, May-2018, accessed on March 16, 2019.

[12]. Prabha Kundur et al., "Overview on Definition and Classification of Power System Stability", On Behalf of IEEE/ClGRE Joint Task Force on Stability Terms and Definitions, accessed on November 30, 2020.

[13]. Rilwan Usman et al, "ANALYSIS OF THE EFFECT OF FLEXIBLE ALTERNATING CURRENT TRANSMISSION SYSTEM (FACTS) ON THE NIGERIAN 330KV TRANSMISSION NETWORK USING ERACS AND MATLAB SIMULLINK", European Journal of Engineering and Technology, Vol. 4 No. 3, 2016, accessed on September 01, 2019.

[14]. B. Rajanarayan Prusty, Bhagabati Prasad Pattnaik et al., "Power System Security Analysis", International Journal of Scientific & Engineering Research, Volume 5, Issue 5, May-2014; accessed on June 18, 2019.

[15]. K. S. SWARUP, and P. BRITTO CORTHIS, "Power system static security assessment using self-organizing neural network", J. Indian Inst. Sci., July–Aug. 2006, accessed on February 20, 2020.

[17]. Sunil Malival, "Study of Power System Security in Indian Utility 62 Bus System", International Journal of Engineering Research and Development (IJERD), (RTEECE 17th – 18th April 2015), accessed on March 4, 2019.

[18]. Akanksha et al, "Contingency management of power system with Interline Power Flow Controller using Real Power Performance Index and Line Stability Index", Ain Shams Engineering Journal (2016) 7, 209–222, accessed on August 23, 2019.

[19]. Swati S. Pande et al, "Voltage Stability Indices Calculation of Large Bus Power System", International Journal of Innovative Research in Electrical, Electronics, Instrumentation and Control Engineering, Vol. 7, Issue 3, March 2019, accessed on May 1, 2019.

[20]. Mostafa Alinezhad and Mehrdad Ahmadi Kamarposhti, "Static Voltage Stability Assessment Considering the Power System Contingencies using Continuation Power Flow Method", International Journal of Electrical and Electronics Engineering, 2010, accessed on May 16, 2019.

[21]. Haruna Musa , "An Overview on Voltage Stability Indices as Indicators of Voltage Stability for Networks with Distributed Generations Penetration", International Journal of Science, Technology and Society, Published online July 21, 2015, December 30, 2020.

[22]. P.R. Sharma et al, "Computation of Sensitive Node for IEEE- 14 Bus system Subjected to Load Variation", International Journal of Innovative Research in Electrical, Electronics, Instrumentation and Control Engineering Vol. 2, Issue 6, June 2014, accessed on July 25, 2019.

[23]. Subrat Kumar Bihari et al., "A Review: Capability of FACTS Device for Performance Improvement of Power System", International Journal of Scientific & Engineering Research Volume 8, Issue 6, June-2017, on January 26, 2020.

[24]. R. Mohan Mathur et al., "THYRISTOR-BASED FACTS CONTROLLERS FOR ELECTRICAL TRANSMISSION SYSTEMS", IEEE PRESS SERIESS ON POWER ENGINEERING, 2002, accessed on February 9, 2020.

[25]. Toshi Mandloi, Anil K Jain, "A STUDY OF POWER SYSTEM SECURITY AND CONTINGENCY ANALYSIS", International Journal of Scientific Research Engineering & Technology (IJSRET), Volume 3, Issue 4, July 2014; accessed on November 11, 2019.

[26]. Federico Milano, "Power System Analysis Toolbox Documentation for PSAT version 1.3.4", July 14, 2005; accessed on May 03, 2019.

[27]. Ch.Kiran Kumar et al., "A comparative analysis of UPFC as a Power Flow controller with applications", IOSR Journal of Electrical and Electronics Engineering (IOSR-JEEE), Volume 4, Issue 6 (Mar. - Apr. 2013), accessed on November 21, 2019.

[28]. Federico Milano, “Power System Analysis Toolbox Documentation for PSAT version 2.0.0”, February 14, 2008; accessed on March 9, 2020

[29]. Nor Rul Hasma Abdullah et al., “Transmission Loss Minimization and UPFC Installation Cost using Evolutionary Computation for Improvement of Voltage Stability”, Proceedings of the 14th International Middle East Power Systems Conference (MEPCON’10), Cairo University, Egypt, December 19-21, 2010, accessed on September 23, 2019.

APPENDICES

Appendix A: The national transmission network of EEP [4]

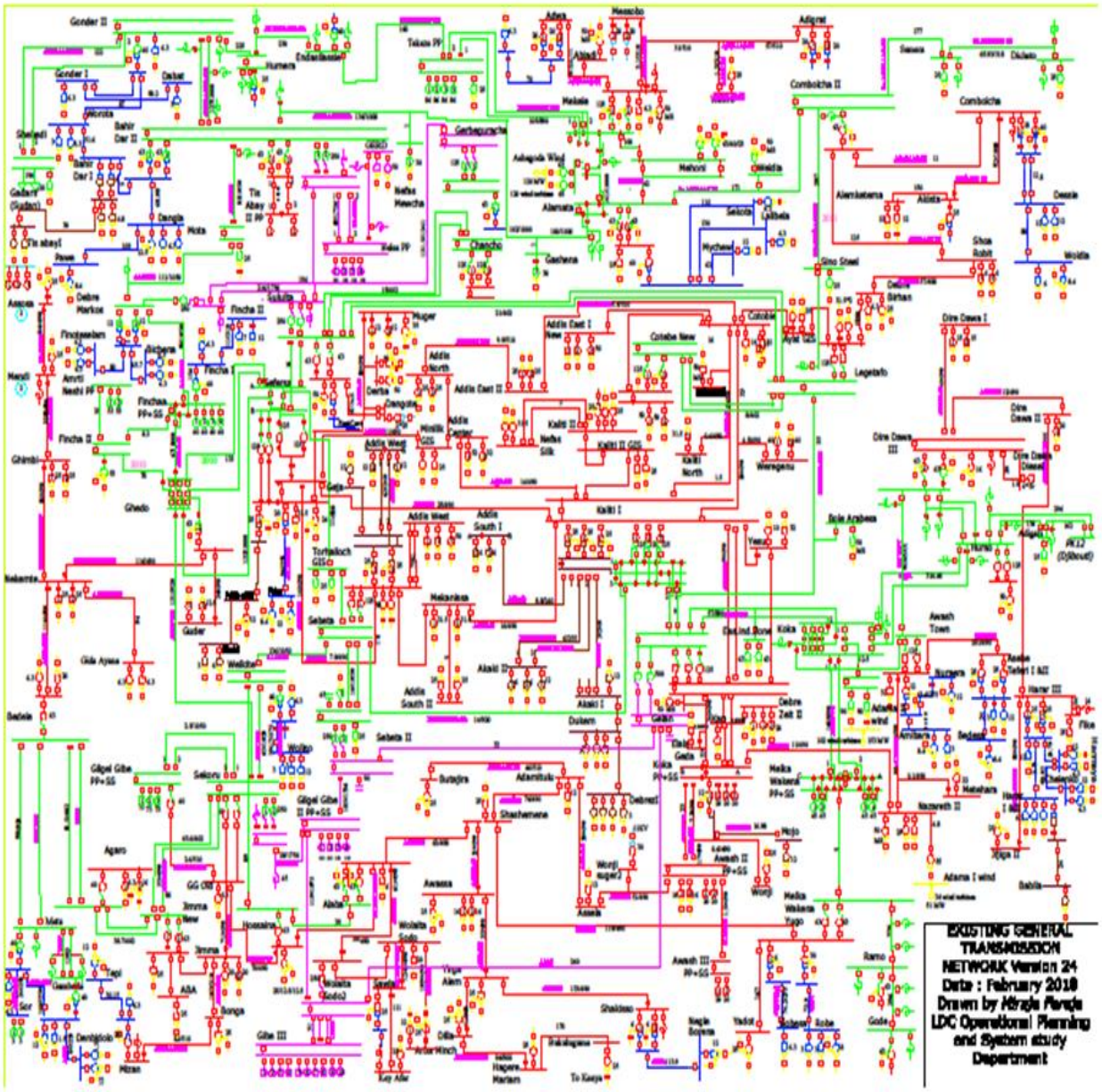

Appendix B. The input load data

SN	Load Bus No.	Load Bus Name	Cumulative Load Name	Total load at the connected bus		Saprox. (MVA)	P (p.u)	Q (p.u)	Vmin (pu)	Vmax (pu)
				P (MW)	Q (MVAr)					
1	51	G. GIBE NEW	Jimma	28.6	13.42	32	0.89	0.42	0.95	1.05
2	99	Metu	Metu	7.36	3.56	9	0.82	0.4	0.95	1.05
3	100	Gambella	Gambella	8.51	4.12	10	0.85	0.41	0.95	1.05
4	53	Agaro	Agaro	7.72	3.74	9	0.86	0.42	0.95	1.05
5	52	Jimma New	Jimma New	0.44	0.21	0.5	0.88	0.42	0.95	1.05
6	85	GG Old	GG Old	2.14	1.04	3	0.71	0.35	0.95	1.05
7	83	Bedele	Bedele	6.09	2.95	7	0.87	0.42	0.95	1.05
8	82	Nekemte	Nekemte	26.59	8.55	28	0.95	0.31	0.95	1.05
9	34	Fincha II	Fincha II	4.96	2.4	6	0.83	0.4	0.95	1.05
10	33	Fincha PP & SS	Fincha	7.75	3.75	9	0.86	0.42	0.95	1.05
11	84	Ghedo	Ghedo	0.75	0.36	0.9	0.83	0.4	0.95	1.05
12	42	Debre Markos	Debre Markos	21.4	10.36	24	0.89	0.43	0.95	1.05
13	106	Bahir Dar I	Bahir Dar I	5.13	3	6	0.86	0.5	0.95	1.05
14	102	Bahir Dar II	Bahir Dar II	31.06	15.23	35	0.89	0.44	0.95	1.05
15	103	Woreta	Woreta	4.54	2.2	6	0.76	0.37	0.95	1.05
16	45	Mota	Mota	2.59	1.25	3	0.86	0.42	0.95	1.05
17	104	Gonder II	Gonder II	33.94	16.43	38	0.89	0.43	0.95	1.05
18	46	Nefas Mewucha	Nefas Mewucha	4.79	0.52	5	0.96	0.1	0.95	1.05
19	43	Gashena	Gashena	4.39	0.23	5	0.88	0.05	0.95	1.05
20	1	Beles PP	GERD	12.35	4.39	14	0.88	0.31	0.95	1.05
21	90	Sululta	Sululta	43.48	14.52	46	0.95	0.32	0.95	1.05
22	68	Gefersa	Gefersa	76.48	37.02	85	0.9	0.44	0.95	1.05
23	93	Dangote	Dangote-Derba-Muger	44.92	12.69	47	0.96	0.27	0.95	1.05
24	19	Torhayloch GIS	Torhayloch	5.62	2.33	7	0.8	0.33	0.95	1.05
25	70	Sebeta 1	Sebeta 1	126.22	53.26	137	0.92	0.39	0.95	1.05
26	23	Sebeta 2	Sebeta 2	18.19	8.81	21	0.87	0.42	0.95	1.05
27	30	Wolkite	Wolkite	21.04	10.18	24	0.88	0.42	0.95	1.05
28	69	Addis North	A/North-Minilk GIS	49.91	16.65	53	0.94	0.31	0.95	1.05
29	72	Addis East 2	Addis East 2	53.84	10.24	55	0.98	0.19	0.95	1.05
30	73	Cotobie	Cotobie	105.01	50.84	117	0.9	0.43	0.95	1.05
31	91	Legetafo	Legetafo	59.72	10.51	61	0.98	0.17	0.95	1.05
32	67	Kaliti 1	Kaliti 1	332.46	140.8	362	0.92	0.39	0.95	1.05
33	71	Mekanisa	Mekanisa	48.48	9.75	50	0.97	0.2	0.95	1.05

34	80	Sheshemene	Sheshemene	98.51	40.28	107	0.92	0.38	0.95	1.05
35	87	Alaba	Alaba	6.85	3.31	8	0.86	0.41	0.95	1.05
36	86	Hosaina	Hosaina	17.62	9.51	21	0.84	0.45	0.95	1.05
37	97	Wolaita Sodo	Wolaita Sodo	43.18	22.68	49	0.88	0.46	0.95	1.05
38	79	Adamitulu	Adamitulu	15.06	7.29	17	0.89	0.43	0.95	1.05
39	78	Asela	Asela	4.76	2.3	6	0.79	0.38	0.95	1.05
40	65	Awash II PP&SS	Awash	35.98	28.35	46	0.78	0.62	0.95	1.05
41	81	M/Wakena Yugo-132	M/Wakena Yugo-132	12.81	4.37	14	0.91	0.31	0.95	1.05
42	64	Koka PP&SS	Koka	22.99	11.13	26	0.88	0.43	0.95	1.05
43	94	Elala-Geda TP	Elala-Geda	8.13	3.94	10	0.81	0.39	0.95	1.05
44	96	Debreziet TP	Debreziet	37.89	23.44	45	0.84	0.52	0.95	1.05
45	29	M/Wakena Yugo-230	M/Wakena Yugo-230	8.78	4.25	10	0.88	0.42	0.95	1.05
46	24	EIZ TAP 1	EIZ TAP	24.11	11.67	27	0.89	0.43	0.95	1.05
47	76	Gelan	Gelan	29.31	14.2	33	0.89	0.43	0.95	1.05
48	77	Yesu	Yesu	33.45	16.19	38	0.88	0.43	0.95	1.05
49	74	Debre Birhan	Debre Birhan	9.23	4.47	11	0.84	0.41	0.95	1.05
50	75	Shoa Robit	Shoa Robit	7.57	2	8	0.95	0.25	0.95	1.05
51	92	Combolcha II	Combolcha II	75.47	30.78	82	0.92	0.38	0.95	1.05
52	40	Woldia	Woldia	15.74	7.62	18	0.87	0.42	0.95	1.05
53	63	Nazereth-II	Nazereth-II	55.66	24.04	61	0.91	0.39	0.95	1.05
54	62	Awash 7 Kilo	Awash 7 Kilo	45.77	20.44	51	0.9	0.4	0.95	1.05
55	32	Hurso	Hurso	100.9	-0.7	101	1	-0.01	0.95	1.05
56	31	Dire Dawa III	Dire Dawa III	79.67	33.79	87	0.92	0.39	0.95	1.05
57	54	Alamata	Alamata	22.03	10.68	25	0.88	0.43	0.95	1.05
58	59	Mehoni	Mehoni	4.27	1.68	5	0.85	0.34	0.95	1.05
59	57	Mekele	Mekele	161.19	76.14	179	0.9	0.43	0.95	1.05
60	55	Shire/Endesilassie	Shire/Endesilassie	14.17	6.86	16	0.89	0.43	0.95	1.05
61	58	Tekeze	Tekeze	2.41	1.22	3	0.8	0.41	0.95	1.05
62	56	Humera	Humera	10.94	5.3	13	0.84	0.41	0.95	1.05
63	60	Welkayt	Welkayt	4.36	1.05	5	0.87	0.21	0.95	1.05
64	15	Shegole	Shegole	68.27	33.06	76	0.9	0.43	0.95	1.05
65	17	Bole Arabsa	B/Arabsa-Lemi	40.33	18.32	45	0.9	0.41	0.95	1.05
66	5	Gebre Guracha	Gebre Guracha	6.95	3.37	8	0.87	0.42	0.95	1.05
67	6	Holeta	Holeta	11.94	0.94	12	0.99	0.08	0.95	1.05
68	95	Elala-Geda DCP	Knoria Textile	8.56	4.14	10	0.86	0.41	0.95	1.05
69	44	Gonder II	Sudan-Gadarf	100	0	100	1	0	0.95	1.05
TOTAL				2451.3	963.39	2688.4	NA	NA	NA	NA

Appendix C: Transmission Lines Input Data

Table C-1. 400 kV transmission line input data of the grid

From Bus Number	From Bus Name	Vn (kV)	To Bus Number	To Bus Name	Vn (kV)	Line R (pu)	Line X (pu)	Charging B (pu)	TL MVA Rate (A,B,C)
2	SULULTA 400	400	5	G/GURCHA 400	400	0.02682	0.363411	0.01860052	1341
2	SULULTA 400	400	6	HOLETA 400	400	0.011838	0.09865	0.01264232	1973
2	SULULTA 400	400	6	HOLETA 400	400	0.011838	0.09865	0.01120375	1973
2	SULULTA 400	400	10	D/MARKOS 400	400	0.04472235	0.5948676	0.04574348	1341
3	GELAN 400	400	4	SEBETA-2 400	400	0.013811	0.112461	0.01119007	1973
3	GELAN 400	400	6	HOLETA 400	400	0.01973	0.155867	0.0176888	1973
3	GELAN 400	400	6	HOLETA 400	400	0.01973	0.155867	0.0176888	1973
3	GELAN 400	400	7	WOLAYTA 400	400	0.108515	0.852336	0.09649721	1973
3	GELAN 400	400	7	WOLAYTA 400	400	0.108515	0.852336	0.09649721	1973
4	SEBETA-2 400	400	6	HOLETA 400	400	0.0033981	0.04074105	0.00861187	1205
4	SEBETA-2 400	400	6	HOLETA 400	400	0.0033981	0.04074105	0.00861187	1205
4	SEBETA-2 400	400	11	GI GIBE-2 400	400	0.03807099	0.50630796	0.07786652	1341
5	G/GURCHA 400	400	10	D/MARKOS 400	400	0.018774	0.24138	0.03712901	1341
7	WOLAYTA 400	400	8	G-GIBE3 400	400	0.01973	0.159813	0.01807045	1973
7	WOLAYTA 400	400	8	G-GIBE3 400	400	0.01973	0.159813	0.01807045	1973
7	WOLAYTA 400	400	8	G-GIBE3 400	400	0.021703	0.163759	0.01843183	1973
7	WOLAYTA 400	400	11	GI GIBE-2 400	400	0.049325	0.408411	0.0403411	1973
9	BAHIRDAR-II 400	400	1	BELES 400	400	0.01284678	0.16305219	0.02812304	1341
9	BAHIRDAR-II 400	400	1	BELES 400	400	0.01284678	0.16305219	0.02812304	1341
9	BAHIRDAR-II 400	400	10	D/MARKOS 400	400	0.04018977	0.5345226	0.04110328	1341
11	GI GIBE-2 400	400	12	GG NEW 400	400	0.00577971	0.07693317	0.01183296	1341

Table C-2. 230 kV transmission line input data of the grid in PSAT

From Bus Number	From Bus Name	Vn (kV)	To Bus Number	To Bus Name	Vn (kV)	Line R (pu)	Line X (pu)	Charging B (pu)	TL MVA Rate (A,B,C)
13	LEGETAFO 230	230	14	SULULTA 230	230	0.01809	0.050652	0.010065	402
13	LEGETAFO 230	230	14	SULULTA 230	230	0.01809	0.050652	0.010065	402
13	LEGETAFO 230	230	16	COTOBEI-I 230	230	0.006834	0.019296	0.003836	402
13	LEGETAFO 230	230	16	COTOBEI-I 230	230	0.006834	0.019296	0.003836	402
13	LEGETAFO 230	230	17	B/ABSTP 230	230	0.003019	0.008442	0.001678	402
13	LEGETAFO 230	230	39	COMBOL-II 230	230	0.183941	0.562329	0.168107	318

14	SULULTA 230	230	15	SHEGOLE 230	230	0.006834	0.019698	0.003709	402
14	SULULTA 230	230	18	GEFERSA 230	230	0.010755	0.031921	0.010138	318
14	SULULTA 230	230	18	GEFERSA 230	230	0.010755	0.031921	0.010138	318
15	SHEGOLE 230	230	18	GEFERSA 230	230	0.007638	0.021708	0.004047	402
17	B/ABSTP 230	230	20	KALITI1 230	230	0.030544	0.085381	0.016968	402
18	GEFERSA 230	230	19	T/HAYILOCH 230	230	0.009491	0.026532	0.005273	402
18	GEFERSA 230	230	35	GHEDO 230	230	0.057361	0.298141	0.068729	280
18	GEFERSA 230	230	35	GHEDO 230	230	0.114763	0.32078	0.06375	402
18	GEFERSA 230	230	35	GHEDO 230	230	0.114763	0.32078	0.06375	402
19	T/HAYILOCH 230	230	22	SEBATA-1 230	230	0.006287	0.017608	0.003499	402
20	KALITI1 230	230	21	GELAN 230	230	0.005359	0.025447	0.004468	331
20	KALITI1 230	230	21	GELAN 230	230	0.005359	0.025447	0.004468	331
20	KALITI1 230	230	22	SEBATA-1 230	230	0.00634	0.030863	0.007551	274
21	GELAN 230	230	24	EIZ TAP 1 230	230	0.040945	0.165222	0.028516	331
21	GELAN 230	230	26	KOKA 230	230	0.036466	0.147149	0.025397	331
22	SEBATA-1 230	230	23	SEBETA-2 230	230	0.006499	0.03297	0.007957	280
22	SEBATA-1 230	230	23	SEBETA-2 230	230	0.006499	0.03297	0.007957	280
22	SEBATA-1 230	230	30	WOLKITE 230	230	0.122389	0.352349	0.065913	402
24	EIZ TAP 1 230	230	26	KOKA 230	230	0.014725	0.069939	0.01792	274
25	AWSH-7KL 230	230	26	KOKA 230	230	0.079259	0.353099	0.054504	353
25	AWSH-7KL 230	230	31	DIRE DAWA3 230	230	0.125643	0.559734	0.0864	353
26	KOKA 230	230	27	M/WAKNA 230	230	0.076301	0.328449	0.094031	257
26	KOKA 230	230	27	M/WAKNA 230	230	0.076301	0.328449	0.094031	257
26	KOKA 230	230	28	ADAMA II WF230	230	0.008844	0.02613	0.004868	402
26	KOKA 230	230	32	HURSO 230	230	0.303735	0.84898	0.168722	402
26	KOKA 230	230	32	HURSO 230	230	0.303735	0.84898	0.168722	402
27	MELKA-WAKNA 230	230	29	M/W-YUGO 230	230	0.002328	0.010023	0.002869	257
30	WOLKITE 230	230	38	HOSAINA 230	230	0.076858	0.221273	0.041393	402
30	WOLKITE 230	230	51	G. GIBE NEW 230	230	0.030181	0.15687	0.036161	280
31	DIRE DAWA3 230	230	32	HURSO 230	230	0.009667	0.027257	0.013204	255
31	DIRE DAWA3 230	230	32	HURSO 230	230	0.009667	0.027257	0.013204	255
33	FINCHA 230	230	34	FINCHA-II 230	230	0.00532	0.016269	0.004865	318
33	FINCHA 230	230	35	GHEDO 230	230	0.03193	0.171249	0.030516	318
33	FINCHA 230	230	42	D/MARKOS230	230	0.041026	0.213231	0.049154	280
34	FINCHA-II 230	230	35	GHEDO 230	230	0.044704	0.136667	0.040855	318
34	FINCHA-II 230	230	36	NESHE 230	230	0.018752	0.057326	0.017138	318
35	GHEDO 230	230	51	G. GIBE NEW 230	230	0.057811	0.281362	0.068832	274
37	ALABA 230	230	38	HOSAINA 230	230	0.033909	0.097626	0.018263	402
39	COMBOL-II 230	230	40	WOLDIYA MOB 230	230	0.068357	0.202862	0.064428	318
40	WOLDIYA MOB 230	230	54	ALAMATA 230	230	0.040163	0.119193	0.037855	318
41	BAHIR DAR2 230	230	44	GONDAR 2 230	230	0.117887	0.339389	0.063489	402

41	BAHIR DAR2 230	230	44	GONDAR 2 230	230	0.117887	0.339389	0.063489	402
41	BAHIR DAR2 230	230	45	MOTA 230	230	0.035787	0.186001	0.042879	280
41	BAHIR DAR2 230	230	46	N/MEW TP230	230	0.087453	0.267355	0.079925	318
42	DEBRE-MARKOS230	230	45	MOTA 230	230	0.048185	0.250452	0.057736	280
43	GASHENA-TAP 230	230	46	N/MEW TP230	230	0.065591	0.200518	0.059943	318
43	GASHENA-TAP 230	230	54	ALAMATA 230	230	0.065591	0.200518	0.059943	318
47	GAMBELA2 230	230	48	METU 230	230	0.120495	0.346898	0.064893	402
47	GAMBELA2 230	230	48	METU 230	230	0.120495	0.346898	0.064893	402
48	METU 230	230	49	BEDELLE 230	230	0.058019	0.177371	0.053025	318
48	METU 230	230	49	BEDELLE 230	230	0.058019	0.177371	0.053025	318
49	BEDELLE 230	230	53	AGARO 230	230	0.070326	0.196566	0.039065	402
49	BEDELLE 230	230	53	AGARO 230	230	0.070326	0.196566	0.039065	402
50	GI GIBE-1 230	230	51	G. GIBE NEW 230	230	0.00223	0.010596	0.002715	274
50	GI GIBE-1 230	230	51	G. GIBE NEW 230	230	0.00223	0.010596	0.002715	274
51	G. GIBE NEW 230	230	52	JIMMA NEW 230	230	0.056606	0.158219	0.031444	402
51	G. GIBE NEW 230	230	52	JIMMA NEW 230	230	0.056606	0.158219	0.031444	402
52	JIMMA NEW 230	230	53	AGARO 230	230	0.033394	0.09334	0.01855	402
52	JIMMA NEW 230	230	53	AGARO 230	230	0.033394	0.09334	0.01855	402
54	ALAMATA 230	230	59	MEHONI 230	230	0.028226	0.081383	0.024317	318
54	ALAMATA 230	230	61	ASHEGODA WF 230	230	0.10653	0.306324	0.057333	402
55	ENDASILASIE 230	230	56	HUMERA 230	230	0.14766	0.438201	0.13917	318
55	ENDASILASIE 230	230	58	TEKEZE 230	230	0.102539	0.304294	0.096642	318
55	ENDASILASIE 230	230	60	WELKAYT 230	230	0.138059	0.3859	0.076692	402
56	HUMERA 230	230	60	WELKAYT 230	230	0.138059	0.3859	0.076692	402
44	GONDAR 2 230	230	60	WELKAYT 230	230	0.137199	0.383488	0.076212	402
57	MEKELE 230	230	58	TEKEZE 230	230	0.067505	0.20033	0.063623	318
57	MEKELE 230	230	58	TEKEZE 230	230	0.067505	0.20033	0.063623	318
57	MEKELE 230	230	59	MEHONI 230	230	0.084348	0.242828	0.045425	402
57	MEKELE 230	230	61	ASHEGODA WF 230	230	0.016482	0.047034	0.008806	402

Table C-3. 132 kV transmission line input data of the grid in PSAT

From Bus Number	From Bus Name	Vn (kV)	To Bus Number	To Bus Name	Vn (kV)	Line R (pu)	Line X (pu)	Charging B (pu)	Appx. MVA Limit
62	AWASH 7 KILO	132	63	NAZRETH II 132	132	0.078889	0.175093	0.025959	112
63	NAZRETH II 132	132	64	KOKA 132	132	0.094129	0.213988	0.031542	112
67	GEFARSA 132	132	67	KALITI I 132	132	0.148708	0.330055	0.048933	112
68	GEFARSA 132	132	70	SEBETA I 132	132	0.086475	0.198508	0.028993	112
71	MEKANISSA 132	132	67	KALITI I 132	132	0.048491	0.111313	0.016258	112
71	MEKANISSA 132	132	70	SEBETA I 132	132	0.035703	0.082219	0.011788	112

68	GEFARSA 132	132	69	ADDIS NORTH 132	132	0.035703	0.082219	0.011788	112
73	COTOBIE 132	132	67	KALITI I 132	132	0.098013	0.223177	0.032843	112
73	COTOBIE 132	132	67	KALITI I 132	132	0.012199	0.028166	0.003983	112
77	YESU FACTORY	132	67	KALITI I 132	132	0.006777	0.015648	0.002213	112
74	DEBRE BIRHAN 132	132	75	SHOA ROBIT 132	132	0.131656	0.299299	0.044117	112
75	SHOA ROBIT 132	132	92	COMBOLCHA 132	132	0.010664	0.024285	0.003561	112
65	AWASH II 132	132	78	ASELA 132	132	0.076251	0.191027	0.031754	112
65	AWASH II 132	132	66	AWASH III 132	132	0.131656	0.299299	0.044117	112
65	AWASH II 132	132	66	AWASH III 132	132	0.067233	0.155240	0.023958	117
79	ADAMITULU 132	132	78	ASELA 132	132	0.027248	0.060957	0.009348	117
82	NEKEMTE 132	132	84	GHEDO 132	132	0.027248	0.060957	0.009348	112
97	W/SODO 132	132	87	ALABA 132	132	0.041655	0.093189	0.014291	117
87	ALABA 132	132	80	SHASHEMENE 132	132	0.041655	0.093189	0.014291	117
80	SHASHEMENE 132	132	79	ADAMITULU 132	132	0.027248	0.060957	0.009348	112
80	SHASHEMENE 132	132	81	M/WAKENA YOUG 132	132	0.041655	0.093189	0.014291	117
85	G/GIBE OLD 132	132	86	HOSAINA 132	132	0.011026	0.024668	0.003783	112
86	HOSAINA 132	132	87	ALABA 132	132	0.011026	0.024668	0.003783	112
89	BAHIR DAR II 132	132	88	TIS ABAY II 132	132	0.030629	0.068522	0.010752	112
89	BAHIR DAR II 132	132	91	TIS ABAY II 132	132	0.030629	0.068522	0.010752	112
85	GEFARSA 132 BB1	132	93	DANGOTE 132	132	0.078889	0.175093	0.025959	112
69	ADDIS NORTH 132	132	72	ADDIS EAST II 132	132	0.094129	0.213988	0.031542	112
73	COTOBIE 132	132	72	ADDIS EAST II 133	132	0.148708	0.330055	0.048933	112
73	COTOBIE 132	132	91	lEGETAFO132KV	132	0.086475	0.198508	0.028993	112
76	GELAN 132	132	77	YESU FACTORY 132	132	0.048491	0.111313	0.016258	112
82	NEKEMTE 132	132	92	BEDELE 132	132	0.035703	0.082219	0.011788	112
91	lEGETAFO132KV	132	74	DEBRE BIRHAN 132	132	0.035703	0.082219	0.011788	112
90	SULULTA 132KV	132	93	DANGOTE 132	132	0.098013	0.223177	0.032843	112
94	ELALA GEDA 132 TP	132	64	KOKA 132	132	0.012199	0.028166	0.003983	112
95	E/GEDA DCP 132	132	64	KOKA 132	132	0.006777	0.015648	0.002213	112
94	ELALA GEDA 132 TP	132	76	GELAN 132	132	0.131656	0.299299	0.044117	112
95	ELALA GEDA DCP 132	132	76	GELAN 132	132	0.010664	0.024285	0.003561	112
64	KOKA 132	132	96	DEBREZIET TP 132	132	0.076251	0.191027	0.031754	112
96	DEBREZIET TP 132	132	76	GELAN 132	132	0.131656	0.299299	0.044117	112
67	KALITI I	132	76	GELAN 132	132	0.067233	0.155240	0.023958	112
67	KALITI I	132	76	GELAN 132	132	0.027248	0.060957	0.009348	112
64	Koka PP	132	65	AWASH II PP	132	0.027248	0.060957	0.009348	112
64	Koka PP	132	65	AWASH II PP	132	0.041655	0.093189	0.014291	112

Table C-4. 66 kV transmission line input data of the grid in PSAT

From Bus Number	From Bus Name	Vn (kV)	To Bus Number	To Bus Name	Vn (kV)	Line R (pu)	Line X (pu)	Charging B (pu)	Appx. MVA Limit
99	METU 66	66	98	SOR 66	66	0.083389	0.067603	0.009740	29
103	WERETA 66	66	101	B/DAR I 66	66	0.179390	0.144062	0.020949	29
101	BAHIR DAR I 66	66	102	B/DAR II 66	66	0.015708	0.012614	0.001834	29
100	GAMBELA 66	66	99	METU 66	66	0.507283	0.411250	0.059250	29
103	WERETA 66	66	104	GONDER II 66	66	0.284341	0.228345	0.033205	29

Table C-5. 45 kV transmission line input data of the grid in PSAT

From Bus Number	From Bus Name	Vn (kV)	To Bus Number	To Bus Name	Vn (kV)	Line R (pu)	Line X (pu)	Charging B (pu)	Appx. MVA Limit
106	BAHIR DAR I 45	45	105	TIS ABAY I 45	45	0.073262	0.11064	0.009247	19

Appendix D: Bus Bar Input Data

Table D-1. 400 kV busbars input data

Bus Number	Bus Name	Base kV	Bus Type	Owner Name	Voltage (pu)	Angle (rad)	Normal Vmax (pu)	Normal Vmin (pu)	Emergency Vmax (pu)	Emergency Vmin (pu)
1	BELES	400	Slack	Generation	1	0	1.05	0.95	1.1	0.9
2	SULULTA	400	PV	Transmission	0.9	-0.479	1.05	0.95	1.1	0.9
3	GELAN	400	PV	Transmission	0.99	-0.812	1.05	0.95	1.1	0.9
4	SEBETA-2	400	PV	Transmission	0.95	-0.108	1.05	0.95	1.1	0.9
5	GEBRE-GURCHA	400	PQ	Transmission	0.89	-0.531	1.05	0.95	1.1	0.9
6	HOLETA	400	PQ	Transmission	0.897	-0.73	1.05	0.95	1.1	0.9
7	WOLAYTA	400	PV	Transmission	0.97	-0.905	1.05	0.95	1.1	0.9
8	GILGEL GIBE-3	400	PV	Generation	1	-0.418	1.05	0.95	1.1	0.9
9	BAHIRDAR-II	400	PV	Transmission	0.94	-0.78	1.05	0.95	1.1	0.9
10	DEBRE MARKOS	400	PV	Transmission	0.96	-0.6	1.05	0.95	1.1	0.9
11	GILGEL GIBE-2	400	PV	Generation	0.99	-0.65	1.05	0.95	1.1	0.9
12	G. GIBE NEW	400	PV	Transmission	0.98	-0.549	1.05	0.95	1.1	0.9

Table D-2. 230 kV busbars input data

Bus Number	Bus Name	Base kV	Bus Type	Owner Name	Voltage (pu)	Angle (deg)	Angle (rad)	Normal Vmax (pu)	Normal Vmin (pu)	Emergency Vmax (pu)	Emergency Vmin (pu)
13	LEGETAFO	230	PV	Transmission	0.9658	-42.01	-0.733	1.05	0.95	1.1	0.9
14	SULULTA	230	PV	Transmission	0.9738	-41.31	-0.721	1.05	0.95	1.1	0.9
15	SHEGOLE	230	PQ	Transmission	1	0	0.000	1.05	0.95	1.1	0.9
16	COTOBEI-I	230	PV	Transmission	0.9641	-42.11	-0.735	1.05	0.95	1.1	0.9
17	BOLEARABSTP	230	PQ	Transmission	0.9661	-41.93	-0.732	1.05	0.95	1.1	0.9
18	GEFERSA	230	PV	Transmission	0.9714	-40.86	-0.713	1.05	0.95	1.1	0.9
19	TORHAYILOCH	230	PV	Transmission	0.971	-40.4	-0.705	1.05	0.95	1.1	0.9
20	KALITI1	230	PV	Transmission	0.9687	-41.1	-0.717	1.05	0.95	1.1	0.9
21	GELAN	230	PV	Transmission	0.9728	-40.88	-0.714	1.05	0.95	1.1	0.9
22	SEBATA-1	230	PV	Transmission	0.9709	-40.08	-0.700	1.05	0.95	1.1	0.9
23	SEBETA-2	230	PV	Transmission	0.979	-38.72	-0.676	1.05	0.95	1.1	0.9
24	EIZ TAP 1	230	PV	Transmission	0.9868	-42.92	-0.749	1.05	0.95	1.1	0.9
25	AWSH-7KL	230	PV	Transmission	0.9964	-48.3	-0.843	1.05	0.95	1.1	0.9
26	KOKA	230	PV	Generation	0.9977	-43.57	-0.761	1.05	0.95	1.1	0.9
27	MELKA-WAKNA	230	PV	Generation	1	-43.85	-0.765	1.05	0.95	1.1	0.9
28	ADAMA II WF	230	PV	Generation	1	-43.25	-0.755	1.05	0.95	1.1	0.9
29	M WAK-YUGO	230	PV	Generation	0.9987	-43.9	-0.766	1.05	0.95	1.1	0.9
30	WOLKITE	230	PV	Transmission	0.9937	-33.33	-0.582	1.05	0.95	1.1	0.9
31	DIRE DAWA3	230	PQ	Transmission	0.9691	-51.23	-0.894	1.05	0.95	1.1	0.9
32	HURSO	230	PQ	Transmission	0.9729	-51.13	-0.893	1.05	0.95	1.1	0.9
33	FINCHA	230	PV	Generation	1.03	-33.84	-0.591	1.05	0.95	1.1	0.9
34	FINCHA-II	230	PV	Transmission	1.0226	-33.66	-0.588	1.05	0.95	1.1	0.9
35	GHEDO	230	PV	Transmission	1	-32.27	-0.563	1.05	0.95	1.1	0.9
36	A/NESHE	230	PV	Generation	0.9664	-33.68	-0.588	1.05	0.95	1.1	0.9
37	ALABA	230	PV	Transmission	0.9767	-33.61	-0.587	1.05	0.95	1.1	0.9
38	HOSAINA	230	PV	Transmission	0.9814	-47.52	-0.829	1.05	0.95	1.1	0.9
39	COMBOL-II	230	PV	Transmission	0.9955	-46.74	-0.816	1.05	0.95	1.1	0.9
40	WOLDIYA MOB	230	PV	Transmission	1.0149	-43.77	-0.764	1.05	0.95	1.1	0.9
41	BAHIR DAR2	230	PV	Transmission	1.0119	-37.2	-0.649	1.05	0.95	1.1	0.9
42	DEBRE-MARKOS	230	PV	Transmission	1.0206	-36.05	-0.629	1.05	0.95	1.1	0.9
43	GASHENA-TAP	230	PV	Transmission	1.0149	-43.77	-0.764	1.05	0.95	1.1	0.9
44	GONDAR 2	230	PV	Transmission	0.9943	-43.02	-0.751	1.05	0.95	1.1	0.9
45	MOTA	230	PV	Transmission	1.0203	-36.81	-0.643	1.05	0.95	1.1	0.9

46	NIFAS MEW TP	230	PV	Transmission	1.0194	-41.2	-0.719	1.05	0.95	1.1	0.9
47	GAMBELA2	230	PV	Transmission	0.9454	-31.84	-0.556	1.05	0.95	1.1	0.9
48	METU	230	PV	Transmission	0.9741	-31.88	-0.556	1.05	0.95	1.1	0.9
49	BEDELLE	230	PV	Transmission	0.9926	-31.62	-0.552	1.05	0.95	1.1	0.9
50	GI GIBE-1	230	PV	Generation	1.02	-28.01	-0.489	1.05	0.95	1.1	0.9
51	G. GIBE NEW	230	PV	Generation	1.017	-28.1	-0.491	1.05	0.95	1.1	0.9
52	JIMMA NEW	230	PV	Transmission	1.0052	-30.04	-0.524	1.05	0.95	1.1	0.9
53	AGARO	230	PV	Transmission	1.0006	-30.76	-0.537	1.05	0.95	1.1	0.9
54	ALAMATA	230	PV	Transmission	1.001	-46	-0.803	1.05	0.95	1.1	0.9
55	ENDASILASIE	230	PV	Transmission	0.9713	-43.58	-0.761	1.05	0.95	1.1	0.9
56	HUMERA	230	PV	Transmission	0.908	-43.43	-0.758	1.05	0.95	1.1	0.9
57	MEKELE	230	PV	Transmission	0.9904	-45.93	-0.802	1.05	0.95	1.1	0.9
58	TEKEZE	230	PV	Generation	1	-43.02	-0.751	1.05	0.95	1.1	0.9
59	MEHONI	230	PV	Transmission	0.9996	-46.07	-0.804	1.05	0.95	1.1	0.9
60	WELKAYT	230	PV	Transmission	1	0	0.000	1.05	0.95	1.1	0.9
61	ASHEGODA WF	230	PV	Generation	1	-46.05	-0.804	1.05	0.95	1.1	0.9

Table D-3. 132 kV busbars input data

Bus Number	Bus Name	Base kV	Owner Name	Voltage (pu)	Angle (rad)	Normal Vmax (pu)	Normal Vmin (pu)	Emergency Vmax (pu)	Emergency Vmin (pu)
62	AWASH 7 KILO	132	Transmission	0.9	-0.733	1.05	0.95	1.1	0.9
63	NAZRETH II	132	Transmission	0.97	-0.6089	1.05	0.95	1.1	0.9
64	KOKA PP	132	Generation	1	0	1.05	0.95	1.1	0.9
65	AWASH II	132	Generation	1	-0.735	1.05	0.95	1.1	0.9
66	AWASH III	132	Generation	1.01	-0.531	1.05	0.95	1.1	0.9
67	KALITI I	132	Transmission	0.9714	-0.813	1.05	0.95	1.1	0.9
68	GEFERSA	132	Transmission	0.97	-0.905	1.05	0.95	1.1	0.9
69	ADDIS NORTH	132	Transmission	0.98	-0.418	1.05	0.95	1.1	0.9
70	SEBETA I	132	Transmission	0.94	-0.713	1.05	0.95	1.1	0.9
71	MEKANISSA	132	Transmission	0.96	-0.6	1.05	0.95	1.1	0.9
72	ADDIS EAST II	132	Transmission	0.979	-0.7	1.05	0.95	1.1	0.9
73	COTOBIE	132	Transmission	0.98	-0.549	1.05	0.95	1.1	0.9
74	DEBRE BIRHAN	132	Transmission	0.98	-0.84	1.05	0.95	1.1	0.9
75	SHOA ROBIT	132	Transmission	0.99	-0.76	1.05	0.95	1.1	0.9
76	GELAN	132	Transmission	1.1	-0.5426	1.05	0.95	1.1	0.9
77	YESU FACTORY	132	Transmission	1.02	-0.495	1.05	0.95	1.1	0.9
78	ASELA	132	Transmission	0.99	-0.766	1.05	0.95	1.1	0.9
79	ADAMITULU	132	Transmission	0.99	-0.817	1.05	0.95	1.1	0.9

80	SHASHEMENE	132	Transmission	0.98	-0.424	1.05	0.95	1.1	0.9
81	M/WAKENA YUGO	132	Transmission	0.98	-0.89	1.05	0.95	1.1	0.9
82	NEKEMTE	132	Transmission	1.03	-0.59	1.05	0.95	1.1	0.9
83	BEDELE	132	Transmission	1.02	-0.58	1.05	0.95	1.1	0.9
84	GHEDO	132	Transmission	1	-0.632	1.05	0.95	1.1	0.9
85	GILGEL GIBE OLD	132	Transmission	0.96	-0.79	1.05	0.95	1.1	0.9
86	HOSAINA	132	Transmission	0.97	-0.586	1.05	0.95	1.1	0.9
87	ALABA	132	Transmission	0.98	-0.829	1.05	0.95	1.1	0.9
88	TIS ABAY II	132	Generation	0.96	-0.587	1.05	0.95	1.1	0.9
89	BAHIR DAR II	132	Transmission	1.01	-0.764	1.05	0.95	1.1	0.9
90	Sululta	132	Transmission	1.01	-0.649	1.05	0.95	1.1	0.9
91	lEGETAFO	132	Transmission	1.02	-0.272	1.05	0.95	1.1	0.9
92	COMBOLCHA II	132	Transmission	1.03	-0.764	1.05	0.95	1.1	0.9
93	Dangote	132	Transmission	0.97	-0.938	1.05	0.95	1.1	0.9
94	ELALA GEDA 132 TP	132	Transmission	1.02	-0.642	1.05	0.95	1.1	0.9
95	ELALA GEDA DCP 132	132	Transmission	1.02	-0.916	1.05	0.95	1.1	0.9
96	DEBREZIET TP 132	132	Transmission	0.98	-0.555	1.05	0.95	1.1	0.9
97	W/SODO 132	132	Transmission	0.9	-0.556	1.05	0.95	1.1	0.9

Table D-4. 66 kV busbars input data

Bus Number	Bus Name	Base kV	Owner Name	Voltage (pu)	Angle (rad)	Normal Vmax (pu)	Normal Vmin (pu)	Emergency Vmax (pu)	Emergency Vmin (pu)
98	SOR	66	Generation	0.98	-0.79	1.05	0.95	1.1	0.9
99	METU	66	Transmission	0.96	-0.69	1.05	0.95	1.1	0.9
100	GAMBELLA	66	Transmission	0.89	-0.578	1.05	0.95	1.1	0.9
101	BAHIR DAR I	66	Transmission	0.99	-0.86	1.05	0.95	1.1	0.9
102	BAHIR DAR II	66	Transmission	0.88	-0.531	1.05	0.95	1.1	0.9
103	WOROTA	66	Transmission	0.95	-0.6	1.05	0.95	1.1	0.9
104	GONDER II	66	Transmission	0.97	-0.8	1.05	0.95	1.1	0.9

Table D-5. 45 kV busbars input data

Bus Number	Bus Name	Base kV	Owner Name	Voltage (pu)	Angle (rad)	Normal Vmax (pu)	Normal Vmin (pu)	Emergency Vmax (pu)	Emergency Vmin (pu)
105	TIS ABAY I	45	Generation	0.99	-0.34	1.05	0.95	1.1	0.9
106	BAHIR DAR I	45	Transmission	0.96	-0.69	1.05	0.95	1.1	0.9

Appendix E: Power plant Input Data

Plant/Bus Name	Sn [MVA]	Bus Type	P [MW]	u [%]	P [pu]	Pmin [MW]	Pmax [MW]	Qmin [MVAr]	Qmax [MVAr]	Pmax [pu]	Qmin [pu]	Qmax [pu]
KOKA	60	PV	20	95	0.34	0	39	-42	36.7	0.6500	-0.7000	0.6117
SOR	6.2	PV	3	100	0.489	0	4.82	-3.8	4.8	0.7774	-0.6129	0.7742
FINCHA	160	PV	112	100	0.7	10	127.99	-82	65	0.7999	-0.5125	0.4063
G/ GIBE I	219	PV	180	100	0.83	0	210	-63	63	0.9589	-0.2877	0.2877
G/GIBE II	500	PV	380	100	0.76	0	420	-200	200	0.8400	-0.4000	0.4000
G/GIBE III	2200	PV	1000	100	0.455	0	1870	-1000	1000	0.8500	-0.4545	0.4545
TIS ABAY I	14.4	PV	12	100	0.84	0	12	-9.64	9.64	0.8333	-0.6694	0.6694
TIS ABAY II	80	PV	54	100	0.675	0	54	-46	40	0.6750	-0.5750	0.5000
M/WAKENA	180	PV	135	97.5	0.75	0	153	-136.5	125.45	0.8500	-0.7583	0.6969
AWASH II	40	PV	12	95	0.3	6	30	-30	26	0.7500	-0.7500	0.6500
AWASH III	40	PV	18	100	0.45	6	30	-30	26	0.7500	-0.7500	0.6500
TEKEZE	344	PV	186	100	0.541	0	312	-152	152	0.9070	-0.4419	0.4419
BELES	520	Slack		100			388	-348	348	0.7462	-0.6692	0.6692
A/NESHI	106	PV	70	100	0.661	0	82	-45	40	0.7736	-0.4245	0.3774
A/GODA WF	120	PV	30	95	0.25		31.2	-21	21	0.2600	-0.1750	0.1750
NAZRETH II	51	PV	10	95	0.1961	0	13	-12	11.6	0.2549	-0.2353	0.2275
A/GODA WF	153	PV	38.25	95	0.25		39.78	-25	25	0.2600	-0.1634	0.1634

Appendix F: Two winding transformers input data in PSAT

From Bus No.	Bus Name	Un1 [kV]	To Bus No.	Bus Name	Un2 [kV]	Sn [MVA]	Leakage Reactance (%)	Winding MVA Base	Xactual (Ohm)	Xbase (Ohm)	X (pu)
12	GG New 400	400	51	GG New 230	230	250	10.3	250	65.9200	640.0000	0.1030
	GG New 400	400		GG New 230	230	250	10.3	250	65.9200	640.0000	0.1030
4	SEBETA II 400	400	23	SEBETA II 230	230	250	9.85	250	63.0400	640.0000	0.0985
	SEBETA II 400	400		SEBETA II 230	230	250	9.85	250	63.0400	640.0000	0.0985
9	Bahir Dar II 400	400	41	Bahir Dar II 230	230	250	11.87	250	75.9680	640.0000	0.1187
	Bahir Dar II 400	400		Bahir Dar II 230	230	250	11.87	250	75.9680	640.0000	0.1187
10	Debre Markos 400	400	42	Debre Markos 230	230	250	11.87	250	75.9680	640.0000	0.1187

2	Sululta 400	400	14	Sululta 230	230	250	11.87	250	75.9680	640.0000	0.1187
	Sululta 400	400		Sululta 230	230	250	11.87	250	75.9680	640.0000	0.1187
7	Wolaita Sodo 400	400	97	Wolaita Sodo 132	132	250	9.85	250	63.0400	640.0000	0.0985
3	Gelan 400	400	21	Gelan 230	230	500	12.5	500	40.0000	320.0000	0.1250
	Gelan 400	400		Gelan 230	230	500	12.5	500	40.0000	320.0000	0.1250
21	Gelan 230	230	76	Gelan 132	132	125	11.84	125	50.1069	423.2000	0.1184
	Gelan 230	230		Gelan 132	132	125	11.84	125	50.1069	423.2000	0.1184
	Gelan 230	230		Gelan 132	132	125	11.84	125	50.1069	423.2000	0.1184
20	KALITI I 230	230	67	KALITI I 132	132	125	20.64	125	87.3485	423.2000	0.2064
	KALITI I 230	230		KALITI I 132	132	125	20.64	125	87.3485	423.2000	0.2064
	KALITI I 230	230		KALITI I 132	132	125	20.64	125	87.3485	423.2000	0.2064
18	GEFARSA 230	230	68	GEFARSA 132	132	125	20.64	125	87.3485	423.2000	0.2064
	GEFARSA 230	230		GEFARSA 132	132	125	20.64	125	87.3485	423.2000	0.2064
	GEFARSA 230	230		GEFARSA 132	132	125	20.64	125	87.3485	423.2000	0.2064
	GEFARSA 230	230		GEFARSA 132	132	125	20.64	125	87.3485	423.2000	0.2064
22	SEBETA I 230	230	70	SEBETA I 132	132	125	20.64	125	87.3485	423.2000	0.2064
	SEBETA I 230	230		SEBETA I 132	132	125	20.64	125	87.3485	423.2000	0.2064
29	M/Wakena Yougo	230	81	M/Wakena Yougo	132	63	6.453	63	54.1847	839.6825	0.0645
	M/Wakena Yougo	230		M/Wakena Yougo	132	63	6.453	63	54.1847	839.6825	0.0645
14	Sululta 230	230	90	Sululta 132	132	63	11.86	63	99.5863	839.6825	0.1186
	Sululta 230	230		Sululta 132	132	63	11.86	63	99.5863	839.6825	0.1186
38	Hossaina 230	230	86	Hossaina 132	132	45	6.371	63	53.4962	839.6825	0.0637
13	Legetafo 230	230	91	lEGETAFO 132	132	125	20.64	125	87.3485	423.2000	0.2064
	Legetafo 230	230		lEGETAFO 132	132	125	20.64	125	87.3485	423.2000	0.2064
50	GG I 230	230	85	GG Old	132	30	8.97	40	118.63	1322.50	0.0897
51	GG NEW	230	85	GG Old	138	30	8.97	40	118.63	1322.50	0.0897
49	BEDELE 230	230	83	BEDELE 132	132	63	10.3	63	86.4873	839.6825	0.1030
101	Bahir Dar I 66	66	106	Bahir Dar I 45	45	12	3.4	12	12.3420	363.0000	0.0340
	Bahir Dar I 66	66		Bahir Dar I 45	45	12	3.4	12	12.3420	363.0000	0.0340

Appendix F: Equivalently converted three winding transformers input data in PSAT

From Bus No.	Bus Name	Un1 [kV]	To Bus No.	Bus Name	Un2 [kV]	Sn12 [MVA]	X12 [%]	X1-2 (p.u)
35	Ghedo 230	230	84	Ghedo 132	132	63	7.36	0.0736
41	Bahir Dar II 230	230	89	Bahir Dar II 132	132	63	9.349	0.09349
	Bahir Dar II 230	230		Bahir Dar II 132	132	63	9.349	0.09349
37	Alaba 230	230	87	Alaba 132	132	63	2.456	0.02456
	Alaba 230	230		Alaba 132	132	63	2.456	0.02456
25	Awash 7Kilo 230	230	62	Awash 7Kilo 132	132	125	12.06	0.1206

	Awash 7Kilo 230	230		Awash 7Kilo 132	132	125	12.06	0.1206
16	Cotobie 230	230	73	Cotobie 132	132	125	12.06	0.1206
	Cotobie 230	230		Cotobie 132	132	125	12.06	0.1206
39	Combolcha II 230	230	92	Combolcha II 132	132	63	6.37	0.0637
41	Bahir Dar II 230	230	102	Bahir Dar II 66	66	63	9.349	0.09349
	Bahir Dar II 230	230		Bahir Dar II 66	66	63	9.349	0.09349
44	Gonder II 230	230	104	Gonder II 66	66	40	4.672	0.04672
48	Metu 230	230	99	Metu 66	66	40	4.672	0.04672
47	Gambella II 230	230	100	Gambella II 66	66	40	4.672	0.04672

Appendix H: Shunt Input Data

Table H-1. The fixed shunt data after merged and lumped at respective buses

Bus Number	Bus Name	Capacity (MVA)	In Service	G-Shunt (MW)	B-Shunt (MVAr)	G-Shunt (pu)	B-Shunt (pu)
32	HURSO 230	30	1	0.1	-30	0.003333333	-1
39	COMBOL-II 230	15	1	0.07	-15	0.004666667	-1
41	BAHIR DAR2 230	60	1	0.24	-60	0.004	-1
44	GONDAR 2 230	30	1	0.14	-30	0.004666667	-1
47	GAMBELA2 230	30	1	0	-30	0	-1
48	METU 230	15	1	0.07	-15	0.004666667	-1
55	ENDASILASIE 230	15	1	0.06	-15	0.004	-1
56	HUMERA 230	45	1	0.18	-45	0.004	-1
3	GELAN 400.00	90	1	0	90	0	1
4	SEBETA-2 400.00	90	1	0	90	0	1
7	WOLAYTA 400 400.00	90	1	0.23	-90	0.002555556	-1
5	Gebre Guracha 400	90	1	0.23	-90	0.002555556	-1
9	BAHIRDAR-II 400.00	45	1	0.12	-45	0.002666667	-1
10	D/Markos 400KV	45	1	0.12	-45	0.002666667	-1
12	GG New 400KV	90	1	0.24	-90	0.002666667	-1
2	Sululta 400KV	45	1	0.12	-45	0.002666667	-1
26	KOKA 230	45	1	0.18	-45	0.004	-1
31	DIRE DAWA III 230	45	1	0.18	-45	0.004	-1
42	D/Markos 230	15	1	0.06	-15	0.004	-1
54	Alamata 230	30	1	0.12	-30	0.004	-1

Table H-2. The switched shunt data

Bus Number	Bus Name	Vhi (pu)	Vlo (pu)	S(MVA)	Qmax (pu)	Qmin (pu)
13	LEGETAFO 230	1.05	0.95	15	0.8	-0.2
54	ALAMATA 230	1.05	0.95	30	0.8	-0.2

59	MEKELE 230	1.05	0.95	15	0.8	-0.2

Appendix I: Base Case Simulation Result at Peak Load

Table I-1. Network statistics and base case power flow result reports

NETWORK STATISTICS						
Buses:				106		
Lines:				146		
Transformers:				51		
Generators:				17		
Loads:				69		
SOLUTION STATISTICS						
Number of Iterations:				4		
Maximum P mismatch [p.u.]				0.000000		
Maximum Q mismatch [p.u.]				0.000000		
Power rate [MVA]				100		
POWER FLOW RESULTS						
Bus	V [p.u.]	phase [rad]	P gen [p.u.]	Q gen [p.u.]	P load [p.u.]	Q load [p.u.]
1_Beles PP	1	0	2.708992	-0.279795	0.123495	0.043858
2_Sululta	0.995809	-0.066874	0.000000	0.000000	0.000000	0.446236
3_Gelan	0.998134	-0.061865	0.000000	0.000000	0.000000	-0.896644
4_Sebeta-II	0.999181	-0.060252	0.000000	0.000000	0.000000	-0.898527
5_G/Guracha	0.990168	-0.056237	0.000000	0.000000	0.069524	0.916040
6_Holeta	0.998108	-0.062838	0.000000	0.000000	0.119369	0.457673
7_Wolyta	1.003078	0.093140	0.000000	0.000000	0.000000	0.905548
8_GG-III PP	1.000000	0.120829	10.010000	-2.768039	0.000000	0.000000
9_Bahirdar II	0.998560	-0.015716	0.000000	0.000000	0.000000	0.448705
10_D/Markos	0.996605	-0.048673	0.000000	0.000000	0.000000	0.446950
11_GG-II PP	1.000000	0.090490	3.800000	-1.205381	0.000000	0.000000
12_GG-New	0.979899	0.082735	0.000000	0.000000	0.000000	4.320912
13_Legetafo	0.976660	-0.141328	0.000000	0.000000	0.000000	0.143080
14_Sululta	0.981222	-0.126797	0.000000	0.000000	0.000000	0.000000
15_Shegole	0.979613	-0.126739	0.000000	0.000000	0.682744	0.330594
16_Cotobie	0.974622	-0.144863	0.000000	0.000000	0.000000	0.000000
17_B/Arabsa TP	0.976575	-0.139755	0.000000	0.000000	0.403283	0.183150
18_Gefersa	0.980906	-0.123453	0.000000	0.000000	0.000000	0.000000
19_T/hailoch	0.983707	-0.116562	0.000000	0.000000	0.056154	0.023317
20_Kaliti-I	0.982344	-0.116180	0.000000	0.000000	0.000000	0.000000
21_Gelan	0.985331	-0.106736	0.000000	0.000000	0.000000	0.000000
22_Sebeta-I	0.985706	-0.111768	0.000000	0.000000	0.000000	0.000000
23_Sebeta-II	0.991987	-0.101268	0.000000	0.000000	0.181896	-0.354727
24_EIZ TAP	0.959764	-0.133588	0.000000	0.000000	0.241098	0.116690

25_Awash-7KL	1.005970	-0.260366	0.000000	0.000000	0.000000	0.000000
26_Koka	0.950186	-0.141728	0.000000	0.000000	0.000000	3.819070
27_M/Wakana PP	0.975000	-0.087278	1.350000	0.027313	0.000000	0.000000
28_Adama-II WF	0.950000	-0.138594	0.382500	-0.164794	0.000000	0.000000
29_M/Wakana Yugo	0.974538	-0.089427	0.000000	0.000000	0.087795	0.042467
30_Wolkite	1.002332	-0.031111	0.000000	0.000000	0.210393	0.101830
31_D/dawa-III	0.966019	-0.331453	0.000000	0.000000	0.796704	0.617899
32_Hurso	0.966096	-0.329330	0.000000	0.000000	1.008984	0.272979
33_Fincha PP	1.000000	-0.023376	1.120000	-0.187368	0.077495	0.037508
34_Fincha-II	1.000015	-0.023898	0.000000	0.000000	0.049629	0.024007
35_Ghedo	0.998439	-0.058407	0.000000	0.000000	0.000000	0.000000
36_A/Neshi	1.000000	-0.009942	0.700660	-0.251882	0.000000	0.000000
37_Alaba	1.001800	-0.055805	0.000000	0.000000	0.000000	0.000000
38_Hossaina	1.003563	-0.048819	0.000000	0.000000	0.000000	0.000000
39_Combolcha-II	1.031407	-0.233357	0.000000	0.000000	0.000000	0.319140
40_Woldiya	1.026362	-0.212322	0.000000	0.000000	0.157442	0.076201
41_Bahirdar-II	0.994346	-0.057799	0.000000	0.000000	0.000000	0.593234
42_D/Markos	0.994818	-0.047446	0.000000	0.000000	0.214015	0.252034
43_Gashana TAP	0.997333	-0.149630	0.000000	0.000000	0.043858	0.002308
44_Gonder-II	0.968710	-0.119506	0.000000	0.000000	1.000000	0.281520
45_Mota	0.999230	-0.055323	0.000000	0.000000	0.025861	0.012518
46_N/Mewcha	1.002298	-0.114654	0.000000	0.000000	0.047871	0.005176
47_Gambella-II	1.028392	0.011061	0.000000	0.000000	0.000000	0.317277
48_Metu	1.033144	0.013786	0.000000	0.000000	0.000000	0.160108
49_Bedele	1.029012	0.018852	0.000000	0.000000	0.000000	0.000000
50_GG-I PP	1.000000	0.053026	1.817700	-0.432618	0.000000	0.000000
51_GG-New	1.000098	0.049657	0.000000	0.000000	0.286034	0.134212
52_Jimma-New	1.014224	0.036349	0.000000	0.000000	0.004385	0.002123
53_Agaro	1.020310	0.029524	0.000000	0.000000	0.077189	0.037360
54_Alamata	0.982457	-0.178544	0.000000	0.000000	0.220310	0.975497
55_Shire-E/Selassie	0.968772	-0.125736	0.000000	0.000000	0.141733	0.631710
56_Humera	0.964296	-0.128218	0.000000	0.000000	0.109442	0.471409
57_Mekele	0.950218	-0.155675	0.000000	0.000000	1.611883	1.573975
58_Tekeze PP	1.000000	-0.113551	1.861040	0.971514	0.024098	0.012161
59_Mehoni	0.974502	-0.173412	0.000000	0.000000	0.042678	0.016793
60_Welkayt	0.958681	-0.126616	0.000000	0.000000	0.043640	0.424031
61_Ashogoda WF	0.950000	-0.153415	0.300000	-0.642962	0.000000	0.000000
62_Awash-7KL	0.992829	-0.283101	0.000000	0.000000	0.457714	0.204422
63_Nazreth-II PP	0.950000	-0.267692	0.100011	0.231541	0.556590	0.240420
64_Koka PP	0.950000	-0.250929	0.204000	-0.355409	0.229939	0.111320
65_Awash-II PP	0.950000	-0.250004	0.240000	-0.366370	0.359825	0.283542
66_Awash-III PP	1.000000	-0.217473	0.180000	0.221300	0.000000	0.000000

67_Kaliti-I	0.954522	-0.223077	0.000000	0.000000	3.324586	1.408014
68_Gefersa	0.963060	-0.211396	0.000000	0.000000	0.764844	0.370221
69_Addis North	0.953808	-0.227808	0.000000	0.000000	0.499106	0.166475
70_Sebeta-I	0.956161	-0.219434	0.000000	0.000000	1.262210	0.532574
71_Mekanisa	0.951918	-0.232508	0.000000	0.000000	0.484835	0.097534
72_Addis East-II	0.953022	-0.229755	0.000000	0.000000	0.538370	0.102396
73_Cotobie	0.955832	-0.222909	0.000000	0.000000	1.050094	0.508439
74_D/Birhan	0.974536	-0.220392	0.000000	0.000000	0.092307	0.044677
75_Shoa Robit	0.979920	-0.254128	0.000000	0.000000	0.075714	0.019997
76_Gelan	0.966277	-0.211291	0.000000	0.000000	0.293105	0.141950
77_Yesu	0.954761	-0.222867	0.000000	0.000000	0.334547	0.161921
78_Assela	0.981828	-0.270256	0.000000	0.000000	0.047597	0.023037
79_Adamitulu	0.998956	-0.275584	0.000000	0.000000	0.150557	0.072880
80_Shashemene	0.963144	-0.219204	0.000000	0.000000	0.985050	0.402766
81_M/Wakana Yugo	0.977193	-0.112785	0.000000	0.000000	0.128079	0.043744
82_Nekemte	0.971865	-0.125875	0.000000	0.000000	0.265928	0.085482
83_Bedele	0.984058	-0.110481	0.000000	0.000000	0.060861	0.029457
84_Ghedo	0.998518	-0.079392	0.000000	0.000000	0.007487	0.003624
85_GG Old	1.009466	0.006042	0.000000	0.000000	0.021392	0.010354
86_Hossaina	1.000514	-0.048810	0.000000	0.000000	0.176182	0.095140
87_Alaba	1.001597	-0.061250	0.000000	0.000000	0.068455	0.033132
88_Tis Abay-II PP	1.000000	0.001850	0.540000	-0.030546	0.000000	0.000000
89_Bahirdar-II	0.992536	-0.017525	0.000000	0.000000	0.000000	0.000000
90_Sululta	0.972315	-0.200072	0.000000	0.000000	0.434819	0.145202
91_Legetafo	0.974582	-0.219573	0.000000	0.000000	0.597162	0.105142
92_Combolcha-II	0.993526	-0.298435	0.000000	0.000000	0.754738	0.307810
93_Dangote	0.954975	-0.246225	0.000000	0.000000	0.449188	0.126899
94_Elala Geda TP	0.957312	-0.239096	0.000000	0.000000	0.081282	0.039376
95_Elala Geda DCP	0.957175	-0.239218	0.000000	0.000000	0.085569	0.041414
96_D/Ziet TP	0.951745	-0.249467	0.000000	0.000000	0.378897	0.234354
97_Wolyta	1.004509	0.050964	0.000000	0.000000	0.431792	0.226834
98_Sor PP	1.000000	-0.054318	0.030318	0.006225	0.000000	0.000000
99_Metu	0.989514	-0.059241	0.000000	0.000000	0.073588	0.035616
100_Gambella-II	1.006730	-0.045548	0.000000	0.000000	0.085142	0.041208
101_Bahirdar-II	0.985748	-0.081420	0.000000	0.000000	0.000000	0.000000
102_Bahirdar-II	0.984350	-0.080670	0.000000	0.000000	0.310568	0.152316
103_Woreta	0.969394	-0.170484	0.000000	0.000000	0.045370	0.021958
104_Gonder-II	0.952717	-0.161937	0.000000	0.000000	0.339446	0.164293
105_Tis Abay-I PP	1.000000	0.012901	0.120960	-0.032871	0.000000	0.000000
106_Bahirdar-I	0.975507	-0.072053	0.000000	0.000000	0.051341	0.029950

Table I-2. Power generated and maximum allowable capacity of plants

Bus	P gen [p.u.]	Q gen [p.u.]	Pmax [pu]	Qmin [pu]	Qmax [pu]
1_Beles PP	2.708992	-0.279795	3.880000	-3.480000	3.480000
8_GG-III PP	10.010000	-2.768039	18.700000	-10.000000	10.000000
11_GG-II PP	3.800000	-1.205381	4.200000	-2.000000	2.000000
27_M/Wakana PP	1.350000	0.027313	1.530000	-1.365000	1.254500
28_Adama-II WF	0.382500	-0.164794	0.397800	-0.300000	0.300000
33_Fincha PP	1.120000	-0.187368	1.279900	-0.820000	0.650000
36_A/Neshi	0.700660	-0.251882	0.820000	-0.450000	0.400000
50_GG-I PP	1.817700	-0.432618	2.100000	-0.630000	0.630000
58_Tekeze PP	1.861040	0.971514	3.120000	-1.520000	1.520000
61_Ashogoda WF	0.300000	-0.642962	0.312000	-0.720000	0.720000
63_Nazreth-II PP	0.100011	0.231541	0.130000	-0.250000	0.250000
64_Koka PP	0.204000	-0.355409	0.390000	-0.420000	0.367000
65_Awash-II PP	0.240000	-0.366370	0.300000	-0.350000	0.260000
66_Awash-III PP	0.180000	0.221300	0.300000	-0.350000	0.260000
88_Tis Abay-II PP	0.540000	-0.030546	0.540000	-0.460000	0.400000
98_Sor PP	0.030318	0.006225	0.048200	-0.038000	0.048000
105_Tis Abay-I PP	0.120960	-0.032871	0.120000	-0.096400	0.096400

Table I-3. Line flow reports and comparison with their respective nominal capacities

LINE FLOWS								
From Bus	To Bus	Line	P Flow [pu]	Q Flow [pu]	P Loss [pu]	Q Loss [pu]	Calculated S(pu) Flow	Thermal limit S(pu)
1_Beles PP	9_Bahirdar II	57	1.292748	-0.161827	0.001602	-0.356258	1.302838	12.17
1_Beles PP	9_Bahirdar II	58	1.292748	-0.161827	0.001602	-0.356258	1.302838	12.17
2_Sululta	5_G/Guracha	1	-0.369522	0.112937	0.000388	-0.240688	0.386395	12.17
2_Sululta	10_D/Markos	60	-0.405925	-0.287787	0.000555	-0.601393	0.497590	12.17
3_Gelan	6_Holeta	3	0.121247	-0.185923	0.000015	-0.347572	0.221964	12.17
3_Gelan	6_Holeta	14	0.121247	-0.185923	0.000015	-0.347572	0.221964	12.17
3_Gelan	4_Sebeta-II	70	-0.300107	-0.256319	0.000078	-0.219550	0.394669	12.17
5_G/Guracha	10_D/Markos	136	-0.439434	-0.562415	0.000420	-0.485936	0.713732	12.17
6_Holeta	4_Sebeta-II	2	-0.783696	-0.302072	0.000192	-0.101195	0.839897	12.17
6_Holeta	4_Sebeta-II	59	-0.783696	-0.302072	0.000192	-0.101195	0.839897	12.17
6_Holeta	2_Sululta	114	0.845243	0.234885	0.000508	-0.243685	0.877272	12.17
6_Holeta	2_Sululta	125	0.845243	0.234885	0.000508	-0.243685	0.877272	12.17
7_Wolyta	3_Gelan	25	3.570146	-1.019689	0.069694	-1.358793	3.712911	12.17

7_Wolyta	3_Gelan	36	3.570146	-1.019689	0.069694	-1.358793	3.712911	12.17
8_GG-III PP	7_Wolyta	54	3.336667	-0.922680	0.011687	-0.262960	3.461890	12.17
8_GG-III PP	7_Wolyta	55	3.336667	-0.922680	0.011687	-0.262960	3.461890	12.17
8_GG-III PP	7_Wolyta	56	3.336667	-0.922680	0.011687	-0.262960	3.461890	12.17
9_Bahirdar II	10_D/Markos	103	0.822733	-0.274136	0.002034	-0.521475	0.867202	12.17
11_GG-II PP	4_Sebeta-II	47	3.975898	-0.499260	0.044880	-0.446478	4.007122	12.17
11_GG-II PP	7_Wolyta	53	-1.755224	-4.016959	0.001156	-4.848593	4.383694	12.17
11_GG-II PP	12_GG-New	92	1.579327	3.310838	0.006029	-0.075276	3.668232	12.17
13_Legetafo	14_Sululta	61	-1.089557	0.024219	0.005609	-0.023068	1.089826	3.55
13_Legetafo	14_Sululta	62	-1.089557	0.024219	0.005609	-0.023068	1.089826	3.55
13_Legetafo	16_Cotobie	63	0.753865	0.075397	0.001052	-0.143808	0.757626	3.55
13_Legetafo	16_Cotobie	64	0.753865	0.075397	0.001052	-0.143808	0.757626	3.55
13_Legetafo	39_Combolcha-II	66	0.390682	-0.661018	0.019254	-0.480439	0.767839	3.55
15_Shegole	14_Sululta	67	-0.089336	-0.297924	0.000164	-0.013859	0.311030	3.55
15_Shegole	18_Gefersa	71	-0.593408	-0.032670	0.000698	-0.013649	0.594306	3.55
17_Bole Arabsa TP	13_Legetafo	65	0.620821	-0.264286	0.000357	-0.005434	0.674734	3.55
17_Bole Arabsa TP	20_Kaliti-I	109	-1.024104	0.081136	0.008459	-0.041794	1.027313	3.55
18_Gefersa	14_Sululta	68	0.278803	-0.139804	0.000328	-0.030058	0.311891	4.18
18_Gefersa	14_Sululta	69	0.278803	-0.139804	0.000328	-0.030058	0.311891	4.18
18_Gefersa	35_Ghedo	73	-0.602876	-0.118656	0.007753	-0.148203	0.614442	3.98
18_Gefersa	35_Ghedo	74	-0.767379	-0.038322	0.017686	-0.201593	0.768336	3.98
18_Gefersa	35_Ghedo	75	-0.767379	-0.038322	0.017686	-0.201593	0.768336	3.98
19_T/hailoch	18_Gefersa	72	1.026590	0.043374	0.002578	-0.013245	1.027506	3.67
20_Kaliti-I	21_Gelan	77	-1.214333	-0.127536	0.002498	-0.002452	1.221012	3.55
20_Kaliti-I	21_Gelan	78	-1.214333	-0.127536	0.002498	-0.002452	1.221012	3.55
20_Kaliti-I	22_Sebeta-I	79	-0.421540	-0.215794	0.000528	-0.017466	0.473564	3.67
21_Gelan	24_EIZ TAP	86	0.598663	0.317344	0.006247	-0.064084	0.677573	3.55
22_Sebeta-I	19_T/hailoch	76	1.084645	0.058375	0.001901	-0.008316	1.086215	3.55
22_Sebeta-I	30_Wolkite	85	-0.857023	0.018633	0.023695	-0.193612	0.857225	4.18
23_Sebeta-II	22_Sebeta-I	83	0.940581	0.337345	0.002373	-0.009748	0.999247	4.18
23_Sebeta-II	22_Sebeta-I	84	0.940581	0.337345	0.002373	-0.009748	0.999247	4.18
25_Awash-7KL	26_Koka	87	-0.942542	-0.133754	0.035357	-1.684531	0.951985	3.55
26_Koka	24_EIZ TAP	80	-0.350117	-0.303810	0.001202	-0.039071	0.463554	3.55
26_Koka	21_Gelan	82	-0.866528	-0.561493	0.012507	-0.028287	1.032543	3.55
27_M/Wakana PP	26_Koka	89	0.414363	-0.008962	0.005713	-0.199294	0.414460	3.55
27_M/Wakana PP	26_Koka	90	0.414363	-0.008962	0.005713	-0.199294	0.414460	3.55
28_Adama-II WF	26_Koka	91	0.382500	-0.164794	0.000416	-0.016436	0.416489	3.55
29_M/Wakana Yugo	27_M/Wakana PP	95	-0.522081	0.002982	0.000260	-0.005887	0.522090	3.55
31_D/dawa-III	25_Awash-7KL	88	-0.463120	-0.408572	0.008767	-0.554207	0.617585	3.67
31_D/dawa-III	32_Hurso	98	-0.166792	-0.104663	0.000124	-0.313881	0.196911	3.55
31_D/dawa-III	32_Hurso	99	-0.166792	-0.104663	0.000124	-0.313881	0.196911	3.55
32_Hurso	26_Koka	93	-0.671408	0.072728	0.048758	-0.486425	0.675335	3.55

32_Hurso	26_Koka	94	-0.671408	0.072728	0.048758	-0.486425	0.675335	3.55
33_Fincha PP	34_Fincha-II	100	0.091198	-0.040470	0.000016	-0.015422	0.099774	3.55
33_Fincha PP	35_Ghedo	101	0.634809	-0.126522	0.004107	-0.074860	0.647294	3.98
33_Fincha PP	42_D/Markos	102	0.316498	-0.057884	0.001469	-0.129281	0.321748	4.18
34_Fincha-II	36_A/Neshi	105	-0.697467	0.207141	0.003193	-0.044741	0.727577	3.55
35_Ghedo	34_Fincha-II	104	-0.730829	0.151519	0.008192	-0.104676	0.746371	3.55
35_Ghedo	51_GG-New	106	-0.998296	0.151701	0.022371	-0.079448	1.009757	3.67
37_Alaba	38_Hossaina	107	-0.280305	-0.011195	0.000666	-0.071893	0.280528	3.55
38_Hossaina	30_Wolkite	96	-0.280913	0.039085	0.001785	-0.162242	0.283619	3.55
39_Combolcha-II	40_Woldiya	108	-0.287652	-0.907592	0.002343	-2.161938	0.952086	3.55
40_Woldiya	54_Alamata	110	-0.447436	1.178144	0.024850	-0.290757	1.260247	3.55
41_Bahirdar-II	44_Gonder-II	111	0.728159	-0.055449	0.015874	-0.200223	0.730267	3.98
41_Bahirdar-II	44_Gonder-II	112	0.728159	-0.055449	0.015874	-0.200223	0.730267	3.98
42_D/Markos	45_Mota	116	0.075377	-0.143219	0.000168	-0.159825	0.161844	4.18
43_Gashana TAP	46_N/Mewcha	117	-0.521117	0.006821	0.005845	-0.172681	0.521162	3.98
45_Mota	41_Bahirdar-II	113	0.049348	0.004088	0.000084	-0.118856	0.049517	4.18
46_N/Mewcha	41_Bahirdar-II	115	-0.574833	0.174326	0.011542	-0.218026	0.600685	3.98
47_Gambella-II	48_Metu	119	-0.047484	-0.178042	0.000109	-0.276856	0.184265	3.67
47_Gambella-II	48_Metu	120	-0.047484	-0.178042	0.000109	-0.276856	0.184265	3.67
48_Metu	49_Bedele	121	-0.064539	0.007900	0.000235	-0.178546	0.065021	3.67
48_Metu	49_Bedele	122	-0.064539	0.007900	0.000235	-0.178546	0.065021	3.67
51_GG-New	50_GG-I PP	52	-0.828974	0.197716	0.000592	-0.004627	0.852226	4.18
51_GG-New	50_GG-I PP	52	-0.828974	0.197716	0.000592	-0.004627	0.852226	4.18
51_GG-New	30_Wolkite	97	1.395468	-0.300660	0.021660	0.011083	1.427490	4.18
52_Jimma-New	51_GG-New	128	-0.187874	0.368496	0.003056	-0.119685	0.413625	3.55
52_Jimma-New	51_GG-New	129	-0.187874	0.368496	0.003056	-0.119685	0.413625	3.55
52_Jimma-New	53_Agaro	130	0.185681	-0.369557	0.001164	-0.073914	0.413582	3.55
52_Jimma-New	53_Agaro	131	0.185681	-0.369557	0.001164	-0.073914	0.413582	3.55
53_Agaro	49_Bedele	123	0.145922	-0.314324	0.001267	-0.161344	0.346544	3.67
53_Agaro	49_Bedele	124	0.145922	-0.314324	0.001267	-0.161344	0.346544	3.67
54_Alamata	43_Gashana TAP	118	-0.472383	-0.162763	0.004875	-0.171893	0.499638	3.98
54_Alamata	61_Ashogoda WF	132	-0.143523	0.361015	0.006688	-0.196004	0.388498	3.98
54_Alamata	59_Mehoni	133	-0.076690	0.295152	0.001071	-0.070950	0.304953	3.98
55_Shire-Endaslassie	60_Welkayt	140	0.039849	-0.057093	0.000339	-0.285401	0.069624	3.55
55_Shire-Endaslassie	56_Humera	141	0.024640	-0.184489	0.000057	-0.413268	0.186128	3.98
56_Humera	44_Gonder-II	51	-0.089102	-0.155435	0.000299	-0.287159	0.179163	3.55
57_Mekele	58_Tekeze PP	138	-0.793589	-0.561438	0.020002	-0.133139	0.972109	3.55
57_Mekele	58_Tekeze PP	139	-0.793589	-0.561438	0.020002	-0.133139	0.972109	3.55
58_Tekeze PP	55_Shire-E/slassie	137	0.209760	0.102757	0.003539	-0.287371	0.233577	3.98
59_Mehoni	57_Mekele	135	-0.120438	0.349309	0.004521	-0.156133	0.369489	3.98
60_Welkayt	56_Humera	142	-0.004130	-0.195723	0.000113	-0.282918	0.195767	3.55
61_Ashogoda WF	57_Mekele	134	0.149789	-0.085943	0.000124	-0.031601	0.172693	3.55

63_Nazreth-II PP	62_Awash-7KL	143	-0.010291	-0.210041	0.002650	-0.149354	0.210293	1.12
63_Nazreth-II PP	64_Koka PP	144	-0.446288	0.201162	0.003350	0.002687	0.489529	1.12
64_Koka PP	94_Elala Geda TP	30	-0.211916	-0.078987	0.001238	-0.092451	0.226158	1.12
64_Koka PP	95_Elala Geda DCP	31	-0.209318	-0.077776	0.001206	-0.092508	0.223300	1.12
65_Awash-II PP	78_Assela	10	0.037324	-0.294890	0.004040	-0.078699	0.297243	1.12
65_Awash-II PP	64_Koka PP	40	0.011379	-0.010514	0.000005	-0.010858	0.015493	1.12
65_Awash-II PP	64_Koka PP	41	0.011379	-0.010514	0.000005	-0.010858	0.015493	1.12
66_Awash-III PP	65_Awash-II PP	11	0.090000	0.110650	0.000046	-0.056347	0.142630	1.12
66_Awash-III PP	65_Awash-II PP	12	0.090000	0.110650	0.000046	-0.056347	0.142630	1.12
67_Kaliti-I	71_Mekanisa	4	0.201578	-0.093475	0.000801	-0.133199	0.222196	1.12
67_Kaliti-I	68_Gefersa	145	-0.194310	-0.092501	0.001184	-0.091460	0.215204	1.12
68_Gefersa	69_Addis North	29	0.576851	0.022167	0.004430	-0.090803	0.577276	1.12
70_Sebeta-I	68_Gefersa	81	-0.321130	-0.148855	0.001468	-0.087953	0.353952	1.12
71_Mekanisa	70_Sebeta-I	50	-0.284059	-0.057809	0.001588	-0.165456	0.289881	1.12
72_Addis East-II	69_Addis North	22	-0.073253	-0.052254	0.000062	-0.105759	0.089980	1.12
73_Cotobie	67_Kaliti-I	5	0.011744	-0.022536	0.000013	-0.084498	0.025413	1.12
73_Cotobie	67_Kaliti-I	6	0.011744	-0.022536	0.000013	-0.084498	0.025413	1.12
73_Cotobie	72_Addis East-II	23	0.466497	-0.052809	0.001380	-0.102951	0.469477	1.12
74_D/Birhan	75_Shoa Robit	8	0.176649	-0.123156	0.002876	-0.018705	0.215342	1.12
74_D/Birhan	91_Legetafo	27	-0.268956	0.078479	0.000095	-0.043504	0.280172	1.12
75_Shoa Robit	92_Combolcha-II	9	0.098059	-0.124448	0.002400	-0.081484	0.158439	1.12
76_Gelan	77_Yesu	26	0.629782	0.223658	0.004545	-0.066531	0.668318	1.12
76_Gelan	67_Kaliti-I	37	0.604554	0.208850	0.004504	-0.068087	0.639612	1.12
76_Gelan	67_Kaliti-I	38	0.604554	0.208850	0.004504	-0.068087	0.639612	1.12
77_Yesu	67_Kaliti-I	7	0.290690	0.128268	0.000043	-0.030728	0.317732	1.12
78_Assela	79_Adamitulu	13	-0.014312	-0.239227	0.000934	-0.227750	0.239655	1.12
79_Adamitulu	80_Shashemene	17	-0.165803	-0.084358	0.008372	-0.661210	0.186029	1.12
80_Shashemene	87_Alaba	39	-0.866803	0.095604	0.061083	-0.145115	0.872059	1.12
81_M/Wakana Yugo	80_Shashemene	18	0.306207	-0.099475	0.013785	-0.020992	0.321960	1.12
83_Bedele	82_Nekemte	43	0.098902	0.014313	0.000758	-0.032118	0.099932	1.12
84_Ghedo	82_Nekemte	15	0.171579	-0.006174	0.003795	-0.045226	0.171690	1.12
85_GG Old	86_Hossaina	19	0.284393	-0.080875	0.006442	-0.018010	0.295669	1.12
87_Alaba	97_Wolyta	16	-0.614900	0.243702	0.031573	-0.042362	0.661432	1.12
87_Alaba	86_Hossaina	20	-0.101136	-0.026448	0.000576	-0.162905	0.104537	1.12
88_Tis Abay-II PP	89_Bahirdar-II	126	0.270000	-0.015273	0.002227	-0.008562	0.270432	1.12
88_Tis Abay-II PP	89_Bahirdar-II	127	0.270000	-0.015273	0.002227	-0.008562	0.270432	1.12
91_Legetafo	73_Cotobie	24	0.034954	0.006095	0.000499	-0.090939	0.035481	1.12
93_Dangote	68_Gefersa	21	-0.147967	-0.071606	0.002182	-0.198021	0.164383	1.12
93_Dangote	90_Sululta	28	-0.301221	-0.055293	0.005994	-0.135676	0.306254	1.12
94_Elala Geda TP	76_Gelan	33	-0.294436	-0.025912	0.003562	-0.110484	0.295574	1.12
95_Elala Geda DCP	76_Gelan	34	-0.296093	-0.026682	0.003600	-0.110381	0.297293	1.12
96_D/Ziet TP	64_Koka PP	32	0.031628	-0.078446	0.000034	-0.189250	0.084582	1.12

96_D/Ziet TP	76_Gelan	35	-0.410525	-0.155908	0.006946	-0.352499	0.439133	1.12
98_Sor PP	99_Metu	42	0.030318	0.006225	0.000281	-0.002567	0.030950	0.29
100_Gambella-II	99_Metu	44	0.009826	-0.008540	0.000167	-0.016984	0.013018	0.29
101_Bahirdar-II	103_Woreta	46	0.054665	-0.089572	0.004863	-0.088125	0.104935	0.29
102_Bahirdar-II	101_Bahirdar-II	45	-0.008889	-0.023152	0.000028	-0.005138	0.024800	0.29
104_Gonder-II	103_Woreta	48	-0.004277	-0.040955	0.000155	-0.064360	0.041178	0.29
105_Tis Abay-I PP	106_Bahirdar-I	49	0.120960	-0.032871	0.006036	0.007402	0.125347	0.19

Table I-4. Transformer flow reports and comparison with their respective nominal capacities

From Bus	To Bus	Line	P Flow [pu]	Q Flow [pu]	P Loss [pu]	Q Loss [pu]	Calculated S(pu) Flow	Nominal S(pu) Flow
10_D/Markos	42_D/Markos	197	-0.0256	0.0375	0.0000	0.0001	0.0454	2.50
14_Sululta	2_Sululta	147	-1.2325	-0.2645	0.0000	0.0784	1.2605	2.50
14_Sululta	2_Sululta	158	-1.2325	-0.2645	0.0000	0.0784	1.2605	2.50
21_Gelan	76_Gelan	164	1.0491	0.2531	0.0000	0.1136	1.0792	1.25
21_Gelan	76_Gelan	165	1.0491	0.2531	0.0000	0.1136	1.0792	1.25
21_Gelan	76_Gelan	166	1.0491	0.2531	0.0000	0.1136	1.0792	1.25
21_Gelan	3_Gelan	169	-3.5293	-0.9300	0.0000	0.1715	3.6497	5.00
21_Gelan	3_Gelan	180	-3.5293	-0.9300	0.0000	0.1715	3.6497	5.00
23_Sebeta-II	4_Sebeta-II	191	-1.0315	-0.1600	0.0000	0.0436	1.0439	2.50
23_Sebeta-II	4_Sebeta-II	194	-1.0315	-0.1600	0.0000	0.0436	1.0439	2.50
41_Bahirdar-II	89_Bahirdar-II	177	-0.2678	0.0175	0.0000	0.0108	0.2683	0.63
41_Bahirdar-II	89_Bahirdar-II	178	-0.2678	0.0175	0.0000	0.0108	0.2683	0.63
41_Bahirdar-II	9_Bahirdar II	195	-0.8798	-0.0697	0.0000	0.0374	0.8825	2.50
41_Bahirdar-II	9_Bahirdar II	196	-0.8798	-0.0697	0.0000	0.0374	0.8825	2.50
51_GG-New	12_GG-New	148	-0.7866	0.5033	0.0000	0.0359	0.9339	2.50
51_GG-New	12_GG-New	149	-0.7866	0.5033	0.0000	0.0359	0.9339	2.50
62_Awash-7KL	25_Awash-7KL	150	-0.2353	-0.1326	0.0000	0.0071	0.2701	1.25
62_Awash-7KL	25_Awash-7KL	151	-0.2353	-0.1326	0.0000	0.0071	0.2701	1.25
67_Kaliti-I	20_Kaliti-I	152	-0.6059	-0.1284	0.0000	0.0695	0.6193	1.25
67_Kaliti-I	20_Kaliti-I	153	-0.6059	-0.1284	0.0000	0.0695	0.6193	1.25
67_Kaliti-I	20_Kaliti-I	154	-0.6059	-0.1284	0.0000	0.0695	0.6193	1.25
68_Gefersa	18_Gefersa	155	-0.5025	-0.0820	0.0000	0.0461	0.5091	1.25
68_Gefersa	18_Gefersa	156	-0.5025	-0.0820	0.0000	0.0461	0.5091	1.25
68_Gefersa	18_Gefersa	157	-0.5025	-0.0820	0.0000	0.0461	0.5091	1.25
68_Gefersa	18_Gefersa	159	-0.5025	-0.0820	0.0000	0.0461	0.5091	1.25
70_Sebeta-I	22_Sebeta-I	160	-0.6134	-0.1380	0.0000	0.0714	0.6287	1.25
70_Sebeta-I	22_Sebeta-I	161	-0.6134	-0.1380	0.0000	0.0714	0.6287	1.25
73_Cotobie	16_Cotobie	162	-0.7528	-0.1568	0.0000	0.0624	0.7690	1.25
73_Cotobie	16_Cotobie	163	-0.7528	-0.1568	0.0000	0.0624	0.7690	1.25

81_M/Wakana Yugo	29_M/Wakana Yugo	167	-0.2171	0.0279	0.0000	0.0051	0.2189	0.63
81_M/Wakana Yugo	29_M/Wakana Yugo	168	-0.2171	0.0279	0.0000	0.0051	0.2189	0.63
83_Bedele	49_Bedele	170	-0.1598	-0.0438	0.0000	0.0232	0.1656	0.63
84_Ghedo	35_Ghedo	171	-0.1791	0.0026	0.0000	0.0038	0.1791	0.63
85_GG Old	50_GG-I PP	172	-0.1586	0.0357	0.0000	0.0078	0.1625	0.63
85_GG Old	51_GG-New	173	-0.1472	0.0348	0.0000	0.0067	0.1513	0.63
86_Hossaina	38_Hossaina	174	0.0001	-0.0215	0.0000	0.0001	0.0215	0.63
87_Alaba	37_Alaba	175	-0.1402	-0.0048	0.0000	0.0008	0.1402	0.63
87_Alaba	37_Alaba	176	-0.1402	-0.0048	0.0000	0.0008	0.1402	0.63
90_Sululta	14_Sululta	179	-0.3710	-0.0324	0.0000	0.0276	0.3724	0.63
90_Sululta	14_Sululta	181	-0.3710	-0.0324	0.0000	0.0276	0.3724	0.63
91_Legetafo	13_Legetafo	182	-0.4506	0.0054	0.0000	0.0353	0.4506	1.25
91_Legetafo	13_Legetafo	183	-0.4506	0.0054	0.0000	0.0353	0.4506	1.25
92_Combolcha-II	39_Combolcha-II	184	-0.6591	-0.3508	0.0000	0.0571	0.7466	0.63
97_Wolyta	7_Wolyta	185	-1.0783	0.0592	0.0000	0.0455	1.0799	2.50
99_Metu	48_Metu	186	-0.0339	-0.0184	0.0000	0.0033	0.0386	0.40
100_Gambella-II	47_Gambella-II	187	-0.0950	-0.0327	0.0000	0.0061	0.1004	0.40
101_Bahirdar-II	106_Bahirdar-I	192	-0.0318	0.0358	0.0000	0.0007	0.0479	1.20
101_Bahirdar-II	106_Bahirdar-I	193	-0.0318	0.0358	0.0000	0.0007	0.0479	1.20
102_Bahirdar-II	41_Bahirdar-II	188	-0.1508	-0.0646	0.0000	0.0041	0.1641	0.63
102_Bahirdar-II	41_Bahirdar-II	189	-0.1508	-0.0646	0.0000	0.0041	0.1641	0.63
104_Gonder-II	44_Gonder-II	190	-0.3352	-0.1233	0.0000	0.0164	0.3571	0.40

Table I-5. Global summary report of the base case grid model simulation

GLOBAL SUMMARY REPORT	
TOTAL GENERATION	
Real Power [p.u.]	25.46968
Reactive Power [p.u.]	-5.25857
TOTAL LOAD	
Real Power [p.u.]	24.51328
Reactive Power [p.u.]	24.71033
TOTAL LOSSES	
Real Power [p.u.]	0.956403
Reactive Power [p.u.]	-29.9689
LIMIT VIOLATION STATISTICS	
All Voltages Within Limits.	
All Reactive Power Within Limits.	
All Current Flows Within Limits.	
All Real Power Flows Within Limits.	
All Apparent Power Flows Within Limits.	

Appendix J: Simulation Result of a Grid Model without UPFC

Table J-1. Network statistics and power flow result reports

NETWORK STATISTICS						
Buses:			106			
Lines:			146			
Transformers:			51			
Generators:			17			
Loads:			69			
SOLUTION STATISTICS						
Number of Iterations:			5			
Maximum P mismatch [p.u.]			0.000000			
Maximum Q mismatch [p.u.]			0.000000			
Power rate [MVA]			100			
POWER FLOW RESULTS						
Bus	V [p.u.]	phase [rad]	P gen [p.u.]	Q gen [p.u.]	P load [p.u.]	Q load [p.u.]
1_Beles PP	1.000000	0.000000	3.301806	0.328231	0.164248	0.058331
2_Sululta	0.962488	-0.078889	0.000000	0.000000	0.000000	0.416872
3_Gelan	0.965817	-0.072645	0.000000	0.000000	0.000000	-0.839522
4_Sebeta-II	0.966751	-0.070460	0.000000	0.000000	0.000000	-0.841146
5_G/Guracha	0.964443	-0.067367	0.000000	0.000000	0.092467	0.881890
6_Holeta	0.965410	-0.073785	0.000000	0.000000	0.158761	0.431874
7_Wolyta	1.004582	0.116985	0.000000	0.000000	0.000000	0.908267
8_GG-III PP	1.000000	0.152948	13.000000	-3.596285	0.000000	0.000000
9_Bahirdar II	0.994740	-0.018865	0.000000	0.000000	0.000000	0.445279
10_D/Markos	0.975956	-0.058848	0.000000	0.000000	0.000000	0.428620
11_GG-II PP	1.000000	0.114441	4.180000	-10.828424	0.000000	0.000000
12_GG-New	0.995190	0.101360	0.000000	0.000000	0.000000	0.891363
13_Legetafo	0.920263	-0.170680	0.000000	0.000000	0.000000	0.127032
14_Sululta	0.930949	-0.154303	0.000000	0.000000	0.000000	0.000000
15_Shegole	0.929659	-0.154747	0.000000	0.000000	0.869580	0.421063
16_Cotobie	0.916866	-0.175050	0.000000	0.000000	0.000000	0.000000
17_B/Arabsa TP	0.921249	-0.169057	0.000000	0.000000	0.504392	0.229069
18_Gefersa	0.932387	-0.150706	0.000000	0.000000	0.000000	0.000000
19_T/hailoch	0.937702	-0.142221	0.000000	0.000000	0.072764	0.030214
20_Kaliti-I	0.940279	-0.142354	0.000000	0.000000	0.000000	0.000000
21_Gelan	0.948379	-0.130969	0.000000	0.000000	0.000000	0.000000
22_Sebeta-I	0.941455	-0.136308	0.000000	0.000000	0.000000	0.000000
23_Sebeta-II	0.950459	-0.123092	0.000000	0.000000	0.241922	-0.289358
24_EIZ TAP	0.943809	-0.171896	0.000000	0.000000	0.316495	0.153182
25_Awash-7KL	0.904005	-0.302472	0.000000	0.000000	0.000000	0.000000
26_Koka	0.946881	-0.184238	0.000000	0.000000	0.000000	0.403463

27_M/Wakana PP	0.975000	-0.125981	1.530000	0.345631	0.000000	0.000000
28_Adama-II WF	0.950000	-0.182150	0.397800	0.312671	0.000000	0.000000
29_M/Wakana Yugo	0.973080	-0.128260	0.000000	0.000000	0.116767	0.056481
30_Wolkite	0.971691	-0.037905	0.000000	0.000000	0.279823	0.135434
31_D/dawa-III	0.849392	-0.381162	0.000000	0.000000	0.847068	0.683964
32_Hurso	0.852651	-0.378983	0.000000	0.000000	1.081015	0.225628
33_Fincha PP	1.000000	-0.043162	1.232000	0.702965	0.103068	0.049886
34_Fincha-II	0.998206	-0.043469	0.000000	0.000000	0.066007	0.031929
35_Ghedo	0.977727	-0.078243	0.000000	0.000000	0.000000	0.000000
36_A/Neshi	1.000000	-0.028698	0.770000	-0.173576	0.000000	0.000000
37_Alaba	0.946366	-0.055926	0.000000	0.000000	0.000000	0.000000
38_Hossaina	0.954967	-0.050848	0.000000	0.000000	0.000000	0.000000
39_Combolcha-II	0.898452	-0.249371	0.000000	0.000000	0.000000	0.121082
40_Woldiya	0.923408	-0.227031	0.000000	0.000000	0.197839	0.095753
41_Bahirdar-II	0.987158	-0.070336	0.000000	0.000000	0.000000	0.584688
42_D/Markos	0.982126	-0.062090	0.000000	0.000000	0.284640	0.282453
43_Gashana TAP	0.963827	-0.172321	0.000000	0.000000	0.058331	0.003070
44_Gonder-II	0.965658	-0.140062	0.000000	0.000000	1.000000	0.279749
45_Mota	0.989419	-0.069090	0.000000	0.000000	0.034395	0.016649
46_N/Mewcha	0.979399	-0.132983	0.000000	0.000000	0.063668	0.006884
47_Gambella-II	1.020501	0.007974	0.000000	0.000000	0.000000	0.312427
48_Metu	1.026179	0.011843	0.000000	0.000000	0.000000	0.157956
49_Bedele	1.022882	0.018093	0.000000	0.000000	0.000000	0.000000
50_GG-I PP	1.000000	0.056585	1.800000	-0.192863	0.000000	0.000000
51_GG-New	0.999806	0.053356	0.000000	0.000000	0.380425	0.178502
52_Jimma-New	1.011619	0.038296	0.000000	0.000000	0.005832	0.002824
53_Agaro	1.016383	0.030442	0.000000	0.000000	0.102661	0.049689
54_Alamata	0.939388	-0.205304	0.000000	0.000000	0.286503	0.403621
55_Shire-E/Selassie	1.006005	-0.159059	0.000000	0.000000	0.188505	0.243044
56_Humera	0.988271	-0.159767	0.000000	0.000000	0.145558	0.509955
57_Mekele	0.948057	-0.190640	0.000000	0.000000	2.135043	1.143284
58_Tekeze PP	1.000000	-0.125646	2.604000	0.449257	0.032050	0.016174
59_Mehoni	0.943358	-0.202701	0.000000	0.000000	0.055971	0.022023
60_Welkayt	1.002994	-0.164659	0.000000	0.000000	0.058041	0.164798
61_Ashogoda WF	0.950000	-0.189778	0.312000	0.062749	0.000000	0.000000
62_Awash-7KL	0.900825	-0.337956	0.000000	0.000000	0.547368	0.244463
63_Nazreth-II PP	0.950000	-0.381497	0.132294	0.735401	0.740265	0.319758
64_Koka PP	0.950000	-0.360380	0.320000	1.386663	0.305819	0.148056
65_Awash-II PP	0.950000	-0.363560	0.216000	0.366457	0.478567	0.377111
66_Awash-III PP	1.000000	-0.324472	0.216000	0.222425	0.000000	0.000000
67_Kaliti-I	0.891513	-0.284864	0.000000	0.000000	3.894012	1.649177
68_Gefersa	0.894304	-0.265760	0.000000	0.000000	0.901462	0.436351

69_Addis North	0.880318	-0.285991	0.000000	0.000000	0.570002	0.190122
70_Sebeta-I	0.886302	-0.276787	0.000000	0.000000	1.461164	0.616521
71_Mekanisa	0.880845	-0.293893	0.000000	0.000000	0.554367	0.111522
72_Addis East-II	0.880267	-0.288699	0.000000	0.000000	0.614772	0.116928
73_Cotobie	0.886050	-0.280499	0.000000	0.000000	1.214925	0.588247
74_D/Birhan	0.897306	-0.275152	0.000000	0.000000	0.109527	0.053011
75_Shoa Robit	0.882072	-0.307487	0.000000	0.000000	0.086814	0.022929
76_Gelan	0.912083	-0.272533	0.000000	0.000000	0.359333	0.174024
77_Yesu	0.891984	-0.284688	0.000000	0.000000	0.392262	0.189855
78_Assela	0.906932	-0.348170	0.000000	0.000000	0.057694	0.027924
79_Adamitulu	0.869204	-0.322757	0.000000	0.000000	0.167629	0.081144
80_Shashemene	0.844509	-0.244658	0.000000	0.000000	1.035313	0.423318
81_M/Wakana Yugo	0.958786	-0.156514	0.000000	0.000000	0.170345	0.058180
82_Nekemte	0.933640	-0.171783	0.000000	0.000000	0.341607	0.109809
83_Bedele	0.950045	-0.152046	0.000000	0.000000	0.080945	0.039178
84_Ghedo	0.974462	-0.107649	0.000000	0.000000	0.009958	0.004820
85_GG Old	0.985878	0.001721	0.000000	0.000000	0.028451	0.013771
86_Hossaina	0.946706	-0.052506	0.000000	0.000000	0.232700	0.125660
87_Alaba	0.940761	-0.061889	0.000000	0.000000	0.089283	0.043213
88_Tis Abay-II PP	1.000000	-0.011262	0.540000	0.034793	0.000000	0.000000
89_Bahirdar-II	0.990222	-0.029676	0.000000	0.000000	0.000000	0.000000
90_Sululta	0.900375	-0.250578	0.000000	0.000000	0.519469	0.173470
91_Legetafo	0.897829	-0.274319	0.000000	0.000000	0.709388	0.124902
92_Combolcha-II	0.859519	-0.344671	0.000000	0.000000	0.821696	0.335118
93_Dangote	0.865513	-0.303634	0.000000	0.000000	0.495883	0.140091
94_Elala Geda TP	0.931133	-0.329771	0.000000	0.000000	0.103854	0.050311
95_Elala Geda DCP	0.930955	-0.329933	0.000000	0.000000	0.109289	0.052894
96_D/Ziet TP	0.916527	-0.339732	0.000000	0.000000	0.469046	0.290113
97_Wolyta	0.990709	0.063158	0.000000	0.000000	0.574283	0.301689
98_Sor PP	1.000000	-0.099092	0.036000	0.027840	0.000000	0.000000
99_Metu	0.982829	-0.099072	0.000000	0.000000	0.097872	0.047369
100_Gambella-II	0.993291	-0.068381	0.000000	0.000000	0.113239	0.054807
101_Bahirdar-II	0.964951	-0.101556	0.000000	0.000000	0.000000	0.000000
102_Bahirdar-II	0.967706	-0.103488	0.000000	0.000000	0.413055	0.202580
103_Woreta	0.906756	-0.156849	0.000000	0.000000	0.054974	0.026606
104_Gonder-II	0.934941	-0.196657	0.000000	0.000000	0.437264	0.211637
105_Tis Abay-I PP	1.000000	-0.020574	0.120000	-0.003027	0.000000	0.000000
106_Bahirdar-I	0.957594	-0.094479	0.000000	0.000000	0.068284	0.039834

Table J-2. Line flow reports and their respective thermal limits

LINE FLOWS

From Bus	To Bus	Line	P Flow [pu]	Q Flow [pu]	P Loss [pu]	Q Loss [pu]	Calculated S(pu) Flow	Thermal limit S(pu)
1_Beles PP	9_Bahirdar II	57	1.568779	0.134950	0.002458	-0.343955	1.574573	12.17
1_Beles PP	9_Bahirdar II	58	1.568779	0.134950	0.002458	-0.343955	1.574573	12.17
2_Sululta	5_G/Guracha	1	-0.397475	-0.153373	0.000344	-0.226877	0.426039	12.17
2_Sululta	10_D/Markos	60	-0.443489	-0.538757	0.000941	-0.563746	0.697812	12.17
3_Gelan	6_Holeta	3	0.138577	-0.130402	0.000022	-0.325239	0.190285	12.17
3_Gelan	6_Holeta	14	0.138577	-0.130402	0.000022	-0.325239	0.190285	12.17
3_Gelan	4_Sebeta-II	70	-0.371704	-0.215113	0.000113	-0.205222	0.429462	12.17
5_G/Guracha	10_D/Markos	136	-0.490286	-0.808386	0.000863	-0.457593	0.945446	12.17
6_Holeta	4_Sebeta-II	2	-0.942960	-0.351145	0.000297	-0.093294	1.006219	12.17
6_Holeta	4_Sebeta-II	59	-0.942960	-0.351145	0.000297	-0.093294	1.006219	12.17
6_Holeta	2_Sululta	114	1.002135	0.330045	0.000775	-0.225317	1.055085	12.17
6_Holeta	2_Sululta	125	1.002135	0.330045	0.000775	-0.225317	1.055085	12.17
7_Wolyta	3_Gelan	25	4.329335	-0.207820	0.105238	-1.022069	4.334320	12.17
7_Wolyta	3_Gelan	36	4.329335	-0.207820	0.105238	-1.022069	4.334320	12.17
8_GG-III PP	7_Wolyta	54	4.333333	-1.198762	0.019819	-0.197632	4.496088	12.17
8_GG-III PP	7_Wolyta	55	4.333333	-1.198762	0.019819	-0.197632	4.496088	12.17
8_GG-III PP	7_Wolyta	56	4.333333	-1.198762	0.019819	-0.197632	4.496088	12.17
9_Bahirdar II	10_D/Markos	103	1.004596	0.140011	0.003573	-0.487695	1.014306	12.17
11_GG-II PP	4_Sebeta-II	47	4.779530	0.435611	0.067458	-0.112924	4.799340	12.17
11_GG-II PP	7_Wolyta	53	-2.919744	-11.863671	0.003120	-15.749992	12.217675	12.17
11_GG-II PP	12_GG-New	92	2.320215	0.599636	0.002519	-0.124389	2.396447	12.17
13_Legetafo	14_Sululta	61	-1.231811	-0.348557	0.008646	-0.010455	1.280176	3.55
13_Legetafo	14_Sululta	62	-1.231811	-0.348557	0.008646	-0.010455	1.280176	3.55
13_Legetafo	16_Cotobie	63	0.888074	0.331733	0.001813	-0.007892	0.948010	3.55
13_Legetafo	16_Cotobie	64	0.888074	0.331733	0.001813	-0.007892	0.948010	3.55
13_Legetafo	39_Combolcha-II	66	0.369841	-0.219366	0.009346	-0.413553	0.430005	3.55
15_Shegole	14_Sululta	67	-0.145736	-0.200492	0.000116	-0.012570	0.247863	3.55
15_Shegole	18_Gefersa	71	-0.723845	-0.220571	0.001252	-0.010544	0.756705	3.55
17_Bole Arabsa TP	13_Legetafo	65	0.718183	0.173410	0.000484	-0.004364	0.738822	3.55
17_Bole Arabsa TP	20_Kaliti-I	109	-1.222575	-0.402478	0.014630	-0.018202	1.287120	3.55
18_Gefersa	14_Sululta	68	0.319944	0.012317	0.000401	-0.026795	0.320181	4.18
18_Gefersa	14_Sululta	69	0.319944	0.012317	0.000401	-0.026795	0.320181	4.18
18_Gefersa	35_Ghedo	73	-0.667212	-0.329835	0.011919	-0.113681	0.744287	3.98
18_Gefersa	35_Ghedo	74	-0.891785	-0.292151	0.027189	-0.157892	0.938420	3.98
18_Gefersa	35_Ghedo	75	-0.891785	-0.292151	0.027189	-0.157892	0.938420	3.98
19_T/hailoch	18_Gefersa	72	1.237495	0.307970	0.004382	-0.006282	1.275241	3.67
20_Kaliti-I	21_Gelan	77	-1.462684	-0.681727	0.004753	0.009379	1.613752	3.55
20_Kaliti-I	21_Gelan	78	-1.462684	-0.681727	0.004753	0.009379	1.613752	3.55

20_Kaliti-I	22_Sebeta-I	79	-0.474960	-0.008309	0.000590	-0.015441	0.475033	3.67
21_Gelan	24_EIZ TAP	86	0.715017	-0.117802	0.007109	-0.055797	0.724656	3.55
22_Sebeta-I	19_T/hailoch	76	1.313508	0.334867	0.003250	-0.003317	1.355522	3.55
22_Sebeta-I	30_Wolkite	85	-1.000005	-0.044358	0.034533	-0.143099	1.000988	4.18
23_Sebeta-II	22_Sebeta-I	83	1.105909	0.505400	0.003825	-0.000532	1.215921	4.18
23_Sebeta-II	22_Sebeta-I	84	1.105909	0.505400	0.003825	-0.000532	1.215921	4.18
25_Awash-7KL	26_Koka	87	-1.031038	-0.174932	0.029462	-0.033616	1.045773	3.55
26_Koka	24_EIZ TAP	80	-0.390263	0.176767	0.001150	-0.038419	0.428430	3.55
26_Koka	21_Gelan	82	-1.014047	0.210359	0.013391	-0.021452	1.035636	3.55
27_M/Wakana PP	26_Koka	89	0.449049	0.007594	0.006766	-0.194073	0.449114	3.55
27_M/Wakana PP	26_Koka	90	0.449049	0.007594	0.006766	-0.194073	0.449114	3.55
28_Adama-II WF	26_Koka	91	0.397800	0.312671	0.000638	-0.015720	0.505972	3.55
29_M/Wak. Yugo	27_M/Wakana PP	95	-0.631414	-0.335342	0.000487	-0.004900	0.714940	3.55
31_D/dawa-III	25_Awash-7KL	88	-0.421722	-0.292918	0.010424	-0.188205	0.513469	3.67
31_D/dawa-III	32_Hurso	98	-0.212673	-0.195523	0.000414	-0.023217	0.288893	3.55
31_D/dawa-III	32_Hurso	99	-0.212673	-0.195523	0.000414	-0.023217	0.288893	3.55
32_Hurso	26_Koka	93	-0.753595	-0.285120	0.059175	-0.385210	0.805729	3.55
32_Hurso	26_Koka	94	-0.753595	-0.285120	0.059175	-0.385210	0.805729	3.55
33_Fincha PP	34_Fincha-II	100	0.157648	0.291384	0.000191	-0.014857	0.331297	3.55
33_Fincha PP	35_Ghedo	101	0.691933	0.247237	0.005686	-0.064409	0.734778	3.98
33_Fincha PP	42_D/Markos	102	0.279350	0.114458	0.001636	-0.126691	0.301889	4.18
34_Fincha-II	36_A/Neshi	105	-0.766377	0.130247	0.003623	-0.043328	0.777367	3.55
35_Ghedo	34_Fincha-II	104	-0.846831	-0.237270	0.010997	-0.093206	0.879443	3.55
35_Ghedo	51_GG-New	106	-1.223777	0.033393	0.033391	-0.021896	1.224232	3.67
37_Alaba	38_Hossaina	107	-0.272364	-0.272953	0.001241	-0.062778	0.385598	3.55
38_Hossaina	30_Wolkite	96	-0.284191	-0.265907	0.002450	-0.147375	0.389193	3.55
39_Combolcha-II	40_Woldiya	108	-0.366256	-0.307508	0.004918	-0.155445	0.478231	3.55
40_Woldiya	54_Alamata	110	-0.569014	-0.247816	0.005368	-0.088507	0.620636	3.55
41_Bahirdar-II	44_Gonder-II	111	0.788383	-0.119374	0.018705	-0.189502	0.797369	3.98
41_Bahirdar-II	44_Gonder-II	112	0.788383	-0.119374	0.018705	-0.189502	0.797369	3.98
42_D/Markos	45_Mota	116	0.058519	-0.169036	0.000209	-0.156008	0.178879	4.18
43_Gashana TAP	46_N/Mewcha	117	-0.598756	-0.119115	0.007981	-0.155565	0.610490	3.98
45_Mota	41_Bahirdar-II	113	0.023915	-0.029676	0.000019	-0.117168	0.038113	4.18
46_N/Mewcha	41_Bahirdar-II	115	-0.670406	0.029566	0.013543	-0.204331	0.671057	3.98
47_Gambella-II	48_Metu	119	-0.062680	-0.181117	0.000172	-0.272696	0.191657	3.67
47_Gambella-II	48_Metu	120	-0.062680	-0.181117	0.000172	-0.272696	0.191657	3.67
48_Metu	49_Bedele	121	-0.088215	0.001086	0.000275	-0.176155	0.088221	3.67
48_Metu	49_Bedele	122	-0.088215	0.001086	0.000275	-0.176155	0.088221	3.67
51_GG-New	50_GG-I PP	52	-0.809050	0.117678	0.000545	-0.004849	0.817564	4.18
51_GG-New	50_GG-I PP	52	-0.809050	0.117678	0.000545	-0.004849	0.817564	4.18
51_GG-New	30_Wolkite	97	1.630396	0.209598	0.029394	0.054373	1.643813	4.18
52_Jimma-New	51_GG-New	128	-0.245857	0.329846	0.002973	-0.119545	0.411393	3.55

52_Jimma-New	51_GG-New	129	-0.245857	0.329846	0.002973	-0.119545	0.411393	3.55
52_Jimma-New	53_Agaro	130	0.242941	-0.331258	0.001176	-0.073385	0.410794	3.55
52_Jimma-New	53_Agaro	131	0.242941	-0.331258	0.001176	-0.073385	0.410794	3.55
53_Agaro	49_Bedele	123	0.190434	-0.282717	0.001302	-0.159629	0.340873	3.67
53_Agaro	49_Bedele	124	0.190434	-0.282717	0.001302	-0.159629	0.340873	3.67
54_Alamata	43_Gashana TAP	118	-0.533011	-0.266026	0.007414	-0.149980	0.595710	3.98
54_Alamata	61_Ashogoda WF	132	-0.202349	-0.160731	0.001334	-0.201861	0.258418	3.98
54_Alamata	59_Mehoni	133	-0.125523	-0.136172	0.000263	-0.067768	0.185200	3.98
55_Shire-E/slassie	60_Welkayt	140	0.062247	-0.146553	0.000135	-0.310706	0.159225	3.55
55_Shire-E/slassie	56_Humera	141	0.043767	-0.109226	0.000692	-0.438013	0.117668	3.98
56_Humera	44_Gonder-II	51	-0.099211	0.119673	0.002914	-0.286156	0.155449	3.55
57_Mekele	58_Tekeze PP	138	-1.104692	-0.468608	0.032191	-0.096553	1.199974	3.55
57_Mekele	58_Tekeze PP	139	-1.104692	-0.468608	0.032191	-0.096553	1.199974	3.55
58_Tekeze PP	55_Shire-E/slassie	137	0.298184	-0.311028	0.003666	-0.298293	0.430874	3.98
59_Mehoni	57_Mekele	135	-0.181757	-0.090428	0.000781	-0.161072	0.203010	3.98
60_Welkayt	56_Humera	142	0.004071	-0.000645	0.000800	-0.301486	0.004122	3.55
61_Ashogoda WF	57_Mekele	134	0.108316	0.103879	0.000119	-0.031545	0.150077	3.55
63_Nazreth-II PP	62_Awash-7KL	143	-0.046322	0.160380	0.005201	-0.035328	0.166935	1.12
63_Nazreth-II PP	64_Koka PP	144	-0.561649	0.255262	0.005316	0.007094	0.616935	1.12
64_Koka PP	94_Elala Geda TP	30	-0.289051	0.461409	0.008109	0.008879	0.544472	1.12
64_Koka PP	95_Elala Geda DCP	31	-0.285642	0.462918	0.008095	0.008847	0.543953	1.12
65_Awash-II PP	78_Assela	10	0.031473	0.297675	0.005960	-0.006757	0.299334	1.12
65_Awash-II PP	64_Koka PP	40	-0.039072	0.012106	0.000056	-0.010744	0.040905	1.12
65_Awash-II PP	64_Koka PP	41	-0.039072	0.012106	0.000056	-0.010744	0.040905	1.12
66_Awash-III PP	65_Awash-II PP	11	0.108000	0.111212	0.000052	-0.055058	0.155023	1.12
66_Awash-III PP	65_Awash-II PP	12	0.108000	0.111212	0.000052	-0.055058	0.155023	1.12
67_Kaliti-I	71_Mekanisa	4	0.234949	0.130936	0.001626	-0.002132	0.268970	1.12
67_Kaliti-I	68_Gefersa	145	-0.221106	0.054589	0.001784	-0.005010	0.227745	1.12
68_Gefersa	69_Addis North	29	0.651001	0.169845	0.006889	0.011664	0.672793	1.12
70_Sebeta-I	68_Gefersa	81	-0.369457	-0.102029	0.002199	0.001079	0.383286	1.12
71_Mekanisa	70_Sebeta-I	50	-0.321045	0.021546	0.002362	-0.000423	0.321768	1.12
72_Addis East-II	69_Addis North	22	-0.074024	0.028529	0.000086	-0.003412	0.079332	1.12
73_Cotobie	67_Kaliti-I	5	0.022148	-0.109658	0.000329	-0.006569	0.111873	1.12
73_Cotobie	67_Kaliti-I	6	0.022148	-0.109658	0.000329	-0.006569	0.111873	1.12
73_Cotobie	72_Addis East-II	23	0.543090	0.148844	0.002342	0.003388	0.563117	1.12
74_D/Birhan	75_Shoa Robit	8	0.186272	0.005928	0.002732	-0.014716	0.186366	1.12
74_D/Birhan	91_Legetafo	27	-0.295799	-0.058939	0.000124	-0.000090	0.301613	1.12
75_Shoa Robit	92_Combolcha-II	9	0.096727	-0.002285	0.001782	-0.041094	0.096754	1.12
76_Gelan	77_Yesu	26	0.725596	0.565717	0.009296	0.017780	0.920068	1.12
76_Gelan	67_Kaliti-I	37	0.697830	0.540957	0.009248	0.017245	0.882950	1.12
76_Gelan	67_Kaliti-I	38	0.697830	0.540957	0.009248	0.017245	0.882950	1.12
77_Yesu	67_Kaliti-I	7	0.324038	0.358082	0.000108	0.000112	0.482932	1.12

78_Assela	79_Adamitulu	13	-0.032181	0.276507	0.005620	-0.005714	0.278374	1.12
79_Adamitulu	80_Shashemene	17	-0.205430	0.201077	0.009809	-0.003643	0.287460	1.12
80_Shashemene	87_Alaba	39	-0.930836	-0.026283	0.085598	0.166750	0.931207	1.12
81_M/Waka.Yugo	80_Shashemene	18	0.344302	0.202150	0.024587	0.009837	0.399260	1.12
83_Bedele	82_Nekemte	43	0.120339	0.028309	0.001241	-0.028442	0.123624	1.12
84_Ghedo	82_Nekemte	15	0.229820	0.018891	0.007311	-0.034168	0.230595	1.12
85_GG Old	86_Hossaina	19	0.322505	0.069361	0.008838	-0.010044	0.329879	1.12
87_Alaba	97_Wolyta	16	-0.742219	0.057704	0.042507	0.068268	0.744459	1.12
87_Alaba	86_Hossaina	20	-0.091133	-0.024233	0.000419	-0.015256	0.094300	1.12
88_Tis Abay-II PP	89_Bahirdar-II	126	0.270000	0.017396	0.002243	-0.008493	0.270560	1.12
88_Tis Abay-II PP	89_Bahirdar-II	127	0.270000	0.017396	0.002243	-0.008493	0.270560	1.12
91_Legetafo	73_Cotobie	24	0.030022	0.006511	0.000233	-0.038781	0.030720	1.12
93_Dangote	68_Gefersa	21	-0.168316	-0.062125	0.003583	-0.020330	0.179416	1.12
93_Dangote	90_Sululta	28	-0.327567	-0.077966	0.008968	-0.000220	0.336718	1.12
94_Elala Geda TP	76_Gelan	33	-0.401014	0.402220	0.014080	0.017902	0.567973	1.12
95_Elala Geda DCP	76_Gelan	34	-0.403026	0.401176	0.014118	0.017990	0.568659	1.12
96_D/Ziet TP	64_Koka PP	32	0.066557	-0.594426	0.010211	0.013721	0.598141	1.12
96_D/Ziet TP	76_Gelan	35	-0.535603	0.304313	0.016985	0.024617	0.616017	1.12
98_Sor PP	99_Metu	42	0.036000	0.027840	0.000619	-0.002275	0.045509	0.29
100_Gambella-II	99_Metu	44	0.012121	-0.015776	0.000355	-0.016487	0.019895	0.29
101_Bahirdar-II	103_Woreta	46	0.059725	-0.005838	0.003758	-0.005424	0.060009	0.29
102_Bahirdar-II	101_Bahirdar-II	45	0.013687	0.044038	0.000124	-0.000397	0.046116	0.29
104_Gonder-II	103_Woreta	48	-0.000032	0.021870	0.000961	-0.005149	0.021870	0.29
105_Tis Abay-I PP	106_Bahirdar-I	49	0.120000	-0.003027	0.005554	0.006704	0.120038	0.19

Table J-3. Global summary report of the grid model simulation

GLOBAL SUMMARY REPORT	
TOTAL GENERATION	
Real Power [p.u.]	30.7079
Reactive Power [p.u.]	-9.819092
TOTAL LOAD	
Real Power [p.u.]	29.376019
Reactive Power [p.u.]	17.850949
TOTAL LOSSES	
Real Power [p.u.]	1.331881
Reactive Power [p.u.]	-27.670041
LIMIT VIOLATION STATISTICS	
All Voltages Within Limits.	37 violations
All Reactive Power Within Limits.	6 violations
All Current Flows Within Limits.	

All Real Power Flows Within Limits.	
All Apparent Power Flows Within Limits.	

Appendix K: PP real power generation setting on their respective nominal apparent power (Sn) as bases for conducting PP outage study

Power Plant Name	No. of units	Generator Bus Number	Sn [MVA]	PPG,max.	PG for PP outage with <=106MW	PG for PP outage with >106MW	PG for PP outage with >=180MW	PG for GGII PP outage
GG III Plant	10	8	2200	0.8500	0.590909	0.650000	0.700000	0.710000
GG II Plant	4	11	500	0.8400	0.836000	0.836000	0.840000	0.840000
Tekeze Plant	4	58	344	0.9070	0.756977	0.756977	0.906977	0.906977
GG I Plant	3	50	219	0.9589	0.821918	0.821918	0.958904	0.958904
M/Wakena Plant	4	27	180	0.8500	0.85000	0.85000	0.850000	0.850000
Fincha Plant	4	33	160	0.7999	0.770000	0.770000	0.799938	0.799938
Amerti Neshi Plant	2	36	106	0.7736	0.726415	0.726415	0.773585	0.773585
Tis Abay II Plant	2	88	80	0.6750	0.675000	0.675000	0.675000	0.675000
Koka Hydro Plant	3	64	60	0.6500	0.533333	0.600000	0.650000	0.650000
Awash II Plant	2	65	40	0.7500	0.540000	0.600000	0.750000	0.750000
Awash III Plant	2	66	40	0.7500	0.540000	0.600000	0.750000	0.750000
TIS ABAY I Plant	3	105	14.4	0.8333	0.821918	0.821918	0.958904	0.958904
Sor PP	2	98	6.2	0.5806	0.5806	0.5806	0.5806	0.5806
Ashogoda	120	61	120	0.2600	0.260000	0.260000	0.260000	0.260000
Adama Wind I	34	63	51	0.2594	0.259400	0.259400	0.259400	0.259400
Adama Wind II	102	28	153	0.2600	0.260000	0.260000	0.260000	0.260000

Appendix L: Simulation Result at Scaled Peak Load with UPFC

Table L-1. Network statistics and power flow result reports of a grid model with UPFC

NETWORK STATISTICS	
Buses:	106
Lines:	146
Transformers:	51
Generators:	17
Loads:	69
SOLUTION STATISTICS	
Number of Iterations:	6
Maximum P mismatch [p.u.]	0.312000*
Maximum Q mismatch [p.u.]	0.534949*

Power rate [MVA]				100		
POWER FLOW RESULTS						
Bus	V [p.u.]	phase [rad]	P gen [p.u.]	Q gen [p.u.]	P load [p.u.]	Q load [p.u.]
1_Beles PP	1.000000	0.000000	4.685402	0.216488	0.164248	0.058331
2_Sululta	0.977192	-0.136792	0.000000	0.000000	0.000000	0.429707
3_Gelan	0.981629	-0.132737	0.000000	0.000000	0.000000	-0.867236
4_Sebeta-II	0.982630	-0.134130	0.000000	0.000000	0.000000	-0.869005
5_G/Guracha	0.970729	-0.119416	0.000000	0.000000	0.092467	0.892838
6_Holeta	0.980863	-0.134884	0.000000	0.000000	0.158761	0.445409
7_Wolyta	0.997212	-0.028345	0.000000	0.000000	0.000000	0.894989
8_GG-III PP	1.000000	0.006974	13.000000	-0.876827	0.000000	0.000000
9_Bahirdar II	0.994953	-0.027372	0.000000	0.000000	0.000000	0.445469
10_D/Markos	0.973549	-0.115526	0.000000	0.000000	0.000000	0.426509
11_GG-II PP	1.000000	-0.028358	4.180000	4.207047	0.000000	0.000000
12_GG-New	0.995887	-0.036268	0.000000	0.000000	0.000000	0.892612
13_Legetafo	0.957015	-0.228755	0.000000	0.000000	0.000000	0.137382
14_Sululta	0.963198	-0.212489	0.000000	0.000000	0.000000	0.000000
15_Shegole	0.961684	-0.213301	0.000000	0.000000	0.908049	0.439690
16_Cotobie	0.954850	-0.231724	0.000000	0.000000	0.000000	0.000000
17_B/Arabsa TP	0.957861	-0.227993	0.000000	0.000000	0.536366	0.243590
18_Gefersa	0.963066	-0.209354	0.000000	0.000000	0.000000	0.000000
19_T/hailoch	0.965392	-0.202501	0.000000	0.000000	0.074685	0.031012
20_Kaliti-I	0.962533	-0.204856	0.000000	0.000000	0.000000	0.000000
21_Gelan	0.968026	-0.205519	0.000000	0.000000	0.000000	0.000000
22_Sebeta-I	0.967146	-0.197647	0.000000	0.000000	0.000000	0.000000
23_Sebeta-II	0.973927	-0.184678	0.000000	0.000000	0.241922	-0.309681
24_EIZ TAP	0.951039	-0.256285	0.000000	0.000000	0.320660	0.155198
25_Awash-7KL	0.938767	-0.300162	0.000000	0.000000	0.000000	0.000000
26_Koka	0.945987	-0.273829	0.000000	0.000000	0.000000	0.402701
27_M/Wakana PP	0.975000	-0.242108	1.530000	0.851937	0.000000	0.000000
28_Adama-II WF	0.950000	-0.272058	0.397800	0.443287	0.000000	0.000000
29_M/Wakana Yugo	0.971043	-0.245486	0.000000	0.000000	0.116767	0.056481
30_Wolkite	0.989314	-0.137762	0.000000	0.000000	0.279823	0.135434
31_D/dawa-III	0.933852	-0.319098	0.000000	0.000000	1.023899	0.826747
32_Hurso	0.937121	-0.316893	0.000000	0.000000	1.305810	0.254370
33_Fincha PP	1.000000	-0.105299	1.232000	0.206508	0.103068	0.049886
34_Fincha-II	0.999412	-0.106281	0.000000	0.000000	0.066007	0.031929
35_Ghedo	0.992190	-0.147176	0.000000	0.000000	0.000000	0.000000
36_A/Neshi	1.000000	-0.091136	0.770000	-0.240177	0.000000	0.000000
37_Alaba	0.979089	-0.161673	0.000000	0.000000	0.000000	0.000000
38_Hossaina	0.983448	-0.155362	0.000000	0.000000	0.000000	0.000000
39_Combolcha-II	0.948045	-0.250542	0.000000	0.000000	0.000000	0.134818

40_Woldiya	0.959166	-0.229749	0.000000	0.000000	0.209398	0.101347
41_Bahirdar-II	0.993064	-0.083547	0.000000	0.000000	0.000000	0.591705
42_D/Markos	0.981293	-0.113469	0.000000	0.000000	0.284640	0.282207
43_Gashana TAP	0.977281	-0.175880	0.000000	0.000000	0.058331	0.003070
44_Gonder-II	0.972152	-0.154042	0.000000	0.000000	1.000000	0.283524
45_Mota	0.992372	-0.098462	0.000000	0.000000	0.034395	0.016649
46_N/Mewcha	0.989927	-0.140864	0.000000	0.000000	0.063668	0.006884
47_Gambella-II	1.024938	-0.110673	0.000000	0.000000	0.000000	0.315149
48_Metu	1.030672	-0.106838	0.000000	0.000000	0.000000	0.159343
49_Bedele	1.027414	-0.100652	0.000000	0.000000	0.000000	0.000000
50_GG-I PP	1.000000	-0.062131	1.800000	-0.707080	0.000000	0.000000
51_GG-New	1.000701	-0.065588	0.000000	0.000000	0.380425	0.178502
52_Jimma-New	1.013814	-0.080602	0.000000	0.000000	0.005832	0.002824
53_Agaro	1.019338	-0.088413	0.000000	0.000000	0.102661	0.049689
54_Alamata	0.955308	-0.204267	0.000000	0.000000	0.293012	0.415825
55_Shire-E/Selassie	0.999158	-0.160143	0.000000	0.000000	0.188505	0.240984
56_Humera	0.975944	-0.156591	0.000000	0.000000	0.145558	0.499059
57_Mekele	0.952481	-0.198839	0.000000	0.000000	2.143804	1.148683
58_Tekeze PP	1.000000	-0.131636	2.604000	-0.021195	0.032050	0.016174
59_Mehoni	0.955905	-0.204433	0.000000	0.000000	0.056762	0.022335
60_Welkayt	0.993307	-0.163680	0.000000	0.000000	0.058041	0.161897
61_Ashogoda WF	0.950000	-0.198437	0.312000	-0.534949	0.000000	0.000000
62_Awash-7KL	0.930473	-0.335813	0.000000	0.000000	0.583991	0.260819
63_Nazreth-II PP	0.950000	-0.368817	0.132294	0.636461	0.740265	0.319758
64_Koka PP	0.950000	-0.348205	0.320000	0.667286	0.305819	0.148056
65_Awash-II PP	0.950000	-0.352576	0.216000	0.181705	0.478567	0.377111
66_Awash-III PP	1.000000	-0.313487	0.216000	0.222425	0.000000	0.000000
67_Kaliti-I	0.940765	-0.279904	0.000000	0.000000	4.336152	1.836430
68_Gefersa	0.927791	-0.296336	0.000000	0.000000	0.970238	0.469641
69_Addis North	0.916097	-0.312499	0.000000	0.000000	0.617277	0.205891
70_Sebeta-I	0.918849	-0.306302	0.000000	0.000000	1.570449	0.662633
71_Mekanisa	0.921301	-0.306003	0.000000	0.000000	0.606460	0.122001
72_Addis East-II	0.918446	-0.311565	0.000000	0.000000	0.669256	0.127290
73_Cotobie	0.925830	-0.301372	0.000000	0.000000	1.326462	0.642251
74_D/Birhan	0.933109	-0.320366	0.000000	0.000000	0.118441	0.057326
75_Shoa Robit	0.921605	-0.341957	0.000000	0.000000	0.094770	0.025030
76_Gelan	0.945961	-0.278895	0.000000	0.000000	0.386522	0.187192
77_Yesu	0.941000	-0.280239	0.000000	0.000000	0.436556	0.211294
78_Assela	0.931633	-0.354322	0.000000	0.000000	0.060880	0.029466
79_Adamitulu	0.918251	-0.347693	0.000000	0.000000	0.187080	0.090560
80_Shashemene	0.929877	-0.302279	0.000000	0.000000	1.255203	0.513226
81_M/Wakana Yugo	0.935286	-0.295030	0.000000	0.000000	0.165109	0.056391

82_Nekemte	0.984060	-0.258594	0.000000	0.000000	0.353684	0.113691
83_Bedele	0.997150	-0.244143	0.000000	0.000000	0.080945	0.039178
84_Ghedo	1.004834	-0.179417	0.000000	0.000000	0.009958	0.004820
85_GG Old	0.999530	-0.109660	0.000000	0.000000	0.028451	0.013771
86_Hossaina	0.979149	-0.159912	0.000000	0.000000	0.234322	0.126536
87_Alaba	0.976839	-0.167330	0.000000	0.000000	0.091045	0.044066
88_Tis Abay-II PP	1.000000	-0.024000	0.540000	-0.018894	0.000000	0.000000
89_Bahirdar-II	0.992123	-0.043204	0.000000	0.000000	0.000000	0.000000
90_Sululta	0.930977	-0.303462	0.000000	0.000000	0.555381	0.185462
91_Legetafo	0.933574	-0.319715	0.000000	0.000000	0.766997	0.135045
92_Combolcha-II	0.906804	-0.353531	0.000000	0.000000	0.914592	0.373004
93_Dangote	0.896146	-0.347405	0.000000	0.000000	0.531606	0.150183
94_Elala Geda TP	0.944797	-0.324142	0.000000	0.000000	0.106924	0.051798
95_Elala Geda DCP	0.944616	-0.324304	0.000000	0.000000	0.112520	0.054458
96_D/Ziet TP	0.929976	-0.334103	0.000000	0.000000	0.482913	0.298690
97_Wolyta	0.989972	-0.073096	0.000000	0.000000	0.574283	0.301689
98_Sor PP	1.000000	-0.214841	0.036000	0.024641	0.000000	0.000000
99_Metu	0.983575	-0.215756	0.000000	0.000000	0.097872	0.047369
100_Gambella-II	0.997023	-0.186771	0.000000	0.000000	0.113239	0.054807
101_Bahirdar-II	0.970163	-0.114125	0.000000	0.000000	0.000000	0.000000
102_Bahirdar-II	0.973233	-0.116372	0.000000	0.000000	0.413055	0.202580
103_Woreta	0.912092	-0.170031	0.000000	0.000000	0.055623	0.026920
104_Gonder-II	0.941163	-0.210642	0.000000	0.000000	0.443103	0.214463
105_Tis Abay-I PP	1.000000	-0.030758	0.120000	-0.009948	0.000000	0.000000
106_Bahirdar-I	0.961814	-0.107121	0.000000	0.000000	0.068284	0.039834

Table L-2. Line flow reports of a grid model with UPFC and their respective thermal limits

LINE FLOWS								
From Bus	To Bus	Line	P Flow [pu]	Q Flow [pu]	P Loss [pu]	Q Loss [pu]	Calculated S(pu) Flow	Thermal limit S(pu)
1_Beles PP	9_Bahirdar II	57	2.260577	0.079078	0.004964	-0.312225	2.261960	12.17
1_Beles PP	9_Bahirdar II	58	2.260577	0.079078	0.004964	-0.312225	2.261960	12.17
2_Sululta	5_G/Guracha	1	-0.587398	0.162591	0.000889	-0.224571	0.609485	12.17
2_Sululta	10_D/Markos	60	-1.520108	0.283642	0.000000	0.033325	1.546345	12.17
3_Gelan	6_Holeta	3	0.269394	-0.106797	0.000079	-0.335407	0.289791	12.17
3_Gelan	6_Holeta	14	0.269394	-0.106797	0.000079	-0.335407	0.289791	12.17
3_Gelan	4_Sebeta-II	70	0.211348	-0.304554	0.000061	-0.212463	0.370703	12.17
5_G/Guracha	10_D/Markos	136	-0.680754	-0.505676	0.000000	0.004121	0.848018	12.17
6_Holeta	4_Sebeta-II	2	-0.255879	-0.541104	0.000090	-0.098941	0.598555	12.17
6_Holeta	4_Sebeta-II	59	-0.255879	-0.541104	0.000090	-0.098941	0.598555	12.17

6_Holeta	2_Sululta	114	0.445813	0.547009	0.000401	-0.235736	0.705669	12.17
6_Holeta	2_Sululta	125	0.445813	0.547009	0.000401	-0.235736	0.705669	12.17
7_Wolyta	3_Gelan	25	5.902959	1.207683	0.000000	0.630836	6.025232	12.17
7_Wolyta	3_Gelan	36	5.902959	1.207683	0.000000	0.630836	6.025232	12.17
8_GG-III PP	7_Wolyta	54	4.333333	-0.292276	0.018791	-0.203332	4.343179	12.17
8_GG-III PP	7_Wolyta	55	4.333333	-0.292276	0.018791	-0.203332	4.343179	12.17
8_GG-III PP	7_Wolyta	56	4.333333	-0.292276	0.018791	-0.203332	4.343179	12.17
9_Bahirdar II	10_D/Markos	103	2.174444	0.192305	0.014970	-0.334939	2.182931	12.17
11_GG-II PP	4_Sebeta-II	47	2.777509	-0.125433	0.022348	-0.728998	2.780340	12.17
11_GG-II PP	7_Wolyta	53	-0.016816	3.796092	0.000000	0.010583	3.796130	12.17
11_GG-II PP	12_GG-New	92	1.419307	0.536387	0.001032	-0.144297	1.517282	12.17
13_Legetafo	14_Sululta	61	-1.200973	-0.179259	0.007091	-0.278517	1.214278	3.55
13_Legetafo	14_Sululta	62	-1.200973	-0.179259	0.007091	-0.278517	1.214278	3.55
13_Legetafo	16_Cotobie	63	0.638486	0.100428	0.000836	-0.209004	0.646336	3.55
13_Legetafo	16_Cotobie	64	0.638486	0.100428	0.000836	-0.209004	0.646336	3.55
13_Legetafo	39_Combolcha-II	66	0.558886	0.248827	0.000000	0.014452	0.611775	3.55
15_Shegole	14_Sululta	67	-0.228998	-0.321101	0.000183	-0.206637	0.394393	3.55
15_Shegole	18_Gefersa	71	-0.679051	-0.118589	0.000947	-0.223338	0.689328	3.55
17_Bole Arabsa TP	13_Legetafo	65	0.417090	-0.072671	0.000188	-0.617688	0.423374	3.55
17_Bole Arabsa TP	20_Kaliti-I	109	-0.953456	-0.170918	0.007695	-0.607384	0.968655	3.55
18_Gefersa	14_Sululta	68	0.256500	-0.113672	0.000275	-0.029089	0.280560	4.18
18_Gefersa	14_Sululta	69	0.256500	-0.113672	0.000275	-0.029089	0.280560	4.18
18_Gefersa	35_Ghedo	73	-0.583373	-0.223089	0.007913	-0.142840	0.624574	3.98
18_Gefersa	35_Ghedo	74	-0.763802	-0.173958	0.018050	-0.194538	0.783361	3.98
18_Gefersa	35_Ghedo	75	-0.763802	-0.173958	0.018050	-0.194538	0.783361	3.98
19_T/hailoch	18_Gefersa	72	0.964775	-0.011431	0.002358	-0.013115	0.964842	3.67
20_Kaliti-I	21_Gelan	77	-3.239874	-0.671941	0.018843	-0.274723	3.308820	3.55
20_Kaliti-I	21_Gelan	78	-3.239874	-0.671941	0.018843	-0.274723	3.308820	3.55
20_Kaliti-I	22_Sebeta-I	79	-0.649008	-0.354569	0.001219	-0.186673	0.739548	3.67
21_Gelan	24_EIZ TAP	86	0.964224	0.025782	0.012445	-0.123599	0.964569	3.55
22_Sebeta-I	19_T/hailoch	76	1.041273	0.011526	0.001813	-0.008054	1.041337	3.55
22_Sebeta-I	30_Wolkite	85	-0.652745	-0.122231	0.013868	-0.213666	0.664091	4.18
23_Sebeta-II	22_Sebeta-I	83	1.106294	0.338947	0.003294	-0.004277	1.157053	4.18
23_Sebeta-II	22_Sebeta-I	84	1.106294	0.338947	0.003294	-0.004277	1.157053	4.18
25_Awash-7KL	26_Koka	87	-1.168829	-0.323386	0.000000	0.033387	1.212741	3.55
26_Koka	24_EIZ TAP	80	-0.628730	-0.115361	0.002389	-0.121178	0.639226	3.55
26_Koka	21_Gelan	82	-1.422936	-0.105911	0.024984	0.023816	1.426872	3.55
27_M/Wakana PP	26_Koka	89	0.266758	0.048140	0.003052	-0.209855	0.271067	3.55
27_M/Wakana PP	26_Koka	90	0.266758	0.048140	0.003052	-0.209855	0.271067	3.55
28_Adama-II WF	26_Koka	91	0.397800	0.443287	0.000884	-0.014976	0.595607	3.55
29_M/Wakana Yugo	27_M/Wakana PP	95	-0.994988	-0.756201	0.001496	-0.000543	1.249736	3.55
31_D/dawa-III	25_Awash-7KL	88	-0.523426	-0.139791	0.000000	0.010674	0.541771	3.67

31_D/dawa-III	32_Hurso	98	-0.250237	-0.343478	0.000440	-0.293417	0.424965	3.55
31_D/dawa-III	32_Hurso	99	-0.250237	-0.343478	0.000440	-0.293417	0.424965	3.55
32_Hurso	26_Koka	93	-0.903582	-0.177246	0.000000	0.040780	0.920802	3.55
32_Hurso	26_Koka	94**	-0.903582	-0.218025	0.000000	0.040780	0.929514	3.55
33_Fincha PP	34_Fincha-II	100	0.207298	0.039432	0.000076	-0.015230	0.211015	3.55
33_Fincha PP	35_Ghedo	101	0.774461	-0.031750	0.006025	-0.063970	0.775111	3.98
33_Fincha PP	42_D/Markos	102	0.147173	0.148941	0.001012	-0.129819	0.209388	4.18
34_Fincha-II	36_A/Neshi	105	-0.766236	0.197214	0.003764	-0.042962	0.791209	3.55
35_Ghedo	34_Fincha-II	104	-0.895694	0.081598	0.011759	-0.092884	0.899403	3.55
35_Ghedo	51_GG-New	106	-0.765955	0.014478	0.012821	-0.124867	0.766091	3.67
37_Alaba	38_Hossaina	107	-0.277539	-0.113773	0.000732	-0.068584	0.299954	3.55
38_Hossaina	30_Wolkite	96	-0.309220	-0.075128	0.001891	-0.156455	0.318216	3.55
39_Combolcha-II	40_Woldiya	108	-0.315230	-0.332187	0.002452	-0.551678	0.457950	3.55
40_Woldiya	54_Alamata	110	-0.527079	0.118143	0.004923	-0.316302	0.540158	3.55
41_Bahirdar-II	44_Gonder-II	111	0.803776	-0.256512	0.019212	-0.437593	0.843714	3.98
41_Bahirdar-II	44_Gonder-II	112	0.803776	-0.256512	0.019212	-0.437593	0.843714	3.98
42_D/Markos	45_Mota	116	-0.179867	-0.163541	0.000709	-0.153748	0.243101	4.18
43_Gashana TAP	46_N/Mewcha	117	-0.540347	-0.100881	0.006308	-0.165145	0.549683	3.98
45_Mota	41_Bahirdar-II	113	-0.214972	-0.026442	0.000614	-0.115128	0.216592	4.18
46_N/Mewcha	41_Bahirdar-II	115	-0.610323	0.057380	0.011382	-0.215059	0.613014	3.98
47_Gambella-II	48_Metu	119	-0.062977	-0.183165	0.000174	-0.275080	0.193689	3.67
47_Gambella-II	48_Metu	120	-0.062977	-0.183165	0.000174	-0.275080	0.193689	3.67
48_Metu	49_Bedele	121	-0.088187	-0.000149	0.000271	-0.177729	0.088187	3.67
48_Metu	49_Bedele	122	-0.088187	-0.000149	0.000271	-0.177729	0.088187	3.67
51_GG-New	50_GG-I PP	52	-0.819937	0.351852	0.000649	-0.004361	0.892242	4.18
51_GG-New	50_GG-I PP	146	-0.819937	0.351852	0.000649	-0.004361	0.892242	4.18
51_GG-New	30_Wolkite	97	1.275047	-0.046617	0.017500	-0.009289	1.275898	4.18
52_Jimma-New	51_GG-New	128	-0.235030	0.359800	0.003229	-0.119226	0.429762	3.55
52_Jimma-New	51_GG-New	129	-0.235030	0.359800	0.003229	-0.119226	0.429762	3.55
52_Jimma-New	53_Agaro	130	0.232114	-0.361212	0.001278	-0.073491	0.429361	3.55
52_Jimma-New	53_Agaro	131	0.232114	-0.361212	0.001278	-0.073491	0.429361	3.55
53_Agaro	49_Bedele	123	0.179505	-0.312566	0.001441	-0.160444	0.360443	3.67
53_Agaro	49_Bedele	124	0.179505	-0.312566	0.001441	-0.160444	0.360443	3.67
54_Alamata	43_Gashana TAP	118	-0.476228	-0.258127	0.005788	-0.160316	0.541685	3.98
54_Alamata	61_Ashogoda WF	132	-0.347180	0.333746	0.000000	0.003873	0.481581	3.98
54_Alamata	59_Mehoni	133	-0.001607	-0.057001	0.000005	-0.070601	0.057023	3.98
55_Shire-Endaslassie	60_Welkayt	140	0.051758	-0.111448	0.000154	-0.305554	0.122880	3.55
55_Shire-Endaslassie	56_Humera	141	0.028381	-0.062109	0.001210	-0.428077	0.068286	3.98
56_Humera	44_Gonder-II	51	-0.125989	0.192913	0.000000	0.001070	0.230410	3.55
57_Mekele	58_Tekeze PP	138	-1.118866	-0.582636	0.031502	-0.485316	1.261478	3.55
57_Mekele	58_Tekeze PP	139	-1.118866	-0.582636	0.031502	-0.485316	1.261478	3.55
58_Tekeze PP	55_Shire-Endaslassie	137	0.271213	-0.232008	0.002570	-0.299435	0.356909	3.98

59_Mehoni	57_Mekele	135	-0.058374	-0.008734	0.000206	-0.165669	0.059024	3.98
60_Welkayt	56_Humera	142	-0.006438	0.032209	0.001164	-0.293795	0.032846	3.55
61_Ashogoda WF	57_Mekele	134	-0.035180	-0.205076	0.000168	-0.031552	0.208071	3.55
63_Nazreth-II PP	62_Awash-7KL	143	-0.059683	0.067738	0.001730	-0.044598	0.090279	1.12
63_Nazreth-II PP	64_Koka PP	144	-0.548288	0.248965	0.005064	0.006531	0.602166	1.12
64_Koka PP	94_Elala Geda TP	30	-0.295109	0.222782	0.003743	-0.001024	0.369758	1.12
64_Koka PP	95_Elala Geda DCP	31	-0.291660	0.224335	0.003707	-0.001102	0.367956	1.12
65_Awash-II PP	78_Assela	10	0.060684	0.099733	0.000984	-0.018603	0.116744	1.12
65_Awash-II PP	64_Koka PP	40	-0.053678	0.018700	0.000105	-0.010633	0.056842	1.12
65_Awash-II PP	64_Koka PP	41	-0.053678	0.018700	0.000105	-0.010633	0.056842	1.12
66_Awash-III PP	65_Awash-II PP	11	0.108000	0.111212	0.000052	-0.055058	0.155023	1.12
66_Awash-III PP	65_Awash-II PP	12	0.108000	0.111212	0.000052	-0.055058	0.155023	1.12
67_Kaliti-I	71_Mekanisa	4	0.641253	0.177338	0.008865	0.013744	0.665322	1.12
67_Kaliti-I	68_Gefersa	145	0.268622	0.076890	0.002413	-0.004440	0.279410	1.12
68_Gefersa	69_Addis North	29	0.561974	0.147092	0.004774	0.006527	0.580905	1.12
70_Sebeta-I	68_Gefersa	81	-0.377331	-0.140827	0.002257	0.000914	0.402754	1.12
71_Mekanisa	70_Sebeta-I	50	0.025928	0.041593	0.000056	-0.006163	0.049012	1.12
72_Addis East-II	69_Addis North	22	0.060171	0.061624	0.000095	-0.003702	0.086128	1.12
73_Cotobie	67_Kaliti-I	5	-0.412252	-0.130173	0.004581	-0.070274	0.432315	1.12
73_Cotobie	67_Kaliti-I	6	-0.412252	-0.130173	0.004581	-0.070274	0.432315	1.12
73_Cotobie	72_Addis East-II	23	0.733323	0.195708	0.003896	0.006793	0.758989	1.12
74_D/Birhan	75_Shoa Robit	8	0.136999	0.004716	0.001375	-0.019609	0.137080	1.12
74_D/Birhan	91_Legetafo	27	-0.255441	-0.062042	0.000087	-0.000204	0.262867	1.12
75_Shoa Robit	92_Combolcha-II	9	0.040855	-0.000705	0.000379	-0.048892	0.040861	1.12
76_Gelan	77_Yesu	26	0.115320	0.452347	0.000000	0.002527	0.466816	1.12
76_Gelan	67_Kaliti-I	37	0.117134	0.168938	0.000472	-0.002715	0.205573	1.12
76_Gelan	67_Kaliti-I	38	0.117134	0.168938	0.000472	-0.002715	0.205573	1.12
77_Yesu	67_Kaliti-I	7	-0.353360	0.262195	0.000000	0.000184	0.440011	1.12
78_Assela	79_Adamitulu	13	-0.001180	0.088870	0.000630	-0.018617	0.088878	1.12
79_Adamitulu	80_Shashemene	17**	-0.192548	0.038779	0.003657	-0.021852	0.196414	1.12
80_Shashemene	87_Alaba	39	-0.735719	0.091606	0.044853	0.073275	0.741401	1.12
81_M/Wakana Yugo	80_Shashemene	18	0.713111	0.574845	0.000000	0.008479	0.915955	1.12
83_Bedele	82_Nekemte	43	0.098268	-0.015140	0.000760	-0.102800	0.099428	1.12
84_Ghedo	82_Nekemte	15	0.265136	-0.118003	0.008961	-0.144035	0.290210	1.12
85_GG Old	86_Hossaina	19	0.277762	-0.015309	0.005963	-0.018100	0.278183	1.12
87_Alaba	97_Wolyta	16	-0.576579	0.161422	0.021823	0.026399	0.598749	1.12
87_Alaba	86_Hossaina	20	-0.068212	-0.079595	0.000214	-0.173674	0.104825	1.12
88_Tis Abay-II PP	89_Bahirdar-II	126	0.270000	-0.009447	0.002225	-0.008560	0.270165	1.12
88_Tis Abay-II PP	89_Bahirdar-II	127	0.270000	-0.009447	0.002225	-0.008560	0.270165	1.12
91_Legetafo	73_Cotobie	24	-0.039534	0.023456	0.000484	-0.041609	0.045969	1.12
93_Dangote	68_Gefersa	21	-0.228948	-0.051101	0.005856	-0.017268	0.234582	1.12
93_Dangote	90_Sululta	28	-0.302658	-0.099082	0.007430	-0.005247	0.318464	1.12

94_Elala Geda TP	76_Gelan	33	-0.405776	0.172008	0.008198	0.004034	0.440727	1.12
95_Elala Geda DCP	76_Gelan	34	-0.407888	0.170978	0.008257	0.004170	0.442274	1.12
96_D/Ziet TP	64_Koka PP	32	0.063916	-0.373636	0.003947	-0.000421	0.379064	1.12
96_D/Ziet TP	76_Gelan	35	-0.546829	0.074947	0.013147	0.015330	0.551941	1.12
98_Sor PP	99_Metu	42	0.036000	0.024641	0.000568	-0.002318	0.043625	0.29
100_Gambella-II	99_Metu	44	0.012715	-0.014479	0.000347	-0.016571	0.019270	0.29
101_Bahirdar-II	103_Woreta	46	0.060408	-0.006448	0.003805	-0.005481	0.060752	0.29
102_Bahirdar-II	101_Bahirdar-II	45	0.014435	0.050517	0.000159	-0.000374	0.052539	0.29
104_Gonder-II	103_Woreta	48	0.000036	0.022707	0.001016	-0.005180	0.022707	0.29
105_Tis Abay-I PP	106_Bahirdar-I	49	0.120000	-0.009948	0.005584	0.006742	0.120412	0.19

Table L-3. Global summary report of the grid model simulated with UPFC

GLOBAL SUMMARY REPORT	
TOTAL GENERATION	
Real Power [p.u.]	32.091496
Reactive Power [p.u.]	5.248717
TOTAL LOAD	
Real Power [p.u.]	31.393912
Reactive Power [p.u.]	18.655761
TOTAL LOSSES	
Real Power [p.u.]	0.697584
Reactive Power [p.u.]	-13.407044
LIMIT VIOLATION STATISTICS	
All Voltages Within Limits.	27 violations
All Reactive Power Within Limits.	6 violations